The characterisation of mycobacterial control profiles and underlying immune signatures in patients with latent tuberculosis infection and active disease



A thesis submitted in fulfilment of the requirements
for the degree of Doctor of Philosophy in Clinical Medicine

Matthew O'Shea

Corpus Christi College, Oxford

Trinity Term 2016

Word Count: ~48,500

The characterisation of mycobacterial control profiles and underlying immune signatures in patients with latent tuberculosis infection and active disease

Matthew O'Shea, Corpus Christi College, University of Oxford

Thesis submitted for the degree of Doctor of Philosophy in Clinical Medicine

Trinity Term 2016

Despite the progress that has been made with global control programmes, tuberculosis (TB) remains a significant challenge to health. Better diagnostics, shorter and more effective treatment regimens and improved vaccines are urgently needed. There is also increasing awareness of the need to tackle the huge burden of latent TB infection, which is estimated to affect one-third of the global population. Targeted preventative therapy is the pragmatic solution to this problem. Unfortunately, current diagnostics lack the necessary resolution to accurately identify individuals at risk of progressing to active TB disease. It has recently been proposed that TB exists on a continuous spectrum, which likely represents the dynamic interaction between the host and pathogen. Delineating this spectrum may identify individuals at risk of disease reactivation who would benefit from targeted treatment. The work presented in this thesis describes the novel use of an *ex vivo* whole blood functional assay to measure the capacity of individuals with active TB disease and latent infection to control mycobacterial growth. The assay identified differential functional responses that discriminated between conventional diagnostic groups, but also showed considerable overlap. Enhanced mycobacterial growth control occurred in patients with active TB disease, which may reflect a general state of immune activation. The wide range of responses seen among latently infected patients is consistent with the concept of a spectrum of infection. Characterisation of different control profiles was undertaken using a multi-platform approach. Differential gene expression was dominated by type I interferon and inflammatory signatures seen in active TB patients and some individuals with latent TB. Clustering analysis showed clear associations with functional responses. Cytokine and chemokine studies revealed strong correlations with mycobacterial growth control. Finally, increases in inflammatory monocytes, polyfunctional T cells, activated and atypical memory B cells and IgG1 responses all demonstrated correlations or associations with functional responses. These findings have potential application in developing a biosignature for TB reactivation and predictive models of risk that warrant further investigation.

Acknowledgements

Firstly I would like to thank my supervisor, Professor Helen McShane, for giving me the opportunity to join her group and undertake such a great project. Your guidance and support during my time in Oxford has been invaluable and I have had an outstanding personal and academic experience.

This project has been a significant task and would not have been possible without assistance and advice from many individuals. I am indebted to all of the members of the TB research group for unceasing help and for making my time at the Jenner so enjoyable. Special thanks go to Iman Satti, Elena Stylianou, Stephanie Harris, Lisa Stockdale, Danny Wright, Rachel Kandt, Jonny Peter, Magali Matsumiya, Janet Pasricha and Paulo Bettencourt. I am particularly grateful to Rachel Tanner who has become a steadfast friend. Always ready to help in the lab you have made much of this work possible. The Jenner is full of great people, too many to list here, but special mention must be made of my officemates Carly Bliss and Pawan Dulal who have made my experience a lot of fun. I am also very appreciative of the considerable efforts of Julius Müller in analysing the transcriptomic data. Lastly, without Julie Furze managing the laboratory so well nothing would be achieved and flow cytometry would cease without the skills and knowledge of Drew Worth. Thank you both.

Beyond Oxford there are several individuals I am extremely grateful to. I thank Professor Adam Cunningham, Dr Martin Dedicoat and Professor Ian Henderson for their friendship, advice and good conversation about science and medicine over a pint of decent beer.

I am very fortunate for the opportunities that the military has given me to date. My Commanding Officer, Surgeon Captain Mike Howell, Royal Navy, and the Defence Professor of Military Medicine, Colonel Duncan Wilson, Royal Army Medical Corps, have

provided me with considerable support and the chance to spend four years undertaking research. I also thank the Wellcome Trust for awarding me a training fellowship, which has been a great start for a career in academic medicine.

My dear parents and sister have encouraged me in all of my various endeavours throughout my life and knowing that they are always there is a wonderful consolation.

Finally, and most importantly, I am indebted to my wife, Sarah, and our children Beatrice, Esmé, Benedict, Matilda and Felicity. You have borne my weekly and many weekend absences with such magnanimity that words cannot describe. I shall be eternally grateful. Without your abiding love and support I would not have completed this work and therefore it is fitting that I dedicate this thesis to you all.

Contents

Abstract i

Acknowledgements ii

Contents iv

List of figures ix

List of tables xii

Acronyms and abbreviations xiii

Introduction

1 Introduction 1

1.1 The global burden of tuberculosis 2

1.2 Microbiology 3

1.3 Natural history and pathogenesis of TB 4

1.4 Clinical manifestations of TB 7

1.5 The global burden of latent TB infection 9

1.5.1 Diagnosing LTBI 10

1.5.2 The need to tackle LTBI 13

1.5.3 Current concepts of LTBI 16

1.5.4 Treatment regimens and outcomes 19

1.6 A proposed 'spectrum of *M. tb* infection' 23

1.6.1 Epidemiological and clinical observations 26

1.6.2 Heterogeneity of the pulmonary granuloma 27

1.6.3 Bacillary diversity 31

1.6.4 Differential gene expression studies 33

1.7 The needs and challenges of TB biomarker 34

1.7.1 Experimental approaches & current progress 38

1.7.2 Transcriptomics 39

1.7.3 Proteomics 42
1.7.4 Metabolomics 43
1.7.5 Multiple biomarkers, large datasets & validating biosignatures ..45
1.8 *Ex vivo* mycobacterial growth inhibition assays 47
1.8.1 Early developments and cellular MGIAs 48
1.8.2 Whole blood MGIAs 51
1.9 Aims and objectives 56

Materials and methods

2 Materials and methods 58
2.1 Statement of authorship 59
2.2 Clinical samples 59
2.2.1 BCG vaccination studies 59
2.2.2 Studies to delineate the spectrum of *M. tb* infection 60
2.3 Mycobacteria Growth Indicator Tube (MGIT) assay 61
2.3.1 Preparation of mycobacterial stocks 61
2.3.2 Titration of mycobacterial stocks 62
2.3.3 Whole blood MGIT assay 62
2.3.4 Calculation of mycobacterial net growth 63
2.4 Immunology assays 64
2.4.1 PBMC isolation, cryopreservation and thawing 64
2.4.2 *Ex vivo* T cell ELISpot assays 65
2.4.3 *Ex vivo* B cell ELISpot assays 66
2.4.3.1 *Ex vivo* antibody secreting cell (ASC) ELISpot assays 66
2.4.3.2 Memory B cell (mBC) ELISpot assays 67
2.4.4 Enzyme-linked immunosorbent assays (ELISAs) 68
2.4.4.1 Total IgG ELISA 68

2.4.4.2 IgG isotype ELISA 69
2.4.5 Whole blood depletions 70
2.4.6 Flow cytometry 71
2.4.6.1 Whole blood depletion efficiency 71
2.4.6.2 PBMC stimulation for T cell characterisation 72
2.4.6.3 Immunophenotyping and ICS T cells 72
2.4.6.4 Immunophenotyping B cells and monocytes 73
2.4.7 Multiplex serum cytokine and chemokine studies 74
2.5 Transcriptomic microarray studies 75
2.5.1 Total RNA extractions 75
2.5.2 Microarrays 76
2.6 Statistical analysis 76
2.7 Reagents 77

Results

3 Characterisation of the whole blood MGIT assay 78
3.1 Statement of authorship 79
3.2 Introduction 79
3.3 Aims 80
3.4 Results 80
3.4.1 Effect of time-to-sample processing 80
3.4.2 Intra-assay variability 82
3.4.3 Inter-assay variability 83
3.4.4 Mycobacterial growth kinetics 83
3.4.5 Differential gene expression 85
3.4.6 Effect of cellular depletions 92
3.5 Discussion 96

4 BCG vaccination as a mycobacterial challenge model 108

4.1 Statement of authorship 108

4.2 Introduction 108

4.3 Aims 109

4.4 Results 109

4.4.1 Study population 109

4.4.2 Effect of BCG vaccination of mycobacterial growth 110

4.4.3 IgG antibody induction following BCG vaccination 112

4.4.4 Evaluating B cell responses following BCG vaccination 114

4.4.5 Immunophenotyping PPD-specific B cells 116

4.5 Discussion 118

5 Delineating the spectrum of *M. tb* infection & TB disease using a MGIA ... 127

5.1 Statement of authorship 127

5.2 Introduction 127

5.3 Aims 128

5.4 Results 128

5.4.1 Study settings 128

5.4.2 Characteristics of study participants 130

5.4.3 Haematological measures among study participants 133

5.4.4 Pre-treatment whole blood MGIT 138

5.4.5 Post-treatment whole blood MGIT 141

5.5 Discussion 143

6 Multiplatform evaluation of MGIA responses 152

6.1 Statement of authorship 152

6.2 Introduction 152

6.3 Aims 153

6.4 Results 154
6.4.1 Patient stratification and experimental approach 154
6.4.2 Multiplex serum cytokine and chemokine analysis 156
6.4.3 Whole blood transcriptomic studies 165
6.4.4 Characterising monocyte subset phenotypes 178
6.4.5 Characterisation of functional T cell responses 185
6.4.6 Characterising IgG subclass distribution 200
6.4.7 Evaluating B cell responses to TB 204
6.4.8 The immunophenotypic characterisation of B cell subsets 205
6.5 Discussion 209

Conclusions and future work

7 Conclusions and future work 232
7.1 Main findings & conclusions 233
7.2 Future work 239
7.2.1 Biomarker refinement and pre-clinical evaluation 239
7.2.2 Evaluation of a putative biosignature of TB reactivation 240
7.2.3 Further MGIT assay characterisation 241
7.2.4 Exploring B cell responses to mycobacteria 242

Appendix

8 Appendix 243
8.1 MGIT standard curve 244
8.2 Reagents and solutions 245
8.3 Supplementary transcriptomic data 249

References

9 References 253

List of figures

Figure 1.1 Global burden of TB 3

Figure 1.2 Global distribution of TB in 2014 4

Figure 1.3 Cellular immune response to *M. tb* 6

Figure 1.4 The immunological life cycle of TB 7

Figure 1.5 Strategies for eliminating TB 16

Figure 1.6 Spectrum of responses to *M. tb* infection 24

Figure 1.7 Heterogeneity of TB granulomas 29

Figure 3.1 Effect of time-to-sample processing on mycobacterial growth 81

Figure 3.2 Inter-assay variability 83

Figure 3.3 Growth kinetics of whole blood MGIT 84

Figure 3.4 Inter-assay variability over 96 hour time-course 85

Figure 3.5 Differential gene expression in blood with mycobacteria 87

Figure 3.6 Changes in gene expression over time 88

Figure 3.7 DGE in whole blood with BCG compared with H37Rv 89

Figure 3.8 Examples of whole blood cell depletions 93

Figure 3.9 Efficiency of cell depletions 94

Figure 3.10 Effect of cell depletions on BCG whole blood MGIT 95

Figure 4.1 BCG vaccination study schedule 111

Figure 4.2 Effect of BCG vaccination on mycobacterial growth control 111

Figure 4.3 IgG antibody responses following BCG vaccination 113

Figure 4.4 BCG-specific ASC and mBC responses to BCG vaccination 115

Figure 4.5 Correlation between ASC responses and IgG antibodies 116

Figure 4.6 Identifying PPD-specific B cells by flow cytometry 117-8

Figure 5.1 Pre-treatment leucocyte profiles 134

Figure 5.2 Patterns of ML relationships 135

Figure 5.3 Pre-treatment haematology parameters 135
Figure 5.4 Changes in leucocyte profiles following treatment 136
Figure 5.5 Patterns of post-treatment ML relationships 137
Figure 5.6 Changes in haematology parameters following treatment 137
Figure 5.7 Pre-treatment whole blood MGIT 139
Figure 5.8 Correlations between pre-treatment haematology and BCG MGIT 140
Figure 5.9 Correlations between pre-treatment haematology and *M. tb* MGIT 141
Figure 5.10 Post-treatment whole blood MGIT 142
Figure 5.11 Correlations between post-treatment haematology and *M. tb* MGIT 143
Figure 6.1 Stratifying LTBI group by pre-treatment MGIT responses 155
Figure 6.2 Pre-treatment Th1/pro-inflammatory cytokine profiles 157
Figure 6.3 Pre-treatment Th2 and Th17 cytokine profiles 158
Figure 6.4 Pre-treatment chemokine profiles 159-60
Figure 6.5 Pre-treatment growth factor profiles 161
Figure 6.6 Changes in cytokines and chemokines after TB treatment 163
Figure 6.7 Changes in cytokines and chemokines after LTBI treatment 164
Figure 6.8 Pre-treatment differential gene expression in whole blood 168
Figure 6.9 Differentially expressed genes between hierarchical clusters 169
Figure 6.10 Modular analysis of DGE between clusters 170
Figure 6.11 Pre-treatment DGE using Berry *et al.* analysis 172
Figure 6.12 Overlap of active TB disease gene signatures 173
Figure 6.13 Relationship between pre-treatment MGIT and DGE clusters 174
Figure 6.14 Changes in DGE following anti-TB treatment 176
Figure 6.15 DGE in hierarchical clusters in response to TB treatment 177
Figure 6.16 Monocyte subset gating strategy 180
Figure 6.17 Pre-treatment monocyte subset characterisation 181

Figure 6.18 Correlations between monocyte subsets and whole blood MGIT 182
Figure 6.19 Baseline monocyte profiles in LTBI subgroups 183
Figure 6.20 Changes in monocyte subsets following anti-TB treatment 184
Figure 6.21 Post-treatment monocyte profiles in LTBI subgroups 185
Figure 6.22 CD4+ and CD8+ T cell gating strategy 186
Figure 6.23 Functional CD4+ T cell characterisation 187
Figure 6.24 Functional CD8+ T cell characterisation 188
Figure 6.25 Pre-treatment T cell cytokine secretion 190
Figure 6.26 Baseline T cell cytokine secretion in LTBI subgroups 192
Figure 6.27 Changes in T cell cytokine secretion after treatment 193
Figure 6.28 Polyfunctional CD4+ *M. tb*-specific cytokine responses 196
Figure 6.29 Polyfunctional CD8+ *M. tb*-specific cytokine responses 197
Figure 6.30 Proportions of polyfunctional T cells responses in LTBI subgroups 198
Figure 6.31 Frequencies of polyfunctional T cells responses in LTBI subgroups 199
Figure 6.32 IgG antibody responses in TB 202
Figure 6.33 IgG antibody responses in LTBI subgroups 203
Figure 6.34 Pre-treatment B cell subset characterisation 206
Figure 6.35 Baseline B cell profiles in LTBI subgroups 207
Figure 6.36 Correlations between baseline B cell subsets and whole blood MGIT 208
Figure 8.1 Example MGIT standard curve 244
Figure 8.2 Quality control evaluation by probe detection 249
Figure 8.3 Quality control evaluation with gender classification 250
Figure 8.4 Assessing microarray processing batch effect 251

List of tables

Table 3.1 Comparison of functional cluster analysis 90

Table 3.2 Immune-related DGE observed during MGIT 91

Table 4.1 Correlation of IgG antibody responses following BCG vaccination 114

Table 5.1 Summary of the characteristics of active TB patients 131

Table 5.2 Summary of the characteristics of patients with latent TB 132

Table 6.1 Correlations between cytokine/chemokines and bacillary growth 162

Table 6.2 Correlation of antigen-specific IgG1 and IgG2 antibody responses 203

Table 8.1 Reagents 245-7

Table 8.2 Solutions 248

Table 8.3 GO DGE annotation top tables 252

Acronyms and abbreviations

AFB	Acid fast bacilli
AFR	African region (WHO classification)
ALP	Alkaline phosphatase
AMR	Americas region (WHO classification)
ANOVA	Analysis of variance
ARI	Annual risk of infection
ART	Anti-retroviral therapy
ASC	Antibody secreting cell
BCG	Bacille Calmette-Guerin
BSA	Bovine serum albumin
CCR	Chemokine receptor
CD	Cluster of differentiation
cDNA	Complementary DNA
CFP-10	Culture filtrate protein-10
cfu	Colony forming unit
CI	Confidence interval
CR	Complement receptor
CRP	C-reactive protein
CT	Computed tomography
CV	Coefficient of variation
CXR	Chest radiograph
DAVID	Database for annotation, visualisation and integrated discovery
DC	Dendritic cell
DGE	Differential gene expression

DMSO	Dimethyl sulfoxide
DNA	Deoxyribonucleic Acid
dosR	Dormancy survival response regulator
DOTS	Directly observed therapy, short-course
DTH	Delayed-type hypersensitivity
DTP	Days-to-positivity
EDTA	Ethylenediaminetetraacetic acid
EHR	Enduring hypoxic response
ELISA	Enzyme-linked immunosorbent assay
ELISpot	Enzyme-linked immunospot
EMR	Eastern Mediterranean region (WHO classification)
ESAT-6	Early secretory antigenic target-6
EUR	European region (WHO classification)
FACS	Fluorescence-activated cell sorting
FCS	Foetal calf serum
FGF	Fibroblast growth factor
FMO	Fluorescence minus one
FSC	Forward scatter
GBP	Guanylate-binding proteins
GCP	Good clinical practice
G-CSF	Granulocyte colony-stimulating factor
GM-CSF	Granulocyte-macrophage colony-stimulating factor
GO	Gene ontology
HEPES	4-(2-hydroxyethyl)-1-piperazineethanesulfonic Acid
HIV	Human immunodeficiency virus
HSC	Haematopoietic stem cell

ICS	Intracellular cytokine staining
ID_{50}	Infectious dose 50%
IFN	Interferon
Ig	Immunoglobulin
IGRA	Interferon-gamma release assay
IL	Interleukin
INH	Isoniazid
iNOS	Inducible nitric oxide synthase
IP	Inducible protein
IQR	Interquartile range
IRIS	Immune reconstitution inflammatory syndrome
kDa	Kilodalton
LAM	Lipoarabinomannan
LH	Lithium heparin
LTBI	Latent TB infection
MALDI	Matrix-assisted enhanced laser desorption/ionisation
mBC	Memory B cell
MCP	Monocyte chemoattractant protein
MCV	Mean cell volume
MDC	Macrophage-derived chemokine
MDR	Multi drug-resistant
MGIA	Mycobacterial growth inhibition assay
MGIT	Mycobacterial growth indicator tube
MHC	Major histocompatibility complex
MIP	Macrophage inflammatory protein
ML	Monocyte to lymphocyte

mRNA	Messenger ribonucleic acid
MS	Mass spectrometry
MSMD	Mendelian susceptibility to mycobacterial disease
M. tb	*Mycobacterium tuberculosis*
MTBC	*Mycobacterium tuberculosis* complex
NAAT	Nucleic acid amplification test
NHP	Non-human primate
NK	Natural killer
NMR	Nuclear magnetic resonance
NNT	Number needed to treat
NTM	Non-tuberculous mycobacteria
OADC	Oleic acid, albumin, dextrose and catalase
OD	Optical density
PAMP	Pathogen-associated molecular pattern
PANTA	Polymyxin B, amphotericin B, nalidixic acid, trimethoprim and azlocillin
PB	Plasmablast
PBMC	Peripheral blood mononuclear cell
PBS	Phosphate-buffered saline
PCA	Principal components analysis
PCR	Polymerase chain reaction
PDGF	Platelet-derived growth factor
PET	Positron emission tomography
PHA	Phytohaemagglutinin
PHE	Public Health England
PHS	Pooled human serum
PPD	Purified protein derivative

PV	Pre-vaccination
PWM	Pokeweed mitogen
qRT-PCR	Quantitative reverse transcription polymerase chain reaction
RANTES	Regulated on activation, normal T cell expressed and secreted
RD1	Region of difference 1
RLU	Relative light units
RMP	Rifampicin
RNA	Ribonucleic Acid
RPM	Revolutions per minute
RR	Relative risk
SAC	*Staphylococcus aureus* Cowan
SEAR	South-East Asia region (WHO classification)
SEB	Staphylococcal enterotoxin B
SELDI	Surface-assisted enhanced laser desorption/ionisation
SEM	Standard error of the mean
SSC	Side Scatter
SSI	Statens Serum Institute
TB	Tuberculosis
TCR	T cell receptor
TGF	Transforming growth factor
Th	T helper
TNF	Tumour necrosis factor
TOF	Time-of-flight
TST	Tuberculin skin test
TTP	Time-to-positivity
US	United States

VEGF	Vascular endothelial growth factor
VOC	Volatile organic compound
W	Week
WHO	World Health Organisation
WPR	Western Pacific region (WHO classification)

Introduction

1 Introduction

1.1 The global burden of tuberculosis

Tuberculosis (TB) has been a cause of pathology among humans for millennia. Evidence suggests that *Mycobacterium tuberculosis* (*M. tb*), the pathogen responsible for most cases of TB, was established as an infection in human populations even before our migration from Africa and subsequent global expansion [1-3]. As population density increased and the dynamics of human-to-human transmission changed, strains of *M. tb* that had caused asymptomatic, chronic infection in ancient populations probably evolved [1-3]. The emergence of virulent *M. tb*, which characterises current human pathology, may therefore be a relatively recent event [4].

Over the past 25 years TB mortality has fallen by 47%, mainly driven by programme-directed advances in diagnosis and effective treatment which has saved approximately 43 million lives [5] (Figure 1.1). Despite this significant progress, TB still represents a huge challenge to global health and is currently equal to human immunodeficiency virus (HIV) as a leading cause of worldwide mortality. In 2014 there were an estimated 9.6 million new cases and 1.5 million deaths due to TB [5]. Approximately 80% of these cases occurred in 22 countries, among which India, Indonesia, Nigeria, Pakistan, China and South Africa were predominant (Figure 1.2). Two of the most important factors driving the on-going TB epidemic are HIV and multi-drug resistant TB (MDR-TB). One quarter of the deaths due to TB and 12% of the new cases in 2014 were in individuals with HIV infection and it is estimated that 480,000 cases of MDR-TB occurred. The cost to treat a single patient for drug-susceptible TB in 2014 ranged from US$100-500, while for MDR-TB it was US$5,000-10,000 [5]. To reduce this burden, shortcomings in detection and treatment must be addressed. Almost 40% of the total estimated new

cases of TB, and 75% of MDR-TB cases, went undiagnosed or were not reported in 2014 [5]. Furthermore, all HIV-positive TB cases are eligible for antiretroviral therapy (ART) however in 2014 only one third of the estimated 1.2 million people living with HIV who developed TB were receiving this therapy [5].

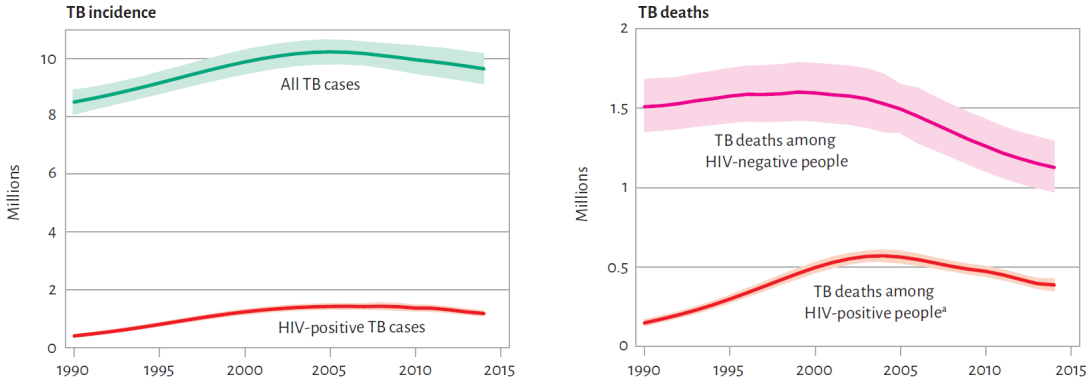


Figure 1.1 Global burden of TB. Estimated absolute numbers of TB cases and deaths worldwide (millions per year), 1990-2014 (image reproduced and text adapted from [5]; permission granted by WHO).

1.2 Microbiology

The genus *Mycobacterium* comprises of aerobic, non-motile, acid-alcohol-fast, Gram-positive, rod-shaped bacilli. *M. tb* is the pathogenic organism responsible for most infection in humans and is a member of the *M. tb* complex, together with *M. bovis*, *M. africanum*, *M. microti*, *M. canetti*, *M. caprae* and *M. pinnipedii*, all of which share considerable genetic homology [6, 7]. TB describes clinical disease resulting from infection with *M. tb*, and to a lesser degree *M. bovis,* which accounts for fewer than 2% of all cases, except in certain populations such as the immunocompromised [8, 9]. Mycolic acid is the major constituent of the mycobacterial cell envelope, defining the genus and its characteristic staining properties [10]. Mycobacteria stain positive with

Gram's stain and the mycolic acids resist de-staining by acid-alcohol after staining with certain aniline dyes (hence the term acid fast bacilli, AFB).

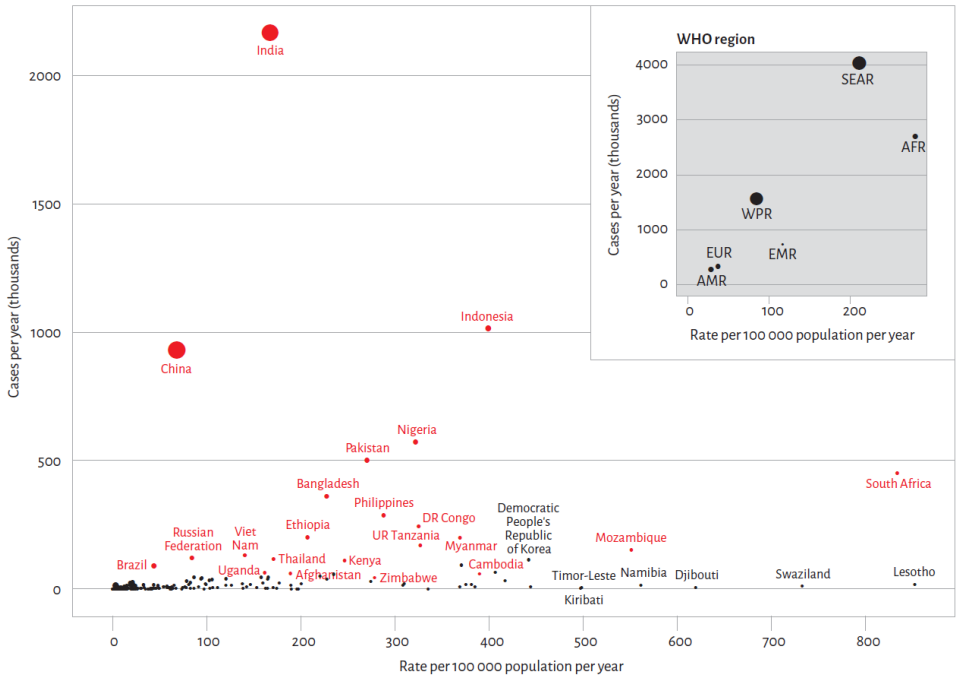
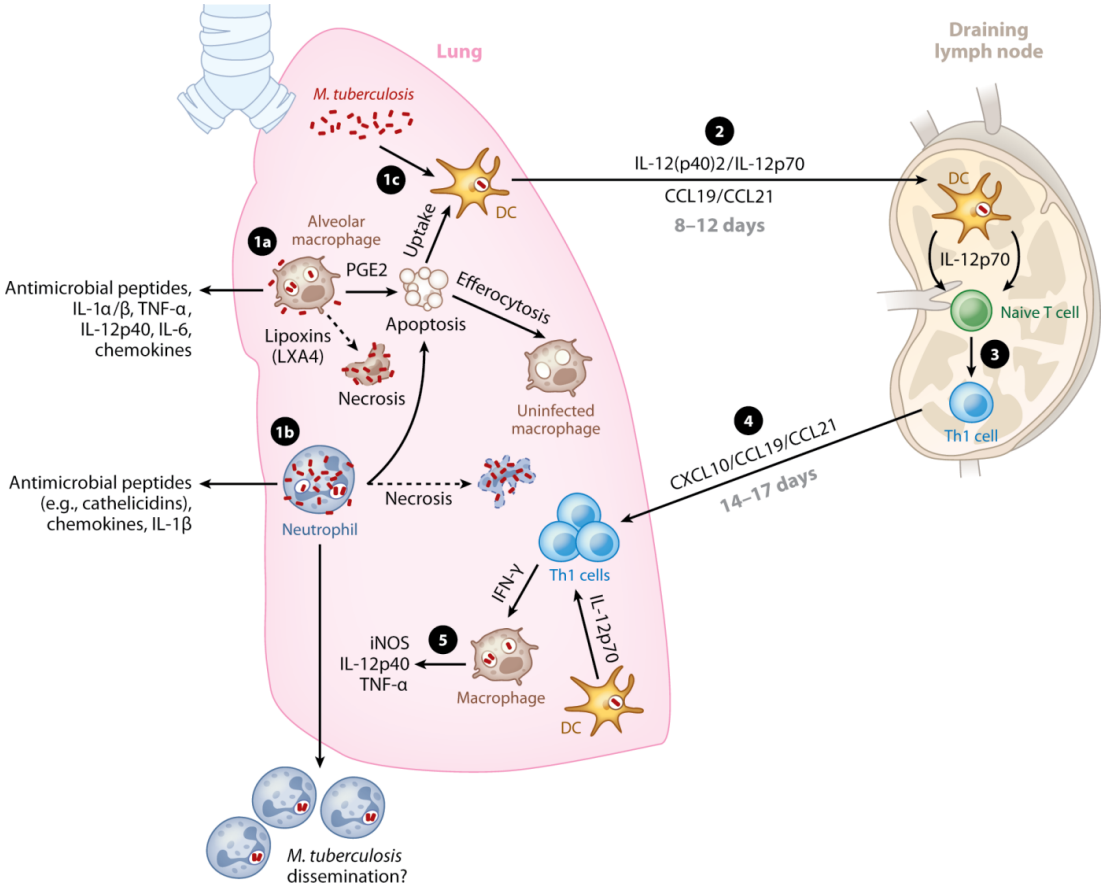


Figure 1.2 Global distribution of TB in 2014. Estimated incidence rate and absolute numbers are shown. The size of each point is proportional to the country's population and red represents high TB burden countries (image reproduced and text adapted from [5]; permission granted by WHO).

1.3 Natural history & pathogenesis of TB

M. tb infection is acquired by aerosol transmission and occurs when an individual with sputum-positive active pulmonary disease expels droplets, each containing up to six bacilli, into the environment by coughing, sneezing or speaking [11, 12]. Droplet nuclei may remain airborne for prolonged periods until undergoing surface deposition, dilution or inactivation. The severity of disease in the index case, proximity and duration of exposure, humidity, ventilation and the presence of inactivating ultraviolet light are factors that can affect transmission likelihood [13, 14]. The infectious dose of

M. tb in humans is very low (ID_{50}<10 bacilli), and inhalation and deposition in the pulmonary alveolar space of bacilli may result in several possible outcomes: immune-mediated clearance of the organism (the majority of cases) or established infection which may cause rapidly progressive active disease (primary disease, 5-10%), chronic (latent) infection (90%) or active disease due to endogenous reactivation after initial infection (post-primary, 5%) [15]. The lifetime risk of an individual developing active TB disease is 5-10%, which is in stark contrast to an annual risk of 5-15% in patients with untreated HIV infection [16, 17]. Most infected individuals who develop primary disease do so within the first 2-3 years after infection. Following alveolar deposition, macrophages phagocytose bacilli, which undergo intracellular replication and eventually cause cell lysis (Figure 1.3). If the host immune response does not eliminate the bacilli there is further phagocytosis by, and proliferation within, alveolar macrophages and subsequent cell apoptosis [15]. Macrophages secrete cytokines and chemokines causing the recruitment of other phagocytic cells and neutrophils, eventually resulting in the formation of a nodular granulomatous structure called the Ghon focus [15]. Further bacillary replication and the involvement of regional draining lymph nodes produces the Ghon (or primary) complex [18]. An effective T lymphocyte-mediated Th1 immune response results in quiescent infection. Failure by the host to mount such a response leads to progressive destruction of the lung. Further proliferation of bacilli may result in haematogenous spread and disseminated disease. Local spread by erosion of caseating lesions through the pulmonary parenchyma and into adjacent airways causes expectoration of bacilli and infectiousness of the host and if untreated, there is significant associated mortality [19]. A proposed immunological life cycle of TB is shown in Figure 1.4 [20].



O'Garra A, et al. 2013.
Annu. Rev. Immunol. 31:475–527

Figure 1.3 Cellular immune response to *M. tb*. Following exposure and aerosol infection with *M. tb*, lung alveolar macrophages (1a), neutrophils (1b) and lung dendritic cells (DCs) (1c) may become infected, leading to the production and secretion of antimicrobial peptides, cytokines, and chemokines. The balance of lipid mediators within infected macrophages contributes to determining downstream pathways leading to either apoptosis or necrosis (e.g. prostaglandin E2 is pro-apoptotic while lipoxin (LX) A4 is pro-necrotic). Infected apoptotic cells may be engulfed by lung DCs or efferocytosed by uninfected lung macrophages (1c). *M. tb*-infected DCs migrate to the local draining lymph nodes within 8-12 days after infection, under the influence of IL-12(p40)2, IL-12p70, CCL19 and CCL21 (2), to drive naïve T cell differentiation toward a Th1 phenotype (3). Protective antigen-specific Th1 cells migrate back to the lungs in a chemokine-dependent manner 14-17 days after initial infection (4) and produce IFN-γ, which results in macrophage activation, cytokine production, the induction of microbicidal factors including iNOS (5), and bacterial control (image reproduced and text adapted from [21]).

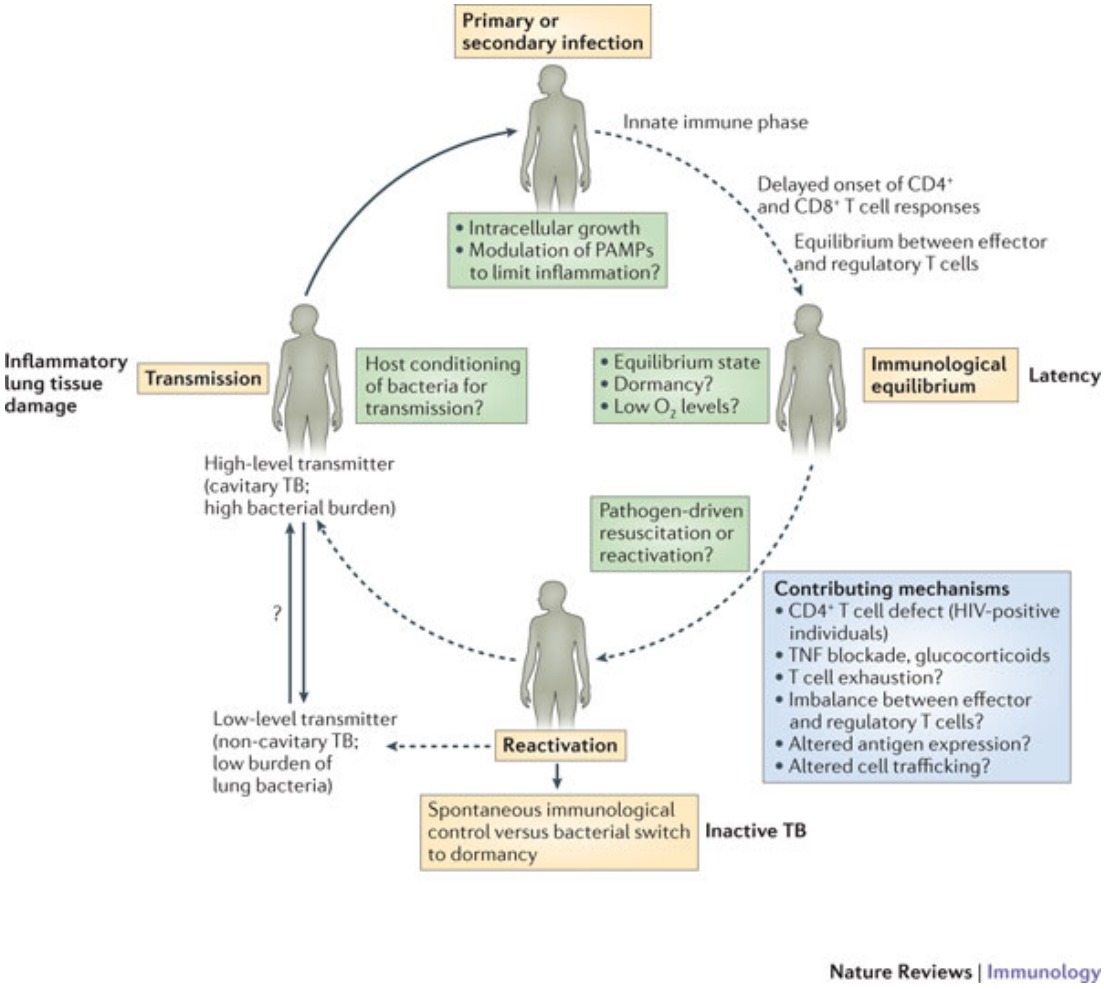


Figure 1.4 The immunological life cycle of TB. The life cycle is based on clinical, epidemiological and immunological studies in humans and includes examples of some of the immunological mechanisms and functions that characterise each stage (where known). Central panels show known or experimentally supported states of the bacteria at distinct stages of the immunological life cycle. Question marks indicate hypothetical mechanisms (image reproduced and text adapted from [20]; permission granted by Nature Publishing Group).

1.4 Clinical manifestations of TB

Active TB disease is clinically defined as being pulmonary or extrapulmonary. Pulmonary TB (involving the lung parenchyma, pleura and mediastinal lymph nodes) accounts for up to 80% of all cases in HIV-negative individuals and typically has an insidious progression over weeks or months. In severe immunosuppression, disease

may be rapidly progressive, occurring over several weeks, and is often accompanied with extensive dissemination. Untreated pulmonary TB has an associated mortality of 50%, with 25% of patients developing chronic disease and the remainder recovering spontaneously [22, 23]. Constitutional symptoms of pulmonary TB include fever, night sweats, weight loss and malaise but these are not assured [24]. An initial dry cough may progress to sputum production and occasionally haemoptysis. Dyspnoea may reflect extensive parenchymal disease, significant pleural effusion, endobronchial obstruction or pneumothorax. Pleural disease may cause significant chest pain [15, 24]. Physical findings on clinical examination are often few and are of limited value in diagnosing pulmonary TB. Classical radiographic abnormalities are suggestive of, rather than specific for, TB and may include pulmonary infiltrates, nodules, cavitation, mediastinal or hilar lymphadenopathy, pleural effusions and atelectasis [25-27]. TB has a predilection for the upper zones of the lungs, possibly due to the high ventilation to perfusion ratio [28, 29]. Extrapulmonary TB occurs in 15-20% of immunocompetent individuals but in more than 50% of HIV-positive patients [16]. Extrapulmonary disease may be due to primary or reactivated TB and includes lymphatic, genitourinary, bone and joint, central nervous system, abdominal and disseminated infection and site-specific investigations are needed for diagnosis [30]. In patients with HIV co-infection, pulmonary cavitation becomes progressively less common with declining immunity while the risk of developing extrapulmonary TB (typically involving lymph nodes and the pleura) and disseminated disease increases [16, 31]. The diagnosis of pulmonary TB in HIV-infected individuals is difficult due to the presence of atypical radiographic findings including non-cavitatory pulmonary infiltrates, and as a consequence of less pulmonary cavitation patients are more likely to have sputum smear-negative disease [16, 31-33].

1.5 The global burden of latent TB infection

In order to develop appropriate TB control strategies, it is necessary to have an accurate estimate of the prevalence of *M. tb* infection. Throughout the TB literature it is often stated that one-third of the global population is latently infected with *M. tb*, but there is seldom consideration of how this figure has been derived and the problems associated with calculating it [4]. As described later, latent infection cannot be diagnosed by direct isolation of the bacillus, but rather by inference from immune sensitisation to mycobacterial antigens. As such, the tuberculin skin test (TST) is the most widely used diagnostic test for LTBI worldwide [34]. However, the global prevalence of TB is not estimated from population-based TST surveys but is calculated from the annual rate of infection (ARI), which can be determined either directly or indirectly. The former approach relies on small TST surveys while the latter is calculated from the TB incidence and a pre-determined coefficient [35]. The incidence of TB disease is estimated from case notifications, disease prevalence or mortality data [4].

In 1999 the WHO attempted to estimate the prevalence of *M. tb* infection for all countries. Contemporaneous TST surveys of sufficient quality were available for only 24 countries, highlighting the several limitations of this method. While logistically and economically viable, TST surveys are confounded by interpreting results in populations with varying exposures to environmental mycobacteria and BCG vaccination [36]. A novel skin test using *M. tb*-specific recombinant antigens is under development and may improve specificity and sensitivity [37, 38]. The WHO therefore relied on the ARI, which was calculated indirectly using the incidence of smear positive TB cases and a coefficient of 50, and estimated that the global burden of *M. tb* infection was 32% [39]. The coefficient was derived from 'Styblo's rule' which states that "smear positive

pulmonary TB incidence of 50/100,000 per year equates to an ARI of 1%" [40]. This relies on several crucial assumptions including that each smear positive case of TB is infectious for two years and results in 10 new infections per year. The use Styblo's rule may overestimate the true global burden of LTBI as the duration of infectiousness of active cases may have declined due to improved diagnostics and earlier treatment [41]. A recent, albeit geographically restricted, study using 20 years of data estimated that 2.6-5.8 infections resulted from each smear positive case each year [42]. Furthermore, other factors such as mycobacterial evolution, population density, HIV infection and MDR-TB may all effect transmission and therefore Styblo's rule [41, 43]. The WHO acknowledged that their estimate of the prevalence of *M. tb* infection was limited by the lack of high quality data and by the models used. Concerns over the dynamics of IFN-γ release assays (IGRA) responses (discussed later), together with increased costs and the difficulties of large-scale deployment of these diagnostics in the field, have limited their use in population estimates of *M. tb* infection. Improvements in the specificity and utility of diagnostics for *M. tb* infection and better modelling platforms, used either alone or in conjunction with traditional TST surveys, may result in a more accurate estimation of latent TB infection (LTBI), but until then the 'one third' statistic is the best we have.

1.5.1 Diagnosing LTBI

Currently the TST and IGRAs are the mainstays of LTBI diagnostics. Robert Koch initially proposed the use of tuberculin, a heat-killed culture filtrate from *M. tb*, as a treatment for TB in 1890 [44]. This was ultimately unsuccessful but the potential use of tuberculin in a diagnostic test for latency was considered after observations that it produced a visible delayed hypersensitivity reaction at the site of subcutaneous injection in asymptomatic individuals, thus demonstrating occult infection. Refinement

over the ensuing decades resulted in the TST in which 2-10 units of purified protein derivative (PPD) of tuberculin are administered by intradermal injection and the resulting induration is measured after 48-72 hours [34]. The diameter of the induration is measured in millimeters as a continuous variable and the threshold for positivity may be altered to reflect population factors (such as prior BCG vaccination) and therefore improve sensitivity and specificity [34].

Until recently the century-old TST has been the cornerstone of LTBI diagnostics and has improved our understanding of the epidemiology of TB. However, it is not a perfect test and is hindered by several limitations. While a positive test is considered a reflection of *M. tb* infection, there are no human studies demonstrating an association between a pre-morbid positive TST and the identification of viable bacilli at post-mortem [4]. Animal models using guinea pigs exposed to air from patients with pulmonary TB disease and therefore considered a natural infection model of airborne transmission, have shown some association between increasing TST induration and the proportion of animals with evidence of infection at autopsy [45-47]. However, not all positive TST results correlated with demonstrable infection. Furthermore, a clear relationship between a positive or negative TST result and the presence or absence of *M. tb* infection may suggest that successful treatment of latent infection would cause reversion of a positive TST [4]. However, a series of large longitudinal studies of isoniazid chemoprophylaxis among household contacts showed that effective therapy was not associated with TST reversion and, in fact, that the reduction in 10-year TB incidence was greater among those remaining TST positive than those reverting to a negative result [48]. In addition, while cheap and easy to perform, the TST is hampered by limited sensitivity (which is reduced in immunocompromised patients) and specificity (showing cross-reactivity with prior BCG vaccination and exposure to non-tuberculous mycobacteria, NTM) and is not suitable for use in repeat testing [49].

The discovery of a genomic region of difference (RD1), which is absent in BCG and many NTMs but present in *M. tb*, resulted in the identification of the RD1-encoded immunodominant antigens early secretory antigenic target-6 (ESAT-6) and culture filtrate protein-10 (CFP-10). This was fundamental in the development of *in vitro* T cell-based immunodiagnostics in which IFN-γ production from T cells is measured in response to these *M. tb*-specific antigens in IGRAs. The two IGRAs currently available for clinical diagnostics include an ELISA-based platform (the QuantiFERON-TB Gold, Qiagen) and an ELISpot-based test (the T-SPOT.TB, Oxford Immunotec). IGRAs have some advantages over the TST including requiring only one patient visit, higher sensitivity compared with the TST, lack of confounding by prior BCG vaccination and their potential for intra-patient repeat use [50-55]. Nonetheless, issues remain for their use in diagnosing LTBI, primarily relating to subject variability, reproducibility, and discordance between assays [50, 56-62]. Unfortunately, neither TST nor IGRA can distinguish between active disease and latent infection. Experimental models have shown an association between *M. tb* inoculum size and the extent of immunopathology and survival [63-65]. Clinically, the size of TST induration and the magnitude of IGRA responses in contacts correlate with duration of exposure to, and the infectiousness of, an index patient [66-68]. There is some evidence that TST size and quantitative IGRA responses may be able to predict the risk of progression to active TB disease [69-74]. However, other studies have been unable to show such an association and currently neither test can be used to stratify risk of TB reactivation [75, 76]. While concordance between IGRAs and TST have similar, high negative predictive values (i.e. a good measure of TB exposure), positive predictive values are low and therefore provide a poor prediction of progression to active disease [70, 73]. A consequence of these shortcomings is that the number needed to treat (NNT) to prevent a single case of TB with chemoprophylaxis among individuals diagnosed with LTBI by these tests is high,

with a large systematic review reporting a NNT of 36-179 [77]. It has been suggested that dynamic responses of TST and IGRAs determined by longitudinal measurements may have greater utility in assessing risk in LTBI. Recent TST conversion, together with TST/IGRA discordance, may indicate lower risk of progression [78]. Conversely, IGRA conversions and reversions may reflect the underlying transitions that occur during *M. tb* infection [79]. Rapid reversion of a positive IGRA after exposure may signal elimination of infection, persistently negative and persistently positive individuals over long duration may have a low likelihood of disease progression, while 'unstable convertors' may be at greater risk [79]. All of these issues highlight the complexity of LTBI diagnostics, the need for longitudinal assessment of a dynamic process, and the need for tests with much improved positive predictive power to enable stratification of disease risk.

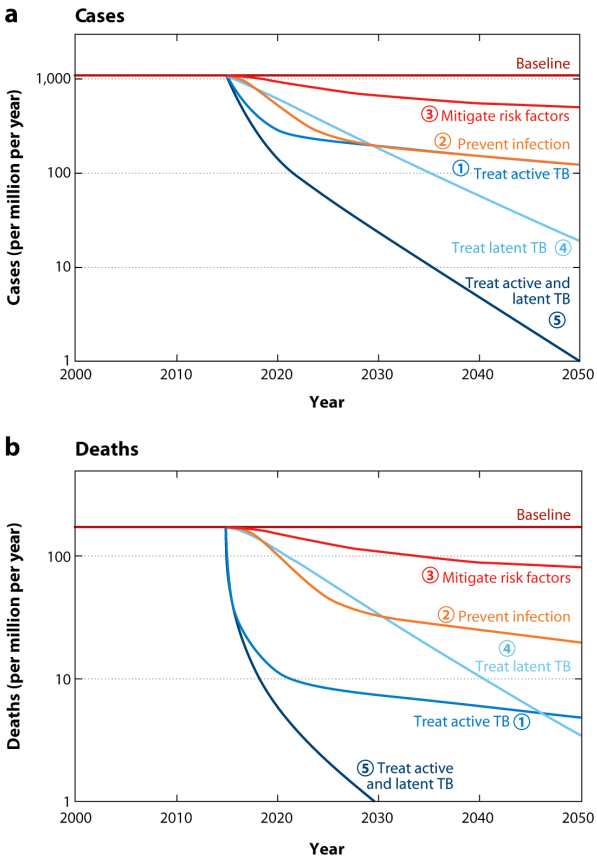
1.5.2 The need to tackle LTBI

In the 1990s the WHO implemented the DOTS (directly observed therapy, short-course) strategy and set a target to identify 70% and cure 85% of TB cases (which was achieved in many countries by 2005) [80]. Subsequently, in 2000 the Stop TB Partnership aimed for a 50% reduction in the global mortality and prevalence of TB disease by 2015, as guided by Millennium Development Goal 6. In 2010, the WHO went further and set a target to eliminate TB as a global public health problem by 2050 (less than 1 case per million per year) [81]. In 2014 there were an estimated 9.6 million new cases and 1.5 million deaths attributed to TB, representing reductions of 40% and 47% in global TB prevalence and associated mortality compared with figures in 1990 (respectively) [5]. While this progress is important, it is insufficient to reach the targets set by the WHO. It represents a reduction in the global TB incidence of approximately 2% per year over recent years to an estimated 1330 cases per million population.

However, to reduce the burden of TB to less than 1 case per million per year by 2050, a 1,000-fold reduction in global TB incidence over the next 34 years is required, corresponding to an unprecedented 20% reduction per year [82]. Substantial improvement of current conventional control strategies may still fail to eliminate TB as planned. Mathematical modeling indicates that even with very high case detection rates, which are rarely achieved in practice, the incidence of TB could be reduced by 100-fold at best [83]. Of significant concern is that these predictions have been based on models that exclude sub-Saharan Africa, accounting for over 30% of the global TB burden, due to the complications of high TB incidence rates attributable to HIV co-infection and the impact of drug resistance on the efficacy of treatment [83].

Until recently, the main focus of TB control and elimination programmes which are underpinned by the DOTS strategy has been the prompt diagnosis and effective treatment of individuals with active disease to interrupt transmission. This strategy is important and has undoubtedly led to substantial declines in TB prevalence and mortality, however the shortcomings of this passive case finding approach have been highlighted recently [84]. A significant number of patients and household contacts have detectable bacilli in sputum but remain asymptomatic and therefore do not seek medical care [85, 86]. In a large population study in South Africa only 67% of HIV-negative and 33% of HIV-positive cases were identified by passive case finding [87]. In addition, even among populations with high rates of treatment compliance in TB endemic settings, little impact on TB incidence has been reported [88]. It has been suggested that an active case finding approach should be adopted to improve detection rates and reduce transmission [89]. However, modeling indicates that even if transmission were interrupted completely and instantly, reactivation of established, and relapse of persisting, *M. tb* infection would still cause an estimated >100 cases per million population in 2050 [82]. Analysis shows that TB incidence rates are

significantly influenced by the proportion of infections that progress rapidly to active TB and the rate of reactivation of latent *M. tb* infection [83]. Combining interventions which target different parts of the clinical spectrum of TB are synergistic, more effective and have greater impact than if deployed independently. Therefore, there is an increasing realisation that the management of latently infected individuals, which represents a huge reservoir of potential new disease and thus infectiousness, will also be required for the elimination of TB. Modeling suggests that the effective treatment of latent *M. tb* infection by either preventative drug therapy or a post-exposure vaccine (or both) would reduce TB disease incidence significantly [90]. Using a baseline incidence of 1,100 new cases of TB per million population per year, it has been estimated that the treatment of 8% of latently infected individuals each year (resulting in cure and permanent protection) would reduce TB incidence to 90 per million by 2050 (with no other intervention), while treating 14% of individuals per year would result in a decrease to 20 per million by 2050. Combining such interventions simultaneously with the effective treatment of active disease would achieve elimination by reducing overall incidence to 1 per million by 2050 (Figure 1.5) [82]. However, this is unlikely to be achieved with currently available diagnostics and treatments given the estimated burden of LTBI and the need for three to nine months of preventive chemotherapy. Together with developing shorter treatment regimes, there is a need to find biomarkers to accurately and efficiently identify individuals at risk of progressing to active TB disease, thus facilitating targeted preventative therapy. To achieve this, our fundamental understanding of the immunological mechanisms of latent *M. tb* infection must be improved [91-98].



Dye C, et al. 2013.
Annu. Rev. Public Health. 34:271–86

Figure 1.5 Strategies for eliminating TB (a) and approaching the elimination phase (b). Based on a model of a high-incidence country (65% case detection, 70% cure) and an incidence of 1,100 cases and 200 deaths/million/year. Improving case detection rates and completion of treatment of active disease could reduce incidence by 10-fold. Better treatments, including vaccination, could move the epidemic to the elimination phase. However, further reductions in incidence and mortality can be achieved only by treating both latent infection and active TB, interventions that would work synergistically together (image reproduced and text adapted from [82]).

1.5.3 Current concepts of LTBI

The term 'latent tuberculosis' was introduced by Clemens von Pirquet, who developed the TST in 1907, to describe children who demonstrated a positive response to tuberculin but did not manifest any symptoms of active TB disease [99, 100]. Currently,

LTBI refers to a state in which bacilli of *M. tb* persist within a host, in the absence of clinical signs and symptoms of disease (such as fever, chills, night sweats, weight loss, cough, hemoptysis, radiographic changes or microbiological evidence), but maintain viability and the potential to replicate and subsequently cause symptomatic disease. Present diagnostics cannot directly identify bacilli in latently infected individuals and, therefore, LTBI is inferred solely through evidence of immune sensitisation to *M. tb* antigens. The relationship between the immune response and the ongoing presence of live bacilli is unclear and is discussed later [101].

The lifetime age-weighted risk of progressing to TB disease following infection is estimated at 12%, with most cases occurring in the first years after infection [17, 102]. Over the following 5-10 years there is a successive decline in incidence after which time rates are similar to those in uninfected individuals [48]. It is often stated that reactivation of latent *M. tb* infection can occur decades after primary infection in humans. This is difficult to accurately assess due to the limited duration of follow-up in most observational studies and the problem of distinguishing reactivation from subsequent reinfection, but available evidence fails to support this assertion [4]. Studies in low-incidence settings have shown that more than 95% of reactivations occur within 10 years of predicted infection [103]. In addition, among migrants moving from high-to-low incidence countries the development of TB is uncommon (0.8%) more than 15 years after arrival in the context of a low risk of re-exposure [104]. Modeling of TB incidence following migration from high burden settings has provided further evidence that what was previously considered as reactivation of latent infection may rather represent re-exposure and reinfection with *M. tb* [105].

Therefore, it is likely that reactivated TB after prolonged latency is less common than previously thought and disease from reinfection is the leading mechanism in the

development of active disease in high prevalence settings. This raises the question of the extent of immunological protection afforded by latent *M. tb* infection. While the potential for reinfection suggests that prior latency or active disease is not completely protective against exogenous reinfection, studies report risk reduction in those with latent infection ranging from 16-81% [102, 106-108]. The mechanism of protection in humans is unknown, but animal studies have shown that control of reinfection is associated with tissue-resident mononuclear cells [109]. Interestingly, a significant proportion (up to 25%) of secondary cases among household contacts produce a different strain of *M. tb* to that isolated from the index patient [110]. Therefore, among latently infected individuals in whom protection from re-exposure fails, evidence suggests that reactivation of a pre-existing latent focus may occur [78]. A parallel with this has been made with the observation that patients successfully treated for active pulmonary TB are at increased risk of re-infection, although this may be largely due to host susceptibility and environmental factors causing re-exposure [111, 112].

However, in some individuals prolonged latency will occur and suggests that latent infection is a dynamic process between the host immune system and bacillary replication [113]. It is likely that the course of *M. tb* infection cycles between episodes of subclinical reactivation and effective host control, which precedes eventual disease presentation when such control finally fails. Several large chest radiograph (CXR) surveys have shown that a significant proportion of asymptomatic patients who went on to develop TB disease had apical fibrotic scarring, considered inactive infection, on CXRs predating their presentation [114-116]. There are several well-recognised risk factors for developing TB disease, among which immunocompromise due to HIV infection is the most important. The degree of this risk is probably dependent upon the extent of HIV-induced immunosuppression and decreases with initiation of appropriate antiretroviral therapy [117-121]. Following HIV infection, the risk of active TB in

individuals with latent *M. tb* infection increases to an estimated 5-15% per year, which is a considerable increase over those without HIV infection [122-124]. Other factors significantly increasing the risk of TB reactivation include immunosuppressive therapies (including TNF-α inhibitors and systemic glucocorticoid therapy) and solid organ transplantation [50, 125-130]. A moderate increase in risk is associated with the presence of chronic systemic conditions such as diabetes mellitus, renal disease, coeliac disease, gastric surgery, malignancy (particularly haematological malignancies and solid head and neck tumours) and silicosis [131-136]. Nutritional status is another important biological factor and malnourished individuals (body mass index <18.5) have an almost threefold increased risk for TB [137, 138].

1.5.4 Treatment regimens and outcomes

The aim of prophylactic drug therapy for LTBI is to prevent progression to active disease. There are currently a number of regimens available to achieve this, which have been recently reviewed [139, 140]. In contrast to active disease, monotherapy for LTBI is often used and is justified on the basis that drug resistant mutations are unlikely to develop due to the lower bacillary burden in latency. Early randomized trials in the 1950-60s demonstrated that isoniazid (INH) monotherapy taken for at least 6 months could reduce incidence of disease by 25-92%, with outcome variability likely due to treatment compliance [48]. Re-analysis of these early data suggested that the effectiveness of INH increased with longer durations of therapy, and therefore 9 months of INH, with an estimated efficacy of 90%, has been the primary regimen in many parts of the world for several years [50, 141]. Interestingly, a recent meta-analysis of 11 trials of TB preventative therapy in over 73,000 HIV-negative individuals showed that there was little difference between the relative risks of progression to active TB whether a 6 or 12 month regimen is used, compared with placebo (RR 0.44 vs

0.38, respectively) [77]. Whilst very cost effective, the main problem with INH monotherapy is the long duration required which is often difficult among individuals who are asymptomatic with a low risk of developing active disease [82]. This regimen has been associated with high rates of non-compliance in several settings and completion of less than 50% has been reported [142-145]. Motivating patients to complete treatment is possible and requires good education early in therapy, close follow-up and on-going support [140]. Interestingly, a recent study among South African gold miners with a high HIV prevalence and annual risk of *M. tb* disease showed that the durability of protection following 9 months of INH monotherapy was lost within 6-12 months of completion [146]. Modeling suggested that both reinfection and reactivation of persistent latent infection contributed to the rapid return to pre-treatment TB disease incidence.

For patients with HIV living in settings with high TB and HIV prevalence and transmission, the WHO recommends continuous INH for at least 36 months, which has been shown to reduce the risk of active disease by 38% compared with a regimen for 6 months [147]. Such prolonged INH therapy is considered a proxy for lifelong treatment because the protective effect wanes over time after completing treatment [148, 149]. In settings with low to moderate TB incidence, INH therapy for 6 months is thought to be durable and sufficient to prevent active TB in HIV-infected individuals receiving ART, although recent modeling indicates that 12 months of treatment may provide additional long-term benefit [150, 151].

Shorter preventative drug regimens improve uptake, patient compliance and therefore completion but must have sterilising and bactericidal components to prevent reactivation [152]. Whilst INH is bactericidal and acts against replicating bacilli, rifampicin and pyrazinamide have a sterilising activity against persisting, non-

replicating bacilli, and therefore have a role in reducing duration of therapy [153]. In addition, a recent report using a non-human primate (NHP) model suggested that mutation rates in latent *M. tb* infection and active disease are similar and that development of resistance due to INH monotherapy is possible [154].

In the UK, a daily schedule of rifampicin and INH (RMP-INH) for 3 months for HIV-negative individuals with LTBI is typically used. A recent network meta-analysis using a mixed treatment comparison methodology, which indirectly infers the relative efficacy and adverse events associated with LTBI treatment regimens, has been completed [155]. It showed that 3-4 months of RMP-INH was as highly efficacious and associated with less hepatotoxicity when compared to prolonged INH monotherapy (although not statistically significant). Furthermore, while reactivation of TB is less likely to occur with rifamycin-containing preventive therapy in the context of HIV infection, drug-drug interactions may occur [146, 156, 157].

Most recently, a directly-observed once-weekly regimen of INH and rifapentine for 3 months in HIV uninfected patients had an efficacy similar to 9 months of self-administered INH alone, but with higher completion rates and less hepatotoxicity [158]. Similar results have been seen in individuals with HIV infection, and while more longitudinal data of efficacy are required, this new regimen is likely to be very cost effective and may represent a significant advance in LTBI chemoprophylaxis [149, 159].

One difficult but increasingly common scenario is the treatment of contacts of individuals with drug resistant pulmonary disease. In the case of INH resistance, 4 months of RMP has been suggested [50]. When the index case has MDR-TB, therapy should be based on the results of drug-susceptibility testing of the original isolate,

although there are few data on the optimal regimen and close follow-up for at least 2 years is required [139, 160, 161].

There are currently several approaches to improving therapy for LTBI. Novel TB drugs such as bedaqualine (TMC207), sutezolid, delaminid and pretomanid (PA-824) have shown potent sterilising activities against mycobacteria and may have a role in LTBI treatment [162-165]. In addition to drug development, vaccine-mediated immunomodulation has been proposed as a potential strategy [101]. Post-exposure vaccination targeted at adolescents and young adults following infection with *M. tb* could prevent post-primary disease and/or reactivation of latent infection by inducing enhanced immunity or boosting pre-existing responses to promote containment or clearance of bacilli [101]. Such vaccines could contain novel antigens expressed by persisting bacilli to generate a sterilising host immune response [166, 167]. Alternatively, therapeutic vaccination may be a valuable adjunct to drug therapy, enhancing efficacy and shortening duration [168].

However, significant hurdles for both TB drug and vaccine development include shortcomings of animal models used in preclinical trials and the costly and lengthy nature of clinical efficacy trials [169]. It will be crucial to improve our understanding of key immune mechanisms and identify robust immunological correlates of protection in order to develop well-characterised models of LTBI for the evaluation of novel drugs and vaccines.

1.6 A proposed 'spectrum of *M. tb* infection'

Considering tuberculosis as either active disease or latent infection has undoubtedly been useful for the prioritisation of clinical management. However, this description of distinct, homogeneous entities is unlikely to reflect the dynamic interaction between the host and pathogen over time, and may limit approaches to drug development, identifying vaccine biomarkers, and determining the risk of reactivation of an individual [100]. The traditional inference that latency represents a dormant, inactive infection is starkly contrasted by the observation that isoniazid, which is active against replicating bacilli, is an effective treatment for LTBI [162]. There is increasing recognition that there is marked heterogeneity within the classifications of active TB disease and latent *M. tb* infection [100]. While a degree of bacterial containment appears to exist in LTBI, latent infection encompasses a diverse range of individuals, from those who have completely cleared the infection to those with subclinical disease who are incubating actively replicating bacilli in the absence of clinical symptoms [91, 93, 100, 170]. Similarly, diverse pathological presentations characterise active TB, ranging from small granulomas and caseous hypoxic lesions containing variable numbers of organisms, to liquefied cavities with a significant burden of replicating bacilli and extrapulmonary or miliary disease [91, 170]. It has been proposed that this clinical diversity reflects the relative numbers, type, and anatomical distribution of lesions [91].

Therefore, several investigators have recently challenged the latent versus active paradigm on the basis that such a binary distribution is an oversimplification and that these conventional designations actually correspond to partially overlapping regions of biological heterogeneity on a spectrum of *M. tb* infection [91, 93, 170]. This spectrum

reflects the changing balance of interaction between the host and pathogen over time (Figure 1.6).

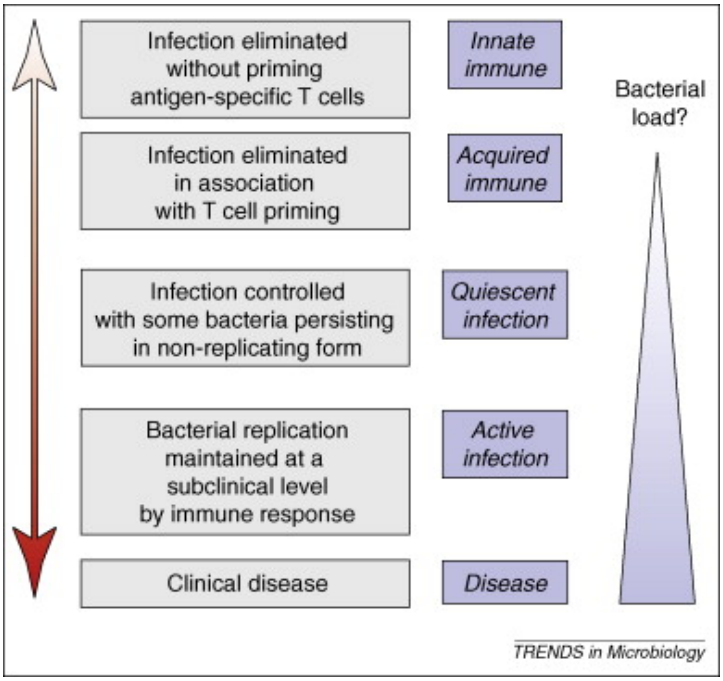


Figure 1.6 Spectrum of responses to *M. tb* infection. Rather than considering infection with *M. tb* as a binary outcome of either active disease or latent infection, it has been proposed that a model of a spectrum of responses is a better representation of the biology of infection (image reproduced and text adapted from [93]; permission granted by Elsevier).

It has been proposed that this continuous spectrum of responses to *M. tb* infection includes innate immunity, acquired (sterilising) immunity, quiescent infection, active (subclinical) infection, and active (fulminant) disease [93]. Innate immunity is proposed for infection that is eliminated in the absence of an acquired response, and acquired immunity for infection that is eliminated by a combination of innate and acquired responses. Quiescent infection has been suggested to represent infection that is controlled by the immune response but in which viable bacilli persist in a non-replicating form. Active infection indicates the subclinical presence of replicating bacilli

controlled by the host immune response, whilst active disease would occur due to bacilli that replicate despite the ongoing immune response causing the development of symptoms and signs of TB [93].

It has been suggested that an important consequence of this model is that treatment of LTBI would be most effective if targeted towards individuals occupying a part of the spectrum that corresponds to the highest risk of progression to active disease [91]. Preventative drug treatment of this group would reduce the NNT considerably and circumvent the economic and logistical issues of treating the global population with evidence of *M. tb* infection. If this were realised, the targets for TB control would then become attainable. However, as described, current diagnostic tests lack the resolution required to determine where an individual with *M. tb* infection exists on the spectrum [91, 100]. A second suggested consequence of this model is its use in designing rational drug development programmes to identify effective agents that target subpopulations of bacilli on the basis of physiological requirements for persistence in different types of lesion [91]. Such drugs would have the potential not only for the treatment of latent infection but also to improve that of active disease [91].

Investigators have attempted to integrate this proposed spectrum of tuberculosis with the known natural history of infection [4]. It has been suggested that shortly after initial infection and immune sensitisation, three outcomes are possible and are dependent on several predisposing and/or precipitating factors [4]. One group, perhaps adults with advanced immunosuppression or infants, may develop primary progressive disease due to predisposing factors including age, HIV infection, malnutrition, diabetes, and pro- or anti-inflammatory imbalance. Another group may control the initial infection rapidly and effectively, possibly sterilising the bacilli, resulting in a very low risk of subsequently developing active disease. The final group

represents high-risk individuals who experience periods of progression followed either by control or the development of active disease. Factors predisposing to these different outcomes include HIV infection, anti-TNF therapy, malnutrition, vitamin D deficiency and viral respiratory infections [171-176]. Preventative drug therapy would likely be most effective in this group [4].

There is increasing evidence supporting the notion of a spectrum of *M. tb* infection, ranging from clinical observations, histological and imaging studies, appreciation of bacterial heterogeneity and the nature of the host immune response to TB.

1.6.1 Epidemiological and clinical observations

It is well recognised that among healthy individuals repeatedly exposed to *M. tb*, such as health care workers and household contacts, a proportion never convert to TST positivity (up to 50% of subjects in some household studies) [177-180]. These 'elite-controllers' may eliminate infection in the absence of an adaptive immune response by solely using innate mechanisms such as macrophages, neutrophils or natural killer (NK) cells [93, 181-183]. Such anti-mycobacterial resistance may be hereditable. For example, *TST1* is a locus on chromosomal region 11p14-15 overlapping with the *TNF1* locus, which controls TNF-α production in response to *M. tb* and has been linked with persistently negative TSTs despite close and prolonged exposure to active TB [184-187]. Alternatively, a negative TST in these cases may actually be due to poor test sensitivity rather than protection against infection, or possibly an inability of the individual to develop a delayed-type hypersensitivity reaction following infection [78]. Finally, the establishment of infection in humans is more likely to result from multiple low dose exposures to *M. tb* and therefore such exposures might not always result in the development of an acquired immune response [188].

As described, the TST and IGRAs are currently the only tests available to diagnose latent infection and are thought to reflect the development of an adaptive immune response to *M. tb*. However, discordance between the tests occurs. IGRA conversion may be delayed compared with TST, perhaps requiring a specific 'window' following exposure for positivity to develop [189-192]. In contrast, TST negativity may persist despite the presence of infection and IGRA conversion [193-195]. Furthermore, serial testing with IGRAs in both low and high TB prevalence settings has shown them to be highly dynamic with significant conversion and reversion rates when compared with TST (e.g. 4-7% IGRA vs 0-0.9% TST conversions) [59, 192, 196-199]. IGRA and TST discordance and episodes of conversion and reversion may not only result from differences in the mechanism of each assay, but also the dynamic host response to *M. tb*, reflecting the control or elimination of infection by adaptive mechanisms. While such variance may cause difficulties in clinical interpretation, they may provide the opportunity to further our understanding of the spectrum of *M. tb* infection [50, 59, 61, 79, 194, 197, 200, 201]. It has been suggested that serial IGRA testing may reveal several immune phenotypes that have predictive value, such as the persistently negative or positive and the unstable and stable IGRA conversions, possibly reflecting lesser or greater risk of disease progression, respectively [79].

1.6.2 Heterogeneity of the pulmonary granuloma

Evidence for a spectrum of *M. tb* infection has also been sought by understanding the basic pathology of *M. tb* infection in humans and animal models. The pulmonary granuloma is the archetypical lesion induced by *M. tb* infection and may be defined as an organised structural collection of diverse immune cells formed in response to pulmonary inflammation due to the interaction of the host adaptive and innate immune system with the antigenic stimuli of mycobacteria [100]. The macrophage is the

primary reservoir of bacilli and the predominant cell type of the granuloma, initiating its development, forming its core and recruiting multiple cell types [202]. These stimulated macrophages display several phenotypes, including mature macrophages, differentiated or epithelioid macrophages, foamy macrophages, and multinucleated giant cells formed from multiple fused macrophages. Macrophages also have anti-mycobacterial effector functions, produce pro- and anti-inflammatory cytokines, and secrete chemokines and proteins associated with tissue modeling [202]. Other cellular constituents surrounding the macrophage core include uninfected macrophages, dendritic cells, NK cells and neutrophils, beyond which is a layer of CD4+ and CD8+ T cells and B cells, and finally a cuff of epithelial cells and fibroblasts [203]. The function of the granuloma is to contain infection, controlling bacillary growth and thus limiting dissemination and pathology. However, it also forms an environmental niche where mycobacteria can persist and replicate. During the early stages of infection granulomas undergo peripheral re-modeling due to continuous lymphocyte recruitment [204]. An excessive pro-inflammatory response causing necrosis of surrounding tissue, or suboptimal granuloma formation due to immunosuppression, will lead to mycobacterial replication and spread, representing failure of initial immunological control [162]. If, however, successful control persists, granulomas undergo fibrosis and calcification [203].

There are several types of granuloma that have been identified in active TB and LTBI in humans and animals and even within the same individual (Figure 1.7) [205]. The caseous granuloma is the typical lesion found in TB and may be seen in both active TB disease and LTBI. Its structure is described above and its name is derived from a caseous core which is necrotic and hypoxic, consisting of dead macrophages and other cells. Caseous granulomas provide bacilli with different microenvironments and mycobacteria may be isolated from several sites. Non-necrotising granulomas are

usually seen in active disease and are composed primarily of macrophages containing bacilli and some lymphocytes. Fibrotic granulomas are predominantly seen in LTBI but may also occur in active disease and consist almost completely of fibroblasts with few macrophages. The microenvironment of fibrotic lesions and the location of bacilli remain unclear.

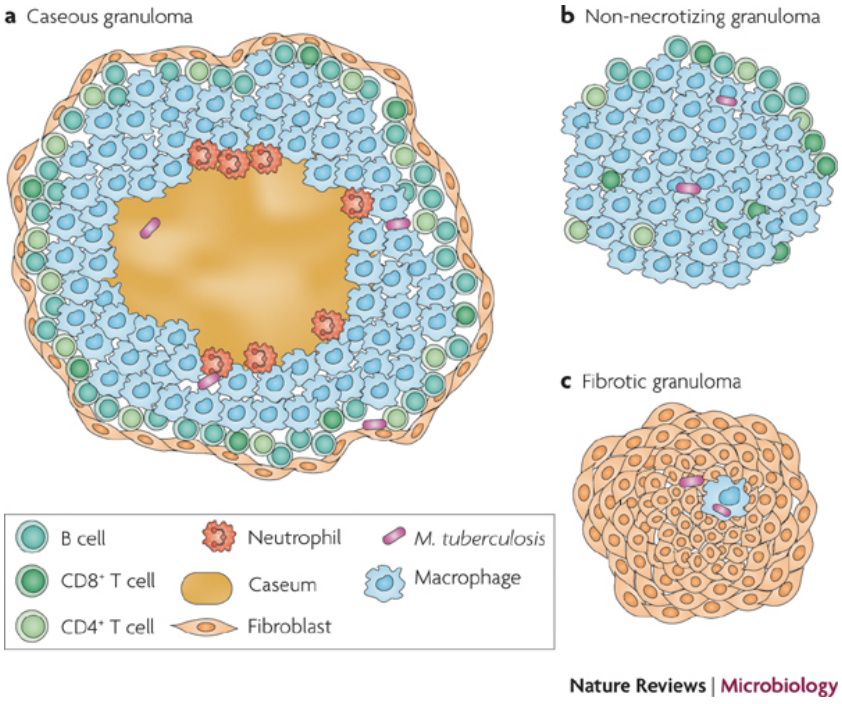


Figure 1.7 Heterogeneity of TB granulomas. In humans and non-human primates, several granuloma types have been described, even within the same individual. Classic tuberculous granulomas (a) are found in both active disease and latent infection and are composed of epithelial macrophages, neutrophils, a cuff of lymphocytes and occasionally a rim of peripheral fibrosis. They are caseous, with a necrotic, hypoxic, centre of dead macrophages and other cells, and forming different microenvironments. Non-necrotising granulomas (b) are typically seen in active disease and are formed mostly of macrophages. Latent TB is characterised by fibrotic lesions (c) but these may also occur in active disease. These lesions are almost entirely fibroblastic and possess few macrophages. Mycobacteria can be isolated from all of these granuloma types but the exact location and conditions within different microenvironments is largely unknown (image reproduced and text adapted from [91]; permission granted by Nature Publishing Group).

Evidence for granuloma heterogeneity has been gathered from a variety of sources. Post-mortem studies of tissues from latently infected humans and NHPs have shown remarkable diversity of granuloma structure both between and even within individuals [91, 205, 206]. In view of the difficulty of obtaining tissue samples for analysis, imaging studies in humans and NHP animal models have proven particularly useful, especially techniques such as high resolution computed tomography (CT) and positron emission tomography (PET). CT imaging provides structural data on the lung and lymph nodes together with spatial information about granulomas, while PET uses probes to identify areas based on cellular function or phenotype in tissues under investigation, such as ^{18}F-fluorodeoxyglucose (FDG) which labels metabolically active cells [91]. Combining ^{18}F-FDG PET/CT imaging provides a detailed structural and functional picture of lung pathology [207]. These techniques are routinely used in the diagnosis, staging, therapeutic monitoring, and follow-up of various malignant tumours and indeed, their use in TB has been mainly been to differentiate LTBI from malignancy [208-210].

CT imaging of patients with LTBI often shows a range of abnormalities, some of which are consistent with those identified in active disease [210]. Pulmonary nodules of varying size are typically seen in LTBI and these are difficult to distinguish from malignant lesions. The use of ^{18}F-FDG PET/CT to improve diagnostic accuracy has shown huge variation in the metabolic activity of lesions. Studies have reported that patients with LTBI and lesions showing increased ^{18}F-FDG uptake may be at higher risk of active TB disease, while another has shown that uptake is reduced in some patients following preventative therapy [211, 212]. These findings have been taken as support for the suggestion that LTBI is a broad spectrum of conditions with elements of latency and active disease overlapping.

Combining imaging with studies of resected and post-mortem tissues in NHP models

has validated findings in human studies and provided further understanding of the spectrum of LTBI by mapping lesions defined by imaging, cellular and molecular measures. Investigators established a low dose *M. tb* infection model in Cynomolgus macaque monkeys resulting in active disease and latent infection [206]. Further studies showed that the type and number of granulomas seen in infected macaques were very similar to those seen in human *M. tb* infection and disease [206, 213-215]. While particular patterns of lesions were often associated with distinct clinical classifications of either active or latent TB, a group of macaques with latent infection demonstrated sporadic growth of *M. tb* from gastric aspirates or bronchoalveolar lavage samples whilst remaining asymptomatic. These were termed 'percolators' and at necropsy, while most of these macaques were similar to latently infected subjects in gross pathology, bacterial burden, histopathology and immune responses, one animal had features more consistent with active disease [215]. It was suggested that this might represent subclinical infection and a probable increased risk of progression to TB disease. Subsequent studies using this NHP model which combined PET/CT imaging with clinical, microbiological and immunological measures showed that while most lung lesions arise from a single bacillus and reach similar maximum burdens, significant lesional heterogeneity occurs within individuals, providing further evidence for the hypothesised spectrum of *M. tb* infection [216].

1.6.3 Bacillary diversity

Mycobacterial differential gene expression, metabolic activity and the response of bacilli to treatment are all further key factors that highlight the variation between TB lesions. In terms of microbiology, TB lesion heterogeneity was shown following early human post-mortem studies that demonstrated varying rates of culture positivity obtained from different types of granuloma [217, 218]. However, the relationship

between the presence of viable *M. tb* and the immune responses that define latent infection is a fundamental question that remains unanswered [93]. Interestingly, the presence of viable bacilli from histologically normal tissues collected from individuals living in TB endemic areas but dying of other causes has also been reported [219]. It has been suggested that possible confounders include the contribution of recently inhaled *M. tb*, rather than established infection, to positive cultures, and the existence of 'dormant' bacilli that require enhanced culture conditions for detection that would result in negative cultures with routine techniques [93].

The corollary to the clinical and immunological concepts of active disease versus LTBI is the idea that replicating or dormant bacilli define the microbiology of these states. The proposal that the bacilli in latent infection are in a state of viable persistence but are non-replicating and 'dormant' is longstanding and may result from the varying microenvironments of different TB lesions. In view of the variety of TB granulomas, it is perhaps unsurprising that *M. tb* must adapt to different conditions to ensure survival and transcriptomic analysis of *M. tb* isolated from surgically resected lung tissue from patients with TB supports this concept [220-222]. Several *in vitro* models have studied, among others, the environmental stresses of hypoxia, low pH and restricted nutrients [223]. Hypoxia is one of the most studied bacillary stressors. An early response to hypoxia is the upregulation of genes under the control of the dormancy survival response regulator (dosR) [224, 225]. With prolonged hypoxia there is induction of the larger gene cluster designated the 'enduring hypoxic response' (EHR) [226]. There has been significant interest in further characterising these responses in an attempt to identify novel antigens for both diagnostics and anti-TB strategies [227]. Some of these hypoxia genes encode *M. tb* antigens that induce T cell IFN-γ responses [228-232]. However, there are conflicting reports about the specificity of responses to such antigens in different states of infection, and there may be considerable overlap across

the *M. tb* infection spectrum [228-231, 233, 234].

Finally, evidence for ongoing bacillary replication in LTBI can be seen from the efficacy of INH in reducing the risk of progression to active disease. INH is a cell wall inhibitor and is active against replicating organisms. Furthermore, while there is some induction under hypoxic conditions, the *M. tb* antigens ESAT-6 and CFP-10 used in IGRAs are mainly secreted during active bacterial replication [92]. Therefore, rather than this simplified view of bacillary 'dormancy' and 'replication' exclusively characterising LTBI and active TB (respectively), it is likely that there is significant bacillary heterogeneity and intra-population diversity at any one time between, and within, different lesions in an individual with TB [154].

1.6.4 Differential gene expression studies

One of earliest genome-wide transcriptional studies using whole blood samples from patients with active TB (before treatment), patients with LTBI and healthy controls, showed a distinct 393-transcript signature in patients with active disease [235]. This signature correlated with radiological extent of disease and reverted to that of healthy controls after treatment. However, the transcriptional profiles of 10-25% of patients with LTBI clustered with patients with active TB. While the authors acknowledged that these findings needed to be verified in a larger number of individuals with LTBI, they speculated that they could reflect the heterogeneity among individuals who are latently infected with *M. tb* and represent subclinical TB at early stages of disease. Interestingly, this subset of patients is very similar to the proportion of individuals with LTBI estimated to reactivate to active disease. Identifying whether those with such a transcriptomic signature progress to develop disease or whether their signature reverts to that of healthy controls and the majority of latently infected individuals would advance our understanding.

1.7 The needs and challenges of TB biomarker development

A biomarker is a unique indicator of a biological or pathological process or a response to intervention that can be objectively measured and evaluated [236]. A biosignature is a combination of independent biomarkers that markedly increases the power of an individual marker [236, 237]. As described, despite important recent advances, efforts to control TB are hampered by limitations on several fronts. Host biomarkers are urgently needed in four main areas: to improve diagnostics; to provide correlates of risk for, and protection against, active disease; for the development of more effective and shorter treatment regimens; and to provide validated correlates to reliably assess the efficacy of candidate TB vaccines.

The perfect biomarker or biosignature for TB would differentiate between patients with active disease and latent infection, return to baseline levels following successful treatment, reproducibly predict clinical outcomes, predict vaccine efficacy and provide endpoints for clinical trials [238]. However, based on our current understanding and knowledge of the biological and immunological responses that underlie discrete states of TB immunopathogenesis, it is unlikely that such a perfect biomarker exists. Therefore, there is now a well-recognised need for, and much research into, identifying TB biomarkers and associated biosignatures not only to improve TB control but also to further our understanding of the underlying mechanisms of *M. tb* infection, immunity, and pathogenesis.

A key area for TB biomarker identification includes diagnostics to reliably discriminate between individuals with active TB and those with LTBI or other pathologies (either infectious or non-infectious). Current diagnostic tests for TB disease rely primarily on the microbiological detection of *M. tb* in clinical samples, typified by identifying AFBs in sputum by microscopic examination. This is the gold standard for diagnosing

pulmonary TB, and while rapid and affordable, its sensitivity ranges from 34-80% and is dependent on both the bacterial load in the sample and experience of the microscopist [239, 240]. Poor sensitivity is of particular note in HIV co-infection [241]. Sputum culture using solid media is more sensitive than sputum smear testing but due to the slow replication time of *M. tb* (20-22 hours) it may take several weeks to obtain a positive result [240, 242, 243]. While automated liquid broth-based culture methods are objective, improve detection time and sensitivity and may provide useful information on the infectiousness of a patient, they require significant laboratory facilities that are seldom available in high incidence settings [244-246]. Nucleic acid amplification tests (NAATs) are molecular techniques that have driven substantial advances in TB diagnostics. The line probe assay directly detects *M. tb* from samples, together with common mutations associated with RMP and INH resistance, with a sensitivity of 58-80% [247, 248]. However this assay still requires PCR facilities. The recently developed GeneXpert MTB/RIF platform circumvents this issue by using a rapid, fully automated and enclosed system that can provide a positive diagnosis and basic drug resistance information within two hours of initiation [249, 250]. While sensitivity and specificity for *M. tb* detection is 99% and 98% (respectively), and for RMP drug resistance is 95% and 98% (respectively) in sputum smear-positive samples, this platform is much less sensitive when applied to sputum smear-negative and extra-pulmonary TB samples [242, 251]. Despite the above progress, approximately 42% of all new TB case notifications are treated on the basis of a presumptive diagnosis [5]. Furthermore, none of these tests can be used to detect latent *M. tb* infection and the many constraints of TST and IGRA testing have been discussed.

Robust and affordable biomarkers for TB disease have the potential to not only improve diagnostic capabilities but may help to delineate the spectrum of *M. tb* infection. This may lead to predictors of progression from primary infection to disease,

risk of reactivation of latent infection to active disease and to identify those who have, or are likely to, eliminate infection. Biomarkers predictive of disease risk would not only allow for targeted preventative therapy of individuals considered likely to develop active TB, but would also be useful in clinical trials. In this context such biomarkers could reduce both the numbers of participants and duration of studies by stratifying participants at most risk of progressing to disease for inclusion. They would also be valuable in evaluating therapeutic outcomes by predicting endpoints of disease before clinical diagnosis and therefore providing surrogate markers of intervention efficacy [237].

Biomarkers assessing response to treatment could be used at various points during therapy. Pre-treatment biomarkers could identify the requirements of individual patients at baseline, potentially reducing the duration of treatment and avoiding drug toxicity [238]. At present, high bacillary load, malnutrition and radiological evidence of extensive disease at diagnosis have some predictive ability for relapse following treatment but limitations and inconsistencies exist [252, 253]. The use of biomarkers during the early stages of treatment could indicate drug efficacy, accelerating the current earliest measure (the conversion of sputum smear or culture from positive at baseline to negative two months after starting therapy) and therefore reducing the likelihood of drug resistance developing due to prolonged suboptimal therapy [238]. On completion of treatment, biomarkers indicating definitive cure or risk of relapse could identify individuals requiring modifications to drug regimens or ongoing monitoring. This would have significant implications not only for the patient, but also for the success of control programmes and our epidemiological understanding of TB recurrence due to relapse or re-infection [238].

Finally, the lack of a correlate of protection is a significant obstacle in TB vaccine development and has recently been reviewed [169]. As underlying the limitations of diagnostic and prognostic tests, this persists in part due to our incomplete understanding of the natural infection and host immunity to *M. tb* and would be improved with biomarker discovery [169]. Parameters commonly measured to assess TB vaccine immunogenicity are those considered important for protection against infection or disease, noted from observational studies of mycobacterial susceptibility in humans and experimental animal models [169]. The importance of IFN-γ production by T cells is demonstrated by the significant increases in rates of *M. tb* in conditions of immune deficiency. These may be primary (e.g. the syndromes of Mendelian susceptibility to mycobacterial diseases, MSMD) or acquired (e.g. HIV infection) and reduce the number and/or function of CD4+ T cells or impair IFN-γ signaling [254-256]. As such, the primary immunological readout of TB vaccine studies is antigen-specific IFN-γ production by T cells, typically using ELISpot assays [238]. Other Th1 cytokines such as TNF-α and frequencies of polyfunctional CD4+ T cells are also thought to be important [238, 257]. However, there is a disparity between immunological responses stimulated by vaccination (correlates of immunogenicity) and those associated with protection from TB disease (correlates of protection) [258]. Several studies have shown that whilst significant increases in antigen-specific IFN-γ secretion and changes in polyfunctional T cell profiles may be induced by vaccination, these responses do not correlate with protection against *M. tb,* although in contrast some recent work shows an association between antigen-specific T cell responses and risk of disease [259-262]. Therefore, the immune responses considered essential for protection may well be necessary but they are not sufficient and as such these parameters do not have utility as correlates of risk or protection in TB vaccine efficacy trials [169]. Similar to their use in drug trials, biomarkers of vaccine efficacy would be valuable as surrogate endpoints

rather than relying on clinical endpoints, reducing the duration and costs of these very expensive studies [169]. Interestingly, the largest such trial of a candidate TB vaccine since the introduction of BCG in the early 1970s has recently shown that the frequency of activated HLA-DR+ CD4+ T cells is associated with increased TB disease risk, an observation subsequently confirmed among TB-infected adolescents [262]. However, in concert with appreciation of a need for such biomarkers comes recognition of several obstacles to realising this goal [263, 264].

1.7.1 Experimental approaches & current progress in TB biomarker discovery

In addition to multiparameter flow cytometry and cytokine profiling studies, transcriptomics, proteomics and metabolomics have been recently used for TB biomarker discovery. These 'omics' are high throughput technologies that profile host responses to *M. tb* infection and have been extensively reviewed [238, 242, 265]. 'Omic' technologies offer an unbiased, hypothesis-generating approach from which findings may be subsequently investigated by more targeted experiments [169]. In view of our incomplete understanding of the basis of host immunity to *M. tb* and that immune responses are heterogeneous and controlled by several levels of regulation, this may be of particular benefit. While targeted approaches assessing specific biomarkers such as cytokine production or the characterisation of immune cell phenotypes have advanced our knowledge, they are insufficient for use as immune correlates to predict risk.

There has been a multitude of studies using these technologies with widely varying numbers of participants and differing demographics, case definitions, sites and states of disease (e.g. active TB disease, LTBI, healthy controls and non-TB disease) that have been applied to diverse types of clinical material (e.g. tissue, whole blood, PBMC, serum and urine) and using different experimental methods (e.g. stimulated or unstimulated samples, different antigens and conditions). These factors undoubtedly contribute to

the difficulties associated with comparing very diverse and complex datasets and considerable validation is required. Notwithstanding the need for greater standardisation across studies, these approaches are relevant and have yielded valuable results, especially given the multifaceted requirements for a TB biosignature.

1.7.2 Transcriptomics

Genome-wide differential gene expression studies measure RNA transcript abundance, typically by gene microarrays or RNA sequencing. The former represents the archetypal 'omic' platform and in humans there is an estimated 50,000-100,000 transcripts that may be targeted for transcriptomic measurements [266].

Since the first report in 2007, several studies have examined gene expression in response to TB and identified signatures that discriminate individuals with TB from healthy controls using peripheral blood samples. Despite the vast array of approaches, similar transcriptional profiles have been identified, commonly indicative of persistent immune activation in TB disease. Among patients with active TB disease, increased IFN-α/β signaling, pro-inflammatory signaling through the Janus kinase pathway, differential expression of Fc-γ receptors, innate immune-related genes such as defensins and guanylate-binding proteins (GBPs), complement factors, and gene clusters involved in apoptosis and natural killer cell activity have all been described [235, 267-276]. Changes in the transcriptome during treatment, as early as one week after initiation and indicative of modulation of the humoral responses, have also been reported [277, 278]. Interestingly, a recent combined 'meta-like' analysis of all transcriptomic data reported in human TB pathogenesis showed a myeloid-derived inflammatory signature and TREM1 signaling to be of particular importance [279, 280]. The optimal number of transcripts that balance high diagnostic sensitivity and specificity with practical utility, accessibility and cost effectiveness is unknown. A study

attempting to address this combined historic transcriptomic data to generate a 360-gene panel, which was tested on samples from a new patient cohort in India [281]. A signature of four genes (*GBP1, ID3, P2RY14* and *IFITM3*) accurately separated individuals with active TB from healthy controls and was subsequently validated in other independent cohorts and datasets, however it performed less well in patients with HIV co-infection [281].

A significant concern is that while peripheral blood samples are easily obtainable, profiles from this compartment may not represent the complete immunological milieu at the principal interface between host and mycobacteria - the pulmonary granuloma. Studies have shown that there is only partial overlap between gene expression profiles from blood and those identified in granulomas and cervical lymph nodes [282, 283]. In addition, detecting heterogeneity between lesions within the same individual is unlikely to be achieved by applying current technologies to peripheral samples [283, 284]. Combining the transcriptomic signatures obtained from disease-specific tissue and blood may provide a framework for developing more sensitive TB biomarkers.

A particular challenge relates to identifying specific transcriptomic signatures for TB to discriminate from general states of immune-mediated inflammation induced by other diseases. Some investigators have attempted to define TB-specific profiles, comparing TB signatures with those from other infectious and non-infectious, pulmonary and multisystemic diseases, including pneumonia, pulmonary sarcoidosis, lung cancer, systemic lupus erythromatosis, Still's disease, Staphylococcal and Group A Streptococcal infections, and in patients with and without HIV co-infection [50, 235, 273, 285-288]. While common expression features occur, profiles unique to TB have been identified.

Finally, in contrast to 'diagnostic' transcript signatures discriminating between active disease and both infected and uninfected healthy controls, far fewer studies have assessed differences between individuals with LTBI and those uninfected. Differential gene expression profiles have been noted in some studies but not in others [235, 269, 271, 272]. This may be because cohorts of LTBI patients have generally been small, case definitions have varied due to different diagnostic tests and thresholds and such patients are considered as a single, homogeneous group rather than a spectrum and therefore true extremes of response may be lost by averaging data. Appreciation of this spectrum in transcriptomic studies is important in identifying correlates of protection and 'prognostic' biomarkers to predict risk for progression to active disease.

The first longitudinal whole blood transcriptome study, which followed HIV-negative household contacts of newly diagnosed TB patients over two years, has very recently been reported [289]. The RNA signature of participants in test and training cohorts was determined by RNA sequencing every six months. The profiles of household contacts who remained healthy were compared with those who developed active TB over the observational period. Analysis of RNA sequencing data derived a candidate risk signature for progression to TB with a sensitivity of 71%, 63% and 48%, at 6, 6-12 and 12-18 months prior to TB diagnosis (respectively) and a specificity of 81%. This signature was then adapted to a 16-gene multiplex qRT-PCR platform and evaluated in an independent validation cohort of household contracts, giving a sensitivity of 54% and specificity of 83% in the 12 months before diagnosis. There was considerable overlap with previously identified genes associated with chronic activation of interferon-mediated inflammatory responses, both at the individual level and by modular enrichment, including *GBPs, FCGR1A* and *1B*, *SERPING1* and *STAT1*. The only other study of gene expression associated with risk of TB progression evaluated the transcriptome of PBMC derived from a small cohort of HIV-positive patients [290].

Whilst limited in approach and not validated, it showed a combined *IL13* and *AIRE* profile had the highest discriminatory power to identify cases up to 8 months prior to diagnosis of TB and that those expressing *IL13* had an expression pattern enriched for type I IFN-related signaling genes [290].

There are also several exciting developments including the increasing availability of affordable RNA sequencing and growing interest in role of microRNAs (miRNAs). These small, non-coding RNAs that regulate post-transcriptional gene expression and have potential utility as biomarkers and even as targets for therapeutic intervention [291-297].

1.7.3 Proteomics

The human proteome encompasses up to 1 million different proteins and proteomic profiling of serum or plasma samples has identified several peptides and antibodies that, in combination, can differentiate individuals with active disease, LTBI and other diseases [298-303]. Differentially expressed proteins in TB disease include serum amyloid A, transthyretin, C-reactive protein (CRP), neopterin, apolipoproteins, fibrinogen, CD14, and complement 3 and proteome signature sizes have varied ranged from 1-10 biomarkers [242, 298, 303-311]. In addition, some proteomics signatures reflect changes during TB treatment [303].

To date, only one study has specifically evaluated proteomic differences between individuals with LTBI and uninfected controls [311]. While a 14-protein plasma signature could discriminate between groups, predominantly consisting of acute phase proteins such as fibrinogen and apolipoproteins, no further stratification of the LTBI cohort was performed [311]. However, several investigators have failed to identify discriminatory protein biomarkers and a lack of standardisation between studies,

including differences in study design, case definition and proteomic techniques, and lack of cross-validation, have been highlighted [242, 299, 301, 312-317].

Technologies used for proteomic fingerprinting include matrix-assisted or surface-enhanced laser desorption/ionisation time-of-flight (MALDI- or SELDI-TOF) mass spectrometry (MS) and protein microarray technology. In the former, proteins are fragmented into peptides, which are then detected by MS on the basis of mass-to-charge ratio. While these technologies offer the advantage of an unbiased 'omic' approach, they are costly, technically complex and therefore of limited availability [298]. The earliest proteomic study not only demonstrated proof-of-concept of using this approach for TB diagnostics but also sought to address accessibility issues. The primary proteomic spectra of 219 peak clusters observed in serum samples that discriminated between patients with pulmonary TB and controls (non-TB diseases and healthy individuals), was refined to a subset of 20 correlation-selected mass clusters. From these clusters two of the most discriminatory proteins were identified as serum amyloid A and transthyretin, which were subsequently tested in a simple immunoassay together with CRP and neopterin giving an accuracy of 84% (82% sensitivity, 86% specificity) [298]. Evaluation in an independent validation cohort showed a similarly promising performance. The need to identify disease-specific signatures and to validate them in appropriate clinical settings is as pertinent to proteomics as it is to other 'omic' technologies [318].

1.7.4 Metabolomics

Metabolic profiling is the identification of small molecular metabolites (e.g. amino acids, lipids, fatty acid, sugars and nucleotides) in clinical samples (typically urine and serum) using high-throughput methods [319, 320]. Volatile organic compounds (VOC), a subgroup of metabolites, can be measured in the breath. Metabolomics has been used

to develop biosignatures for several diseases including malignancy, cardiovascular disease and diabetes [321-323]. This approach has shown metabolic biosignatures associated with different TB disease states and responses to treatment in serum, urine, sputum, CSF and breath from TB patients and uninfected controls [242, 324-328]. Profiles have included metabolites associated with inflammatory processes, immunosuppression and oxidative stress [327]. Differential profiles have also been reported between different lineages of infecting mycobacteria following anti-TB therapy [329].

The potential of metabolomic profiling in TB to identify compounds derived directly from the site of infection has also been suggested. In one serum-based study, fibrinopeptide A, postulated to be released following fibrin deposition during granuloma formation, was elevated in patients with TB disease and LTBI compared with an uninfected group [327]. Similarly, kynurenine occurred at higher levels in TB patients. This compound is synthesized from tryptophan by indoleamine 2,3-dioxygenase 1 (IDO1) which is induced in macrophages and dendritic cells in contact with *M. tb*. A reciprocal decrease in serum tryptophan was also observed, although a statistical correlation between these molecules did not exist [327]. The authors derived clusters of functionally related metabolites, demonstrating significant correlations within clusters and suggesting co-dependence on specific metabolic processes or systemic response. Furthermore, the study showed 211 significant correlations between metabolites and cytokines/chemokines, such as IL-6, IP-10 and sIL2ra with tryptophan and glutamine, perhaps reflecting a relationship between metabolic function and immune response indicative of disease progression. Interestingly, this study also identified several metabolites that differed significantly between the latently infected individuals and uninfected controls including inosine, hypoxanthine, glycylvaline, 5-oxoproline and two unidentified compounds [327]. Together with

endogenous metabolites produced by the host, exogenous metabolites may be secreted by an infecting pathogen and *M. tb*-derived cell wall glycolipids have been identified in the plasma of patients with active TB disease [330].

The number of metabolites measured to date has varied from 34 to over 23,000 and the resulting signatures from 1-130 molecules [242]. This is due, in part, to the different techniques used and their capacities, which may limit the ability to compare studies. Generally, a two-step process of separation of molecules by gas or liquid chromatography, followed by detection and identification of the constituents by nuclear magnetic resonance (NMR) or MS, has been used, which, as with proteomic platforms, have limited availability. Also, differences in subject characteristics and environmental factors, such as dietary intake, may make comparative analyses difficult. Only one TB metabolomics study to date has taken this into consideration and matched participants appropriately [330]. The focus of many studies has been to examine TB pathogenesis rather than the diagnostic potential of metabolites, therefore validation of profiles in independent cohorts is often absent. Metabolic profiling in TB is potentially a very valuable tool to identify diagnostic and prognostic markers but considerable development in techniques, application and analysis is required.

1.7.5 Multiple biomarkers, large datasets and validating biosignatures

The advantages of using multiple biomarkers have been elegantly described recently [265]. A combinatorial approach using several independent variables to generate a biosignature has been shown to not only increase power but also reduce the overall error rate of predictive models [237, 265, 327]. However, using too many variables may result in overfitting of models whereby minor fluctuations in the data are exaggerated due to increased model complexity [331]. Therefore the ideal number of

individual biomarkers for a TB biosignature has yet to be determined and a fine balance between too many and too few will be required [265].

Notwithstanding the numbers of variables, investigators have highlighted the importance of using biomarkers that are independent from one another, stressing the difference between dependence and correlation [265, 332]. Examples supporting this approach include the development of biosignatures for assessing risk of HIV-associated Immune Reconstitution Inflammatory Syndrome (IRIS), diagnosing sepsis and predicting responses to influenza vaccination [333-335].

Of the several platforms for biomarker discovery described, many are high throughput and can generate multiple variables from multiple samples simultaneously. Analysing and integrating large datasets from different techniques is computationally complex and data reduction is often used to improve the utility of the data [336]. Approaches to this include unsupervised and unbiased filtering by identifying and excluding factors with low variability based on interquartile range, and using principal components analysis (PCA), a mathematical method that creates composite variables by linear combination to reduce the number of variables of a dataset [337]. A further development is the rationalisation of large numbers of variables into smaller, distinct biological modules in which the constituents are highly related and typically expressed in a coordinated way [338]. This is logical as biological processes occur in a modular manner and it allows simpler data analysis and more intuitive interpretation. It has been applied successfully to several diseases and infections, including *M. tb* [235, 339, 340]. It has recently been proposed that considering underlying biological processes is an important aspect of data evaluation and may provide novel insights into immunopathogenesis [237]. Most of these techniques have been applied to data obtained from differential gene expression studies, but the principles are relevant to

other high throughput platforms too.

As part of developing a robust biosignature, models require both internal and external validation to test sensitivity and specificity. During internal validation, supervised analysis is used to classify the data into groups. The overall dataset is then randomly divided into two subsets, a training set and a test set, the latter requiring a substantial proportion of samples. The training set is used to generate a model to classify samples into the pre-defined groups, which is then applied to the test set for further evaluation [337]. A problem with dividing data into subsets is the reduction in sample number and therefore the statistical power of the analysis [337]. Re-sampling methods such as bootstrapping and leave-out-one randomisation use repeated analyses to increase the power and model performance [331]. External cross-validation by applying the model to an independent validation set of samples is the final step of assessing performance. Together with validating any model against data derived from a different, unrelated cohort, it is important to test the general applicability of a model to diverse populations, with and without the target disease or infection. Using standardised measures that are comparable between different studies must also be considered [237].

1.8 *Ex vivo* mycobacterial growth inhibition assays

In view of our incomplete understanding of the host immune response to *M. tb*, which has hampered the identification of correlates of protective immunity and markers of prognostic risk, there has been increasing interest in the use of *ex vivo* mycobacterial growth inhibition assays (MGIAs). These functional assays provide an unbiased, summative assessment of a range of immune mechanisms and their complex interactions rather than measuring single, pre-defined parameters. This is important given the conflicting data on the role of T cells, macrophages, neutrophils, humoral

responses and other immune effector mechanisms to control mycobacterial growth [21]. These assays use whole blood or cellular fractions and measure the ability to control growth following *in vitro* infection with bacilli. Over the past 35 years several variations of MGIA have been developed, but most have focussed on evaluating immune responses to vaccination and the bactericidal/bacteriostatic effects of drugs. To date, there are no published studies that have assessed mycobacterial growth inhibition in clinical samples from individuals with TB disease.

1.8.1 Early developments and cellular MGIAs

'Lymphokine' was the term used to describe secretory products release by immune mouse splenocytes upon stimulation with tubercle bacilli [341]. Mouse peritoneal macrophages supplemented with lymphokine showed enhanced inhibition of *M. tb* growth *in vitro* [341]. Advances in the culture of human macrophages led to the adaptation of this technique for use with human samples and the first description of a MGIA in 1981 [342]. PBMC were isolated from healthy volunteers considered either immune (TST-positive or recently vaccinated with BCG) or non-immune (TST-negative) to BCG. Lymphocytes were cultured for 72 hours with a BCG-derived antigen to induce the production of lymphokine. Monocyte-derived macrophages were then infected with bacilli and cultured for a further 7 days with or without the addition of lymphokine. [^{3}H]thymidine uptake was used to detect inhibited bacillary replication, together with direct bacillary counts and morphological evidence of 'tuberculoimmunity'. This approach showed that only lymphocytes from immune donors were able to produce lymphokine upon stimulation, and macrophages incubated with this lymphokine showed enhanced inhibition of intracellular bacillary replication. The authors extended their studies to demonstrate the inhibitory effect of vitamin D3 on mycobacterial growth in macrophages, a finding independently confirmed by others [343, 344]. A

similar assay assessed inhibition of mycobacterial growth in murine peritoneal macrophages and human alveolar lavage cells, showing that both cell types could inhibit *M. tb* growth [345].

The first application of an MGIA in a vaccine study involved isolating monocytes from healthy British school children pre- and 8 weeks post-BCG vaccination and pulsing monolayers with autologous stimulated lymphocytes for 2 hours each day for 3 days (rather than adding lymphokine) [346]. Monocyte monolayers were infected with *M. microti* for 24 hours and the change in number of live bacteria in monolayers and supernatants over 4 days quantified by colony counts on agar. The cells were bacteriostatic during the first day, after which growth accelerated in pre-vaccination but not post-vaccination monolayers. Mycobacterial growth was significantly inhibited at days 3 and 4 of the culture using cells from post- compared with pre-BCG, reflecting the protective effect of BCG vaccination in this population. Surprisingly, mycobacterial growth was actually increased by exposures to stimulated lymphocytes, regardless of vaccination status. The authors suggest that two opposing effects of lymphocyte exposure may be at play: one occurring after vaccination to enhance bacteriostasis, the other causing impairment of bacteriostasis and occurring both before and after vaccination [346]. The same group later applied this assay to a study of BCG vaccination in PPD-negative children receiving BCG vaccination in Chingleput, India [347]. There was no change in mycobacterial growth following BCG vaccination, in keeping with epidemiological evidence for a lack of protective efficacy in this population, possibly due to pre-existing sensitisation by environmental mycobacteria. Overall, growth rates were higher in monolayers from British compared with Indian vaccinees.

Following these early studies several PBMC-based MGIAs of varying technical complexity were developed. A 'primary lymphocyte inhibition assay' involved the low-level infection of isolated monocytes with *M. tb,* followed by culture either alone or with non-stimulated autologous lymphocytes for several days [348]. Cells were then lysed and mycobacteria quantified by solid culture. Addition of non-stimulated lymphocytes resulted in significant inhibition of mycobacterial growth for both PPD-negative and -positive subjects, suggesting measurement of early innate non-specific aspects of immunity. It was also demonstrated that soluble lymphocyte mediators from the supernatants of co-cultures could mediate a modest reduction in *M. tb* growth in freshly infected monocytes alone [348]. Taken together the authors concluded that protective memory responses to *M. tb* required CD4+ T cells, that CD4-CD8- T cells contributed to innate immunity and that soluble mediators were only partially responsible for activating *M. tb*-infected monocytes. The primary lymphocyte inhibition assay subsequently demonstrated enhancement of mycobacterial growth inhibition at 4 months post-primary BCG and 2 months post-revaccination compared with baseline in PPD-negative individuals (although not statistically significantly) [349].

In a 'secondary lymphocyte inhibition assay', antigen-specific T cells were expanded by stimulation prior to co-culture with infected monocytes [350]. Adherent monocytes were cultured for 6 days followed by infection with BCG and removal of extracellular BCG by washing. In parallel, PBMC were cultured for 7 days in media alone or with the addition of mycobacterial antigen. Expanded effector cells were then added to autologous monocyte targets at varying ratios for 72 hours. Target cells were lysed and mycobacteria quantified by radiolabelling. Interestingly, stimulation with mycobacterial antigens caused a significant expansion of predominantly γδ TCR+ T cells. Inhibition of BCG growth was significantly enhanced in co-cultures containing antigen-expanded T cells compared with unexpanded lymphocytes, and this inhibition

was increased twofold following BCG vaccination in 3 of 5 individuals. A similar trend was seen using this assay following primary BCG vaccination and re-vaccination [349].

1.8.2 Whole blood MGIAs

An early version of a whole blood MGIA used BCG transfected with luciferase (BCG *lux*) as a reporter [351]. Heparinised, diluted whole blood was inoculated with BCG *lux* for 96 hours followed by hypotonic cell lysis. Mycobacterial growth was measured in relative light units (RLU) and expressed as a ratio of growth in the sample relative to a control. This MGIA showed *in vitro* growth of BCG *lux* was significantly lower in whole blood, but not plasma, from tuberculin-positive compared with tuberculin-negative individuals [351]. In a subsequent study in US adults, three different MGIAs were compared in the evaluation of mycobacterial growth following primary BCG vaccination and a BCG boost. The luciferase assay demonstrated a significant vaccine-induced reduction in BCG *lux* growth at 8 months (2 months after revaccination), but not following primary vaccination [349]. The effect of BCG vaccination on mycobacterial growth in the whole blood was further demonstrated using this BCG *lux* MGIA in a TB endemic setting [352]. Among a South African infant cohort, 33 of 50 participants showed a reduction in BCG *lux* growth at 3 to 6 months post primary BCG vaccination, but not in a small, unvaccinated control group. BCG vaccination induced significantly higher IFN-γ production in response to BCG *lux* and PPD, although cytokine secretion did not correlate with luminescence. An adult control group (BCG-vaccinated in infancy) did not show changes in either growth of BCG *lux* or cytokine production over the study period. Finally, this assay demonstrated reduced ability of HIV-infected infants to control mycobacterial growth compared with healthy controls which was associated with low CD4+ T cell counts and reduced IFN-γ production [353]. The addition of exogenous IFN-γ did not improve the reduced control in the HIV-

positive infants. This MGIA was later optimised for use with smaller blood volumes to improve suitability for paediatric studies and the methodology and reproducibility data described in detail [354, 355].

The authors highlighted several advantages of using this whole blood assay such as its technical simplicity requiring reduced manipulation of clinical samples, the low volumes of samples needed, and the ability to assess the combined inhibitory effects of several cellular constituents, as well as serum-based factors, on mycobacterial growth and anti-mycobacterial immunity [349, 351]. Limitations included the use of an attenuated, recombinant strain of BCG, which may affect responses and also that whole blood assays cannot distinguish between intracellular and extracellular inhibition of mycobacterial growth and are therefore less suitable for studying the underlying mechanisms of control than lymphocyte-based assays. In summary, several studies using a whole blood BCG luminescence-based MGIA have shown growth control to correlate with immune status and immunogenicity of BCG vaccination.

In 2001 an alternative *ex vivo* whole blood assay was described to measure the bactericidal activity of drugs by whole blood culture [356]. The objective was to determine the influence of drug, host, and strain factors on mycobacterial growth and to assess the potential of this method for the future evaluation of new anti-mycobacterial drugs. Whole blood was collected before, and at intervals following, drug administration and inoculated with bacilli at ~10^4 cfu (calculated to show positivity at 4.5 days using the BD BACTEC MGIT liquid culture system). Cultures were incubated at 37^{o}C with constant mixing for 72 hours. After 72 hours, host cells were disrupted by hypotonic lysis, bacilli were sedimented, resuspended and inoculated into BACTEC MGIT tubes. Control cultures were established on day 0 by direct inoculation of the same titre of mycobacterial stock into BACTEC tubes. The difference between the days-

to-positivity (DTP) of the control and experimental cultures were used to determine mycobacterial growth. Using several drugs (with bactericidal and bacteriostatic functions) against both drug-sensitive and multi-drug resistant strains, the authors showed a model of intracellular infection in which microbial killing reflected the combined effects of therapeutic agent and immune mechanism. There were several proposed advantages to this system. The summative effects of immune functions were tested, drug concentrations reflected those in the circulation and the small inocula used underwent rapid and complete phagocytosis, eliminating the need to remove extracellular bacilli. Furthermore, the use of the BACTEC MGIT system rather than a luciferase reporter construct permits the study of a wide range of strains and not a single genetically engineered strain. Finally, it was suggested that calculating DTP rather than BACTEC growth indices improved accuracy and increased dynamic range. However, as BACTEC MGIT is more sensitive than agar for detecting viable bacilli this may have resulted in an underestimation of bactericidal activity of drugs in the assay. Conversely, an overestimation of bactericidal activity may occur by misinterpretation of true bacillary killing due to prolongation of lag phase.

The BACTEC MGIT assay was then used to study responses of BCG vaccination in ten tuberculin-negative volunteers from the US [357]. Eight participants received primary BCG vaccination followed by a boost 6 months later. Four subjects showed increased mycobacterial growth inhibition 2 months following the first vaccination, and while their responses waned at 6 months, they were restored after re-vaccination. Three subjects responded only after the second vaccination and the remaining three subjects showed no response. The authors suggest that such heterogeneity among subjects may be influenced by host genetic factors. Inhibition of *M. tb*-induced TNF-α production and the combined depletion of CD4+ and CD8+ T cells significantly reduced control of mycobacterial growth in tuberculin-positive participants only. They also highlighted

that in order to serve as a model of intracellular infection, a very low ratio of mycobacteria to monocytes (multiplicity of infection, MOI) is required to ensure complete bacillary phagocytosis. A highly sensitive method of detection is then needed such as the BACTEC system, which offers the additional advantage of being unaffected by bacterial clumping (associated with virulence). However the BACTEC MGIT does rely on bacillary replication and this may be affected by mycobacteria in a prolonged lag phase of replication, although it has been suggested that this may paradoxically be more reflective of natural infection in which containment rather than eradication occurs [357].

This system was subsequently applied to samples from 36 HIV-negative volunteers receiving standard 6 months of treatment for pulmonary TB [358]. Following the initiation of therapy, whole blood was collected at weeks 8 and 12 (immediately before dose administration and 2 and 6 hours thereafter), and at a single time-point at week 28 (2 weeks after completion of treatment). Subjects were studied using that individual's isolate and the drug-susceptible *M. tb* clinical isolate MP-28. In the absence of chemotherapy, bacteriostasis was noted and attributed to immune mechanisms while administration of chemotherapy resulted in bactericidal activity, which was greatest during the intensive phase of treatment. The cumulative bactericidal activity observed during treatment correlated with the rate of decrease of sputum bacillary load during the first 4 weeks and was associated with time to conversion to sputum negativity by week 8 of treatment. Such an assay may have a role in assessing the sterilising activity of novel anti-TB drugs and provide a surrogate marker of TB relapse. In this study, bactericidal activity and sputum bacillary clearance were most closely correlated when patients were studied using their own *M. tb* isolates, perhaps indicating that unique strain characteristics have a potentially important role in this model for phenotypic drug tolerance.

This finding was investigated further by using the BACTEC MGIT system to measure the capacity of different mycobacterial strains to survive phagocytosis and replicate in whole blood cultures [359]. Six healthy TST-negative volunteers provided whole blood and 18 clinical isolates and 5 reference strains of *M. tb* were used in a 72 hour culture. The supernatants of 24 hour cultures were analysed for a variety of cytokines using a protein microarray. Attenuated strain H37Ra showed the least capacity to replicate whereas virulent H37Rv showed increased replication. Interestingly, replication rates in whole blood varied greatly between clinical isolates. Intracellular mycobacterial growth was most restricted during the first 24 hours of whole blood culture. While limited by the study size, it was also observed that higher concentrations of IFN-α and IL-10 after 24 hours of culture were associated with greater bacillary replication. However, the authors did note that limitations of the whole blood assay include a lack of understanding of the exact cellular localisation of bacilli during the initial phase of whole blood culture. This was compounded by the low inoculum used, which also provided suboptimal stimulation for cytokine expression.

The whole blood bactericidal activity assay was subsequently used to examine anti-mycobacterial immunity in patients after TB cure, assessing the potential suitability of attenuated TB strains as indicators of protection [360]. The control of mycobacterial growth of three strains of *M. tb* (the infecting strain, H37Ra and the clinical isolate MP-28) was examined in patients who had successfully completed TB treatment (from whom the individual strains were isolated), and healthy TST-negative volunteers (in whom the same isolates were studied). The study showed that the whole blood from cured TB patients demonstrated greater control of the *M. tb* strain with which they had previously been infected compared to TB-naïve volunteers. No correlation was evident between the control of these strains and that of attenuated H37Ra, however, correlation with strain MP-28 was noted (although this was weak). The authors

suggested that differential antigen expression may account for the findings and that *M. tb* MP-28 may be a suitable strain to assess mycobacterial immunity using growth inhibition in whole blood culture.

Most recently, the whole blood BACTEC MGIT assay was used by the host group to evaluate responses to BCG vaccination among UK adults, together with a PBMC-based adaptation [361]. Participants received either a primary BCG vaccination or homologous boost to historical BCG. At baseline, historically vaccinated individuals showed a trend for enhanced mycobacterial growth inhibition compared with naïve volunteers in whole blood (although this did not reach significance). Following primary BCG vaccination, a non-significant enhancement of mycobacterial growth inhibition was observed at 8 weeks compared with pre-vaccination in whole blood, while in participants with historic vaccination, there was no effect of re-vaccination. This MGIA was also used by the host group in a BCG challenge study, comparing anti-mycobacterial immunity induced by candidate vaccine MVA85A. While volunteers with a history of BCG vaccination showed some degree of protective immunity to challenge (regardless of MVA85A status), this was not detected by the BACTEC MGIT [362].

1.9 Aims and objectives

Delineating the proposed spectrum of TB would not only improve our understanding of the immunopathogensis of TB, but also has the potential to identify individuals at highest risk of progression to active disease, therefore facilitating targeted preventative therapy. I sought to use a MGIA, which provides an unbiased, summative assessment of a range of immune mechanisms and their complex interactions, in an attempt to dissect the host immune response to *M. tb*.

My specific aims were to:

i. Characterise a whole blood MGIA, investigate the underlying mechanisms of action and assess its suitability for use in this study.

ii. Use recent BCG vaccination as a model of mycobacterial exposure to assess anti-mycobacterial responses and to develop assays to measure surrogates of antigenic burden.

iii. Determine whether individuals with active TB disease, LTBI and uninfected healthy controls demonstrate different capacities to control mycobacterial growth using a MGIA.

iv. Use functional control responses to stratify individuals and investigate the characteristics of subgroups using several techniques in a multi-platform approach to develop a putative biosignature of reactivation risk.

Materials and methods

2 Materials and methods

2.1 Statement of authorship

The author performed all of the work described herein except where explicitly detailed. Specifically, some of the blood samples used in the experiments were collected by Donna Tupper (Infantry Training Centre, Catterick) and Sheila Churchill (Churchill Hospital, Oxford). Rachel Tanner, Stephanie Harris and Lisa Stockdale (The Jenner Institute, Oxford) provided assistance with PBMC isolation. Rachel Tanner also occasionally assisted with MGIT assays. Whole depletion flow cytometry was performed by Iman Satti and T cell flow cytometry by Danny Wright (The Jenner Institute). Gene expression microarrays were performed by Eneida Parizotto-Lee and Magali Matsumiya, with subsequent bioinformatics analysis undertaken by Julius Müller (The Jenner Institute). Assistance with Luminex was provided by Steve Smith (The London School of Hygiene and Tropical Medicine, London).

2.2 Clinical samples

All of the studies involving samples collected from human adult volunteers were conducted in accordance with the principles of the Declaration of Helsinki and Good Clinical Practice (GCP). The storage of all human samples for subsequent exploratory immunological analysis and transcriptomic studies was in agreement with the conditions of ethical approval granted by independent committees.

2.2.1 BCG vaccination studies

Samples used in BCG vaccination studies were collected from healthy adult volunteers having provided valid, informed, written consent. Individuals were enrolled from the Medical Centre, Infantry Training Centre, Catterick, under the ethical approval granted

by the Ministry of Defence Research Ethics Committee (MoDREC 237/PPE/11). Peripheral blood samples were collected for the whole blood MGIT assay, serum was stored for ELISA and multiplex cytokine and chemokine studies and PBMC were isolated and cryopreserved for subsequent exploratory immunology assays.

2.2.2 Studies to delineate the spectrum of *M. tb* infection

After gaining valid, informed, written consent, peripheral blood samples were collected from adult volunteers according to the following inclusion criteria:

i. Suspected or confirmed new diagnosis of pulmonary or extrapulmonary TB disease (later confirmed by positive microbiological culture or patients treated with high clinical suspicion on the basis of clinical symptoms and signs and radiological or histological evidence).
ii. Confirmed new diagnosis of LTBI (as determined by positive TST and/or IGRA in the context of recent exposure to an active case).
iii. HIV-negative and without any other significant co-morbidity.
iv. Competent to participate and provide consent as judged by the investigator.
v. Over the age of 18 years.

Participants were enrolled at one of three clinical sites:

i. The respiratory/infectious disease out-patient clinic at the Birmingham Chest Clinic, Birmingham (Heart of England Foundation Trust), under ethical approval granted by the National Research Ethics Service (NRES), Heart of England NHS Foundation Trust (REC reference 2012107RM).
ii. The respiratory out-patient clinic at the Churchill Hospital, Oxford (Oxford University Hospitals NHS Foundation Trust), under ethical approval granted by

the National Research Ethics Service (NRES), Committee South Central - Oxford C (REC reference 12/SC/0299).

iii. The Medical Centre, Infantry Training Centre, Catterick, under the ethical approval granted by the Ministry of Defence Research Ethics Committee (MoDREC 237/PPE/11).

In addition, samples were also collected from BCG-vaccinated and unvaccinated healthy volunteers, with no past medical history of TB, exposure to TB or evidence of LTBI, as control subjects from the above sites and also at the Jenner Institute, Oxford, with written consent and in accordance with Oxford University policy. Together with the sampling described above, PAXgene® tubes were collected and stored in accordance with the manufacturer's instructions for later microarray transcriptomic studies.

2.3 Mycobacteria Growth Indicator Tube (MGIT) assay

2.3.1 Preparation of mycobacterial stocks

Two strains of mycobacteria were used throughout this study: BCG Pasteur and *M. tb* H37Rv. A frozen 1ml aliquot of strain seed stock (at a titre of 10^7 cfu/ml) was thawed at room temperature, vortexed and added to 9ml Middlebrook 7H9 broth in a 50ml Falcon tube. A mock inoculation was also prepared to monitor for contamination. This was then incubated at 37°C, 5% CO_2, with rotational shaking for 5-7 days or until the suspension had become cloudy. The 10ml culture was then added to a fresh 90ml Middlebrook 7H9 broth in a 500ml flask and incubated at 37°C, 5% CO_2, with rotational shaking. From day 5-7, 1ml aliquots were used to measure the optical density (OD) at 600nm (against a blank of the mock culture). An OD between 0.3-0.5 was considered to represent mid-log phase growth, at which time the culture was divided into 1ml aliquots in 2ml microtubes and stored at -80°C until required.

2.3.2 Titration of mycobacterial stocks

A 1ml aliquot of stock was thawed at room temperature and vortexed and five serial 10-fold dilutions were prepared in supplemented Middlebrook 7H9. For each titration twelve BACTEC MGIT tubes were supplemented with 800µl of PANTA antimicrobials (containing polymixin B, amphotericin, nalidixic acid, trimethoprim and azlocillin) and OADC enrichment broth (containing oleic acid, bovine albumin, dextrose and catalase). 500µl of each stock dilution, together with an undiluted sample, was added to each MGIT tube in duplicate. Tubes were placed in the BACTEC 960 machine and incubated at 37°C until the detection of positivity by fluorescence. A standard curve was created using the inoculum volume against time-to-positivity (TTP) values using the equation: $y = m\ (ln\ x) + c$, where y is TTP, m is the slope, x is the inoculum volume and c is the y intercept. An example of a standard curve is provided (Appendix 8.1). In addition, two 7H10 agar plates were divided into 3 sectors and 10µl of each dilution was spotted 3 times into each sector. Plates were incubated at 37°C, 5% CO_2, and colonies were counted after 3-4 weeks. A standard curve was created using the inoculum volume calculated from the TTP-derived values and the cfu enumerated by solid culture and the stock cfu/ml was subsequently determined.

2.3.3 Whole blood MGIT assay

A 1ml aliquot of BCG Pasteur or *M. tb* H37Rv was thawed at room temperature, vortexed for 1 minute then resuspended in pre-warmed (37°C) RPMI-MGIT media. The volume of the mycobacterial stock was calculated to give a TTP of 6.5 days, which has previously been determined to give optimal differential responses in the whole blood assay. 300µl RPMI-MGIT/mycobacterial suspension was added to duplicate 2ml microtubes for each sample. 300µl of whole blood was added to each tube and cultures were incubated at 37°C for 96 hours with 360° rotation. After 96 hours cultures were

centrifuged at 11000xg for 5 minutes, the supernatants were removed and stored at -80°C and 1ml of sterile water was added to the cell pellet for lysis. Tubes were vortexed for 30 seconds and incubated at room temperature for 5 minutes. This was repeated twice, after which a further centrifugation at 11000xg for 10 minutes was performed, supernatants were discarded and 500µl of supplemented Middlebrook 7H9 media from a spare MGIT tube was added. Tubes were vortexed for 30 seconds and the suspension transferred to a BACTEC MGIT tube supplemented with PANTA antibiotics and OADC enrichment broth (as described above). Tubes were placed in the BACTEC 960 machine and incubated at 37°C until the detection of positivity by fluorescence. In addition, on day 0, duplicate viability control tubes were set up by directly inoculating supplemented BACTEC MGIT tubes with the same volume of mycobacteria as the samples.

2.3.4 Calculation of mycobacterial net growth

The readout of the BACTEC MGIT assay is net growth. To calculate this value the mean TTP for matched duplicates of both the samples and controls was converted to an inoculum volume based on the stock titration curve (described above). The value of x (inoculum volume) was determined from re-arrangement of the standard curve equation to: $x = (y - c) / m$. This value was then converted to a cfu count by multiplying it by the concentration of the stock (determined by agar plating solid culture, as described above). The net growth ratio of viable bacilli was calculated as: (sample cfu / control cfu) then $\log_{10}$ transformed. Therefore, a smaller net growth value indicated less bacillary replication and was interpreted as greater mycobacterial control.

2.4 Immunology assays

2.4.1 PBMC isolation, cryopreservation and thawing

PBMC were separated from fresh heparinised whole blood obtained from study participants by gradient centrifugation. 15ml of Lymphoprep was loaded into 50ml Leucosep tubes and centrifuged at 700xg for 1 minute. 15-30ml of whole blood collected in lithium heparin (LH) tubes was carefully layered onto the Leucosep tube membrane and centrifuged at 1000xg for 13 minutes at room temperature without a brake. PBMC were collected from the interface using a Pasteur pipette and transferred to a 50ml Falcon tube, which was topped up to 45ml with R0 media and centrifuged at 700xg for 5 minutes at room temperature with a brake. The supernatants were removed, pellets flicked and then pooled for each donor into a single 50ml Falcon tube and resuspended in 45ml of R0 for a second wash. Cells were resuspended in 10ml R10 and counted using a CASY® counter. Briefly, 10µl of cell suspension was added to 10ml of CASY®ton solution in duplicate and the mean cell count was determined.

For cryopreservation, cells were centrifuged at 700xg for 5 minutes and resuspended in ice-cold FCS to a concentration of 10-20x10^6 cells per ml. An equal volume of ice-cold 20% DMSO in FCS was added to the cell solution and mixed by inversion. Cells were immediately aliquoted into cryovials at 1ml/vial (5-10x10^6 cells/vial) and placed in a CoolCell® cell freezing container which was stored at -80°C. After 1-2 days, vials were transferred to liquid nitrogen.

For thawing, vials were retrieved from liquid nitrogen and placed on dry ice. Cells were thawed in a water bath at 37°C until a small amount of ice remained. Using a Pasteur pipette, the cell suspension was gently pipetted up and down to encourage complete thawing. The cells were then transferred to a 15ml Falcon tube containing 9ml R10 and

centrifuged at 700xg for 5 minutes. The supernatant was removed and cells were resuspended in 10ml R10 containing 2µl/ml of benzonase and rested at 37°C for a minimum of 2 hours before counting and use in subsequent immunology assays.

2.4.2 *Ex vivo* T cell ELISpot assays

T cell *ex vivo* IFN-γ ELISpot assays were performed using the human IFN-γ ELISpot (ALP) kit. Briefly, ELISpot plates were coated with 50µl anti-IFN-γ capture antibody prepared in 0.05M carbonate-bicarbonate buffer to a final concentration of 15 µg/ml. Plates were incubated at 4°C overnight then washed five times with sterile PBS. Plates were blocked with 100µl/well R10 and incubated for 2-5 hours at 37°C. 3×10^5 PBMC, suspended in 80µl media, were added to each ELISpot well (in triplicate). An ESAT-6/CFP-10 peptide pool was added in 20µl volumes to give a total volume of 100µl/well (final concentration of 10µg/ml). Staphylococcus enterotoxin B (SEB) and phytohemagglutinin (PHA) were used as positive controls (10µg/ml). Unstimulated PBMC were used as a measure of background IFN-γ production. ELISpot plates were incubated for 18-20 hours at 37°C, 5% CO_2, before being developed. Following washing five times with PBS containing 0.05% Tween 20 (PBS/T), 50µl of biotin anti-IFN-γ antibody, diluted 1:1000 in PBS, was added to each well and plates were incubated for 2 hours at room temperature. After washing, 50µl/well of streptavidin-alkaline phosphatase (ALP), diluted 1:1000 in PBS, was added and plates were incubated for 1 hour at room temperature. After further washing, 50µl/well of BCIP/NBT substrate was added and spots were developed for approximately 3-15 minutes. The substrate reaction was terminated by washing the plate in tap water 3-4 times and plates were dried overnight before being read the following day. Spots were counted on an ELISpot reader (AID Germany, software v5.0). Results are reported as spot-forming cells (SFC) per million PBMC, calculated by subtracting the mean count of the unstimulated PBMC

from the mean count of triplicate antigen wells and correcting for the number of PBMC in the well. Responses were considered positive if the count was twice (but at least 5 spots greater) than that of the unstimulated wells.

2.4.3 *Ex vivo* B cell ELISpot assays

2.4.3.1 Ex vivo antibody secreting cell (ASC) ELISpot assays

ELISpot plates were coated with 50µl per well of test antigen in triplicate. Six wells were coated for each antigen which included (at final concentrations): BCG SSI ($2x10^5$ cfu/well), PPD (6µg/ml), cell membrane fraction (6µg/ml), ESAT-6 (10µg/ml) and CFP-10 (10µg/ml) prepared from *M. tb* H37Rv (ESAT-6 and CFP-10, purchased from BEI Resources, were recombinant proteins expressed in *Escherichia coli* and purified by immobilised-metal affinity chromatography). For negative control wells sterile PBS was used and for the detection of total IgG secreting cells, six wells were coated with 50µl per well of polyvalent goat anti-human IgG at 50 µg/ml in PBS. Plates were incubated overnight at 4°C. ELISpot plates were then washed three times with sterile PBS (100µl/well) and wells were blocked with R10 media (100µl/well) for at least 1hr at 37°C. Blocking media was flicked out and replaced with 50µl/well of fresh R10. Cryopreserved PBMC were thawed and prepared as described above and resuspended to a concentration of $5x10^6$ cells/ml in R10. 50µl of the cell suspension was added to the negative control wells and to the first three antigen-coated wells per volunteer. Cells were diluted 1:2 in R10 for the second three antigen-coated wells. PBMC dilutions for the total IgG controls were 1:1, 1:25 and 1:50 in R10. 50µl of the IgG control dilutions were added to duplicate wells. ELISpot plates were then transferred to an incubator at 37°C, 5% CO_2, for 16-18 hours. Cells were discarded by flicking off the cell suspension into suitable disinfectant and plates were washed six times with PBS/T. Washing solution was flicked off and plates blotted onto absorbent paper. 50µl/well of

anti-human IgG (gamma specific) conjugated to ALP and diluted 1:5000 in PBS was added and plates were incubated for 4 hours at room temperature. Plates were then washed six times with PBS/T, washing solution was flicked off and plates blotted onto absorbent paper. 50µl/well of developer was added and plates were developed for approximately 3-5 minutes until spots developed. Plates were washed well with tap water (six times) then dried overnight. Spots were counted on an ELISpot reader. The frequencies of antigen-specific ASCs were calculated by subtracting the mean count of the negative control wells from the test antigen wells and correcting for number of PBMC in the well. ASC frequency was reported as both the number of ASCs per $1x10^6$ PBMC and also as the percentage of the total IgG secreting cells $1x10^6$ PBMC. Responses were considered positive if the count was of two or more spots in each replicate well, with the total number of spots in the antigen-coated wells being twice that observed in the negative control wells [363].

2.4.3.2 Memory B cell (mBC) ELISpot assays

PBMC were thawed and resuspended to a concentration of $2x10^6$ cells/ml in R10 media. A minimum of $6x10^6$ cells per volunteer was required. For each volunteer 500µl of the cell suspension was added to six wells of a 24-well flat bottom plate, yielding $1x10^6$ cells per well. Mitogen stimulation mix was prepared containing *Staphylococcus aureus* Cowan (SAC, 1:2400 dilution), CpG (5µg/ml) and pokeweed mitogen (PWM, 1:6000 dilution from a 1mg/ml stock) and 500µl was added to five wells per volunteer, leaving an unstimulated well as a control, to which 500µl of R10 was added. Plates were incubated at 37°C, 5% CO_2, for 6 days. On day 5, ELISpot plates were coated overnight as described above. On day 6, ELISpot plates were washed and blocked as described. The cultured cells set up on day 0 for each volunteer were harvested by gentle re-suspension with a Pasteur pipette. The stimulated cells were pooled into a

50ml Falcon tube and the unstimulated cells were transferred into a 15ml Falcon tube. Pooled cells were made up to 30ml, and the unstimulated cells to 10ml, with R10. Suspensions were centrifuged at 700xg for 5 minutes at room temperature then resuspended in the same volume of R10. The supernatant was discarded, cell pellets were resuspended by flicking and 10ml R10 was added. After another wash, cells were resuspended in 2ml R10 for counting as previously described. Cells were then resuspended at $2x10^6$ cells/ml in R10 and 100µl was added to the negative control wells and the first three antigen-coated wells. A 1:2 dilution was added to the second three antigen-coated wells. For the total IgG wells, dilutions of 1:1, 1:50 and 1:100 were added to each well in duplicate. 100µl of unstimulated cells were also added to duplicate IgG wells. Plates were then incubated at 37°C, 5% CO_2, for 16-18 hours and developed and counted as described above. Frequencies of antigen specific ASCs were reported as mBC-derived ASCs [363].

2.4.4 Enzyme-linked immunosorbent assays (ELISAs)

2.4.4.1 Total IgG ELISA

96-well flat-bottom microtitre plates were coated (in duplicate) overnight at room temperature with 100µl/well of BCG SSI ($2x10^5$ cfu/well), cell membrane fraction, culture filtrate or whole cell lysate (2µg/ml stock) or LAM (1µg/ml stock), prepared from *M. tb* H37Rv. Each antigen was diluted in coating buffer, which was also used for the negative control. The plates were then flicked and washed six times with PBS/T, followed by blocking with 200µl/well of casein for 1 hour at room temperature. The blocking solution was flicked off and plates were blotted. Serum samples were prepared at dilutions of 1:100 in casein. A sample of pooled serum from active TB patients was used as a positive control. 50µl of sample was added per well (50µl casein to the negative control wells), and the plates were incubated for 2 hours at room

temperature. The contents were then discarded and the plates washed six times with PBS/T. Secondary antibody (goat anti-human gamma-chain whole IgG ALP conjugate) was diluted 1:1000 in casein, vortexed and 50µl/well was added. The plates were then incubated for 1 hour at room temperature, flicked and washed six times with PBS/T. 100µl/well of development buffer was added and the plates were covered in foil. Plates were read every 10 minutes using an ELx800 Microplate Reader with Gen5 software at 405nm until the positive control reached an OD of 1.0. The mean OD values of duplicate negative controls were subtracted from the mean OD of duplicate samples and reported.

2.4.4.2 IgG isotype ELISA

96-well flat-bottom microtitre plates were coated overnight at room temperature with 50µl/well of the following antigens (at final concentrations) prepared from *M. tb* H37Rv in duplicate: cell membrane fraction (2µg/ml), culture filtrate (2µg/ml), LAM (2µg/ml) and a 1:1 mix of ESAT-6/CFP-10 (10µg/ml each). Each antigen was diluted in PBS, which was also used as a negative control. Each plate was prepared in duplicate to test for IgG1 and IgG2 responses. Each plate was also coated with native human IgG1 and IgG2 (2µg/ml) in duplicate wells. The plates were then flicked and washed six times with PBS/T, followed by blocking with 200µl/well of casein for 1 hour at room temperature. Serum samples were prepared at dilutions of 1:100 in casein for all antigens except for ESAT-6/CFP-10 when a 1:10 dilution was used. The blocking solution was flicked off and plates were blotted and washed six times with PBS/T. 50µl/well of sample was added except for isotype control wells where 50µl/well of casein was added. Plates were incubated for 2 hours at room temperature. The contents were then discarded and the plates washed six times with PBS/T. 50µl/well of the corresponding biotinylated secondary antibody (e.g. anti-IgG1 or anti-IgG2) at

1:1000 dilution was added and the plates were then incubated for 1 hour at room temperature, flicked and washed six times with PBS/T. 50µl/well of Extravidin-ALP (1:5000) was added and plates were incubated for 30 minutes at room temperature. Contents were flicked and washed six times with PBS/T. 100µl/well of pNPP substrate was added and plates were read every 10 minutes using an ELx800 Microplate Reader with Gen5 software at 405nm until the IgG1 and IgG2 isotype controls reached an OD of 0.6 and 1.2, respectively. These values were previously determined from the gradient of a standard curve of native human IgG1 or IgG2 ranging from 0.1 to 100 µg/ml (doubling dilutions) to avoid saturation. The mean OD values of duplicate negative controls were subtracted from the mean OD of duplicate samples and reported. Sample readings with an OD greater than the negative control plus 3 SD were considered positive.

2.4.5 Whole blood depletions

EasySep® depletion kits were used with substantial modifications to the manufacturer's protocol. This resulted from several optimisation experiments assessing different antibody concentrations, incubation periods and temperatures (data not shown). Five 5ml polystyrene round-bottom tubes were set up per volunteer. 2.4ml of heparinised whole blood per volunteer was aliquoted into each tube and diluted with 1.6ml RPMI-MGIT. EasySep® positive selection cocktail containing cell-specific antibodies were added as follows to each tube: 200µl of anti-CD66b, anti-CD3 and anti-CD19 and 400µl of anti-CD14 (50-100µl/ml of whole blood/media suspension). A negative control without addition of any antibodies was also included. Samples were mixed well by pipetting and incubated for 15 minutes at room temperature, with mixing at the midpoint by further pipetting. EasySep® whole blood magnetic nanoparticles were mixed by vigorous pipetting to ensure a uniform

suspension and 200µl was added to each tube except for the CD14 depletion to which 400µl was added. 200µl of nanoparticles was also added to the negative control. Mixing was performed by gentle pipetting, followed by 15 minute incubation at room temperature. Each tube was then placed in an EasySep® magnet for 5 minutes. With the tube still *in situ* the magnet was inverted in one continuous motion and the depleted fraction decanted into a new tube. A second depletion was performed as described above to improve depletion efficiency. 300µl of each depleted sample and undepleted sample was then used in the MGIT assay as previously described. 1ml of each of these samples was also assessed by flow cytometry to determine the efficiency of depletion.

2.4.6 Flow cytometry

2.4.6.1 Whole blood depletion efficiency

1ml whole blood was lysed with 9ml FACS lysing buffer in 50ml Falcon tubes, mixed and incubated for 10 minutes at room temperature. The surface antibody mix was prepared containing: anti-CD3 AF700, anti-CD19 PECy5, anti-CD56 PECy7, anti-CD66b FITC and anti-CD14 PB (final volume 100µl/well in FACS buffer) and stored in the dark on ice (antibody titrations were performed on every new vial). Lysed samples were centrifuged at 700xg for 5 minutes at room temperature and the supernatant was discarded. The cell pellet was resuspended in 20ml PBS and centrifuged at 700xg for 5 minutes at room temperature. The supernatant was discarded, cells were resuspended in the residual fluid and transferred to V-bottomed 96-well plates. The plate was centrifuged at 700xg for 5 minutes at 4°C, the contents were flicked and blotted and 100µl/well of antibody mix was added. Cells were incubated at 4°C for 30 minutes in the dark. Cells were washed twice and fixed as described below. Stained cells were acquired using an LSRII flow cytometer (BD Biosciences) within 24 hours and analysed using FlowJo v8.3 (Tree Star Inc.).

2.4.6.2 PBMC stimulation for functional T cell characterisation

Cryopreserved PBMC were thawed and prepared as previously described. Supplemented R10 was prepared for the stimulated incubation using warmed R10 and adding 1µg/ml of anti-CD28 and anti-CD49d antibodies (diluted in sterile PBS). Sufficient R10 was made for 4µl/well (containing $1x10^6$ PBMC in 200µl R10). PBMC were counted and diluted to a final concentration of $5x10^6$/ml in supplemented R10. 200µl/well of PBMC was aliquoted into U-bottomed 96-well plates containing 10µl/well of antigen (final concentration): SEB (1µg/ml), PPD (20µg/ml), or ESAT-6/CFP-10 peptide pools (5µg/ml). An unstimulated well was also included (R10). Plates were incubated at 37°C, 5% CO_2, for 2 hours then Brefeldin A was added to each well (3µg/ml final concentration). Plates were incubated at 37°C, 5% CO_2, for 14-16 hours. Cells were transferred to a 96-well V-bottom plate and centrifuged at 700xg for 5 minutes at 4°C. The pellet was checked then plates were flicked and blotted. 200µl/well of PBS was added and cells were resuspended by pipetting. The plate was centrifuged at 700xg for 5 minutes at 4°C, the pellet was checked before flicking and blotting and cells were stained immediately (below).

2.4.6.3 Immunophenotyping and intracellular cytokine staining (ICS) T cells

Red live/dead stain was diluted 1:100 with PBS and 5µl was added to each well and mixed by pipetting. Plates were incubated at 4°C for 10 minutes in the dark. The surface antibody mix was prepared containing: anti-CD14 ECD, anti-CD19 ECD and anti-CD4 PB (final volume 100µl/well in FACS buffer) and stored in the dark on ice. The ICS antibody mix was prepared containing: anti-CD3 AF-700, anti-CD8 APC-H7, anti-IFN-γ PE-Cy7, anti-IL-2 PE, anti-TNF-α AF647 and anti-IL-17 FITC (final volume 100µl/well in perm/wash buffer) and stored in the dark on ice. Antibody titrations were performed on every new vial. After live/dead staining, 100µl/well surface

antibody mix was added and cells were incubated at 4°C for 30 minutes in the dark. During this time compensation beads were prepared according to the manufacturer's instructions and after staining and washing, 200µl/well of FACS buffer was added and these were stored in dark on ice until acquisition. After surface staining the cells, 100µl/well of FACS buffer was added and the plate was centrifuged at 700xg for 3 minutes at 4°C, the pellet was checked before flicking and blotting, then cells were washed twice with 200µl/well of FACS buffer as above. 200µl/well of undiluted fix/perm buffer was added, mixed, and plates were incubated for 20 minutes at 4°C in dark. Cells were then washed with 200µl/well of perm buffer and plates were centrifuged at 700xg for 3 minutes at 4°C, flicked and blotted. 100µl/well of ICS antibody mix was added, mixed and plates were incubated for 30 minutes at 4°C in the dark. Two washes with 200µl/well of perm buffer were performed as described and cells were resuspended in 100µl/well of FACS buffer/1% paraformaldehyde. Stained cells were transferred into labeled cluster tubes, wrapped in aluminium foil and stored at 4°C until acquisition. Stained cells were acquired using an LSRII flow cytometer (BD Biosciences) within 24 hours and analysed using FlowJo v8.3 (Tree Star Inc.).

2.4.6.4 Immunophenotyping B cells and monocytes

Cryopreserved PBMC were thawed and prepared as previously described. PBMC were counted and diluted to a final concentration of $5x10^6$/ml in R10. 200µl/well of PBMC was aliquoted into V-bottomed 96-well plates and washed twice with 200µl/well of FACS buffer as described. Aqua live/dead stain was diluted 1:10 in PBS and 2.5µl/well was added and plates were incubated at 4°C for 20 minutes in the dark. The B cell surface antibody mix was prepared containing: anti-CD10 APC, anti-CD19 PECy7, anti-CD21 PB, anti-CD27 Qdot605, CD20 APC-Cy7, anti-CD38 PECy5 and anti-IgG PE (final volume 100µl/well in FACS buffer). The monocyte surface antibody mix was prepared

containing: anti-CD3 AF700, anti-CD19 PB, anti-CD56 PB, anti-HLA-DR APC-Cy7, anti-CD14 PE and anti-CD16 PE-Cy7 (final volume 100µl/well in FACS buffer). Antibody titrations were performed on every new vial and mixes were stored in the dark on ice. Fluorescence minus one (FMO) controls were included in each batch for complex gating. Cells were stained in batches with either the B cell or monocyte mix, washed and fixed as described above. Compensation beads were prepared as described. Stained cells were acquired using an LSRII flow cytometer (BD Biosciences) within 24 hours and analysed using FlowJo v8.3 (Tree Star Inc.). For assays using fluorescently labeled PPD, 100µg of PPD was conjugated with either AlexaFluor488 or Fluorescein according to the manufacturer's instructions.

2.4.7 Multiplex serum cytokine and chemokine studies

The Milliplex® Map human cytokine/chemokine kit testing 41 analytes was used according to the manufacturer's instructions. Briefly, cryopreserved serum samples were thawed completely, vortexed and centrifuged to remove particulates. 200µl/well of wash buffer was added to a luminex plate, which was then sealed and mixed on a plate shaker for 10 minutes at room temperature. Wash buffer was decanted by inverting and blotting. Standards were prepared by six serial dilutions (3.2-10,000pg/ml) in assay buffer. Two quality controls were also prepared by reconstituting lyophilised concentrate in 250µl deionised water, vortexing, and incubating for 10 minutes at room temperature. Assay buffer was used to determine background. 25µl of serum matrix was added to the background, standard, and control wells. 25µl of each serum sample was added per well, followed by 25µl of cytokine bead mix. The plate was sealed, wrapped in foil and incubated with agitation for two hours at room temperature. The plate was rested on a magnet for 1 minute before gently decanting and blotting. The plate was removed from the magnet, 200µl of wash buffer

was added and the plate was agitated for 30 seconds before re-applying to the magnet. This was repeated twice. 25µl of detection antibody was added to each well, and the plate was sealed, covered with foil and incubated with agitation for 1 hour at room temperature. 25µl of streptavidin-phycoerythrin was added to each well, and the plate was sealed, covered with foil and incubated with agitation for 30 minutes at room temperature. Plate washing was performed twice using the magnet as described above. 150µl of sheath fluid was added to each well, and the beads resuspended on a plate shaker for 5 minutes. The plate was then run on the Luminex^{200} plate reader and analysed using xPONENT software.

2.5 Transcriptomic microarray studies

2.5.1 Total RNA extractions

Total intracellular RNA was extracted from PAXgene® samples using the Blood RNA Kit (Qiagen) according to the manufacturer's instructions. Briefly, PAXgene® tubes were thawed over 2 hours at room temperature and then centrifuged to pellet the nucleic acids. The pellet was then resuspended and incubated with proteinase K for protein digestion. An additional centrifugation through a shredder spin column was performed to homogenise the cell lysate and remove residual cell debris. The supernatant of the flow-through fraction was transferred to a fresh microcentrifuge tube, ethanol was added to adjust binding conditions, and the lysate was applied to another column and briefly centrifuged for RNA binding. Any remaining contaminants were removed with several washes. Bound RNA was treated with DNase I to remove trace amounts of bound DNA and after further washes the RNA was eluted in elution buffer and heat-denatured. The purity and quantity of the isolated total RNA was assessed spectrophotometrically prior to storage at -20^{o}C until required.

2.5.2 Microarrays

Microarrays were performed by Eneida Parizotto and Magali Matsumiya. Briefly, globin mRNA was depleted from total RNA extractions using a biotin/streptavidin/magnetic bead-based assay, according to the manufacturer's instruction (GLOBINclear Kit, Ambion). The depleted RNA was then amplified using the TotalPrep RNA Amplification Kit (Illumina) according to the manufacturer's instruction. Briefly, cDNA was synthesised by reverse transcription and purified before being used as a template for the synthesis of biotin-labeled cRNA. This was purified and assessed using the Agilent bioanalyser. Amplified and labeled cRNA was hybridised to Illumina HumanHT-12 (v4.0) expression beadchips according to the manufacturer's instructions. Arrays were scanned with an Illumina bead array reader confocal scanner.

2.6 Statistical analysis

Statistical analyses were performed using Prism (v6.0) and SPSS (v22). The D'Agnostino-Pearson omnibus test was used to assess normality of data. Parametric data from experiments comparing two groups were analysed using a paired t-test (for matched pairs) or an unpaired t-test. Non-parametric data, or small datasets where normality could not be determined, were analysed using a Wilcoxon matched-pairs signed rank test (for matched pairs) or a Mann-Whitney test. For parametric data from experiments comparing more than two groups, repeated measures ANOVA (where the same individuals were tested over time or conditions) or one-way ANOVA (where different individuals were tested over time or conditions, or where values were missing) were performed. For multiple comparisons Dunnett's post-test correction was used. For non-parametric data from experiments comparing more than two groups, a Kruskal-Wallis test with Dunn's post-test was performed. For correlation analyses, after testing for normality, a Pearson's correlation for parametric data or a Spearman's

correlation for non-parametric data were performed. Transcriptomic data were analysed using 'R' statistical software by Julius Müller and are described in detail later.

2.7 Reagents

Lists of all of the reagents and solutions used above are given in Appendix 8.2 (Tables 8.1 and 8.2, respectively).

Results

3 Characterisation of the whole blood MGIT assay

3.1 Statement of authorship

Gene expression microarrays and subsequent bioinformatics analysis was performed by Magali Matsumiya and Julius Müller, respectively (The Jenner Institute, Oxford). Assistance with Luminex was provided by Steve Smith (The London School of Hygiene and Tropical Medicine, London) and flow cytometry by Iman Satti (The Jenner Institute).

3.2 Introduction

It has previously been shown that MGIAs can detect a functional ability to control bacillary growth and discriminate between subjects [346, 357, 361]. Most studies have investigated vaccine-induced anti-mycobacterial activity using these assays and to date there has only been one report of using a MGIA in the context of LTBI, which used a modified secondary lymphocyte inhibition assay [364].

The focus of the present study is to assess mycobacterial growth inhibition in samples from individuals with a range of *M. tb* infection statuses using a whole blood BACTEC MGIT assay that provides an unbiased, summative assessment of control.

In view of the limited studies to date, I sought to assess its robustness and characterise the assay to ensure it was a suitable platform for subsequent use with clinical samples, and also to investigate some of the mechanisms contributing to mycobacterial control.

3.3 Aims

The aims of the experiments described in this chapter were to:

i. Assess the effect of time from sampling to beginning the whole blood MGIT on mycobacterial growth.
ii. Determine the precision and reproducibility of the assay by assessing intra- and inter-assay variability.
iii. Assess mycobacterial growth kinetics over time.
iv. Study differential gene expression in response to different mycobacterial strains over time.
v. Investigate the effect of depleting different cellular fractions on mycobacterial growth.

3.4 Results

3.4.1 Effect of time-to-sample processing

Whole blood was collected from 6 healthy volunteers (PPD positive, ESAT-6/CFP-10 negative by IFN-γ ELISpot, data not shown) and left to stand in LH vacutainer tubes at room temperature. A whole blood MGIT was set-up at 1, 3, 6, and 9 hours following blood draw using BCG Pasteur and *M. tb* H37Rv. A fresh vial of mycobacterial stock (from the same preparatory batch) was used for each time-point for both controls and samples, which were established in duplicate.

Using BCG, the mean net growth of all volunteers across all time-points (n=24) was 0.51 $\log_{10}$ cfu (range 0.34-0.72) and the coefficient of variation (CV) and 95% confidence interval (95% CI) was 9.9% (5.6-14.3) (Figure 3.1 A). While there was some variation in net growth among individuals across the time-course, in particular

increased growth at 6 hours delay in time-to-processing, this was not statistically significant by repeated measures analysis (p=0.1) (Figure 3.1 B).

Mean net growth using H37Rv was 1.0 $\log_{10}$ cfu (range 0.83-1.18) and the CV (95% CI) was 4.3% (2.7-5.9) (Figure 3.1 C). Similarly, there was no significant difference in net growth among individuals (p=0.3) (Figure 3.1 D).

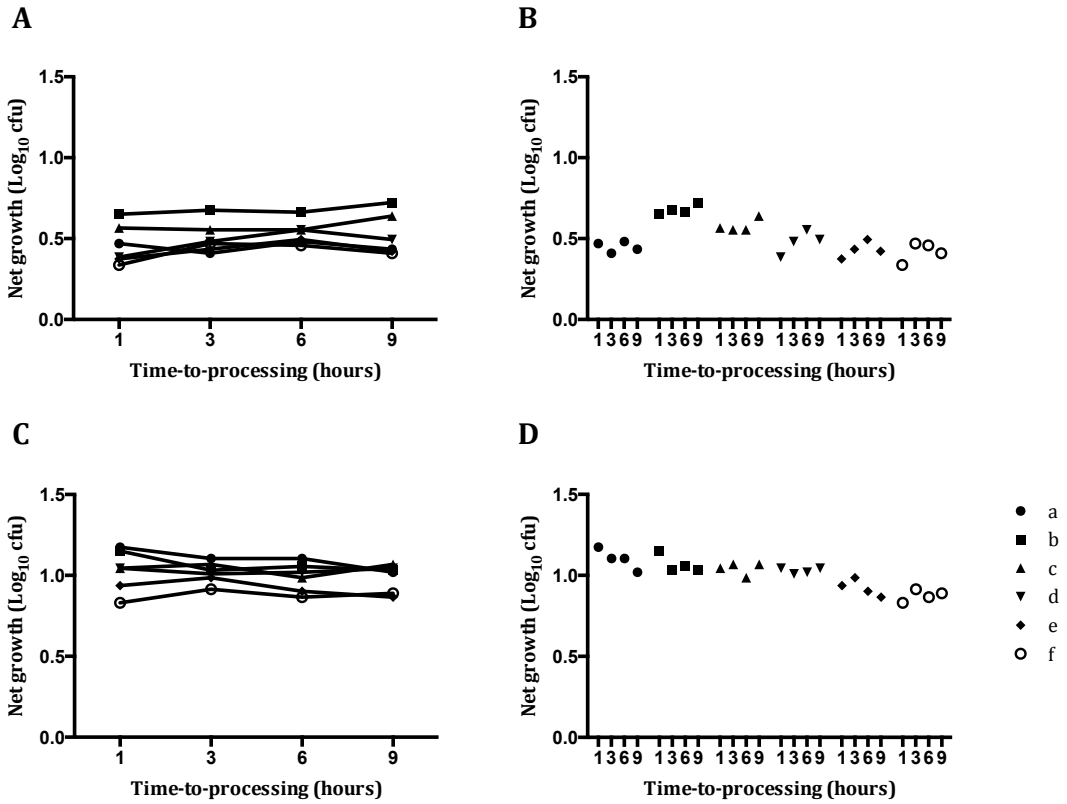


Figure 3.1 Effect of time-to-sample processing on mycobacterial growth using the whole blood MGIT assay. Whole blood was collected from 6 healthy volunteers (a-f) followed by a delay of 1-9 hours before starting the MGIT assay using BCG Pasteur (A & B) and *M. tb* H37Rv (C & D). Points represent the mean of duplicates; horizontal lines between points show net growth for each volunteer over time. There was no significant difference in net growth over time for either strain by repeated measures ANOVA.

3.4.2 Intra-assay variability

Throughout the use of this time course experiment, each control and sample was run in duplicate. As each duplicate was subject to independent culture over 96 hours, this was more than just a technical repeat.

As control and sample tubes were established for multiple time-points during the above experiments, these data could also be used to determine intra-assay variability. This was calculated using the time-to-positivity (TTP) of cultures. I chose this readout as TTP represents the primary data prior to extrapolation to net growth values and is therefore a more valid measure of variability. The net growth value readout is a more appropriate measure for inter-assay comparisons and allows for a more biologically intuitive assessment.

The mean TTP CV (95% CI) for BCG and H37Rv control tubes was 0.7% (0.2-1.3) and 0.5% (0.1-0.8), respectively, and for samples it was 1.2% (0.7-1.7) and 1.7% (1.2-2.2). The difference in TTP between duplicates (ΔTTP, hours) was further examined to set exclusion criteria for subsequent work, with a threshold set at the mean ΔTTP plus two standard deviations of the mean. The mean ΔTTP for control tubes using BCG and H37Rv (n=8) was 1.7 hours (1.4 SD, 95% CI 0.6-2.8) and 1.0 hour (0.9 SD, 95% CI 0.3-1.7), respectively (p=0.3). Therefore, exclusion criteria for control tubes was set at a ΔTTP of >4 hours for BCG and >3 hours for H37Rv. For samples (n=24) a single ΔTTP exclusion threshold of >6 hours was set (BCG, mean ΔTTP 2.2 hours, 1.9 SD 95% CI 1.3-3.0; H37Rv mean ΔTTP 2.5 hours, 1.8 SD 95% CI 1.8-3.3). There was no significant difference in sample ΔTTP between BCG and H37Rv (p=0.4).

3.4.3 Inter-assay variability

To assess inter-assay variability, whole blood was collected from 4 healthy volunteers (PPD positive, ESAT-6/CFP-10 negative by IFN-γ ELISpot, data not shown) at three time-points: baseline, then 4 and 8 months thereafter. Full blood counts were determined at each time-point. Whole blood MGIT was set-up using BCG and H37Rv at each of these time-points. Mean net growth (95% CI) at 96 hours of culture was 0.38 log_{10} cfu (0.32-0.44) using BCG and 0.52 log_{10} cfu (0.45-0.59) for H37Rv (p=0.003) (Figure 3.2). In terms of variability, the mean CV (95% CI) for net growth using BCG was 21.7% (5.7-37.8) and using H37Rv it was 15.7% (7.9-23.6) (p=0.3).

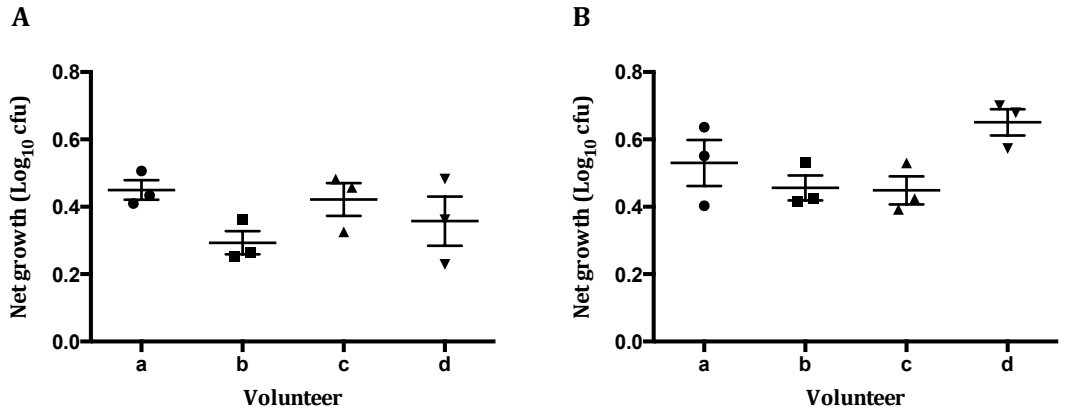


Figure 3.2 Inter-assay variability. Whole blood was collected from 4 healthy volunteers (a-d) and the MGIT culture established with BCG Pasteur (A) and *M. tb* H37Rv (B) for 96 hours. Points represent the mean of duplicates; bars represent mean values with SEM. A paired t-test was performed showing a significant difference of pooled, matched net growth values between BCG and H37Rv.

3.4.4 Mycobacterial growth kinetics

The growth kinetics of BCG and H37Rv in the whole blood MGIT and associated inter-assay variability were investigated using the samples from 4 healthy volunteers

(described above). Samples and mycobacteria were cultured for 24, 48, 72 and 96 hours in duplicate for each individual at each time-point. At these culture times, samples were processed for MGIT as described.

Net growth of both strains of mycobacteria increased over the culture period, with more growth being observed with H37Rv (Figure 3.3). Between 24 and 96 hours, mean net growth for BCG increased from -0.07 to 0.38 $\log_{10}$ cfu ($p<0.0001$) and for H37Rv from -0.16 to 0.52 $\log_{10}$ cfu ($p<0.0001$) (analysis by repeat measure one-way ANOVA).

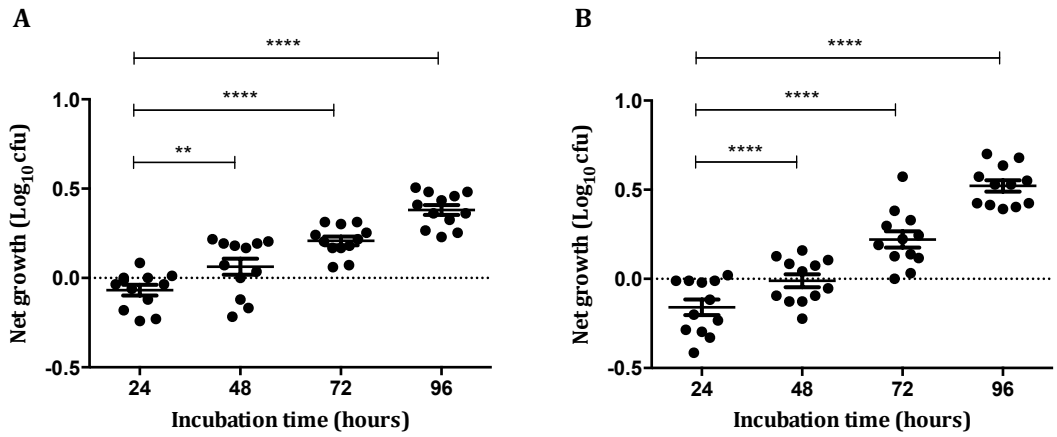


Figure 3.3 Growth kinetics of whole blood MGIT. Pooled data from whole blood MGIT using samples from 4 healthy volunteers at 3 different time-points, cultured with BCG Pasteur (A) or *M. tb* H37Rv (B) for 24, 48, 72 and 96 hours. Points represent the mean of duplicates; bars represent mean values with SEM. A matched repeated measures multiple comparison ANOVA with Dunnett's post-test correction was performed using 24 hours as the control data. ** represents a p-value of <0.005 and **** a p-value of <0.0001.

Analysis of reproducibility for each individual and strain showed differences in inter-assay variability over the time-course (Figure 3.4). More variability was seen using BCG than H37Rv, with a mean CV of 148.7% (range 21.7-344.6%) and 113.2% (range 15.7-249.3%), respectively. Both mycobacterial strains demonstrated a similar pattern of

variability over time, with maximal CV at 48 hours of culture and minimal CV on completion, at 96 hours.

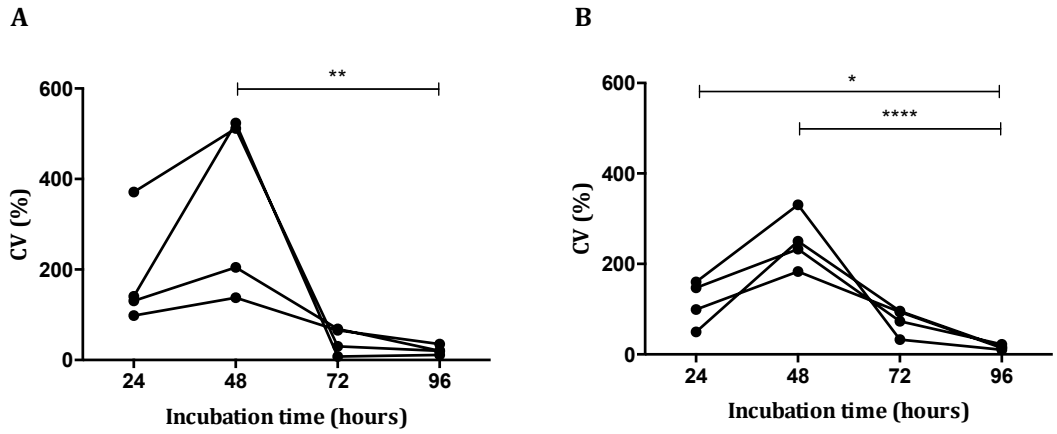


Figure 3.4 Inter-assay variability over 96 hour time-course. Changes in the coefficients of variation (CV) for whole blood MGIT using samples from 4 healthy volunteers at 3 different time-points, cultured with BCG Pasteur (A) or *M. tb* H37Rv (B) for 24, 48, 72 and 96 hours. Points represent the mean CV for each individual, calculated from duplicates over 3 different experiments. A one-way multiple comparison ANOVA with Dunnett's post-test correction was performed using 96 hours as the control data. * represents a p-value of <0.05, ** a p-value of <0.005 and **** a p-value of <0.0001.

3.4.5 Differential gene expression over time

The relationship between mycobacterial growth in whole blood MGIT and changes in differential gene expression (DGE) over time was investigated using transcriptomic studies. Samples from 4 healthy volunteers (described above) were cultured with BCG, H37Rv or media (negative control) for 24, 48, 72 and 96 hours. At each time-point, total RNA was extracted and microarrays performed. Of the 48 samples processed, three were excluded as outliers due to probe detection three times below the median absolute deviation. Following background correction, 23,203 probes, corresponding to 16,188 genes, were detected ($p<0.05$). Covariates of interest included categorical

variables of condition (mycobacteria or control) and incubation period. In order to adjust for elements considered likely to cause confounding, the model *Expression~[gender+neutrophil count+monocyte:lymphocyte ratio+batch]* was used in the analysis. Whole blood incubated with mycobacteria showed distinct DGE when compared with negative controls over time (Figures 3.5 and 3.6). In addition, while BCG and H37Rv assays showed few differences in DGE at early time-points, increasing differences in expression profile occurred over time until reaching a peak at 96 hours (Figure 3.7).

In order to better understand the relationship between the varying conditions and DGE, the top 200 genes showing most significant changes in expression (both increases and decreases) were further analysed using the Database for Annotation, Visualisation and Integrated Discovery (DAVID). DAVID uses gene-annotation enrichment analysis and functional annotation clustering of numerous sets of genes in a gene list to identify associations with cellular functions and pathways. Over the 96 hour time-course, the four most prominent functional clusters associated with mycobacterial culture were defence response, inflammatory response, response to wounding and immune response (Table 3.1). The differences in DGE between BCG and H37Rv primarily involved metabolic processes, particularly those related to mitochondrial function, although these occurred at considerably lower statistical significance (Table 3.1). Indeed, the only immune-related pathways identified when comparing DGE associated with BCG and H37Rv did not reach significance and concerned T cell activation and included the genes *IFNAR1, CD74* (involved in MHC class II antigen processing), and *FK506 binding protein 1A* (a member of the immunophilin protein family, which plays a role in immunoregulation and protein folding and trafficking). Some of the immune-related genes differentially expressed in response to mycobacteria are shown in Table 3.2

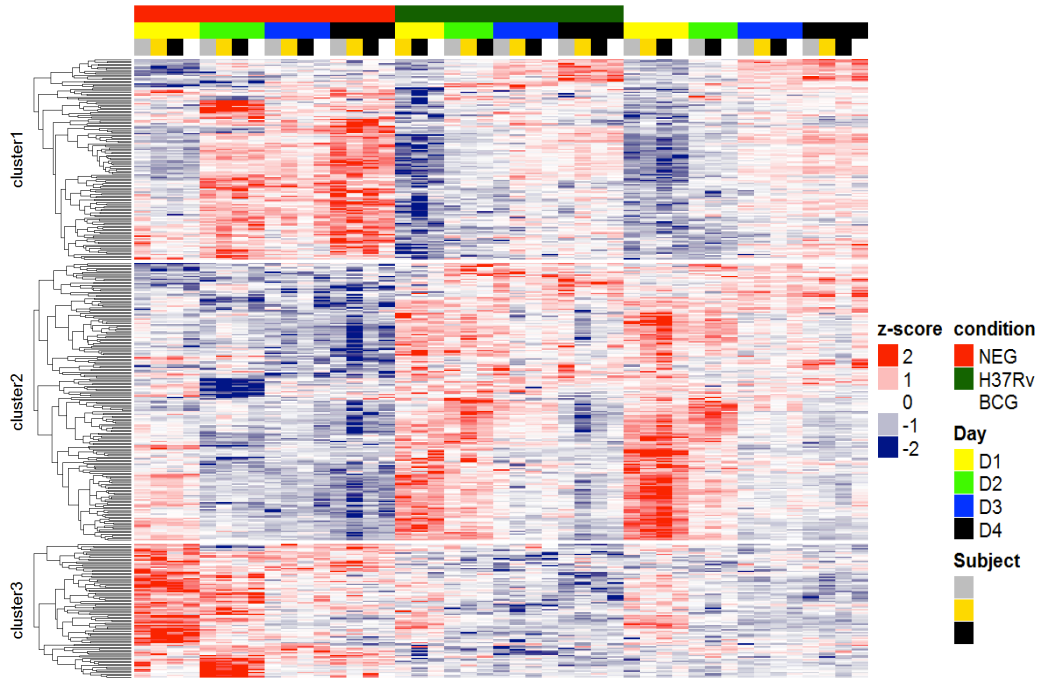


Figure 3.5 Differential gene expression in whole blood following culture with mycobacteria over 96 hours. A heatmap of differential gene expression derived from whole blood ordered by condition (negative vs BCG vs H37Rv), followed by incubation period (day 1 to 4) and then subject. Profiles with mycobacteria were distinct from the negative control, but showed some differences between individual strains. The y-axis was subject to unsupervised hierarchical clustering of similarity in gene expression. Rows were scaled to z scores of gene expression (e.g. red indicates 4 SD from mean expression).

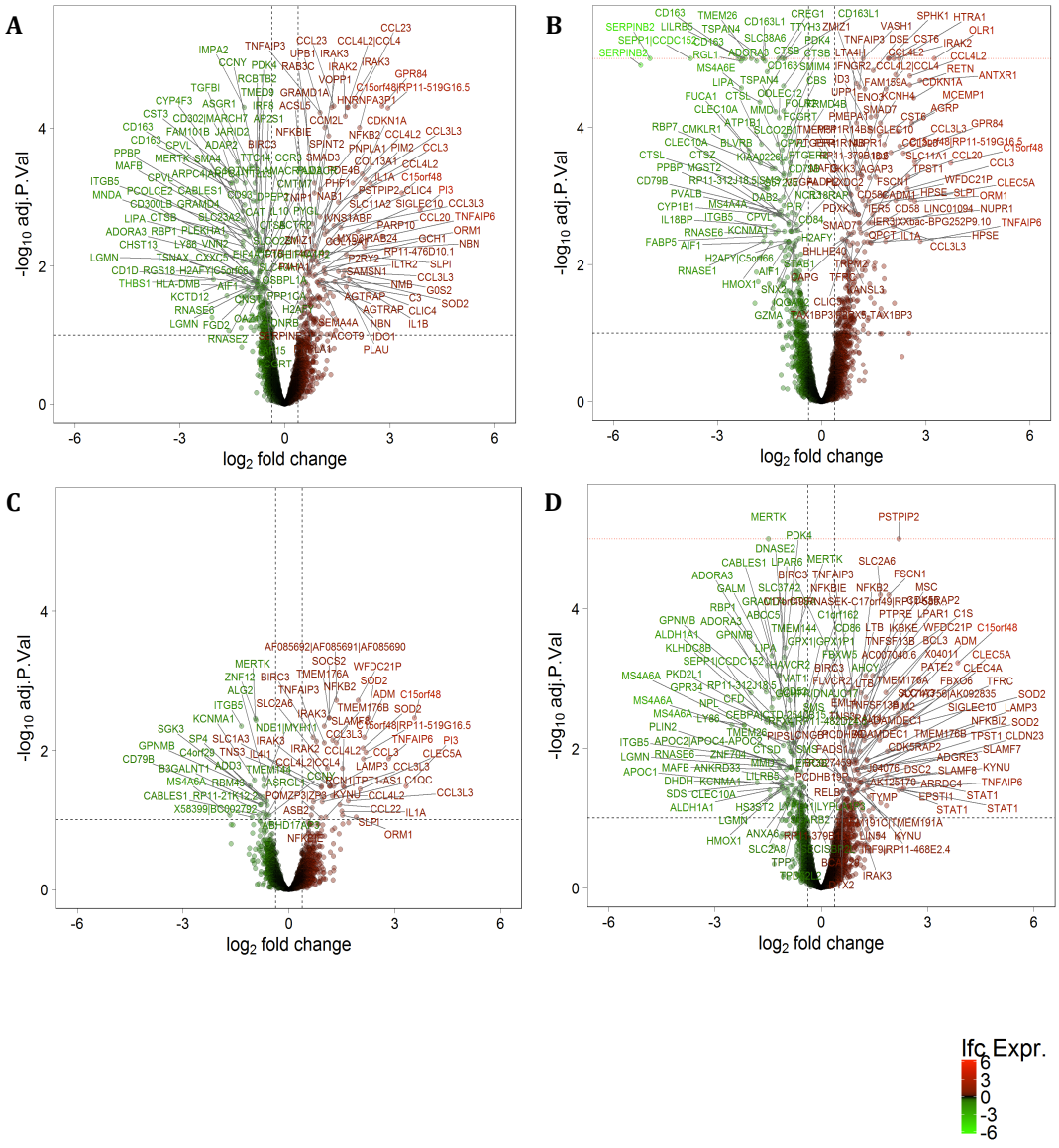


Figure 3.6 Changes in gene expression in whole blood following culture with mycobacteria compared with negative controls over 96 hours. Volcano plots showing the changes in differential gene expression in whole blood incubated with mycobacteria (BCG and H37Rv) or media (controls) over 96 hours. DGE at 24 (A), 48 (B), 72 (C) and 96 (D) hours is shown. The x-axis indicates the fold change in expression (red=increase in expression units; green=decrease) and the y-axis the significance (Benjamini-Hochberg adjusted p-value, the false detection rate (FDR)).

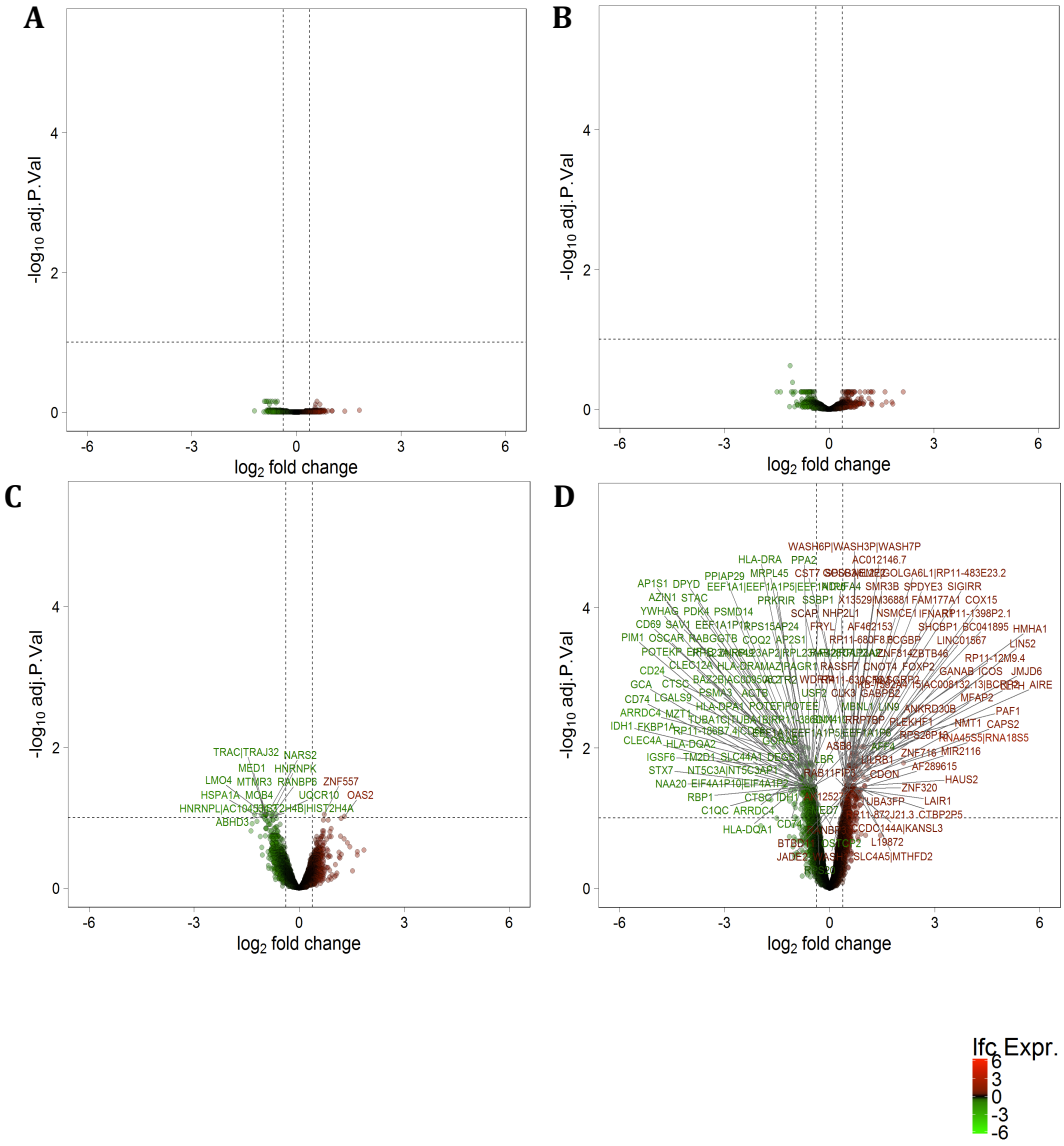


Figure 3.7 Differential gene expression in whole blood following culture with BCG compared with H37Rv over 96 hours. Volcano plots showing the changes in differential gene expression in whole blood between BCG Pasteur and *M. tb* H37Rv. DGE at 24 (A), 48 (B), 72 (C) and 96 (D) hours is shown. The x-axis indicates the fold change in expression (red=increase in expression units; green=decrease) and the y-axis the significance (Benjamini-Hochberg adjusted p-value (the FDR)).

Condition	Functional cluster	No. of genes	p-value	q-value
H37Rv vs Negative	Defence response	35	$6.4x10^{-17}$	$1.6x10^{-13}$
	Inflammatory response	25	$9.1x10^{-15}$	$6.8x10^{-12}$
	Response to wounding	30	$2.7x10^{-14}$	$1.3x10^{-11}$
	Immune response	26	$1.2x10^{-8}$	$4.6x10^{-6}$
BCG vs Negative	Response to wounding	37	$6.4x10^{-20}$	$9.3x10^{-17}$
	Defence response	39	$1.3x10^{-19}$	$9.2x10^{-17}$
	Inflammatory response	30	$2.8x10^{-19}$	$1.3x10^{-16}$
	Immune response	29	$4.5x10^{-10}$	$1.6x10^{-7}$
H37Rv vs BCG	Mitochondrion	24	$5.6x10^{-5}$	$1.2x10^{-2}$
	Mitochondrial matrix	10	$1.7x10^{-4}$	$1.9x10^{-2}$
	Mitochondrial lumen	10	$1.7x10^{-4}$	$1.9x10^{-2}$
	Mitochondrial part	15	$6.8x10^{-4}$	$4.9x10^{-2}$

Table 3.1 Comparison of functional cluster analysis. For each combination of conditions the top 200 genes with the most significant change in expression were assessed by functional cluster analysis using DAVID. Cluster definitions (according to the European Molecular Biology Laboratory, European Bioinformatics Institute (EMBL-EB)) are as follows:

Defence response: reactions, triggered in response to the presence of a foreign body or the occurrence of an injury, which result in restriction of damage to the organism attacked or prevention/recovery from the infection caused by the attack.

Inflammatory response: the immediate defensive reaction (by vertebrate tissue) to infection or injury caused by chemical or physical agents. The process is characterised by local vasodilation, extravasation of plasma into intercellular spaces and accumulation of white blood cells and macrophages.

Response to wounding: any process that results in a change in state or activity of a cell or an organism as a result of a stimulus indicating damage to the organism.

Immune response: Any immune system process that functions in the calibrated response of an organism to a potential internal or invasive threat.

Gene	q-value	Gene name	Average fold change
SEPP1|CCDC152	$1.31x10^{-11}$	Selenoprotein P, plasma, 1	-1.42
CD163	$1.33x10^{-10}$	CD163 molecule	-1.36
MERTK	$1.33x10^{-10}$	MER proto-oncogene, tyrosine kinase	-0.89
IRAK2	$1.33x10^{-10}$	Interleukin-1 receptor-associated kinase 2	1.32
CCL4L2|CCL4	$1.33x10^{-10}$	Chemokine ligand 4| 4-like 2| 4-like 1	1.37
ADORA3	$1.54x10^{-10}$	Transmembrane and immunoglobulin domain containing 3	-1.29
GPR84	$7.64x10^{-10}$	G protein-coupled receptor 84	1.71
LIPA	$8.12x10^{-10}$	Lipase A, lysosomal acid, cholesterol esterase	-1.27
IRAK3	$9.19x10^{-10}$	Interleukin-1 receptor-associated kinase 3	0.98
NFKB2	$9.46x10^{-10}$	Nuclear factor of kappa light polypeptide gene enhancer	0.94
CTSB	$1.91x10^{-9}$	Cathepsin B	-0.98
CCL3L3	$2.97x10^{-9}$	Chemokine ligand 3-like 3	1.54
IRAK3	$2.99x10^{-9}$	Interleukin-1 receptor-associated kinase 3	1.21
CCL3	$3.39x10^{-9}$	Chemokine ligand 3	2.04
LILRB5	$4.05x10^{-9}$	Leukocyte immunoglobulin-like receptor, subfamily B, memb 5	-0.91
SIGLEC10	$4.75x10^{-9}$	Sialic acid binding Ig-like lectin 10	1.32
SOD2	$5.70x10^{-9}$	Superoxide dismutase 2, mitochondrial	1.89
TNFAIP6	$9.13x10^{-9}$	Tumor necrosis factor, alpha-induced protein 6	2.69
PSTPIP2	$1.00x10^{-8}$	Proline-serine-threonine phosphatase interacting protein 2	1.01
CCL3L3	$1.02x10^{-8}$	Chemokine ligand 3-like 1| 3-like 3	1.79
CREG1	$1.11x10^{-8}$	Cellular repressor of E1A-stimulated genes 1	-0.64
RBP1	$2.63x10^{-8}$	Retinol binding protein 1, cellular	-0.89
BIRC3	$2.63x10^{-8}$	Baculoviral IAP repeat containing 3	0.56
ITGB5	$3.30x10^{-8}$	Integrin, beta 5	-1.09
IL1A	$3.30x10^{-8}$	Interleukin 1, alpha	1.59
CCL23	$5.05x10^{-8}$	Chemokine ligand 23	0.86
CCL20	$5.33x10^{-8}$	Chemokine ligand 20	1.72
IFNGR2	$1.21x10^{-7}$	Interferon gamma receptor 2 (interferon gamma transducer 1)	0.59
LY86	$1.43x10^{-7}$	Lymphocyte antigen 86	-0.77
RETN	$1.56x10^{-7}$	Resistin	1.35
FCGRT	$1.90x10^{-7}$	Fc fragment of IgG, receptor, transporter, alpha	-0.59
SLPI	$1.98x10^{-7}$	Secretory leukocyte peptidase inhibitor	1.42
HMOX1	$2.14x10^{-7}$	Heme oxygenase (decycling) 1	-1.20
MMD	$4.03x10^{-7}$	Monocyte to macrophage differentiation-associated	-0.71
IL1B	$4.36x10^{-7}$	Interleukin 1, beta	1.73
IRF8	$6.47x10^{-7}$	Interferon regulatory factor 8	-0.61

Table 3.2 Immune-related differential gene expression observed during MGIT. Immune-related genes were selected from the top 200 genes showing the most significant changes in expression observed in whole blood incubated with either mycobacteria (BCG and H37Rv) or media (controls) over 96 hours.

3.4.6 Effect of cellular depletions

In an attempt to investigate the contribution of different cells to mycobacterial growth, neutrophils (CD66b+), monocytes (CD14+), T cells (CD3+) and B cells (CD19+) were depleted from the whole blood of 10 healthy volunteers, three of whom were BCG naïve. An assay using magnetic nanoparticles was optimised by testing multiple conditions, including different concentrations of cell-specific monoclonal antibodies, incubation times and temperature (data not shown). A technical control of whole blood processed with magnetic nanoparticles but without the addition of depleting antibody (WB+NP) was compared with whole blood without nanoparticles (WB) in BCG and H37Rv 96 hour MGIT. There was a trend for slightly increased growth of both mycobacterial strains with the addition of nanoparticles, but this was not significant (mean net growth WB+NP vs WB: BCG, 0.56 vs 0.51, p=0.16; H37Rv, 0.84 vs 0.80, p=0.14; paired t-test). Net growth of BCG and H37Rv cultures correlated significantly with one another (WB, r=0.64, p=0.04, data not shown).

Depleted fractions were used in a BCG 96 hour MGIT. The efficiency of the depletions, and the impact on other cell types, was assessed by flow cytometry. Efficiency was calculated as: ([undepleted fraction cell count – depleted fraction cell count]/undepleted fraction cell count) x 100 (Figure 3.8). Overall efficiency of depletion varied widely across all cell types, ranging from 44-99%. The hierarchy of depletion efficiency was CD19+>CD3+>CD66b+>CD14+ (mean efficiency 88%, 83%, 80%, and 70%, respectively) (Figure 3.9). Cell-specific depletions had no effect on the frequency of other cell types in a depleted fraction (data not shown).

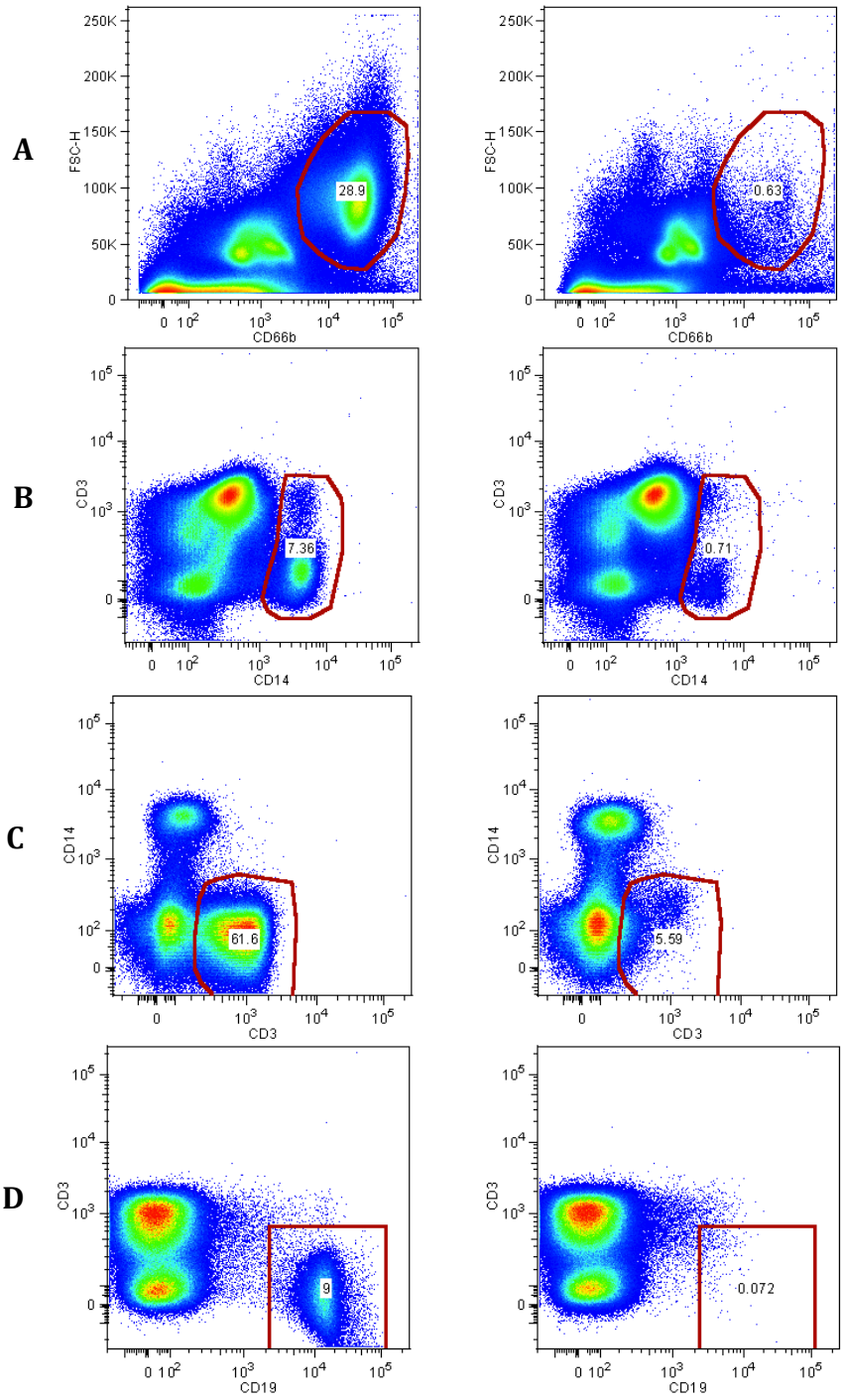


Figure 3.8 Examples of whole blood cell depletions. Neutrophils (CD66b+) (A), monocytes (CD14+) (B), T lymphocytes (CD3+) (C), and B cells (CD19+) (D) were depleted from whole blood. The efficiency of depletions was assessed by flow cytometry. Cells were gated initially by size (SSC-A vs FSC-H), followed by selection of live cells (not shown). Cell subtypes were identified by staining cell surface markers and histograms were constructed to assess the change in cell frequency following depletion.

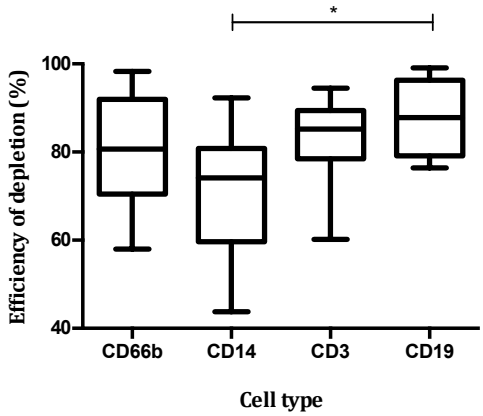


Figure 3.9 The efficiency of cell depletions. Neutrophils (CD66b+), monocytes (CD14+), lymphocytes (CD3+), and B cells (CD19+) were depleted from whole blood and the depletion efficiency was determined by flow cytometry: ([undepleted fraction cell count - depleted fraction cell count]/undepleted fraction cell count) x 100. Bars represent median values, boxes 25th and 75th centiles and the whiskers minimum and maximum values. A matched multiple comparisons one-way ANOVA with Tukey's post-test correction was performed comparing mean efficiency of depletion for each cell subset. * represents a p-value of <0.05.

The effect of depleting cell subsets on BCG growth varied considerably, although overall the pattern of increased mean change in net growth was CD66b+>CD14+>CD3+>CD19+ (mean change in net growth 0.18, 0.12, 0.08, 0.06 $\log_{10}$ cfu, respectively) (Figure 3.10). Overall, removing neutrophils and monocytes resulted in increased net growth for all volunteers, although the magnitude of the observed increases varied between them. For neutrophils, there was a positive correlation between increasing depletion of these cells and net growth (r=0.63, p=0.05, Pearson's correlation), however for monocytes such a relationship was not evident. The effect of removing lymphocytes and B cells resulted in changes in BCG growth in 6 and 7 of the 10 volunteers, respectively, and the magnitude of increased growth was less than that seen with other cell subsets. No significant correlation between efficiency of depletion and change in net growth was noted, although there was a negative trend for B cells.

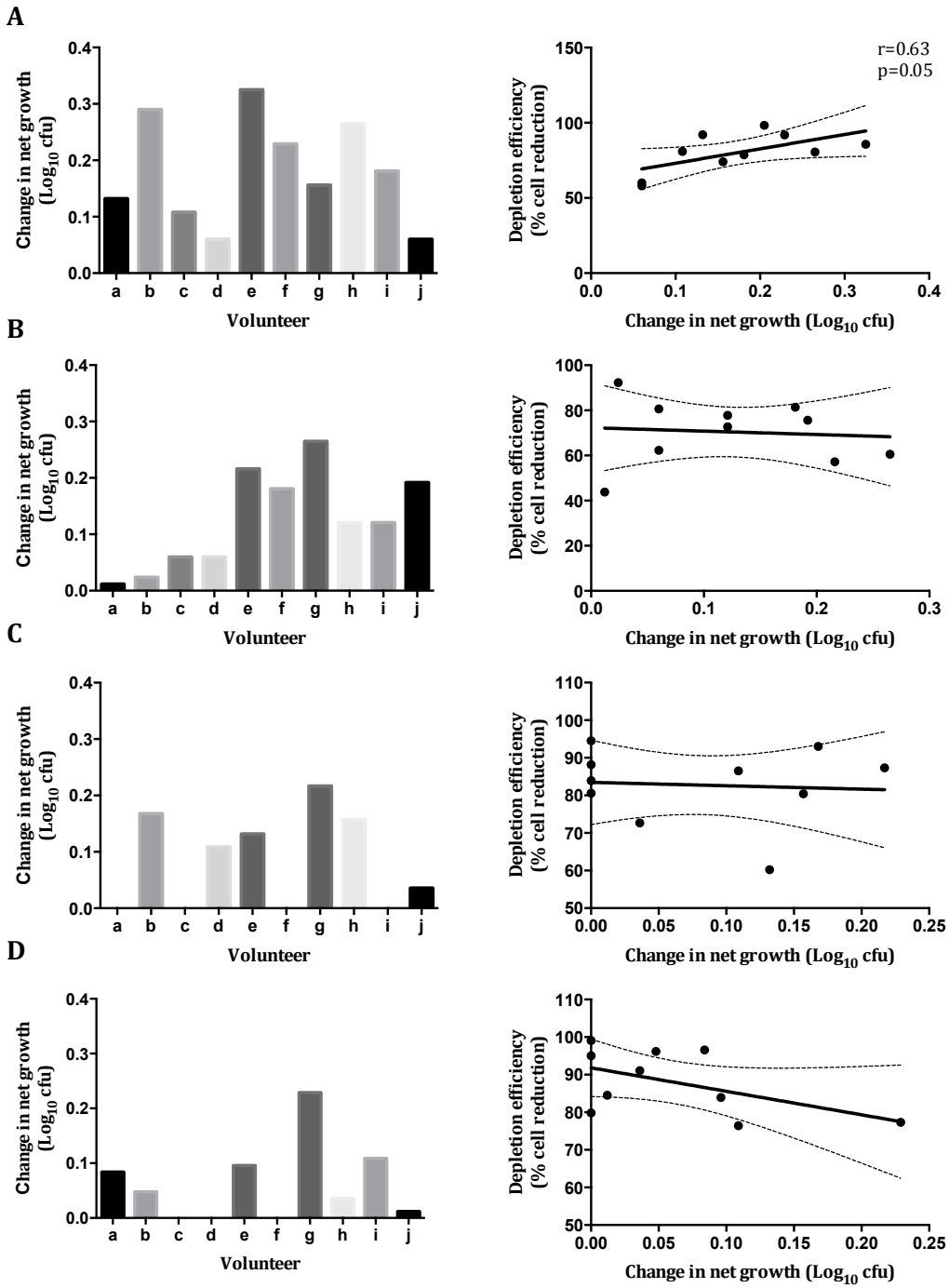


Figure 3.10 The effect of cell depletions on BCG whole blood MGIT. Neutrophils (A), monocytes (B), lymphocytes (C), and B cells (D) were depleted from the whole blood of 10 healthy volunteers (a-j). Left panels show changes in BCG net growth following depletions (mean values of duplicates). Right panels show the correlation between absolute change in BCG net growth and the percentage depletion efficiency for each volunteer. A linear regression model was used to fit trend lines based on mean values (solid lines) and 95% CI (dashed lines).

3.5 Discussion

As described in the introduction, over the past 30 years many variations of MGIA have been developed. The host group has selected the BACTEC MGIT system using a PBMC-based assay to investigate effects of candidate TB vaccines on *in vitro* mycobacterial growth. This approach offers an automated, rapid, very sensitive readout of bacillary growth, while using a cellular compartment thought to be most reflective of vaccine-induced adaptive T cell responses and therefore offering greatest discrimination of vaccine immunogenicity [361, 365].

In contrast to vaccine-induce responses, there is increasing evidence for the role of multiple innate and adaptive immune factors in the control, and pathology, of TB [21]. Therefore, for the current study a whole blood BACTEC MGIT assay was chosen to investigate the postulated spectrum of *M. tb* infection and disease [357]. This approach gives an unbiased readout based on the summative contributions of all components of the blood compartment, both cellular and non-cellular, in the absence of defined mechanisms. Furthermore, there is minimal manipulation of the sample and the effects of cryopreservation and thawing of cells seen with PBMC-based assays are avoided [365]. The potential limitation of using peripheral blood samples in terms of studying mycobacterial immunity is that this compartment is unlikely to simulate the complexity of the primary pathological manifestation of TB - the pulmonary granuloma. However, lymphohaematogenous spread is known to occur during early dissemination of *M. tb* and mycobacteraemia is increasingly recognised [366, 367]. Peripheral blood samples are easily accessible and are the most frequently used samples for biomarker discovery, allowing comparison between studies. This was a novel application for the host laboratory, therefore it was necessary to validate and characterise the whole blood BACTEC MGIT assay.

One of the key parameters assessed was CV, and values of less than 50% are considered an acceptable level of variation when using a functional, cell-based assay [368]. This study planned to recruit volunteers from three clinical sites, ranging in distance from 0.5 to 216 miles to the laboratory. This introduced considerable variation in the time from blood collection to processing and assay set-up, therefore delays in time-to-processing from 1 to 9 hours were studied (thought to represent the extremes of collection and processing intervals). Throughout, greater mycobacterial growth was seen with H37Rv than BCG, which is consistent with other studies showing enhanced growth of clinical and virulent strains of mycobacteria over BCG and attenuated strains [357]. The CV was less than 10% for each strain and there was no significant difference in net growth over the time-course for BCG or H37Rv, indicating acceptable variability and suggesting this is a reproducible platform when using samples collected remotely.

Precision is an important component of any assay and has been defined as "the closeness of agreement between a series of measurements obtained from multiple sampling of a homogenous sample under prescribed conditions" [368]. Intra-assay variability ('within' variation of multiple assays performed using a single sample at a single time) and inter-assay variability ('between' variation of multiple assays performed using a single sample at different times) are the two constituent parts of precision and each were evaluated for the whole blood MGIT.

Intra-assay variability was minimal, with CVs of less than 1% for controls and less than 2% for samples. These data are similar to those previously reported and are well within acceptable limits [365]. Analysis of ΔTTP allowed for the calculation of statistically robust exclusion criteria for duplicates in subsequent experiments. Variability was consistently less in both controls and samples when using H37Rv compared to BCG. This is likely related to the increased virulence of H37Rv and

associated enhanced growth and it has been shown previously in human and macaque PBMC MGIT that a higher TTP, indicative of slower growth, is strongly positively correlated with increased variability [365]. The observation that CVs were marginally higher in samples than controls is likely due to the procedures for each assay. Control and sample tubes were established using the same volume of master mix of bacillary stock. However, control tubes were set-up on day 0 and mycobacteria were inoculated directly into supplemented Middebrook OADC enrichment (MGIT) media. In contrast, samples underwent a 96 hour rotational culture before processing and inoculation into liquid MGIT media. While aliquots of whole blood were taken from the same LH vacutainer tube, even very small pipetting errors that may have arisen due to the viscosity of blood could affect the relative frequencies of the constituents (some of which may support growth, e.g. iron-rich haemoglobin, while others may restrict it, e.g. innate and adaptive immune cells) and therefore introduce variability. In addition, variability may have occurred during the several steps of post-96 hour culture processing. Notwithstanding this, CVs were still very low. And well below the 50% limit suggested.

A greater degree of inter-assay variability was noted, although over an 8 month period CVs were only 22% for BCG and 16% for H37Rv which are similar to those previously reported and acceptable for a functional assay [349, 361]. The controls are probably very important in minimising these CVs as they allow for normalisation of mycobacterial stocks and growth conditions within and between experiments. However, the increase in inter- versus intra-assay variability is unsurprising given the natural variation of biological samples. While all volunteers were healthy at each time-point of blood collection, sampling occurred at different times of the day and differences in several haematological parameters were noted. It has been shown that

neutrophil function, and the concentration of iron and glucose may affect mycobacterial growth [369-371].

Time-course experiments showed a significant increase in net growth with increasing culture time. The rate of mean net growth between 24 to 96 hours was greater for H37Rv than BCG (0.23 versus 0.15 $\log_{10}$ cfu/day, respectively), consistent with preceding data and other studies [351, 357]. Mean net growth of H37Rv was less at 24 hours than that of BCG. Despite increased virulence and overall growth kinetics, this initial delay may be due to increased bacillary recovery time for H37Rv after cryopreservation and thawing, particularly if lag-phase organisms are present, which is a risk when culturing faster growing strains despite care to prepare stocks of mycobacteria from mid-log cultures. This is circumstantial and net growth was comparable at 48 hours between strains. Interestingly, the inter-assay CVs peaked at 48 hours for both BCG and H37Rv before declining to a nadir at 96 hours. This may be related to the slow replication time of mycobacteria (20-24 hours) [372]. Bacillary replication may reach a significant threshold at 48 hours after culture onset and 1-2 generation times, which may stimulate a dynamic immune response, causing variable outputs until stabilisation at 96 hours.

As noted, the more virulent H37Rv consistently showed greater mycobacterial growth than BCG, although there was a good correlation in net growth between the strains. While BCG is logistically easier to use than *M. tb*, the latter is the causative pathogen of TB disease which is the focus of this study, and the importance of studying immune responses and bactericidal activity against both virulent and attenuated mycobacteria has previously been highlighted [357, 360].

In order to gain a greater understanding of the contributions of BCG and *M. tb* during the whole blood MGIT, DGE over time was evaluated. Unsurprisingly, a clear difference was evident in patterns of DGE between both mycobacteria and the control cultures over the time-course. The most significant changes in expression were in defence and inflammatory gene clusters and many of the genes identified have been previously reported to play a role in human responses to mycobacteria, such as interferon and Fc-γ receptor-related genes [235]. While this assay is not designed to replicate the complexity of *in vivo* human *M. tb* infection, it is reassuring that appropriate DGE appears following *ex vivo* challenge of whole blood with mycobacteria.

Between H37Rv and BCG, it was not until 72-96 hours that significant differences in gene expression were seen. Interestingly, when analysing these differences over the duration of the culture, it was mitochondrial pathways that dominated functional gene clusters. This is consistent with the hypothesis that virulence-specific perturbations in mitochondrial function and morphology can occur. In contrast to avirulent strains, virulent mycobacteria suppress macrophage apoptosis early in infection to promote survival, maintain an environment for bacillary replication and disrupt normal antigen presentation [373, 374]. Mitochondria play a critical role in apoptotic pathways and therefore would be potential targets for manipulation by *M. tb* [373, 374]. A recent study of the early perturbations in mitochondrial function induced by *M. tb* showed that human monocytes infected with H37Ra rapidly underwent apoptosis, which was significantly attenuated in cells infected with H37Rv [375]. Structural and functional perturbations in the mitochondria of host cells occurred soon after infection resulting in exhausted H37Ra-infected monocytes, whereas the mitochondria in cells infected with H37Rv demonstrated increased activity [375]. Such differences in virulence may be due to differential antigen expression and in particular the presence of RD1 antigens. Unlike H37Rv, BCG lacks RD1 genes, which have been shown to attenuate *M.*

tb when deleted [376, 377]. Furthermore, *M. tb* appears to manipulate the timing and mode of death of infected host cells and favours necrosis over apoptosis in order to facilitate dissemination and transmission [378]. Intriguingly, evidence suggests that some virulence factors of H37Rv are encoded for by RD1 and may contribute to host cell necrosis after *M. tb* infection through induction of mitochondrial dysfunction and depletion of intracellular ATP [379]. The human whole blood transcriptomic data reported here are the first of their type and support the approach of using both BCG and H37Rv in order to capture a broad range of host immune responses.

Depletion experiments were performed to investigate the contribution of different cell types to the MGIT assay output. Most positive and negative cell selection systems rely on column technology, which typically requires significant dilution of samples to allow flow-through. This may have an effect on a whole blood functional assay and therefore the EasySep® system was used for cell depletion studies due to minimal sample manipulation and dilutions, which are comparable with a normal whole blood MGIT assay. However, there were limitations to the system. The range of cell subsets for depletion was chosen as they are the major immune constituents of the blood compartment, but also due to the limited preparatory reagents available for use. The EasySep® system is recommended for the positive selection of cells using small volumes of blood and requires red blood cell lysis and repeated elutions to enhance purity. The experimental design here used larger volumes of blood for negative selection and erythrocyte lysis and multiple elutions were not possible due to the potential effects on sample function.

Despite several adaptations and optimisations of the protocol, the efficiency of depletion was variable. It is noteworthy that the hierarchy of depletion efficiency was B cells, T cells, neutrophils and monocytes (high to low efficiency). This generally reflects

the relative proportions of these subsets in whole blood, with the exception of monocytes (1-7, 7-24, 30-80, 2-12%, respectively) [380]. The declining efficiency of depletion with increasing cell number is intuitive. For monocytes, the worse-than-expected depletion efficiency may be due to soluble CD14. CD14 exists in two forms, one bound to the cell membrane (mCD14) and a soluble form (sCD14) that appears either after shedding of mCD14 or by direct secretion from intracellular vesicles [381]. sCD14 may have competed with mCD14 for binding to anti-CD14 antibodies, therefore reducing the depletion efficiency of monocytes.

The technical controls with nanoparticles showed increased net growth, albeit non-significant. The assay uses bi-specific tetrameric antibody complexes (TAC) directed against both the cell subset of interest and dextran. Following incubation, magnetic dextran iron nanoparticles are added which bind to the TAC, pulling the entire cell-bound complex to the periphery of the reaction tube by magnetism. The manufacturer states that the nanoparticles are biologically inert and do not interfere with subsequent assays. However, any unbound nanoparticles may have been carried over to the culture and it is possible that the increased iron content could have augmented mycobacterial growth [382].

In terms of the effect of cell depletions it is perhaps unsurprising that neutrophil depletion showed the most consistent and greatest impact, increasing mycobacterial net growth to some extent in all samples. In animal models of *M. tb* infection, neutrophils are abundant during early lesion formation and in humans they are found in the airways of patients with pulmonary TB in significant numbers [383-387]. Furthermore, an inverse relationship between neutrophil counts and risk of infection among contacts of patients with pulmonary TB has been reported [182]. Neutrophils have been shown to phagocytose and either restrict or kill mycobacteria in several *in*

vitro studies [388]. Consistent with the findings here, a BCG *lux* bioluminescence assay demonstrated the capacity of whole blood to restrict the growth of mycobacteria, which was reduced following neutrophil depletion [182]. Another study reported significant and rapid killing of virulent *M. tb* shortly after phagocytosis by neutrophils [389]. Interestingly, this study also showed inconsistencies between individuals in the capacity of their neutrophils to kill mycobacteria, suggesting a contribution of neutrophils to host variability in susceptibility to *M. tb* infection and disease, consistent with observational studies [390]. However, the role of neutrophils in TB is not fully defined and controversies exist. In contrast to the view of having a protective function, some investigators suggest that they may actually exacerbate TB pathology [370].

Despite the relatively low frequency of monocytes in peripheral blood, and even with suboptimal depletion efficiency, reduced monocyte counts were associated with increased mycobacterial growth in most volunteers. Monocytes are known to play an important role in innate immune responses to *M. tb.* Early *in vitro* studies showed reduced or completely inhibited mycobacterial replication in monocytes from BCG-vaccinated animals [391]. *In vivo*, monocytes accumulate early in infection and differentiate to effector macrophages, which produce TNF-α and help control *M. tb* replication and granuloma formation [392]. Dysfunctional cell trafficking due to abnormal chemokines and/or chemokine receptors decrease the recruitment of monocytes to the site of infection and mycobacterial control subsequently declines. In mice, this has been reported with overexpression of CCL-2 (MCP1) and the absence of CCR2 [393-395]. In humans, gene polymorphisms in *CCL2*, *CCL3L1* and *CCR5* have been associated with increased susceptibility to pulmonary TB [396, 397]. It has been suggested that since these associations have been noted in adults, it is likely that monocytes are crucial to maintain durable control of *M. tb* and the prevention of reactivation of latent infection [20]. Indeed, the TNF-α antagonists adalimumab and

infliximab are known to increase the risk of reactivation of *M. tb* and have been shown to induce apoptosis of human monocytes [398, 399]. In contrast to neutrophils, the lack of correlation between the magnitude of monocyte depletion and change in net growth may reflect the functional heterogeneity of these cells. 'Classical monocytes', defined as CD14+CD16+ cells, form the major human subtype and make up 90-95% of the total cellular population, and therefore were the primary target of monocyte depletion assays [400]. However, recent studies have suggested that qualitative effects are more important than quantitative effects in explaining the capacity of monocytes to control mycobacterial growth and have also highlighted important functional relationships with other cells types [401]. Experiments of mixing monocytes and lymphocytes from healthy individuals at different ratios suggested that differences in monocyte function and differential gene expression were dependent on the monocyte:lymphocyte (ML) ratio, but on neither constituent alone, and therefore qualitative differences in monocytes may be better reflected by the ML ratio than solely by monocyte counts [401]. Observational studies have identified what has been termed a 'Goldilocks effect' where extremes of numbers of monocytes relative to lymphocytes results in poor mycobacterial control. The risk of TB disease was been shown to be significantly higher among individuals with ML ratios lower than the 5th or greater than the 95th percentiles of a population [402]. It is particularly interesting that the two individuals in the experiments reported here at the extremes of monocyte depletion, which resulted in the greatest and smallest changes in ML ratios, showed the least increase in mycobacterial growth following depletion, highlighting the complex interaction between qualitative and quantitative elements. The ML ratio appears prognostic in both influenza and malaria and may reflect differences in microenvironment [403, 404]. Subsets of haematopoietic stem cells (HSCs) have biases in the ratio of myeloid and lymphoid cells they generate [405-408]. It has been suggested that the peripheral

ML ratio results from differences in the proportions of myeloid-biased, balanced, or lymphoid-biased HSCs and that the ontogeny of monocytes and lymphocytes, reflected in their ratio, may affect mycobacterial control [402]. The lineage biases of HSCs and hence the ML ratio may be altered directly by *M. tb* infection. Recent studies have shown that mycobacteria can infect bone marrow mesenchymal stem cells and alter haematopoiesis [409, 410]. Alternatively, the ML ratio may reflect an individual's position on the spectrum of *M. tb* infection and TB disease [402, 411].

The mean depletion efficiency of CD3+ lymphocytes was relatively high but the effects were variable, with decreased control noted in only some individuals. No correlation between the degree of cell depletion and change in mycobacterial growth was seen. In a previous study using a whole blood MGIT, the depletion of CD4+ or CD8+ T cells alone resulted in modest reductions in mycobacterial control to an attenuated strain of *M. tb* only among PPD-positive individuals, while simultaneous depletion of both T cells subsets produced additive effects [357]. In a further study, only TST-positive children showed increased growth of BCG *lux* following CD4+ or CD8+ T cell depletion in a whole blood assay [353]. Interestingly, three of the five individuals here that showed no or little change in growth after CD3+ T cell depletion were BCG unvaccinated. In prior studies, individuals received contemporaneous BCG vaccination while here most volunteers were historically BCG vaccinated, some up to 20 years previously. The heterogeneous functional capacity of T cells from such individuals may be partly due to the interval between vaccination, with waning immunity and reduced ability to generate an effective memory response occurring over time [412]. Observational studies have indicated that the protective effects of BCG against TB disease are maintained for only 15 years following vaccination, although some studies show the effects can persist for 50-60 years [413-416]. While the role of CD4+ T cell-mediated responses to, and control of, mycobacterial infection are well known, the impact of

CD8+ T cells are less well understood [21]. While there is no evidence to suggest that different CD3+ T cell subsets were preferentially depleted or retained, it is not possible to comment on the individual functional contributions of the relative proportions of these cells following depletion on mycobacterial growth.

Finally, despite representing the smallest proportion of immune cells in whole blood, depletion of CD19+ B cells resulted in an increase in mycobacterial net growth in several individuals. There is increasing recognition of the role of B cells and antibodies in host responses to TB and the methodological basis of the whole blood MGIT allows for the postulation of the mechanism of B cell-mediated control. Passive transfer experiments of *M. tb*-specific monoclonal antibodies, human polyclonal IgG or homologous immune sera have shown improved outcome following *M. tb* infection in murine models [417-425]. In human and animal studies, an inverse association between *M. tb*-specific antibody titre and susceptibility to *M. tb* infection and TB disease has been described [426-429]. Antibodies may have many diverse functions against *M. tb* ranging from the direct, including pathogen opsonisation and complement activation, to the indirect such as immunomodulation through activating and inhibitory Fc receptors [430]. However, given the short duration of the whole blood MGIT assay and the absence of lymphoid tissue, it may be difficult to generate such antibody responses. Insufficient time between antigenic stimulation and assay termination may preclude the proliferation of antigen-specific resting B cells and their differentiation into antibody-producing plasmablasts and plasma cells, particularly as there are no lymphoid structures to facilitate this. Even if one considers a potential role for thymus-independent antigens, these are not known to have a prominent role in mycobacterial responses and again, the kinetics of such a response are not feasible here. However, other studies have shown the spontaneous release of BCG-specific IgG from unstimulated cultures, but using purified PBMC fractions [431]. Currently, there are no

data to support a role for B cell proliferation or *M. tb*-specific antibody production during the whole blood MGIT assay therefore it would be interesting to study these dynamic aspects. An alternative explanation for the effects of B cells seen here could relate to their effector functions and interactions with T cells, neutrophils, monocytes and dendritic cells through antigen-presentation and cytokine production, as previously described [432, 433].

In summary, the effect of cellular depletions on mycobacterial growth in a whole blood MGIT has highlighted several issues. Firstly, there are considerable technical difficulties associated with depleting cells from whole blood using minimal manipulation in order to maintain *ex vivo* properties. As a result, the efficiency of depletion varied widely. Secondly, for logistical reasons, each cell subset was depleted in isolation and further combinatorial depletion studies may dissect the complexity of cellular interactions in the assay. Finally, the variability of the effect of cell depletions is dependent not only on differences in the efficiency but also on the functional capacity of cells to control growth, both within and between individuals. The advantage of the whole blood MGIT is that it captures this heterogeneity as a single functional output of net mycobacterial growth, reflective of the summative effects of the both cellular and non-cellular constituents of whole blood.

4 BCG vaccination as a mycobacterial challenge model

4.1 Statement of authorship

The blood samples used in the experiments described here were collected by Donna Tupper (Infantry Training Centre, Catterick). The author performed all of the assays with occasional assistance from Rachel Tanner and Stephanie Harris (The Jenner Institute, Oxford).

4.2 Introduction

It has been proposed that part of the spectrum of responses to infection with *M. tb* will include quiescent and subclinical infection before leading to symptomatic active disease [100]. These conditions are likely to consist of persisting bacilli in various states of senescence or replication. Therefore, bacillary load *in vivo* will likely have a crucial influence on immunological control by the host. Correlating antigenic load with MGIA profiles would explore fundamental aspects of the host-pathogen relationship and allow delineation of the clinical spectrum of infection with mycobacteria. BCG is a live, replicating mycobacteria and therefore BCG vaccination can be considered as a timed mycobacterial challenge. Using such a model, in parallel with studies of patients with *M. tb* infection and TB disease, would provide a further point on the spectrum of host-pathogen interactions and the opportunity to investigate markers of antigenic burden. As described, currently there are no sufficiently sensitive methods of determining antigenic load directly in asymptomatic individuals with *M. tb* infection. Diagnosis is made indirectly by demonstrating immune sensitisation to *M. tb*-specific antigens. Measuring *M. tb*-specific immune responses, cell-mediated and also humoral, may be valuable surrogate markers of bacillary burden. Parallels to this may be drawn when considering the clinical spectrum of disease associated with *M. leprae* infection,

in which humoral responses play a key role. Therefore, differences in B cell responses may reflect the clinical status of *M. tb*-infected individuals. While there is increasing interest in the role of B cells and antibodies in TB, data are limited. IgG and IgA antibodies are produced in response to *M. tb* infection but poor sensitivity and specificity limits the diagnostic utility of serological assays [434-438]. Greater resolution may be gained by studying cellular responses, specifically, *M. tb*-specific plasmablasts as indicators of active infection and memory B cells (mBCs) as indicators of resolved or subclinical infection [431, 439, 440].

I therefore sought to study a group of recent BCG vaccinees as a model of mycobacterial challenge to assess MGIA responses following vaccination and to investigate the utility of B cell assays as surrogate measures of bacillary burden

4.3 Aims

The aims of the experiments described in this chapter were to:

i. Assess the ability of the whole blood MGIT assay to demonstrate enhanced mycobacterial control following BCG vaccination.
ii. Develop a mycobacterial antigen-specific ELISA to assess humoral responses.
iii. Develop BCG-specific antibody secreting cell (ASC) and memory B cell (mBC) assays to evaluate responses to BCG vaccination.
iv. Immunophenotype PPD-specific B cells following BCG vaccination.

4.4 Results

4.4.1 Study population

This study used samples collected from healthy adult volunteers from a cohort of Gurkha recruits undergoing initial military training at the Infantry Training Centre,

Catterick, UK. The general characteristics of this population are described in detail in Chapter 5. Ethical approval was granted by the Ministry of Defence Research Ethics Committee (MoDREC Protocol 237/PPE/11). Written informed consent was obtained from each volunteer prior to participation.

A group of volunteers shown to be negative for LTBI by T-SPOT.TB IGRA (performed by Oxford Immunotec, Oxford, UK) and without known history or physical evidence of prior BCG vaccination (naïve group) were enrolled (n=11). In addition, a small control group of volunteers (n=4), negative for LTBI and historically vaccinated with BCG in infancy, were also enrolled (control group). All volunteers were male and there was no significant difference in the median age between naïve and control groups (18.9 vs 20.5 years, respectively, p=0.3).

The naïve group received a single intradermal vaccination with BCG SSI in accordance with current British Army public health policy. The control group did not receive BCG vaccine. Peripheral blood samples were collected pre-vaccination, 1 week and 10 weeks following vaccination for real-time MGIT assays, PBMC isolation and serum storage (Figure 4.1).

4.4.2 Effect of BCG vaccination on mycobacterial growth

The whole blood MGIT assay using BCG Pasteur was performed with samples collected pre- and 10 weeks post-vaccination with BCG from naïve and control groups. At pre-vaccination baseline, there was less mycobacterial net growth in control versus naïve volunteers (mean net growth 0.68 and 0.81 $\log_{10}$ cfu, respectively; p=0.05) (Figure 4.2 A). Net growth remained stable within the control group over the study period. However, using the MGIT assay, a reduction in mycobacterial growth, suggesting enhanced control, was detected 10 weeks post-vaccination in the naïve group (mean

net growth 0.81 and 0.69 log_{10} cfu, respectively; p=0.01) (Figure 4.2 A). Of the 11 volunteers receiving BCG vaccination, 7 demonstrated a reduction in net growth while the remaining volunteers showed no change (Figure 4.2 B).

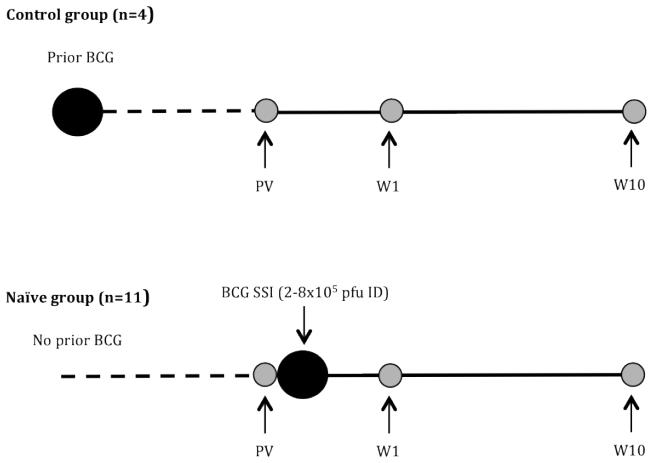


Figure 4.1 BCG vaccination study schedule. Peripheral blood samples were collected from two groups of volunteers (BCG naïve and BCG vaccinated) at pre-vaccination (PV), 1 week (W1) and 10 weeks (W10) following BCG vaccination of the naïve group.

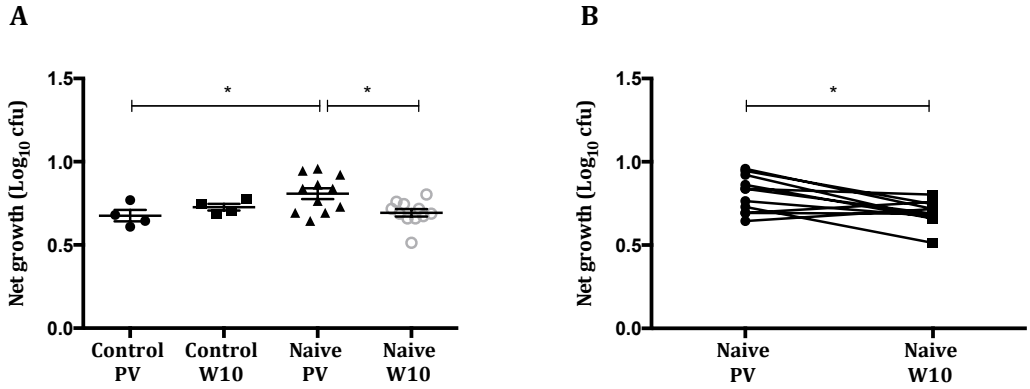


Figure 4.2 Effect of BCG vaccination on mycobacterial growth control. A whole blood MGIT assay with BCG Pasteur using samples collected pre- and 10 weeks post-vaccination from naïve (n=11) and control (n=4) groups (A). Points represent the mean of duplicates; bars represent mean values with SEM. Changes in individual responses within the naïve group are also shown (B). A paired t-test was performed within each group. * represents a p-value of <0.05.

4.4.3 IgG antibody induction following BCG vaccination

An ELISA was used to evaluate the induction of IgG antibodies to a variety of mycobacterial antigens following BCG vaccination. Total IgG was measured, as this was the class of antibody detected in subsequent B cell ELISpot assays. Antigen-specific total IgG was determined against the BCG used for vaccination (BCG SSI) and several antigens derived from virulent *M. tb* (H37Rv whole cell lysate, cell membrane fraction, culture filtrate and LAM). Baseline responses at pre-vaccination and subsequently at 1 week and 10 weeks after BCG vaccination of naïve volunteers were determined. The control group who had been historically BCG vaccinated did not receive further BCG vaccination but matched time-course antibody levels were measured. While there was no difference in IgG antibody responses between pre- and 1 week post-vaccination, significant increases were noted between pre- and 10 weeks post-vaccination (Figure 4.3). These increases were seen against all of the antigens tested, but most significantly to BCG and H37Rv cell membrane fraction (Figure 4.3). Furthermore, there were highly significant positive correlations between the relative increases in IgG antibodies to all of the antigens, suggesting that individuals mounted similar magnitudes of IgG induction to several mycobacterial antigens (Table 4.1). No correlation between whole blood MGIT mycobacterial net growth and antibody responses was seen (data not shown).

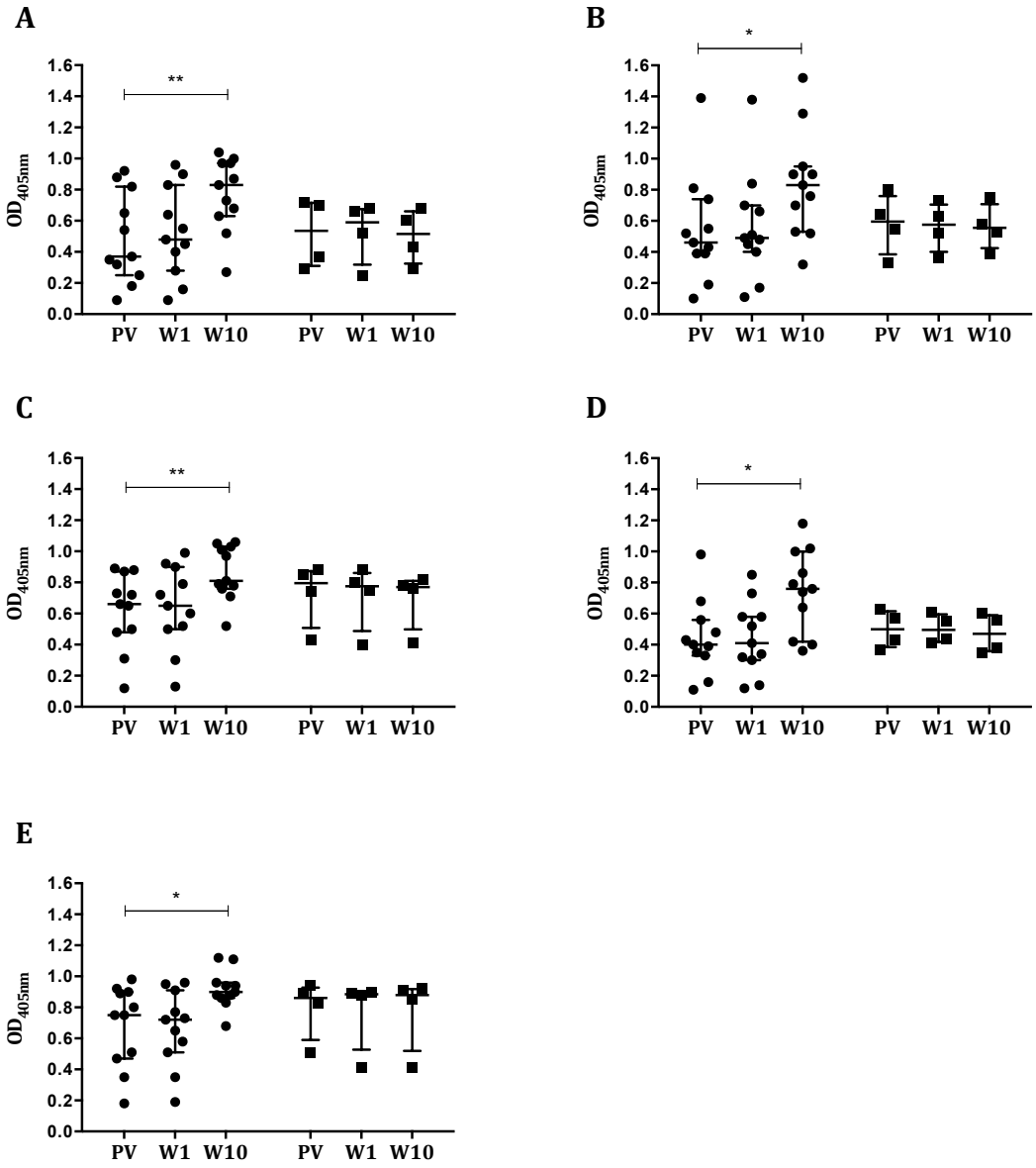


Figure 4.3 IgG antibody responses following BCG vaccination. Antigen-specific total IgG responses at pre-vaccination (PV) and at 1 week (W1) and 10 weeks (W10) after BCG vaccination of naïve volunteers (n=11) were determined by ELISA. A control group with prior BCG did not receive secondary BCG (n=4). Antigens used were whole BCG SSI (A), whole cell lysate (B), cell membrane fraction (C), culture filtrate (D) and LAM (E) prepared from *M. tb* H37Rv. Optical densities are reported following subtraction of the background. Points represent the mean of duplicates; filled circles indicate naïve volunteers and filled squares controls; bars represent median values with the interquartile range. A matched repeated measures multiple comparisons ANOVA with Dunnett's post-test correction was performed using PV as the control data. * represents a p-value of <0.05 and ** a p-value of <0.005.

Antigen	BCG	Whole cell lysate	Cell membrane fraction	Culture filtrate	LAM
BCG		0.954 ****	0.881 ***	0.887 ***	0.800 **
Whole cell lysate	0.954 ****		0.864 **	0.919 ****	0.797 **
Cell membrane fraction	0.881 ***	0.864 **		0.946 ****	0.941 ****
Culture filtrate	0.887 ***	0.919 ****	0.946 ****		0.901 ***
LAM	0.800 **	0.797 **	0.941 ****	0.901 ***	

Table 4.1 Correlation of antigen-specific IgG antibody responses following BCG vaccination. Relative increases in IgG antibody responses in the naïve group were calculated ([OD_{405} week 10] – [OD_{405} baseline]) for each ELISA antigen and a Pearson correlation matrix was generated. Pearson r correlation coefficients are shown with significance, where ** represents a p-value of <0.005, *** a p-value of <0.0005 and **** a p-value of <0.0001.

4.4.4 Evaluating B cell responses following BCG vaccination

B cell ELISpot assays were developed to detect BCG-specific IgG-secreting ASCs indicative of either antigen-specific plasmablasts (overnight assay) or mBC, enumerated following several days of culture and stimulation with polyclonal mitogens (causing differentiation into ASCs). The antigen used was the same BCG given during vaccination (BCG SSI). The transient induction of plasmablasts was noted 1 week following BCG vaccination in the naïve group (mean of 20 ASC per million PBMC or 1.7% of total IgG+ ASC), which was undetectable by week 10 (Figure 4.4 A and B). No plasmablast responses were seen among the control group. The controls did however show persisting BCG-specific mBC responses (mean of 16 mBC-derived ASC per million cultured PBMC or 0.06% of IgG+ mBC-derived ASC) (Figure 4.4 C and D). In addition,

mBC responses were seen in the naïve group at 1 week after vaccination and increased significantly by week 10 (Figure 4.4 C and D). A strong correlation between ASC responses at week 1 and BCG-specific IgG antibody induction at week 10 was seen, and while there was similar trend with week 1 anti-BCG IgG antibodies, this was not significant (Figure 4.5).

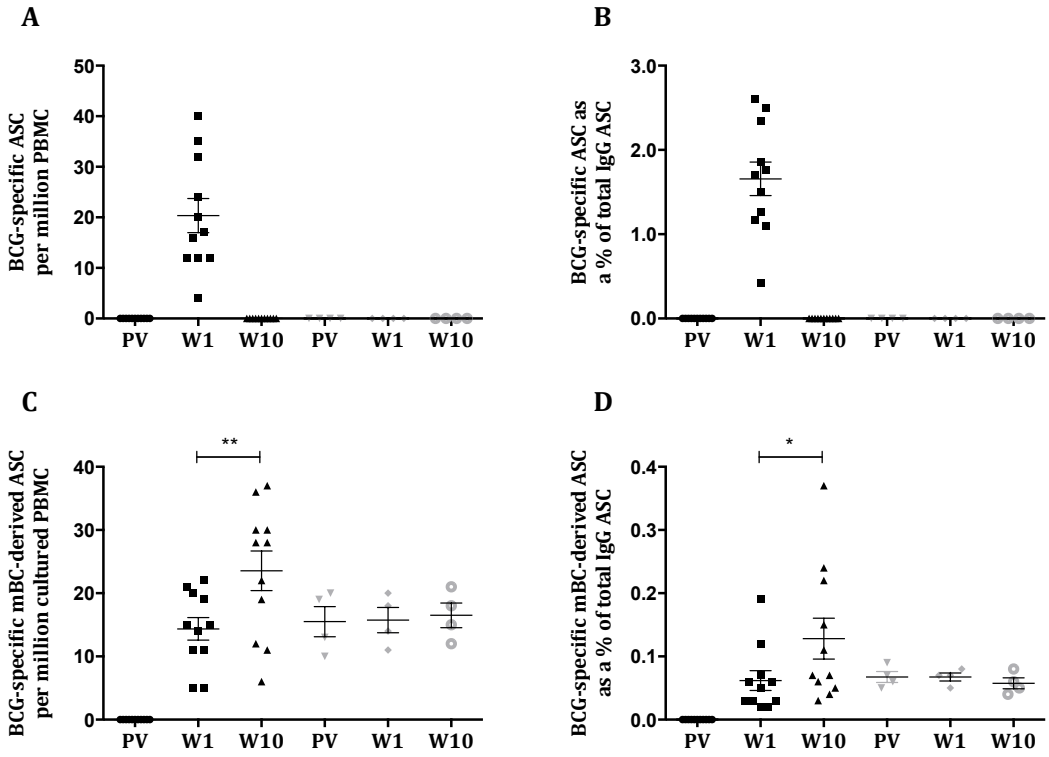


Figure 4.4 BCG-specific IgG-secreting ASC and mBC responses following BCG vaccination. IgG-secreting plasmablast (ASC) and mBC (mBC-derived ASC) responses to BCG were determined at pre-vaccination (PV) and at 1 week (W1) and 10 weeks (W10) after vaccination of naïve volunteers (n=11, black symbols) and for a control group with prior BCG who did not receive secondary BCG (n=4, grey symbols). ASC responses are presented as the number of BCG-specific ASCs per million PBMC (A) and as the proportion (%) of total IgG-secreting ASC (B). mBC responses are shown as the number of BCG-specific mBC-derived ASC per million cultured PBMC (C) and as the proportion (%) of mBC-derived ASC of total IgG-secreting ASC (D). Points represent the mean of triplicates at two dilutions; bars represent the mean with SEM. A paired t-test comparing mBC responses between W1 and W10 was performed. * represents a p-value of <0.05 and ** a p-value of <0.005.

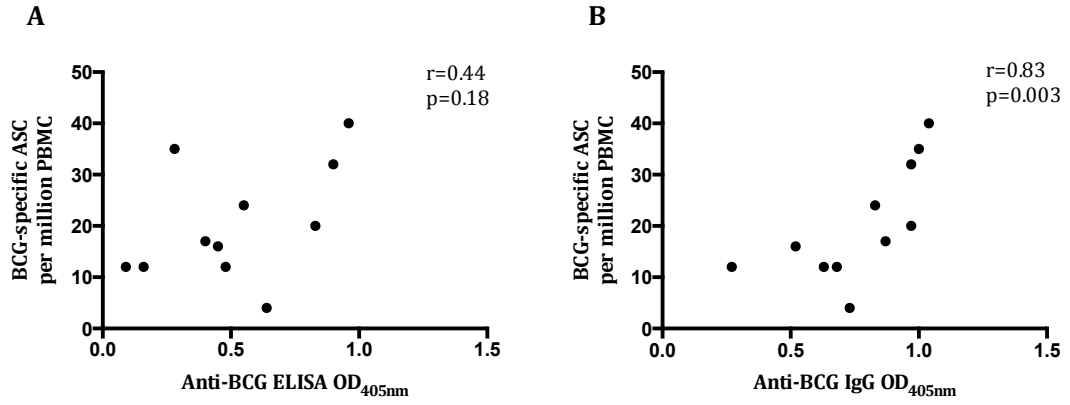


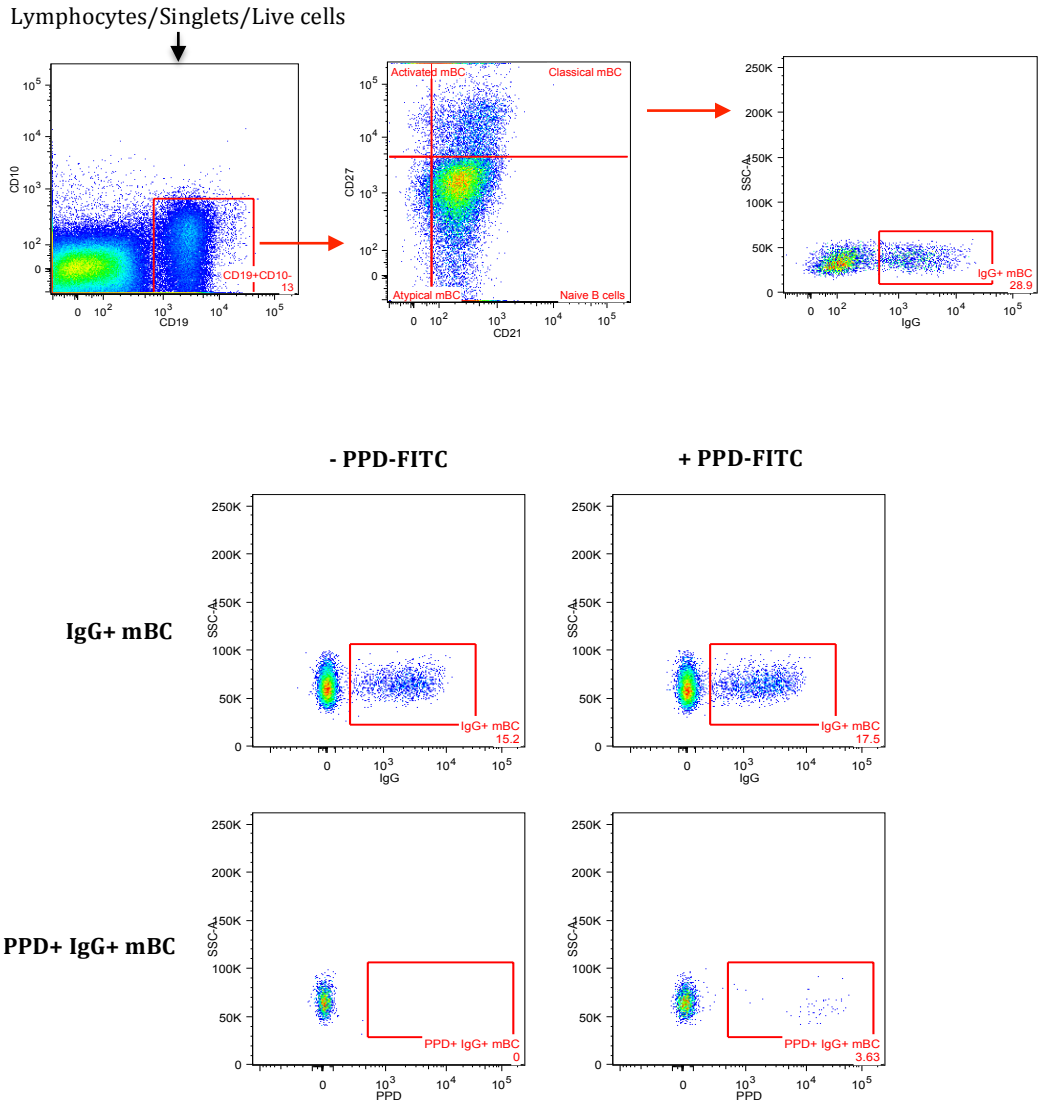
Figure 4.5 Correlation between BCG-specific ASC responses and IgG antibody induction following BCG vaccination. A Spearman rank correlation was performed between ASC responses and anti-BCG IgG induction measured at 1 week (A) and 10 weeks (B) after BCG vaccination (naïve group, n=11). Spearman rank correlation coefficient (r) and p-values are shown.

4.4.5 Immunophenotyping PPD-specific B cell responses following BCG vaccination

To develop a method for quantitation of mycobacterial-specific ASCs and mBCs by flow cytometry using fluorochrome-conjugated PPD, PPD was labeled with FITC and Alexa Fluor® 488 using proprietary peptide labeling kits. Initial experiments were performed to determine the success of labeling by analysing emission spectra by flow cytometry, which indicated that the PPD-FITC conjugate should be used in subsequent experiments (data not shown). In order to evaluate the specificity of PPD-FITC, cryopreserved PBMC from 4 volunteers who had been screened for participation in a clinical vaccine trial were used. Each individual was born in the UK, had never received BCG vaccination and was negative for PPD and *M. tb*-specific antigen responses by IFN-γ ELISpot. These cells were surface stained with a seven-colour panel and after selecting lymphocytes and singlet cells by size parameters, followed by live cells, IgG+

classical mBC were identified (CD19+, CD10-, CD21+, CD27+, IgG+) (Figure 4.6 A). A comparison of PPD-FITC stained and unstained controls unfortunately showed the presence of PPD+ IgG+ classical mBC (Figure 4.6 A and B). Several PPD-FITC titrations were performed in an attempt to reduce background responses, but clear discrimination could not be achieved (data not shown). In view of the apparent lack of exposure of these individuals to mycobacterial antigens, these results were suggestive of non-specific binding and therefore this approach was not pursued.

A



B

Volunteer	± PPD-FITC	CD19+ (%)	Classical mBC (%)	IgG+ mBC (%)	PPD+ IgG+ mBC (%)
001	-	10.9	11.0	12.7	0
	+	11.0	10.6	12.7	3.7
002	-	13.9	17.1	23.8	0
	+	14.4	17.4	25.0	2.6
005	-	13.4	11.8	7.7	0
	+	13.9	11.5	7.8	5.8
006	-	11.7	17.0	15.2	0
	+	11.6	16.9	16.5	3.6

Figure 4.6 Identifying PPD-specific B cells by flow cytometry. A PPD-FITC conjugate was generated and tested in a mycobacterial-naïve cohort to determine specificity (n=4). Cells were gated initially by size (SSC-A vs FSC-H), followed by selection of live cells (not shown). IgG+ classical mBC were identified as CD19+, CD10-, CD21+, CD27+, IgG+ and a comparison of PPD-FITC stained and unstained cells from naïve individuals showed non-specific binding (A). The proportion of CD19+ cells is calculated from live singlet lymphocytes, classical mBC from total mature CD19+ cells, and IgG+ mBC from total mBC (B).

4.5 Discussion

The purpose of the experiments described above was to develop B cell and humoral assays to measure responses to mycobacterial antigens as surrogate markers of bacillary load. Sample from naïve individuals receiving routine BCG vaccination were used as proof-of-concept for this approach as they would be known to have controlled, recent exposure to live, replicating mycobacteria. The overall aim of this study was to stratify individuals by ability to control mycobacterial growth based on the readout of a whole blood MGIA. Therefore, it was important to assess whether the MGIA could identify differences in control following BCG vaccination, considering recent BCG

vaccination as a live, replicating, mycobacterial challenge model. The stability of net growth over time was evaluated in a control group and was consistent with the findings reported earlier during MGIT assay characterisation (Chapter 3). The majority of naïve healthy adults showed significant enhanced mycobacterial control between pre-vaccination and 10 weeks after receiving BCG vaccine. These results are consistent with the reduced growth seen using this MGIA as early as week 4 following primary BCG vaccination in Rhesus and Cynomolgus macaques and after 8 weeks in human vaccinees [361, 365]. Other studies using variations of a whole blood MGIA have reported similar findings [349, 351, 357]. Furthermore, the heterogeneity among subjects in their responses to BCG vaccination seen here is consistent with these studies, which have shown no improvement in control of *in vitro* mycobacterial growth with repeated BCG vaccination [441]. It is well documented that the efficacy of BCG is highly variable, ranging from 0-80% in different settings, and that vaccine-induced immunity may wane with time, failing to confer adequate protection against pulmonary disease, particularly among adolescents and young adults in high-endemic regions [442-446]. Several reasons have been proposed for reduced BCG vaccine efficacy in these settings, such as poor nutritional status, exposure to non-tuberculous mycobacteria (NTM), helminth infection and the effect of host genetic heterogeneity on susceptibility [447-450]. A recent systematic review of randomised controlled trials found that the absence of sensitisation with environmental NTMs was associated with higher efficacy of BCG against pulmonary (and also possibly miliary and meningeal) TB [451]. Pre-existing immunity to NTM may either 'block' the effects of BCG vaccination by inhibiting the replication of BCG and preventing the induction of protective immune responses or 'mask' the effects as BCG is unable to further boost background immunity induced by NTMs [448, 452]. In addition, chronic helminth infections may also have a modulatory effect on vaccine efficacy, causing a shift towards Th2-type immunity,

impaired antigen-specific and Th1-type responses and the induction of regulatory T cells producing TGF-β and other inhibitory cytokines, which suppress pro-inflammatory cytokines. These responses have been associated with reduced efficacy of BCG in endemic settings [453-456]. The volunteers receiving BCG in this study were all recent arrivals in the UK from Nepal and while their nutritional status was good it is very likely that they would have been exposed to NTM and helminths, which may account for the heterogeneity of responses to vaccination observed. However it should be noted that faster and more significant reductions in net growth of mycobacteria have been shown using PBMC-based assays following BCG vaccination, and this may be a more appropriate compartment to detect vaccine-induced cellular-mediated responses [361]. Nonetheless, enhanced control was detected using a whole blood MGIA after primary BCG vaccination in this population, allowing for onward studies.

The induction of antibodies following antigenic stimulation is the key response of adaptive B cell immunity. As the development of B cell assays was an important aspect of these studies, it was appropriate to evaluate whether mycobacterial-specific humoral immune responses were induced by BCG vaccination. Significant increases in IgG responses were seen following BCG vaccination, specific not only for BCG but also several *M. tb*-derived antigens. As *M. tb* is the target mycobacterium for human BCG vaccination it was interesting to measure these responses. In general, IgG antibody levels in the control group were higher than those measured in the naïve group at baseline and 1 week after BCG vaccination, however levels exceeded the control group after week 10.

While the role of antibodies in BCG vaccine efficacy and in protective immunity against *M. tb* is debated, several other studies have shown the induction of humoral immunity following BCG vaccination. One study showed significant increases in total IgG and

IgG1, IgG2 and IgG3 isotypes to *M. tb* whole cell lysate in naïve individuals 2 months after vaccination with two different BCG vaccines (BCG TICE and Connaught) [457]. The group confirmed their findings in another cohort showing significantly increased LAM-specific IgG following primary BCG vaccination, which was boosted after secondary vaccination [426]. The LAM-specific IgG was reported to mediate enhanced innate (increased uptake of BCG by neutrophils and macrophages and subsequent improved growth inhibition) and cell-mediated (increased proliferation and IFN-γ production by *M. tb*-specific CD4+ and CD8+ T cells) responses [426]. Independent findings of IgG responses against a related cell wall glycolipid, arabinomannan (AM), induced by primary and secondary BCG vaccination and which were associated with enhanced mycobacterial opsonophagocytsosis and intracellular growth reduction have been recently reported [458].

Other authors have also observed high baseline reactivity to mycobacterial antigens among some BCG-naïve individuals and have suggested cross-reactive memory responses due to prior exposure to NTM as one cause [349, 426]. Enrolling volunteers with negative IGRA or TST responses to NTM-specific antigens may surmount this problem. The highest pre-vaccination IgG antibody responses were seen against LAM, a lipoglycan and major constituent of the cell wall of mycobacteria with significant homology across species [459]. Interestingly, individuals with the highest baseline responses consistently generated the smallest increases in IgG antibody levels following vaccination, consistent with the view that prior exposure may attenuate immunity and reduce BCG vaccine efficacy.

A limitation of this study was that total IgG specific for an 'irrelevant' antigen, such as diphtheria toxin, was not measured as an additional control. There is no reason to suspect that the changes observed were a non-specific humoral response to polyclonal

stimulation of B cells. Indeed, no changes in IgG responses were seen in the control group over time, who experienced the same conditions as the naïve group except for not receiving BCG vaccination. Finally, the lack of correlation between IgG levels and net growth in the whole blood MGIA is perhaps unsurprising. Studies that have shown mycobacterial growth inhibition seemingly mediated by *M. tb*-specific antibodies have used purified PBMC fractions or cultured cells [426, 458]. The whole blood MGIA contains multiple specific and non-specific, cellular and non-cellular factors, which are likely to contribute to anti-mycobacterial immunity (hence its use). Therefore, any effect of antibodies may be concealed by the activity of these other constituents.

The rationale for developing assays to detect mycobacterial-specific B cell responses arose from the increasing appreciation of the possible role that these cells may have in host immunity to *M. tb*. Recent findings include the presence of follicle-like B cell aggregates in pulmonary granulomas in humans and animal models and it has been suggested that B cells and antibodies may differentially shift immune responses towards protection and/or pathogenesis in TB [21, 460, 461]. There is precedence for this when considering diseases associated with *M. leprae*. Both cause chronic granulomatous infections with long incubation periods. Most infected individuals do not progress to disease and there is a spectrum of presentations depending on cell-mediated immune responses [462, 463]. Milder tuberculoid disease (TT) is pauci-bacillary and infection is contained by Th1 and cell-mediated responses [464]. Multi-bacillary infection occurs in more severe lepromatous leprosy (LL), and is characterised by a poor cell-mediated response, Th2 responses and elevated antibodies [464]. This model could be applied to *M. tb*, supported by recent findings of type I IFN-β signatures in patients with LL, similar to the neutrophil-driven type I IFN-αβ response in patients with active TB [235, 465]. Transcriptomic studies show increased

expression of FcγR (high affinity IgG receptor) discriminating between active disease and LTBI groups, and elevated expression of B cell genes during treatment [268, 271, 272, 277]. Therefore, differences in humoral responses may reflect the clinical status of *M. tb*-infected individuals. Specifically, *M. tb*-specific plasmablasts (ASCs) may reflect active disease whilst memory B cells (mBCs) may indicate resolved or contained infection [431, 439, 466-469]. Plasmablasts are proliferative, short-lived antibody-secreting cells dominating early antibody responses during active infection [470, 471]. mBCs contribute to long-term humoral immunity and respond to antigen-specific re-stimulation [472-474]. Evaluating these cells would provide a more dynamic, discriminative measure of humoral responses compared to detecting stable serum antibodies by conventional serology [475, 476]. Samples from individuals recently vaccinated with BCG provided the opportunity to develop appropriate assays, especially in view of a recent report showing that long-lived mBC responses can occur following BCG vaccination [466].

ASCs appear in the peripheral circulation within days of infection or vaccination, peaking at 6-8 days, irrespective of pre-existing antibodies, then decrease rapidly to undetectable levels after 2 weeks [477]. While no BCG-specific IgG secreting ASCs were detectable in the control group at any time-point, an ASC response was seen in the naïve group 1 week after BCG, before dissipating by week 10. While there have been no other reports of ASC responses following BCG vaccination, the results here are consistent with those seen in studies of the kinetics of B cell responses to rabies, influenza and candidate malaria vaccines in naïve adults [478-480]. The magnitude of ASC responses observed here is comparable to these studies which also showed that antibody and B cell responses appeared more rapidly and of greater magnitude after secondary immunisation, suggesting that these cells may be derived from previously formed mBCs which not only have a lower threshold for activation but may also have

the ability to differentiate into plasma cells without needing to re-enter germinal centres [480, 481]. This is interesting because as described previously, ELISA detected relatively high baseline IgG responses, perhaps suggesting prior NTM exposure. Therefore, an element of the ASC response to BCG vaccination may be due to the generation of plasmablasts from pre-existing mycobacterial-specific mBCs.

BCG-specific mBC responses were detectable in the control group, who had received BCG up to 20 years previously, at all time-points. Similar findings have been reported among historic BCG vaccinees assessed 13-45 years post-vaccination [466]. The responses noted here are higher than previously seen, which may be due to the use of different antigens (PPD rather than whole BCG) and study populations. In the naïve group, mBCs induced by BCG vaccination were apparent at week 1 and peaked at week 10. These observations are consistent with the detection of mBCs in peripheral blood by 1 week of immunisation in a murine model [482]. A study assessing longitudinal mBC responses following exposure to candidate malaria vaccines showed a gradual increase in specific mBC after immunisation which peaked at 84 days until declining by 140 days [479]. The kinetics seen here are consistent with this and one would expect contraction of the mBC response to a persisting residual level over time [483]. It would be very interesting to further study the kinetics of B cell responses to BCG by evaluating earlier time-points post-vaccination and over a longer duration to assess ASC and mBC generation and persistence. Contrary to the suggestion that pre-existing mycobacterial-specific mBCs may have contributed to the ASC response in the naïve group, no mBC responses were seen pre-vaccination among these individuals. It is possible that these were not detected due to very low frequencies exceeding the limit of detection of the ELISpot assay.

The poor correlation between ASC responses and early IgG antibody induction, which improved over time, is perhaps to be expected. At 1 week following vaccination, BCG-specific antibodies would still be in the very early stages of production and would not peak for several weeks. Indeed, it may be that at 10 weeks antibody levels have started to wane and that determining responses at an earlier time-point may provide an even stronger correlation. Strong correlations of IgG plasma cell responses with IgG antibody responses after primary immunisation by area under the curve analysis has been reported elsewhere [480].

Finally, while B cell ELISpot assays are sensitive and provide information about antigen-specific cells, they require several million PBMC to perform, are very labour intensive, are dependent on the functional ability of mBCs to proliferate and differentiate into ASCs and typically take several days to complete. Therefore I sought to develop a method for quantitation of mycobacterial-specific ASCs and mBCs by flow cytometry using fluorochrome-conjugated PPD. This would have the potential to enumerate multiple B cell subsets rapidly using fewer cells. While commonly adopted for detecting viral antigen-specific B cells, this approach has not been described before for mycobacteria [484, 485]. Unfortunately, substantial non-specific staining of mBC from mycobacteria-naïve individuals was seen, limiting the utility of this approach to detect antigen-specific B cell subsets. The problem of high background due to non-specific fluorochrome binding has been previously reported, particularly when using complex multi-protein antigens [486]. PPD is prepared from cultures of *M. tb*, *M. bovis* or *M. avium*, which are heat and filter sterilised and then undergo protein concentration by ultrafiltration or ammonium sulphate precipitation [487, 488]. A recent proteomics-based characterisation of PPD identified 171 different proteins among four PPD samples [488]. Most of the proteins were between 10 and 50 kDa in size, but the size distribution ranged from 7.2 to 220 kDa [488]. One way to overcome

high background staining is to use dual antigen-specific labeling to detect very small populations of antigen specific cells [489, 490]. It would be interesting to investigate this approach further.

There were several limitations to the experimental work described here including the limited size of the control group and the inclusion of naïve individuals from a resource-poor setting where prior NTM exposure may have confounded responses to BCG. Furthermore, while BCG vaccination was used as a convenient model of exposure to mycobacterial antigens, the intradermal inoculation of attenuated bacilli may not fully represent the immune response induced following natural infection with virulent *M. tb* by an aerosol route, although there is increasing interest in developing an intradermal BCG human challenge model as a surrogate for *M. tb* infection with some promising early results [362, 491, 492]. However, as a proof-of-concept I have shown that it is possible to detect humoral and *ex vivo* B cell responses following BCG vaccination using a variety of assays, supported by functional MGIA data, which have potential application in evaluating bacillary burden in patients with *M. tb* infection and disease.

5 Delineating the spectrum of *M. tb* infection and TB disease using a MGIA

5.1 Statement of authorship

Some of the blood samples used in the experiments described here were collected by Donna Tupper (Infantry Training Centre, Catterick) and Sheila Churchill (Churchill Hospital, Oxford). The author performed all of the assays with assistance from Rachel Tanner, Stephanie Harris, Lisa Stockdale and Danny Wright (The Jenner Institute, Oxford).

5.2 Introduction

It has been proposed that the pathology associated with *M. tb* exists as a spectrum rather than as a binary classification of active disease or latent infection [91, 93, 100]. This spectrum is likely to reflect the changing balance of interactions between the host and pathogen over time and there is increasing clinical, immunological and microbiological evidence to support this hypothesis. Delineating the spectrum of *M. tb* infection and identifying subgroups within it could have the potential to define the risk of reactivation of an individual, allow targeted preventative therapy and provide new approaches to drug development and vaccine biomarker discovery. Traditional approaches and current diagnostic tests lack the resolution to dissect the proposed spectrum of *M. tb* infection.

A whole blood BACTEC MGIT assay has been shown to discriminate between individuals by their functional ability to control bacillary growth following vaccination. In the absence of defined mechanisms, this assay provides an unbiased, summative assessment of mycobacterial control as a measure of anti-mycobacterial immunity.

I sought to apply a whole blood MGIA using the BACTEC MGIT system to a large population of *M. tb*-infected individuals and healthy controls to delineate the clinical TB spectrum. Identification of subgroups based on ability to control mycobacterial growth would then allow for the stratification of individuals and their subsequent characterisation using several immunological assays.

5.3 Aims

The aims of the experiments described in this chapter were to:

i. Recruit adult volunteers with active TB disease, latent *M. tb* infection and healthy controls from three centres in the UK.
ii. Collect detailed clinical information and, where relevant, to obtain blood samples before and after treatment for TB.
iii. Apply the whole blood MGIT assay using mycobacterial strains of different virulence to characterise the spectrum of phenotypes exhibited by individuals through their capacity to control bacillary growth.
iv. Assess the impact of chemoprophylaxis for latent *M. tb* infection and TB treatment for active disease on mycobacterial growth control.
v. Determine whether MGIT assay output correlates with standard clinical and/or laboratory measures.

5.4 Results

5.4.1 Study settings

Adult volunteers were recruited to this study from three clinical centres. Birmingham is the second-largest city in the United Kingdom, with a population of approximately 1 million and a surrounding conurbation of almost 2.3 million residents [493]. TB

remains a major public health concern in central Birmingham, which has one of the highest TB incidences of any European city [494]. The number of cases of active disease has risen steadily over the past 10 years and at a rate almost twice as fast as in England as a whole. The city has an overall incidence rate of TB of 35 cases per 100,000 population, but this ranges from 27 to 99 cases per 100,000 in different areas [494, 495]. Between 2012-2014, an average of 385 active cases were reported annually. Almost one third of the cases of TB diagnosed in Birmingham are acquired in Birmingham, highlighting the problem of ongoing transmission. Similar to other European cities, the majority of cases occur in people born outside the UK and their descendants [496]. The Birmingham Chest Clinic, located in the centre of the city, has provided an out-patient clinical TB service since 1934 and assesses and treats approximately 3000 patients each year. The population seen here was considered appropriate for recruiting individuals across the spectrum of *M. tb* infection and TB disease. Ethical approval was granted by the National Research Ethics Service (NRES), Heart of England NHS Foundation Trust (REC reference 2012107RM).

With a population of 158,000 and of a very different demographic, it is unsurprising that the burden of TB in the city of Oxford is considerably less than that seen in Birmingham, with an average of 36 new cases reported each year [493, 495]. The Department of Respiratory Medicine at the Churchill Hospital, Oxford, provides an out-patient service which predominantly assesses referrals from occupational health screening. Therefore the focus of recruiting individuals from this centre was on those with LTBI. Ethical approval was granted by the NRES, Committee South Central - Oxford C (REC reference 12/SC/0299).

Finally, Gurkha recruits at the Infantry Training Centre, Catterick, were invited to participate. Gurkha soldiers have been an enduring feature of the British Army since

1817. Each year up to 230 new recruits leave Nepal and arrive in the UK for a 10 month programme of intensive training. Annual selection occurs in Nepal amidst significant competition from approximately 17,000 applicants. Recruits receive a clinical assessment and CXR to exclude active TB disease and on arrival in the UK screening for LTBI is undertaken in accordance with current British Army Public Health and national guidelines [30]. Single-step IGRA testing is performed and following exclusion of active disease and in the absence of contraindications, recruits with evidence of LTBI receive a standard course of preventative therapy (3 months RMP-INH). The incidence of TB in Nepal is approximately 160 cases per 100,000 population and the rate of latent *M. tb* infection among Gurkha recruits is 10-15% [5, 497]. Ethical approval was granted by the Ministry of Defence Research Ethics Committee (MoDREC 237/PPE/11).

5.4.2 Characteristics of study participants

Between April 2013 and January 2015 a total of 211 individuals volunteered to take part in this study. Twenty-one individuals with active TB disease, defined as culture-confirmed or clinically suspected TB, participated, of whom 19 were enrolled in Birmingham. The mean age was 33.9 years and over three quarters were male (Table 5.1). Just over half of individuals were born outside the UK (57.1%) and the majority were of Indian or Pakistani ethnicity (61.9%), followed by African (19.0%). The vast majority (95.2%) reported, or had evidence of, prior BCG vaccination. Patients were enrolled with a diverse range of pulmonary and extrapulmonary TB diagnoses (Table 5.1). Pulmonary TB was the most common diagnosis (71.4%) and 38.1% of all diagnoses were confirmed microbiologically. All *M .tb* isolates were shown to be fully drug-sensitive. Each patient completed anti-TB treatment based on a standard regimen for 6 months, guided by sputum conversion to negativity and/or clinical response to therapy. Follow-up samples were obtained from 12 of the participants (63.1%).

	n=21 (%)
Mean age (years)	33.9, range 18-60
Male sex	16 (76.2)
Place of birth	
UK	9 (42.9)
Outside UK	12 (57.1)
Ethnic group	
White Caucasian	2 (9.5)
Sub-Saharan African	4 (19.0)
Indian subcontinent	13 (61.9)
Other	2 (9.5)
BCG vaccinated	20 (95.2)
Culture confirmed diagnosis	8 (38.1)
System	
Pulmonary	15 (71.4)
Extrapulmonary	5 (23.8)
Lymph node	4
Bone	1
Disseminated (miliary)	1 (4.8)

Table 5.1 Summary of the characteristics of active TB patients. Description of the demographic details and basic clinical information for the 21 patients with active TB disease enrolled into the study.

Across all of the study sites, 139 patients with LTBI, as evidenced by a positive TST and/or IGRA conversion after recent exposure, were recruited (Table 5.2). Seventy-nine volunteers were Gurkha recruits (54.7%) and of the civilian participants most were enrolled in Birmingham (n=53, 38.1%). The mean age was 30.2 years, and as with the active TB cohort, most individuals were non-UK born although represented a greater proportion of the total (89.2 vs 57.1%, respectively). The predominance of male

participants from the Indian sub-continent was mostly driven by the contribution of Gurkha recruits. There was evidence of prior BCG vaccination in 79.9% of participants. The majority of individuals completed 3 months preventative therapy (94.2%). Of those who did not, age and pregnancy were the most common reasons (Table 5.2). Follow-up samples, collected on completion of treatment, were obtained from 78 (56.1%) of these participants.

	n=139 (%)
Mean age (years)	30.2, range 18-56
Male sex	107 (77.0)[1]
Place of birth	
UK	15 (10.8)
Outside UK	124 (89.2)
Ethnic group	
White Caucasian	8 (5.6)
Sub-Saharan African	23 (16.5)
Indian subcontinent	99 (71.2)[2]
Other	9 (3.6)
BCG vaccinated	111 (79.9)
TST and/or IGRA positive	138
TST positive	1
Completed chemoprophylaxis	131 (94.2)[3]

Table 5.2 Summary of the characteristics of patients with latent TB. Description of the demographic details and basic clinical information for the 139 patients with latent TB infection enrolled into the study. Notes: [1]n=79 (73.8%) and [2]n=79 (79.8%) were Gurkha recruits; [3]n=8 (5.8%) volunteers were untreated due to the following reasons: n=4 were >35 years of age; n=3 were pregnant; n=1 reported drug intolerance shortly after commencing therapy.

Finally, 51 healthy BCG-vaccinated and BCG-naïve controls with no past history of TB or evidence of latent infection were also enrolled. Mean age was 24.6 years (range 18-56) and 38 (74.5%) were male. Thirty-three (64.7%) of these participants were born outside the UK and 32 (62.7%) were of Indian sub-continent ethnicity. A history of BCG vaccination was reported by 31 (60.8%) of individuals. Single samples were obtained from each healthy control.

5.4.3 Haematological measures among study participants

Full blood counts were determined for samples obtained from individuals before starting anti-TB treatment for those with active TB disease or latent infection, and for healthy controls. The profiles of pre-treatment white blood cell subsets showed that patients with active disease had significantly more monocytes and fewer lymphocytes than those with LTBI or the controls (Figure 5.1). The ML ratio was calculated for each individual and was seen to be significantly increased in active disease, and distinct patterns of relationships between absolute monocyte and lymphocyte counts were seen within cohorts (Figure 5.2). Among the haematological measures, haemoglobin concentration was significantly reduced in both active disease and latent infection, while platelets were elevated in patients with TB disease (Figure 5.3).

These measures were repeated on completion of treatment and compared with pre-treatment results. Among active patients, significant reductions were noted in total white cell, neutrophil and monocyte counts, with a trend to increased lymphocytes after treatment (Figure 5.4). A similar pattern was seen for individuals with latent infection after treatment, but also included declines in eosinophils and basophils (Figure 5.4). The ML ratio fell significantly in active patients after treatment and the previously seen patterns of absolute monocyte and lymphocyte counts was lost (Figure 5.5). Finally, patients with active disease and latent infection showed increases in

haemoglobin concentrations and decreases in platelet counts following treatment (Figure 5.6).

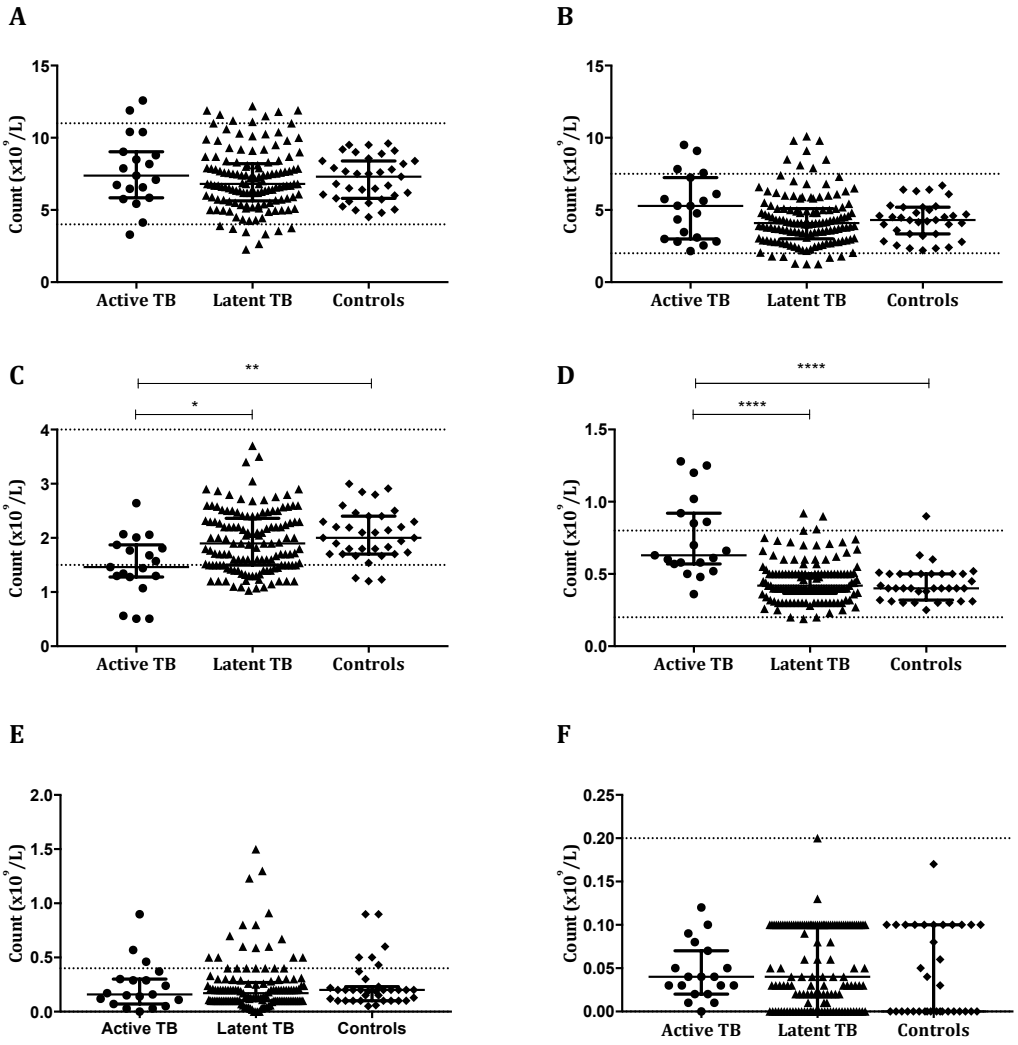


Figure 5.1 Pre-treatment leucocyte profiles. White blood cell subset counts were determined for samples from individuals before starting anti-TB treatment. Results were available for patients with active TB disease (n=19), latent infection (n=129) and healthy controls (n=35). Total leucocyte (A), neutrophil (B), lymphocyte (C), monocyte (D), eosinophil (E) and basophil (F) counts are shown. Points represent individual values; bars represent median values with the interquartile range; dashed lines are the upper and lower limits of the normal range for each cell type. After testing for normality, a Kruskal-Wallis test with Dunn's correction for multiple comparisons was performed. * represents a p-value of <0.05, ** a p-value of <0.005, *** a p-value of <0.0005 and **** a p-value of <0.0001.

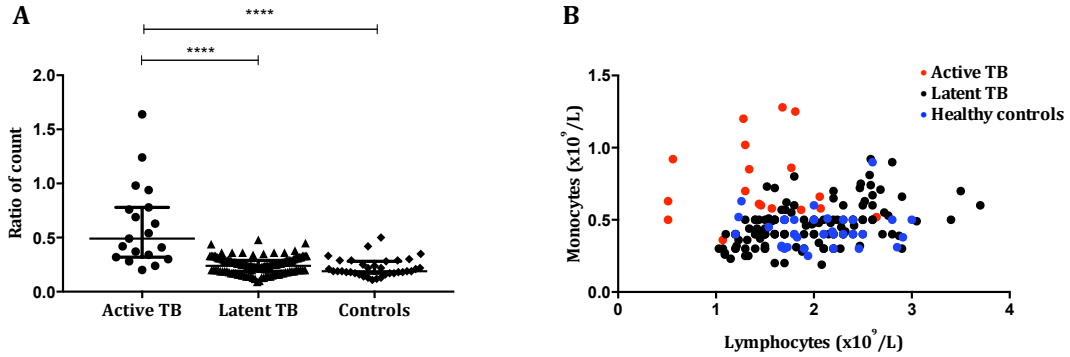


Figure 5.2 Patterns of monocyte-to-lymphocyte relationships. The ML ratio was calculated (A) and the relationship between absolute monocyte and lymphocyte counts examined (B) for individuals before starting anti-TB treatment. Points are individual values; bars are median values with the interquartile range. After normality testing a Kruskal-Wallis test with Dunn's correction for multiple comparisons was performed. **** represents a p-value of <0.0001.

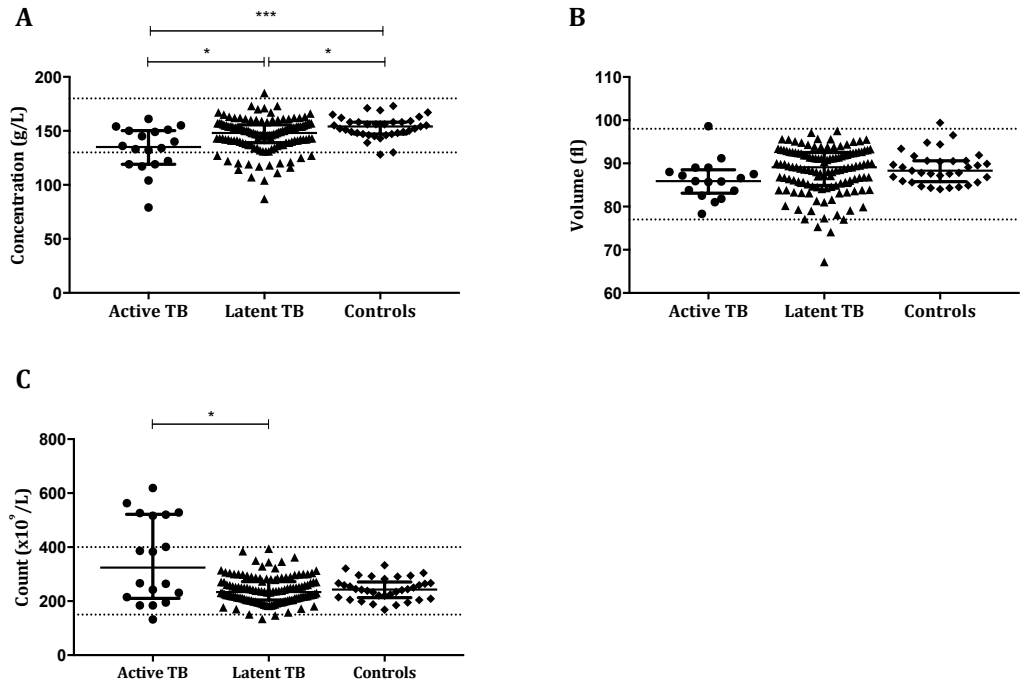


Figure 5.3 Pre-treatment haematology parameters. Haemoglobin concentration (A), mean cell volume (B), and platelet counts (C) are shown. Points and bars are as described above. After normality testing a Kruskal-Wallis test with Dunn's correction for multiple comparisons was performed. * represents a p-value of <0.05 and *** a p-value of <0.0005.

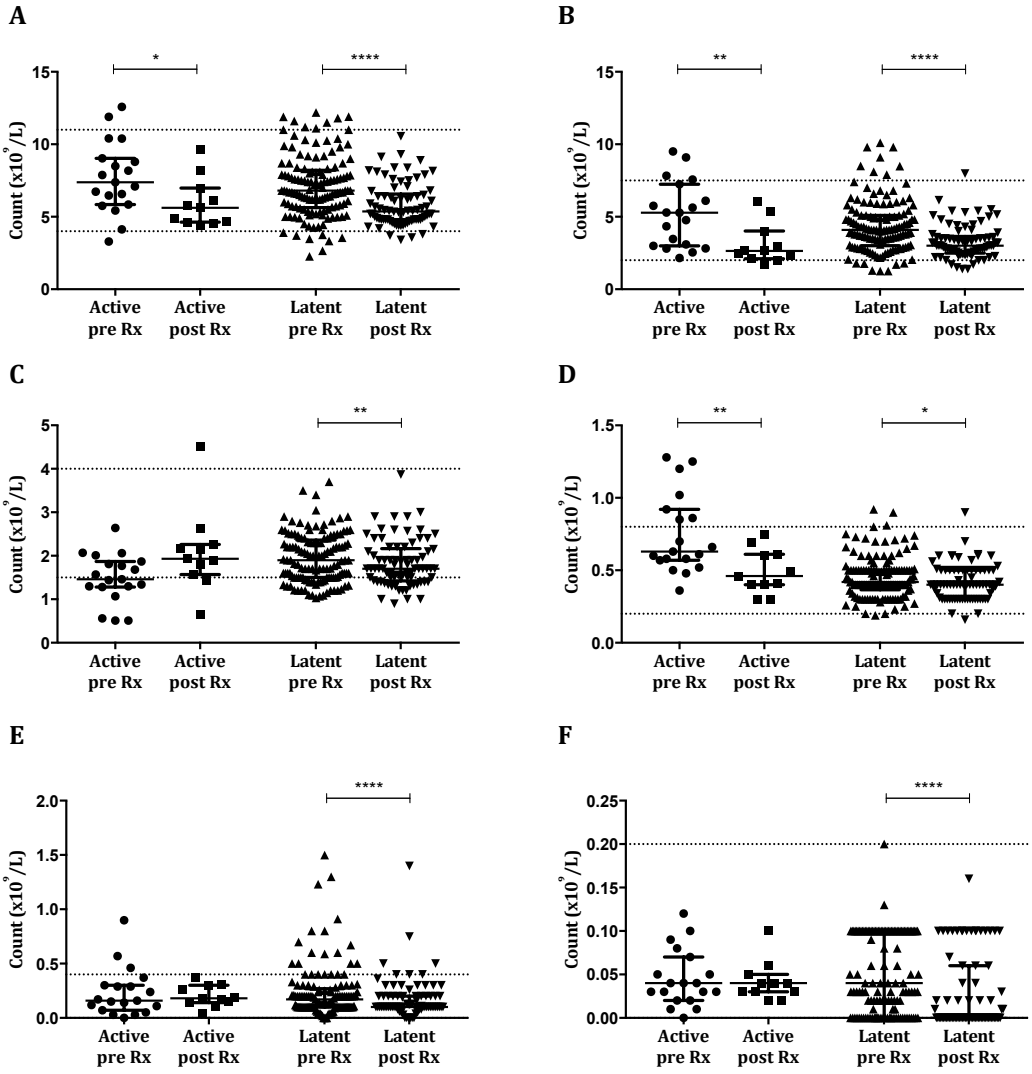


Figure 5.4 Changes in leucocyte profiles following treatment. White blood cell subset counts were determined for samples from individuals on completion of anti-TB treatment and compared with those obtained pre-treatment. Matched results were available for patients with active TB disease (n=9) and latent infection (n=77). Total leucocyte (A), neutrophil (B), lymphocyte (C), monocyte (D), eosinophil (E) and basophil (F) counts, pre- and post-treatment, are shown. Points represent individual values; bars represent median values with the interquartile range; dashed lines are the upper and lower limits of the normal range for each cell type; Rx signifies treatment. After testing for normality, a Wilcoxon matched-pairs signed rank test was performed. * represents a p-value of <0.05, ** a p-value of <0.005 and **** a p-value of <0.0001.

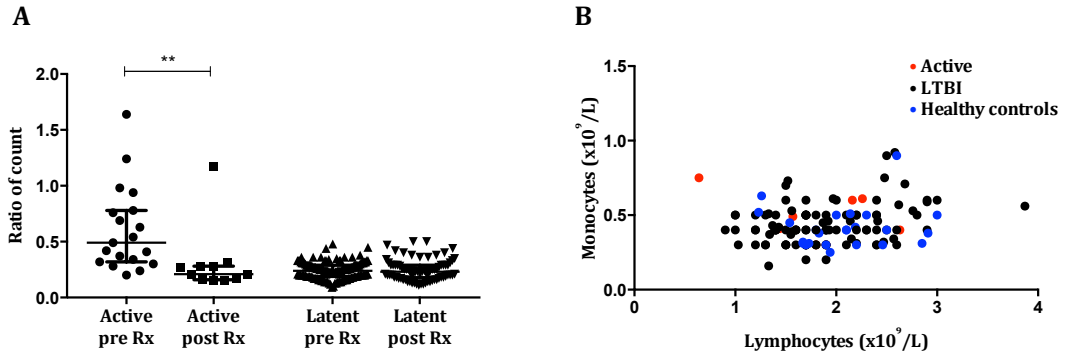


Figure 5.5 Patterns of post-treatment monocyte-to-lymphocyte relationships. The ML ratio pre- and post-treatment for TB (A) and the relationship between monocyte and lymphocyte counts after treatment (B). Matched results: active TB disease (n=9), LTBI (n=77). Points are bars are as described above; Rx signifies treatment. After testing for normality, a Wilcoxon matched-pairs signed rank test was performed. ** represents a p-value <0.005.

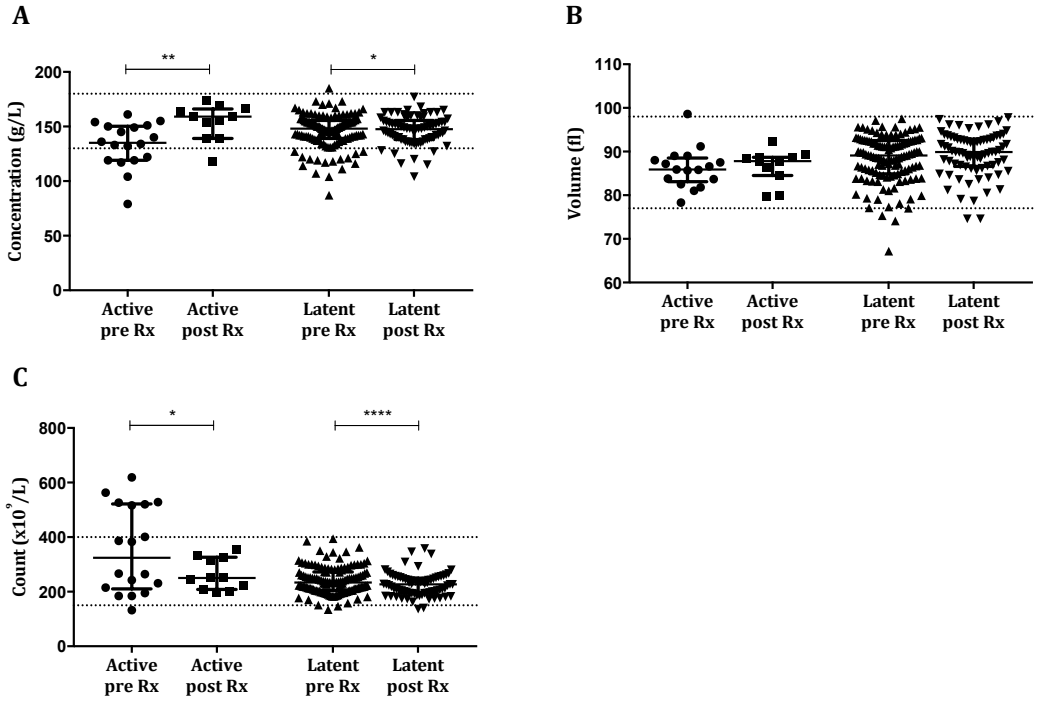


Figure 5.6 Changes in haematology parameters following treatment. Haemoglobin concentration (A), mean cell volume (B), and platelet counts (C) are shown. Points, bars, dashed lines and statistical analysis is as described above.

5.4.4 Pre-treatment whole blood MGIT

Whole blood MGIT using the BACTEC system was performed as described using pre- and post-treatment samples infected *ex vivo* with BCG Pasteur or *M. tb* H37Rv. All 211 baseline samples were tested. Following application of the previously determined exclusion criteria for samples (samples excluded if ΔTTP between duplicates was >6 hours), a total of n=11, n=93 and n=35 samples from active, LTBI and controls groups (respectively) were included for MGIT assays using BCG. The mean net growth of BCG for each of these groups was 0.24, 0.37 and 0.49 $\log_{10}$ cfu (respectively) and a significant difference in net growth was seen between each group (Figure 5.7 A). For H37Rv, n=19, n=132 and n=51 samples from active, LTBI and controls groups (respectively) met the inclusion criteria and were eligible for further analysis. Unfortunately, a large batch effect for the 2015 cohort of Gurkha volunteers resulting in net growth significantly higher than previously seen in comparable individuals was noted and therefore these samples were excluded from further analysis. This reduced the LTBI group to n=101. The mean net growth of H37Rv for each of the study groups was 0.56, 0.59 and 0.71 $\log_{10}$ cfu (respectively) and a significant difference in net growth was seen between all groups except for active TB and latent infection (Figure 5.7 B). Net growth was significantly higher in H37Rv vs BCG for active, LTBI and control groups ($p=0.01$, $p<0.0001$, $p<0.0001$, paired student t-test, respectively). There was a strong correlation between pre-treatment net growth values for BCG and H37Rv ($r=0.41$, $p<0.0001$) (Figure 5.7 C). In addition, on dividing the healthy controls on the basis of BCG vaccination status, the naïve group demonstrated a trend for reduced bacillary control of BCG when compared to individuals with historic vaccination, although this was non-significant (data not shown).

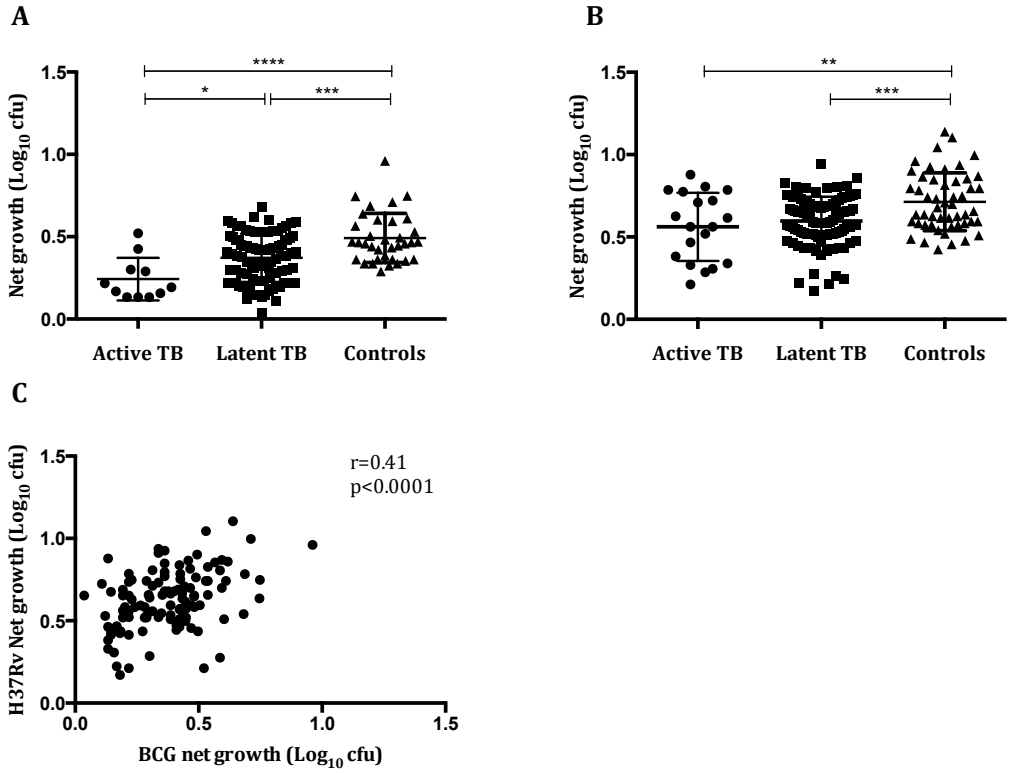


Figure 5.7 Pre-treatment whole blood MGIT. Samples were collected from volunteers with active TB, latent infection and healthy controls before starting anti-TB treatment (where appropriate). Whole blood MGIT using BCG Pasteur (A) and *M. tb* H37Rv (B) was performed and data meeting the inclusion criteria (duplicate ΔTTP <6 hours) are shown. Points represent the mean of duplicates; bars represent mean values with SD. The association between BCG and H37Rv pre-treatment MGIT results was evaluated by Pearson's correlation (C). A one-way multiple comparison ANOVA with Tukey's post-test correction was performed between the groups. * represents a p-value of <0.05, ** a p-value of <0.005, *** a p-value of <0.0005 and **** a p-value of <0.0001.

The relationship between pre-treatment mycobacterial net growth and the haematological parameters previously described was investigated. For BCG, significant positive correlations were seen between lymphocyte count and haemoglobin concentration with net growth (Figure 5.8 A and C). There was a trend towards a negative association between ML ratio and mycobacterial growth but this did not reach significance (Figure 5.8 B). However, for H37Rv monocyte count and ML ratio were

significantly negatively correlated and haemoglobin concentration and mean cell volume were positively correlated with net growth (Figure 5.9).

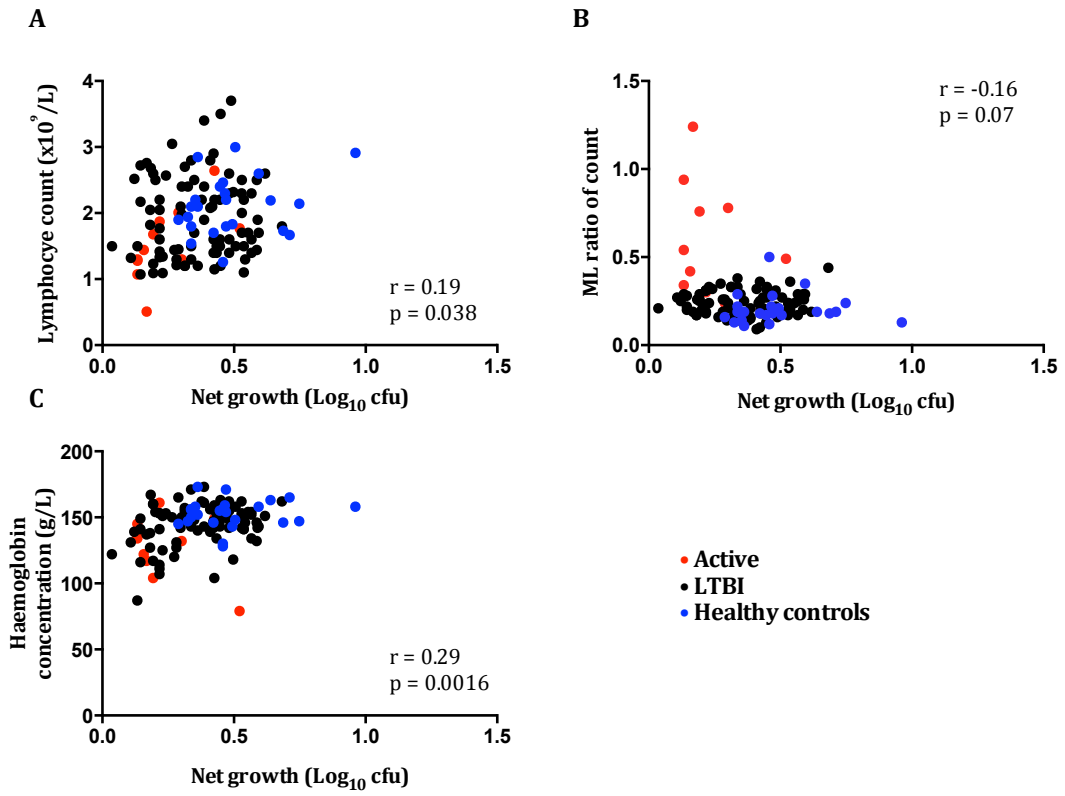


Figure 5.8 Correlations between pre-treatment haematology and whole blood BCG MGIT. The relationship between baseline BCG net growth and the haematology parameters previously described was investigated. After testing for normality, Spearman's correlations were calculated and associations were found between mycobacterial growth and lymphocyte count (A), monocyte-to-lymphocyte ML ratio (B) and haemoglobin concentration (C).

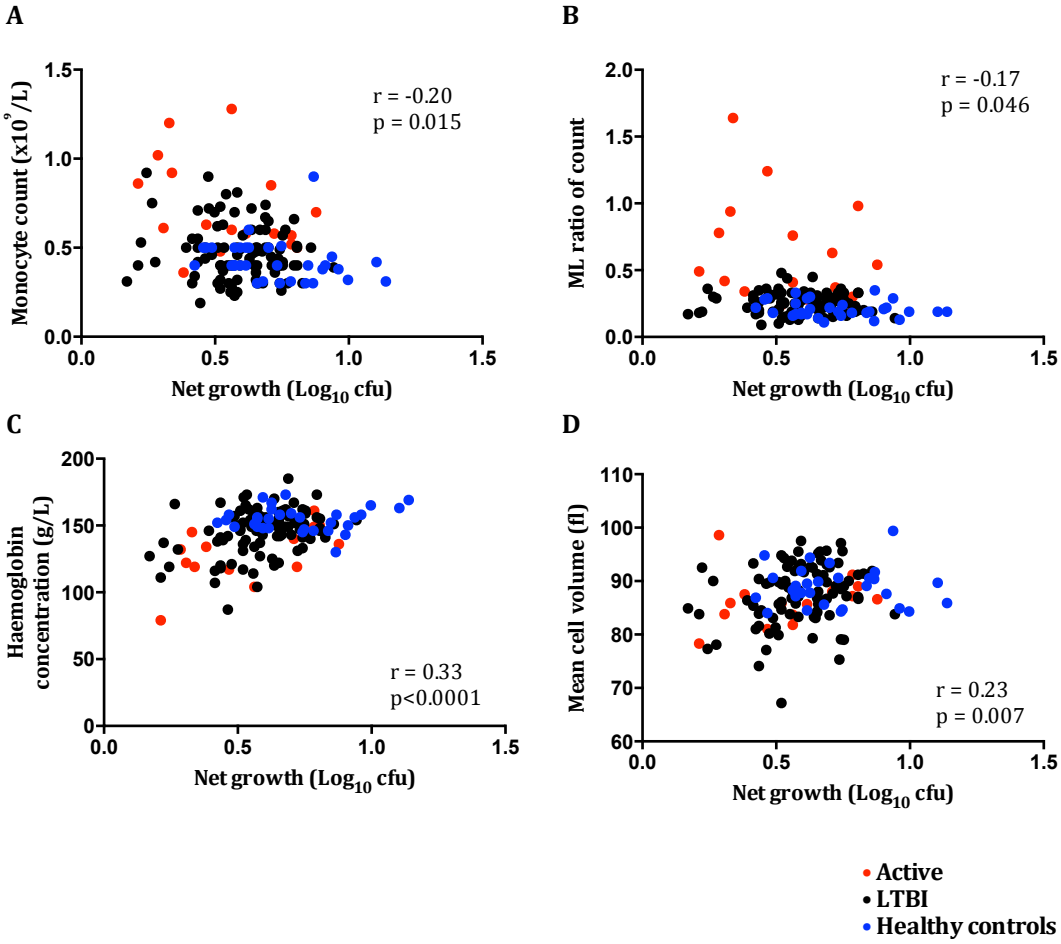


Figure 5.9 Correlations between pre-treatment haematology and whole blood *M. tb* MGIT. The relationship between baseline H37Rv net growth and the haematology parameters previously described was investigated. After testing for normality, Spearman's correlations were calculated and significant associations were found between mycobacterial growth and monocyte count (A), monocyte-to-lymphocyte (ML) ratio (B), haemoglobin concentration (C) and mean cell volume (D).

5.4.5 Post-treatment whole blood MGIT

Whole blood MGIT was repeated using samples from participants after completion of treatment for active disease and latent infection. Following application of the exclusion criteria for samples, a total of n=12 and n=50 samples from active and LTBI groups (respectively) were included for MGIT assays using BCG, while for H37Rv these values

were n=10 and n=52, respectively. Comparing pre- and post-treatment results, there were significant increases in net growth of BCG and H37Rv seen in both active TB and latently infected groups following treatment. The increases were greatest in the active TB group and for BCG MGIT (mean growth pre- vs post-treatment: active TB, 0.24 vs 0.58, p=0.006; LTBI, 0.37 vs 0.52, p<0.0001, log_{10} cfu) (Figure 5.10 A). Increased growth of H37Rv MGIT following treatment was also seen (mean growth pre- vs post-treatment: active TB, 0.56 vs 0.89, p=0.03; LTBI, 0.59 vs 0.76, p<0.0001, log_{10} cfu) (Figure 5.10 B).

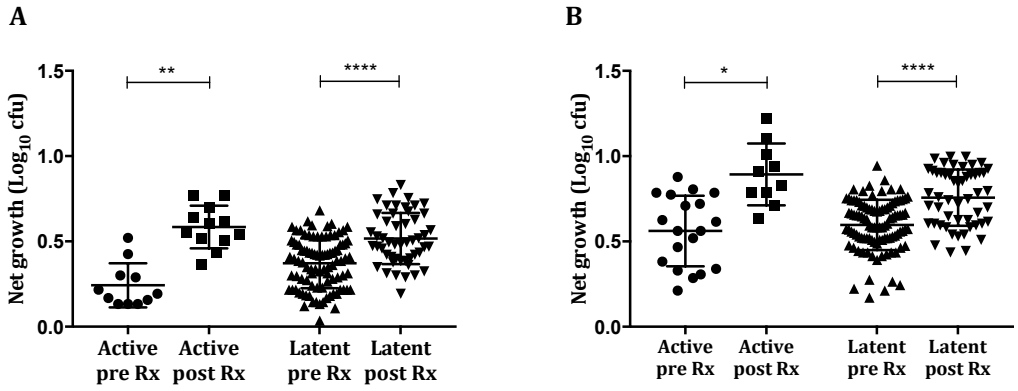


Figure 5.10 Post-treatment whole blood MGIT. Samples were collected from volunteers with active TB and latent infection between 1 to 6 months following completion of anti-TB treatment (where appropriate). Whole blood MGIT using BCG Pasteur (A) and *M. tb* H37Rv (B) was performed. Data meeting the inclusion criteria (duplicate ΔTTP <6 hours) are shown. Points represent the mean of duplicates; bars represent mean values with SD. A paired t- test was performed to assess net growth before and after treatment. * represents a p-value of <0.05, ** a p-value of <0.005 and **** a p-value of <0.0001.

The previously observed correlations between pre-treatment net growth values for BCG and the haematological parameters described were no longer evident after treatment. However, significant positive correlations between post-treatment H37Rv

net growth with monocyte count and ML ratio were seen, together with a negative correlation with lymphocyte count (Figure 5.11).

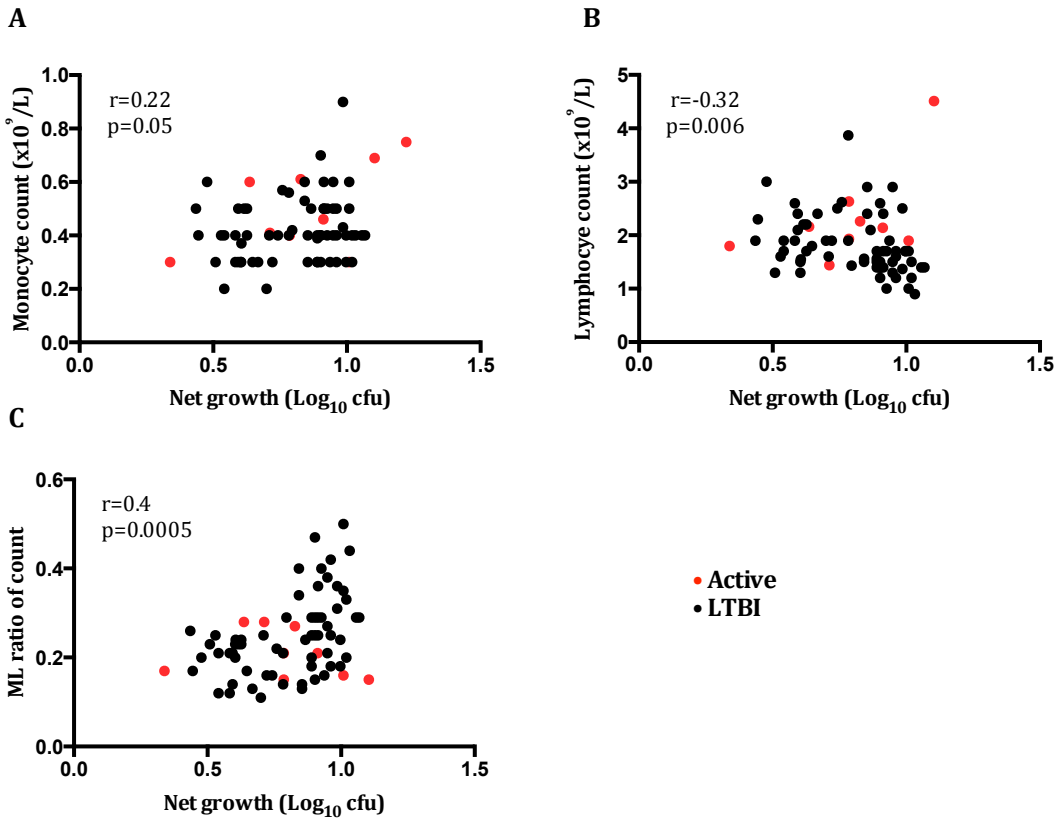


Figure 5.11 Correlations between post-treatment haematology and whole blood *M. tb* MGIT. The relationship between baseline H37Rv net growth and the haematology parameters previously described was investigated. After testing for normality, Spearman's correlations were calculated and significant associations were found between mycobacterial growth and monocyte count (A), lymphocyte count (B) and monocyte-to-lymphocyte (ML) ratio (C).

5.5 Discussion

A multi-centre approach to enroll patients for this study was used in order to recruit not only sufficient numbers, but also patients across the spectrum of *M. tb* infection and TB disease. A relatively modest number of patients with active TB were recruited but as they could be seen as a 'control' group for one extreme of TB pathology, the total was

considered acceptable. A key element of the study protocol was that samples should be obtained from patients before starting anti-TB treatment. This is often a logistical challenge and many studies investigating human TB disease recruit patients who may be in the very early stages of therapy. Whilst pragmatic, this is not ideal as the response to therapy may be rapid which could potentially affect whole blood MGIT output. For example, significant changes in the whole blood transcriptome have been shown to occur as early as one week after starting anti-TB treatment [277]. Furthermore, anti-TB drugs used in a standard regimen, such as rifampicin, are rapidly absorbed, reaching peak serum concentration within 2 hours after oral administration [498, 499]. This therefore precludes the use of such samples in a functional assay in which whole blood is co-cultured with mycobacteria. In addition, and most importantly, it is clearly not ethically acceptable to delay the commencement of therapy in order to meet the need for collecting pre-treatment samples. These factors, together with the distance between the main clinical centre for recruiting patients with active disease and the host laboratory, added to the logistical challenge of recruiting active patients. Post-treatment samples were obtained in just over 60% of these cases, highlighting the difficulty of sustaining the engagement of a patient with healthcare services and research studies once they are well, particularly after a long duration of therapy. When post-treatment sampling was achieved, it occurred at least one month after completion of treatment, as the half-life of anti-TB drugs is typically 1-5 hours and this interval would therefore avoid the potential confounding effect of residual drug [498, 499].

The demographics of the active TB patients who participated was generally consistent with the profile of such patients seen in the UK, that of young, foreign-born men. In 2014 almost 60% of new TB cases reported in England were male, occurred mostly among individuals aged 30-34 years and over 70% patients were non-UK born, commonly from the Indian sub-continent [500]. The proportion of culture-confirmed

diagnoses of pulmonary TB were below those typically reported (38% vs 60%), which may reflect difficulties with patient sampling or a lower threshold among clinicians to commence empirical therapy based on an individual's history, clinical examination and radiographic findings [495, 500]. Among the culture-negative patients, no alternative diagnoses were made as symptoms resolved and patients made clinical improvements with anti-TB treatment. It could be considered that one limitation of the cohort of patients with active TB disease was the heterogeneity of diagnoses. In human clinical studies it is often preferred to enroll a homogenous group of pathologies in order to control for confounding factors associated with differences in disease manifestations. However, although clinical definitions and currently available tests may appear to place patients within a homogenous group, the significant variation both between and within individuals with active TB has already been described. Furthermore, the proportions of pulmonary and extrapulmonary cases recruited to this study are characteristic and therefore reflective of the range of pathologies usually seen [500].

Significantly more patients with latent infection were enrolled to allow thorough evaluation of the broad spectrum of states hypothesised to exist. Power calculations using the standardised difference to yield a power of 80% and p-value for significance of 0.05 suggested that a minimum sample size of 100 individuals was required [501]. The standardised difference was calculated from the target difference and standard deviation from previous experiments that distinguished individuals on the basis of BCG vaccine-induced anti-mycobacterial responses using the whole blood MGIT. The significant numerical contribution made by the Gurkha recruits may have skewed the gender and ethnicity profile of the LTBI group. However, the overall proportion of males from the Indian sub-continent were similar to figures reported in England [500].

Pre-treatment full blood counts showed several interesting differences between study cohorts but also considerable overlap between some measures. While no significant difference in total white cell counts was noted between groups at baseline, there was a trend for increased neutrophils in the active TB group. It has previously been shown that up to 18.5% of patients with active TB disease and 3.7% of healthy contacts have a neutrophilia (peripheral blood neutrophil count ≥7.5 $\times 10^9$/L), very similar to the profiles of the cohorts here (15.8% vs 6.2%, respectively) [502]. There was no evidence of other infections or non-tuberculous bacteremia among patients enrolled in this study. The significant reductions in white cell counts noted in both active and latent cohorts following treatment probably reflected the decline in neutrophils, which would be expected following successful anti-TB therapy.

The significantly reduced lymphocyte and elevated monocyte counts seen in patients with active TB disease is consistent with earlier reports. As described in Chapter 3, it is perhaps more appropriate to consider the ML ratio rather than individual mononuclear cell subsets for several reasons. Studies in the early twentieth century first identified a relationship between the peripheral blood ML ratio and the extent and severity of mycobacterial disease in animal models and humans [503-505]. More contemporary observational studies have shown an association between the risk of TB disease in infants and HIV-infected adults in high TB incidence settings [402, 506, 507]. In addition, a recent study stratified individuals into three groups based on ML ratio and concluded that extremes of ratios were good predictors of active TB [508]. Similar findings have been reported in cattle and humans following *ex vivo* manipulation of ML ratio and subsequent ability to control mycobacterial growth [401, 509, 510]. The active TB patients described here did not show the extreme reductions in ML ratio previously reported in a subset of patients [508]. This may be an effect of size, as earlier studies have shown that it is a minority group of patients (up to 16%) who

display decreased ratios, which would be difficult to demonstrate with a small cohort [508].

The effect of *M. tb* on ML ratio may result from either alteration in HSC subsets or by infection of bone marrow mesenchymal stem cells [409, 410]. This is a reasonable hypothesis as human and animal studies have shown that HSCs are biased towards myeloid or lymphoid cells, therefore *M. tb* may alter the proportions of these biased HSCs and thus alter the ML ratio [405-408, 508]. Importantly, following anti-TB treatment, high ML ratios declined while low ML ratios increased to levels seen in healthy controls [508]. These findings perhaps support the assertion that reductions are due to effective therapy rather than drug-associated suppression of cell production or cell destruction. The ML ratio may also have a prognostic value beyond active disease. Most recently, a prospective longitudinal study of clinical and laboratory markers associated with the risk of developing active TB in HIV-negative household contacts with latent infection has shown that the appearance of disease symptoms was significantly associated with an elevated peripheral blood monocyte count and an increased ML ratio [511].

Anaemia is a common haematological abnormality, which occurs in up to one third of patients with TB, but is typically mild and resolves with anti-TB treatment [512]. This is very consistent with the data presented here. Chronic infection, such as TB, can cause anaemia, which may be due to suppression of erythropoiesis by direct infection of bone marrow by *M. tb*, nutritional insufficiency or reduced iron absorption and utilisation [512-514]. It has also been suggested that inflammatory cytokines such as IFN-γ, TNF-α, IL-1 and IL-6 induce the sequestration of iron into the reticulo-endothelial system resulting in reduced haemoglobin synthesis, inhibition of erythroid progenitor cell and erythropoietin activity [513, 515, 516]. Of note, one study reported that a high

proportion of TB patients had reduced haemoglobin and haematocrit concentrations after completion of the intensive phase of TB therapy and suggested drug-induced anaemia as the cause [517].

It is well recognised that platelets play crucial roles in haemostasis, thrombosis and in chronic inflammatory diseases. However, recent studies have shown a variety of platelet functions in response to infection and sepsis, including entrapping pathogens, the activation and recruitment of neutrophils and monocytes and the modulation of T and B lymphocyte functions [518-523]. In relation to TB, activation of thrombocytopoiesis and elevated peripheral platelet counts has been reported in active disease [524]. Whether this reflects a non-specific inflammatory response to chronic infection is unknown. Interestingly it has been recently shown that platelets can induce monocyte differentiation into epithelioid-like multinucleated giant foam cells, which retain phagocytic capacity but also suppressive features when exposed to mycobacteria, suggesting a role for platelets in TB pathogenesis [522]. Among our cohorts, platelet counts declined significantly in patients with active and latent infection following anti-TB therapy, although it was only the former group demonstrating abnormally elevated counts pre-treatment. It is difficult to determine the precise mechanism for this, but it may involve a combination of resolution of infection and also the suppressive effects of anti-TB drugs [525-527].

Eosinophilia is a characteristic feature of parasitic infection. The changes in eosinophil counts in the LTBI cohort over time observed here are likely an artifact due to treatment of gastrointestinal parasite infections which is routinely administered to Gurkha recruits due to the high rates in this group (up to 20% of recruits, unpublished data).

In terms of functional evaluation, the whole blood MGIT discriminated between individuals with different states of *M. tb* infection. Overall, mycobacterial net growth was higher with H37Rv than BCG across all groups as has been seen previously and likely a result of differences in relative virulence of these strains. However, irrespective of strain, net growth followed a similar pattern of active TB<latent infection<healthy controls. This may appear counterintuitive when considering the clinical phenotypes of each study group. Individuals with active TB disease have clinically failed to control their *M. tb* infection *in vivo*, hence the manifestation of symptoms. One could speculate that a similar loss of control may be seen within the whole blood MGIT. However, in the MGIT assay the pathological burden seen *in vivo* is absent and the reduced mycobacterial growth and improved control seen using this *ex vivo* model may reflect a general state of immune activation. Different profiles in pre-treatment haematological parameters have been described, and increases in absolute numbers of monocytes and platelets (that may have immune-modulatory and anti-mycobacterial functions), together with the likely presence of activated CD3+ and CD19+ cells, would all contribute to reducing net growth seen among patients with active disease. This concept is supported by data in the preceding chapter describing whole blood MGIT responses in a human intradermal BCG challenge model. Whilst the route of exposure and the virulence of the organism are different to that of natural aerosol infection with *M. tb*, the administration of live replicating mycobacteria during BCG vaccination can be used as a surrogate model. Following challenge, which would probably have resulted in immune activation as has been extensively reported previously, reduced net growth of BCG in a whole blood MGIT assay occurred, confirmed by other studies [361, 528]. This may also account for the wide spectrum of mycobacterial growth control responses seen among latently infected participants, with many overlapping with the active and control groups. Some individuals, perhaps with subclinical disease, may demonstrate

immune activation and thus bacillary control similar to the active group, whilst those with quiescent infection would cluster with the healthy controls. The differences in the discriminatory power of the MGIT assay with BCG and *M. tb* may be due to the virulence of the mycobacteria. While significant differences between all groups were seen with BCG, these were seen in the H37Rv assay between healthy controls and the two *M. tb*-positive groups. The increased virulence of H37Rv may have reduced the ability to distinguish between the active and the LTBI groups, hence the large overlap between them. However, the very strong correlation of an individual's growth inhibition between strains is reassuring and is consistent with previous experiments. Therefore, while the magnitude of net growth may have been different, the general observation was that individuals demonstrating improved control of BCG growth also did so for H37Rv, and the converse was evident for those with poor anti-mycobacterial responses. This is an important observation for later stratification.

Reduced bacillary growth correlated with lower haemoglobin concentrations, which may be a direct association as iron is known to augment bacillary replication [382]. Indeed, a positive correlation between haemoglobin concentration and net growth in whole blood MGIT assays with both human and NHP samples has previously been shown, further supported by the experimental addition of haemoglobin and the chelation of iron in PBMC and splenocyte-based assays [365]. Alternatively, this association may be an artifact of patients with similar profiles clustering together.

Interestingly, a positive correlation was seen between BCG net growth and lymphocyte count, while a negative correlation was noted between *M. tb* growth and monocyte count. The former correlation may reflect the contribution of an adaptive immune response to BCG control among vaccinees. The latter association may be due to a more intense innate response to a virulent strain. The association between ML ratio and

mycobacterial net growth seen for BCG and *M. tb* perhaps highlights the approach of considering this combined measure rather than absolute counts independently.

A key objective of the study was to assess the impact of anti-TB treatment on mycobacterial control. Investigating longitudinal responses following intervention has the potential to add to understanding the mechanism of the MGIT assay. Significant increases in BCG and *M. tb* net growth were seen after treatment in both of the study cohorts. The mean magnitude of the increase was 1.5-fold greater in patients treated for active disease (although the differences in the degree of statistical significance of these changes may be due to a size effect of the groups). These changes are intuitive as one may speculate that individuals with the highest bacillary burden, and therefore the greatest immune activation, would demonstrate larger changes in growth control after successful treatment. Normalisation of the haematological measures are consistent with this hypothesis. Furthermore, while the previous positive correlation between pre-treatment haemoglobin concentration and net growth was no longer evident after treatment, fascinatingly, the correlations with monocyte and lymphocyte counts and also ML ratio reversed. These changes resulted in profiles very similar to those reported among healthy individuals and infer that treatment alters not only the absolute number of myeloid and lymphoid cells, but also their function [401]. It appears that the functional ability of monocytes to inhibit mycobacterial growth declines, whilst that of lymphocytes improves following treatment, which warrants further investigation.

6 Multiplatform evaluation of MGIA responses

6.1 Statement of authorship

Rachel Tanner, Stephanie Harris and Lisa Stockdale (The Jenner Institute, Oxford) provided assistance with PBMC isolation. T cell flow cytometry was performed by Danny Wright and advice provided by Iman Satti (The Jenner Institute). For transcriptomic studies, the author extracted RNA from samples and gene expression microarrays and subsequent bioinformatics analysis were performed by Eneida Parizotto-Lee and Julius Müller, respectively (The Jenner Institute). Assistance with Luminex was provided by Steve Smith (The London School of Hygiene and Tropical Medicine, London).

6.2 Introduction

The preceding chapter described the use of the *ex vivo* BACTEC MGIT assay to determine the functional ability of individuals with states of *M. tb* infection and disease to control mycobacterial growth. While clear differences in these responses discriminated between extremes of diagnostic group (e.g. active TB and healthy uninfected controls), this was less apparent among individuals with LTBI who showed considerable overlap. Some individuals with LTBI clustered with the healthy controls, while others demonstrated responses similar to the active disease group. This is consistent with the proposed spectrum of TB. The relationship between MGIA data and certain haematological measures, together with the dynamic changes seen in response to anti-TB therapy, all support the biological plausibility of these findings. However, further exploratory analyses were required to both validate these results and to investigate underlying mechanisms.

The need to identify TB biomarkers has been discussed and includes risk stratification for reactivation of LTBI and progression to active disease. However, it is very unlikely that a single measure will suffice and rather a composite of a number of markers will be required to generate an *M. tb*-specific biosignature. There is increasing appreciation that a multi-platform approach will be required to achieve this.

I therefore sought to stratify individuals within the spectrum of LTBI by ability to control bacillary growth as determined by the whole blood MGIT assay and then to characterise the profiles of these subgroups using several techniques in a multi-platform approach.

6.3 Aims

The aims of the experiments described in this chapter were to:

i. Stratify individuals with LTBI (before treatment) into groups based on ability to control mycobacterial growth as demonstrated by the whole blood MGIT assay.
ii. Characterise differential bacillary control using broad assessments applied to the entire study cohort in an unselected manner, including:
    a. multiplex serum cytokine and chemokine profiling,
    b. whole blood transcriptomic studies.
iii. Select subgroups based on stratification for characterisation using exploratory techniques assessing:
    a. the immunophenotype of monocytes,
    b. functional T cell responses,
    c. humoral responses to *M. tb*-specific antigens and B cell subsets,
    d. *M. tb*-specific plasmablast and memory B cell responses.

iv. Assess the associations and correlations between these data with continuous and categorical variables based on MGIT net growth and stratification definitions, respectively.

6.4 Results

6.4.1 Patient stratification and experimental approach

For immunological assays, samples from a subset of healthy controls and active TB patients were used and the LTBI group was stratified by MGIT responses. Individuals with LTBI and net growth values for BCG and H37Rv below the 25th centile were considered as sharing the greatest similarity with active patients and given the notation LTBI(a), while those a net growth above the 75th centile were assigned as LTBI(l), representing a more latent profile from the MGIT data (Figure 6.1 A). The correlation between BCG and H37Rv net growth values were then used to strengthen the stratification and samples were used where the concordance of net growth values for BCG and H37Rv was greatest (Figure 6.1 B). Immunological assays were subsequently performed with subsets of samples defined by the categorical variables of active disease, LTBI(a), LTBI(l), and healthy controls. Where appropriate (and dependent on sample availability) matched and pre- and post-treatment samples were used. In order to counter the prospect of introducing bias through sample selection, further assays were performed using samples collected from the entire study cohort (where available). This approach was used for serum cytokine and chemokine evaluation and whole blood transcriptomic studies. Where sufficient data points were available analyses using continuous data (MGIT net growth values) and categorical data (defined above) were performed. Again, where possible and appropriate, matched and pre- and post-treatment samples were used for the analysis.

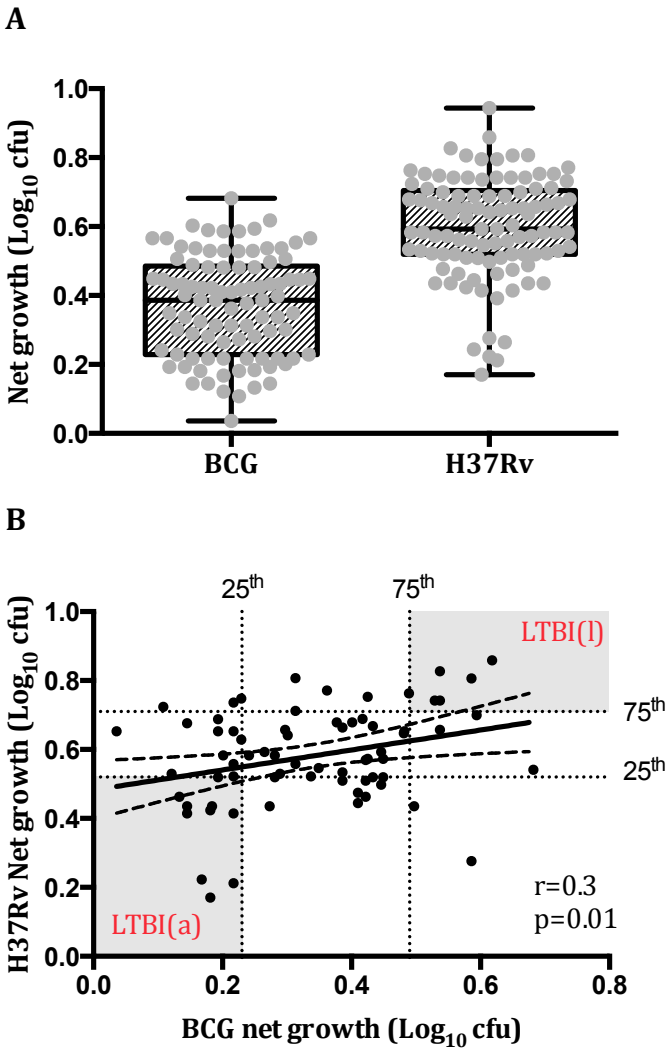


Figure 6.1 Stratifying LTBI group by pre-treatment whole blood MGIT responses. Individuals with LTBI were stratified as either LTBI(a) or LTBI(l), based on whole blood MGIT responses to BCG Pasteur and *M. tb* H37Rv, using samples collected before starting anti-TB treatment (A). Box-and-whisker plots show the median, 25th and 75th centiles, and whiskers the maximum and minimum values. The Pearson r correlation between BCG and H37Rv net growth values was used to further strengthen the stratification of the LTBI subgroups (B). Where possible, LTBI(a) was defined as net growth <25th centile for both BCG and H37Rv, while LTBI(l) was defined as net growth >75th centile for both strains.

6.4.2 Multiplex serum cytokine and chemokine analysis

Serum cytokine and chemokine concentrations were measured in a total of 173 samples from active TB (n=21) and LTBI (n=122) patients before anti-TB treatment, and healthy controls (n=30). Post-treatment samples were available for 50.3% of individuals (active n=10, LTBI n=77). From a multiplex panel of 41 cytokines and chemokines, 23 were detected in unstimulated serum samples. Concentrations of Flt-3L, Fractalkine, G-CSF, GM-CSF, IFN-α2, IL-1α, IL-1β, IL-1RA, IL-2, IL-3, IL-9, IL-10, IL-12p40, IL-12p70, IL-13, IL-15, MCP-3 and TNF-β were consistently below the limit of detection in either all or most samples. In serum samples collected before anti-TB therapy, TNF-α was the only Th1/pro-inflammatory cytokine significantly elevated in patients with active TB and LTBI (Figure 6.2). Several Th2/anti-inflammatory cytokines were elevated in these groups, including IL-4, IL-5 and IL-6, with higher levels noted in the individuals with active TB disease (Figure 6.3). Of the chemokines, IP-10 showed highest concentrations in active patients when compared to healthy controls, followed by Gro and MDC (Figure 6.4). IP-10 was also significantly elevated when compared with LTBI, although levels of MIP-1α and MIP-1β were reduced in active TB versus LTBI patients. Finally, the growth factors PDGF-BB, PDGF-AA, EGF and VEGF were detected at greater concentrations in samples from *M. tb*-infected individuals, and generally those with active disease showed the highest levels (Figure 6.5).

Using unselected MGIT data (i.e. net growth values as a continuous variable from all study participants), significant correlations between pre-treatment mycobacterial growth using BCG and H37Rv and the concentration of several cytokines and chemokines were noted (Table 6.1). Of particular interest were negative correlations between levels of Gro and PDGF-BB and net growth, and positive correlations between net growth and serum concentration of TNF-α and MIP-1β.

Following treatment, there were significant changes in certain chemokine and cytokine profiles. Among the active disease group, these were characterized by chemokines and growth factors, with reduced concentrations of IP-10, Gro, PDGF-AA and PDGF-BB, together with increased concentrations of MIP-1α and MIP-1β levels (Figure 6.6). While some of these patterns were common to the LTBI group following chemoprophylaxis, with decreased concentrations of Gro, MDC and TGFα, in addition there were also reductions in pro-inflammatory (IFN-γ and TNF-α) and anti-inflammatory (IL-4) cytokines (Figure 6.7).

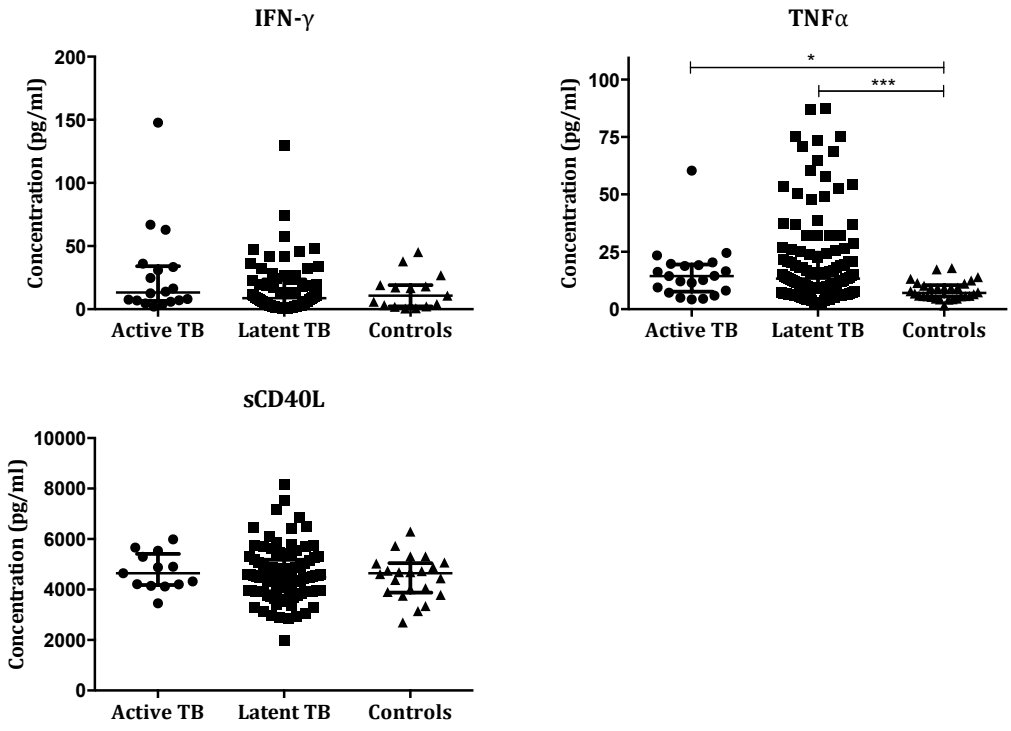


Figure 6.2 Pre-treatment Th1/pro-inflammatory cytokine profiles. Concentrations of a panel of Th1/pro-inflammatory cytokines were measured in unstimulated serum collected from individuals with active disease, LTBI and healthy controls before starting anti-TB treatment (where appropriate). Points are single measurements and bars the median with interquartile range. Only values within the upper and lower limits of detection for each analyte are included. After testing for normality, a Kruskal-Wallis test with Dunn's correction for multiple comparisons was performed. * represents a p-value of <0.05, and *** a p-value of <0.0005.

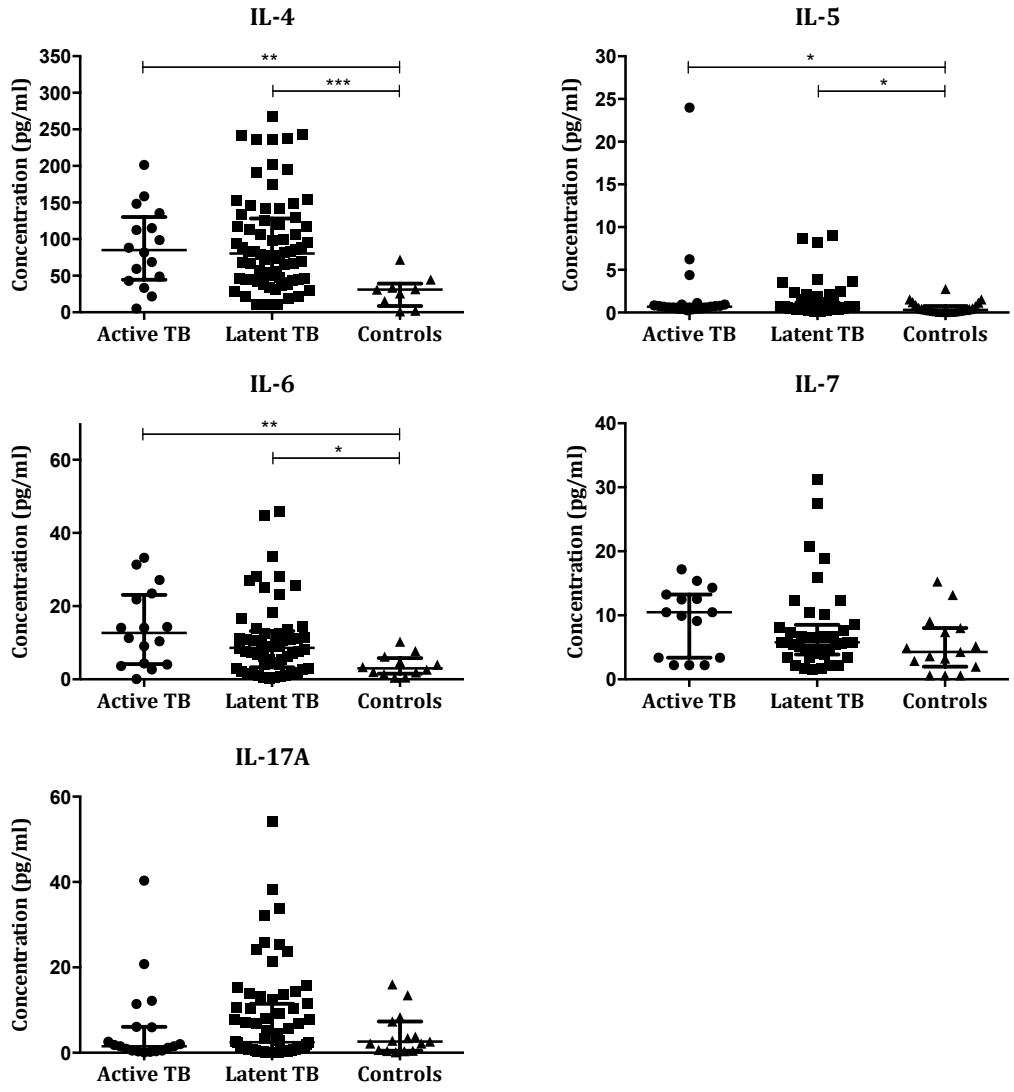
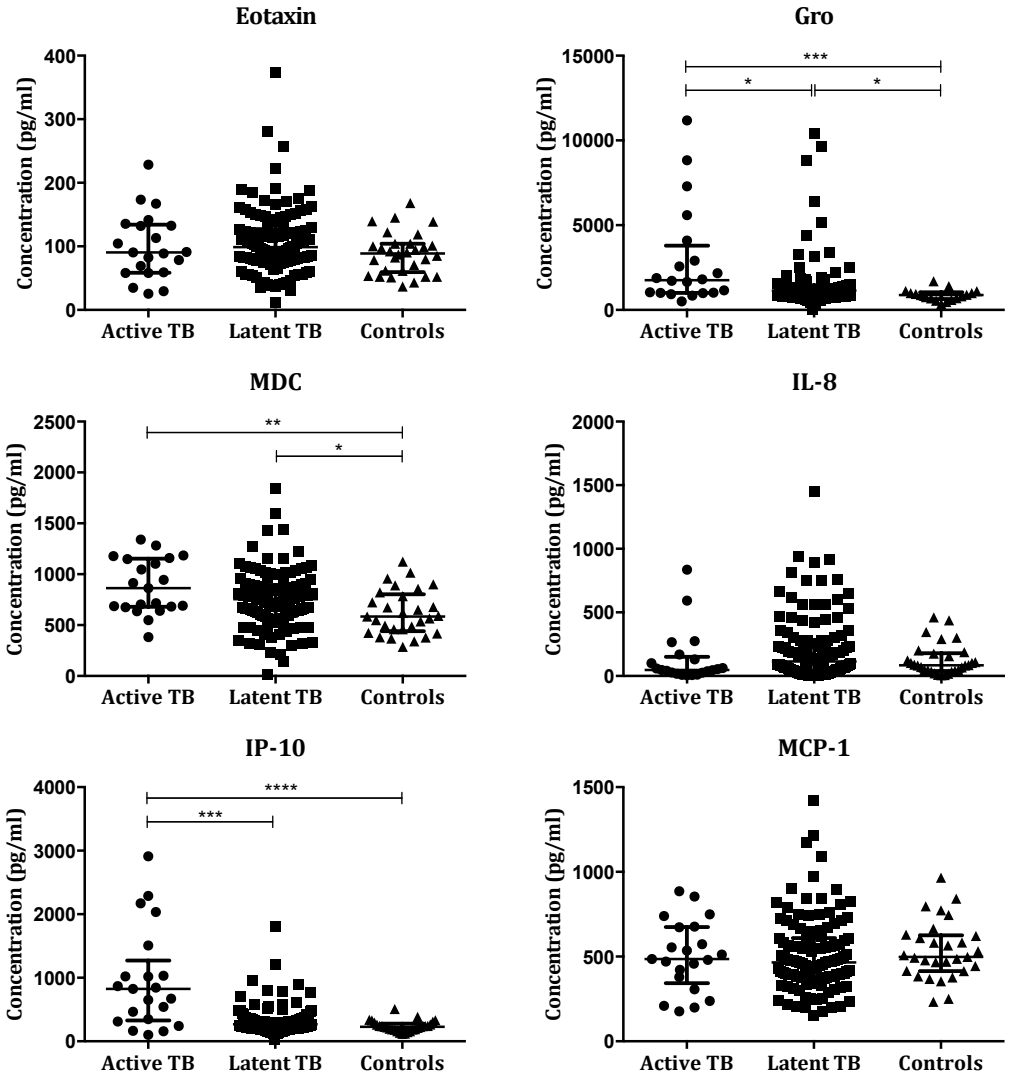


Figure 6.3 Pre-treatment Th2/anti-inflammatory and Th17/regulatory cytokine profiles. Absolute concentrations of a panel of Th2/anti-inflammatory and Th17/regulatory cytokines were measured in unstimulated serum collected from individuals with active disease, LTBI and healthy controls before starting anti-TB treatment (where appropriate). Points are single measurements and bars the median with interquartile range. Only values within the upper and lower limits of detection for each analyte are included. After testing for normality, a Kruskal-Wallis test with Dunn's correction for multiple comparisons was performed. * represents a p-value of <0.05, ** a p-value of <0.005 and *** a p-value of <0.0005.


Eotaxin
Concentration (pg/ml)
400
300
200
100
0
Active TB
Latent TB
Controls
Gro
15000
10000
5000
0
***
*
*
MDC
2500
2000
1500
1000
500
**
*
IL-8
IP-10
4000
3000
****
***
MCP-1

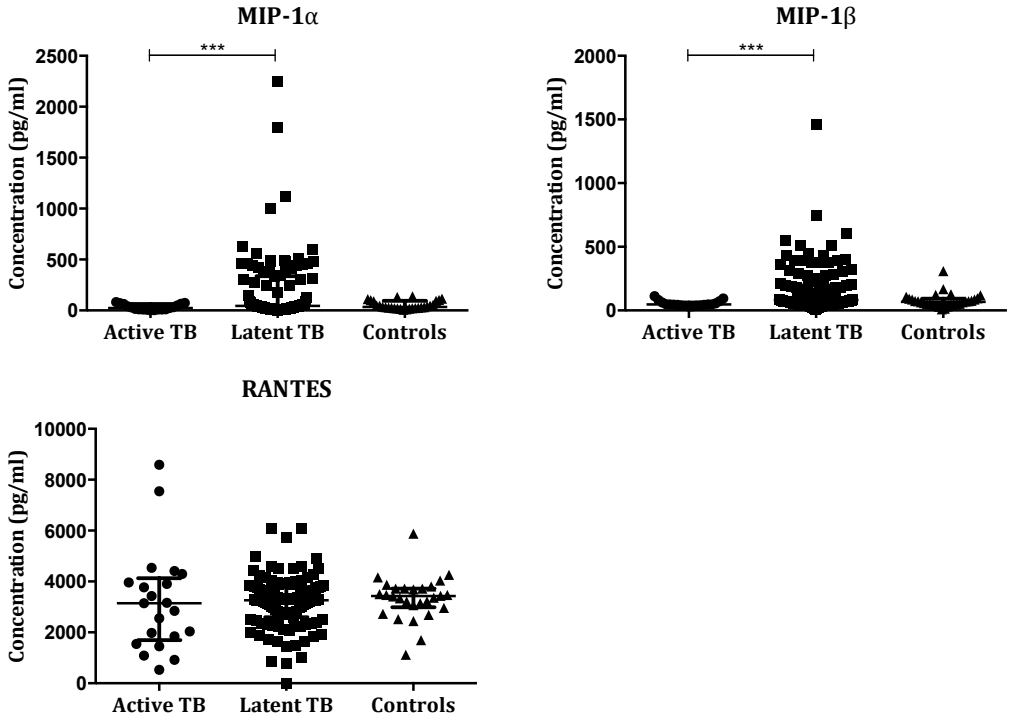


Figure 6.4 Pre-treatment chemokine profiles. Absolute concentrations of a panel of chemokines were measured in unstimulated serum collected from individuals with active disease, LTBI and healthy controls before starting anti-TB treatment (where appropriate). Points are single measurements and bars the median with interquartile range. Only values within the upper and lower limits of detection for each analyte are included. After testing for normality, a Kruskal-Wallis test with Dunn's correction for multiple comparisons was performed. * represents a p-value of <0.05, ** a p-value of <0.005, *** a p-value of <0.0005 and **** a p-value of <0.0001.

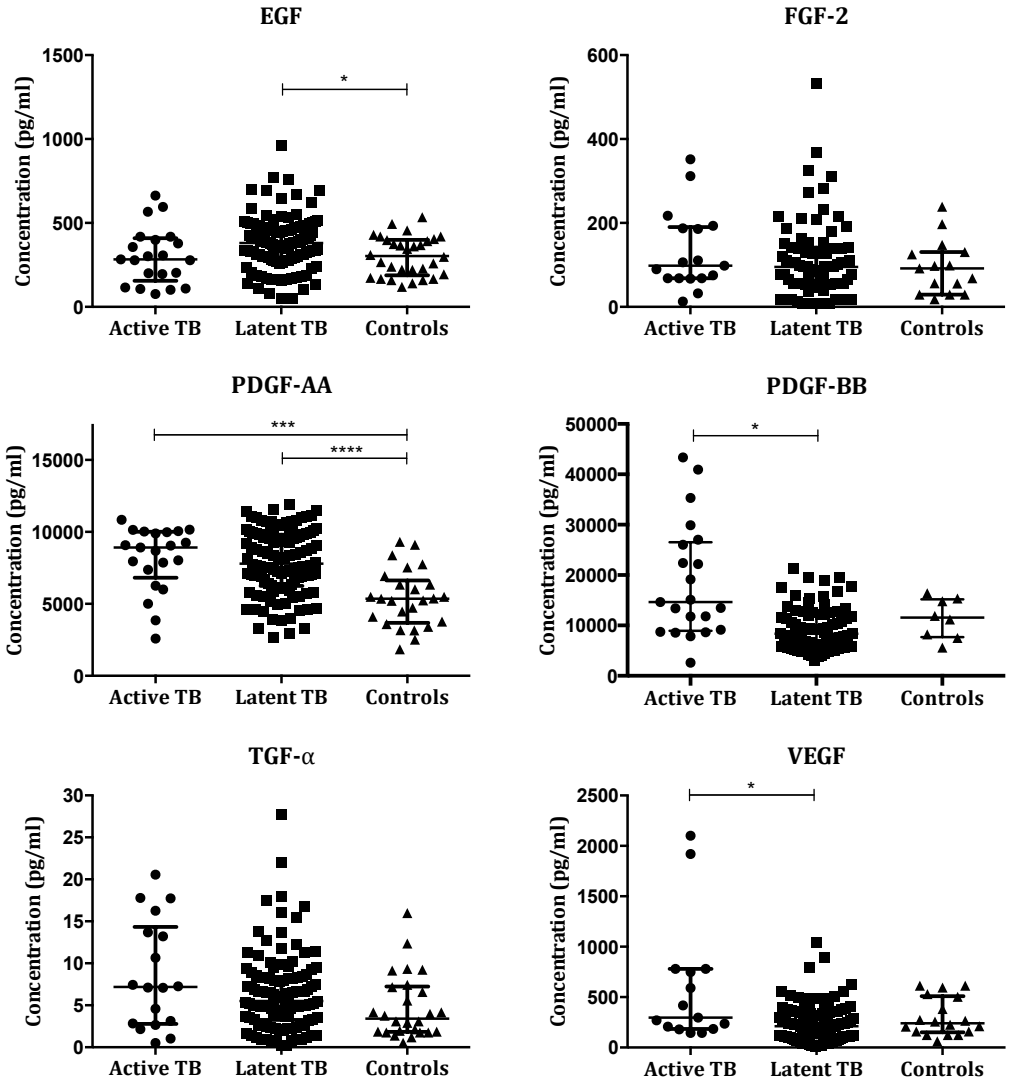


Figure 6.5 Pre-treatment growth factor profiles. Absolute concentrations of a panel of growth factors were measured in unstimulated serum collected from individuals with active disease, latent TB infection and healthy controls before starting anti-TB treatment (where appropriate). Points are single measurements and bars the median with interquartile range. Only values within the upper and lower limits of detection for each analyte are included. After testing for normality, a Kruskal-Wallis test with Dunn's correction for multiple comparisons was performed. * represents a p-value of <0.05, *** a p-value of <0.0005 and **** a p-value of <0.0001.

Category	Cytokine/Chemokine	BCG		H37Rv	
		r	p-value	r	p-value
Th1	IFN-γ	-0.02	0.850	0.06	0.637
	TNF-α	0.21	0.020*	0.24	0.006*
	sCD40L	0.02	0.878	0.11	0.286
Th2/Th17	IL-4	0.16	0.187	0.18	0.090
	IL-5	0.00	0.996	0.33	0.001*
	IL-6	0.17	0.233	-0.10	0.515
	IL-7	0.08	0.592	0.18	0.201
	IL-17A	0.10	0.435	0.17	0.154
Chemokine	Eotaxin	0.16	0.090	0.10	0.272
	Gro	-0.22	0.030*	-0.16	0.098
	MDC	-0.16	0.092	0.09	0.311
	IL-8	-0.05	0.602	-0.03	0.762
	IP-10	-0.02	0.789	0.01	0.907
	MCP-1	0.12	0.210	0.06	0.532
	MIP-1α	0.18	0.074	0.04	0.662
	MIP-1β	0.21	0.023*	0.22	0.014*
	RANTES	-0.07	0.476	0.02	0.805
Growth factor	EGF	0.20	0.031*	0.27	0.002*
	FGF-2	-0.06	0.568	-0.06	0.594
	PDGF-AA	-0.07	0.435	0.14	0.111
	PDGF-BB	-0.21	0.085	-0.26	0.038*
	TGFα	-0.05	0.612	-0.02	0.864
	VEGF	-0.08	0.472	-0.12	0.239

Table 6.1 Correlations between cytokine/chemokine levels & bacillary growth. The association between concentrations of detectable cytokines and chemokines in baseline serum samples and whole blood MGIT net growth values for BCG and H37Rv were investigated. Results from all study participants (active disease, LTBI and healthy controls) were analysed. A Spearman's correlation matrix was performed. Spearman r, together with the associated p-values, are shown. * indicates a significant p-value.

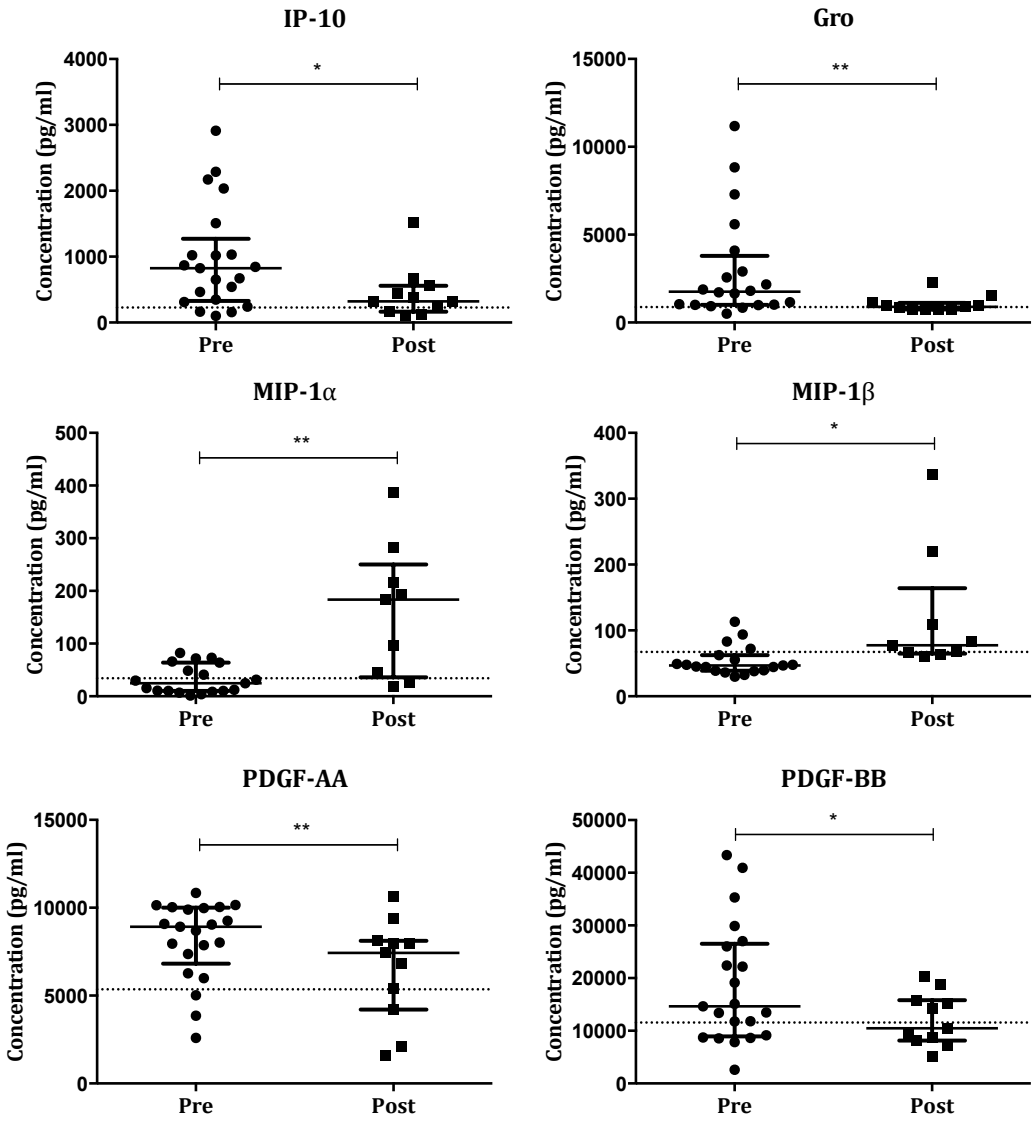


Figure 6.6 Changes in cytokines and chemokines following treatment for active TB. Absolute concentrations of a panel of cytokines and chemokines were measured in unstimulated serum collected from individuals with active disease after completing anti-TB treatment (post) and compared with pre-treatment levels (pre). Only significant changes are shown. Points are single measurements and bars the median with interquartile range. Only values within the upper and lower limits of detection for each analyte are included. Dashed line shows the median of control samples. After testing for normality, a Wilcoxon matched pairs signed rank test was performed. * represents a p-value of <0.05 and ** a p-value of <0.005.

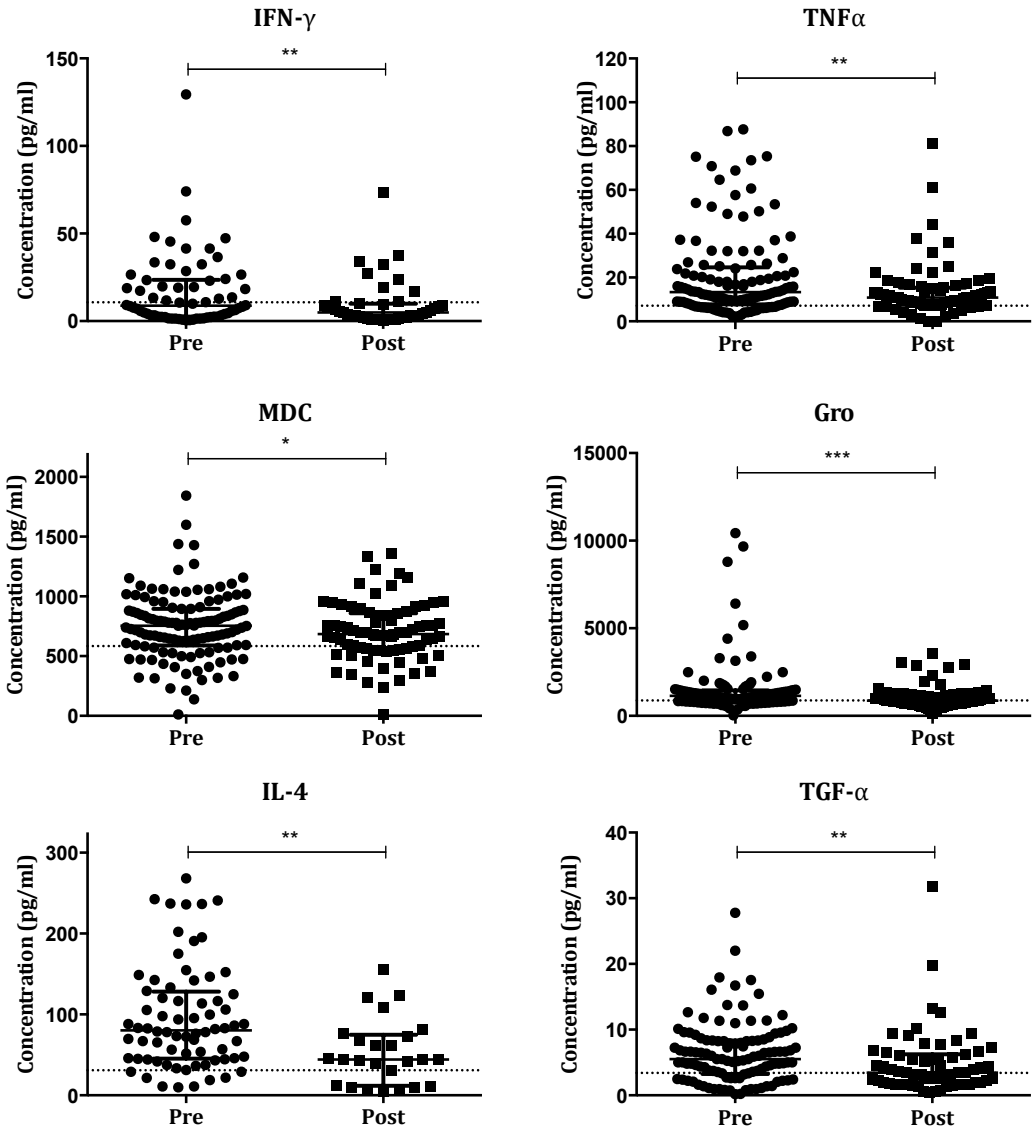


Figure 6.7 Changes in cytokines and chemokines following treatment for LTBI. Absolute concentrations of a panel of cytokines and chemokines were measured in unstimulated serum collected from individuals with LTBI after completing TB chemoprophylaxis (post) and compared with pre-treatment levels (pre). Only significant changes are shown. Points are single measurements and bars the median with interquartile range. Only values within the upper and lower limits of detection for each analyte are included. Dashed line shows the median of control samples. After testing for normality, a Wilcoxon matched pairs signed rank test was performed. * represents a p-value of <0.05 and ** a p-value of <0.005.

6.4.3 Whole blood transcriptomic studies

The relationship between mycobacterial growth in the whole blood MGIT assay and differential gene expression (DGE) profiles were investigated in a large transcriptomic study. Total RNA was extracted from 197 PAXgene samples. Four samples failed extraction and another was excluded during microarray quality control evaluation (exceeding four times the median absolute deviation) (Appendix Figure 8.2). The remaining 192 samples comprised of pre-treatment whole blood collected from individuals with active TB disease (n=18), LTBI (n=86) and healthy controls (n=21). Post-treatment samples were available from active TB (n=9) and LTBI (n=58) patients. This latter component is unique among transcriptomic studies and provided a novel approach to assessing anti-TB treatment responses in this group. Further quality control analysis showed that no outliers were detected based on gender (Appendix Figure 8.3). In addition, a principal components analysis (PCA) was performed to assess the effect of processing samples in batches and microarray hybridization batch effects were then removed (Appendix Figure 8.4). The expression data were normalised and only probes with a detection p-value <0.05 in at least 10% of the samples were flagged as detected above background. After removing undetected and unmapped probes a total of 23,412 probes, which mapped to 17,434 genes, were retained for subsequent analysis (from an initial 47,323 probes mapping to 27,624 genes). Disease state was coded as a categorical variable with five levels: active TB pre-treatment, LTBI pre-treatment, active TB post-treatment, LTBI TB post-treatment and control. Continuous variables of interest included MGIT data (net growth). An F-test was performed to test for differential expression for active versus LTBI samples as well as LTBI versus healthy control samples at the same time, and only genes with an FDR <0.1% were selected. Hierarchical clustering analysis was then performed on batch, age, gender and ethnicity subtracted residuals. A 1 – Pearson correlation was used as a

dissimilarity matrix and distances were agglomerated using the complete linkage method of the hclust command in R.

The analyses was undertaken to address three primary questions, which were whether:

i. Before starting anti-TB treatment, different diagnostic groups have distinct DGE patterns on hierarchical clustering.
ii. Continuous MGIT net growth data correlates with whole transcriptomic profiles.
iii. The DGE patterns change following completion of TB therapy in active disease and latently infected individuals.

Hierarchical cluster analysis revealed that within the cohort three distinct clusters existed before anti-TB treatment (n=125) (Figure 6.8). One consisted of a majority of active patients, one of mostly LTBI and the third of controls. The majority of healthy controls (n=20, 90.9%) occupied the largest cluster of 52 subjects, in which there was a significant number of LTBI patients (n=29, 55.8% of the cluster) and three individuals with active TB disease. The second cluster (n=37) comprised mostly of patients with LTBI (n=34, 91.9%), but also included one with active disease and two healthy controls. Finally, the third cluster of 36 individuals contained the majority of active patients from the study (n=14, 77.8% of the active cohort), but also 22 with LTBI. These clusters were categorised as 'control', 'latent' and 'active' (respectively) for convenience and while distinct clusters were identified, considerable overlap between patients with LTBI was noted. The most significant differences in DGE were noted to occur between the active and control clusters, and between active and latent clusters (Figure 6.9 A and B). Fewer differences were noted between control and latent clusters (Figure 6.9 C). Some of the genes most significantly expressed in the active cluster included many which have been

described before in the context of TB, and among others included *GBPs, FCGR1A, ANKRD22, C1QB, TAP1, BATF2, SEPT4, IFITM1, STAT1, SERPING1, SOCS1, ETV7* and *IFIT3*. In order to gain insight into functional associations of expression profiles, a gene ontology classification analysis was performed between clusters. Gene ontology (GO) uses gene-annotation enrichment analysis and functional annotation clustering of genes to identify common associations. It has a hierarchical structure for the analysis of transcriptomic data and allows for the classification of gene products into molecular functions, biological processes, and cellular components [529]. This allows for a more biologically intuitive interpretation of large DGE datasets.

Significant differences in DGE between active and control clusters were mainly seen with increased gene expression in the former group, characterised by immune response. Type I interferon signalling, innate and defence responses and cytokine-mediated signalling pathways were particularly prominent (Appendix Table 8.3 A). On comparing active with latent clusters, the GO analysis showed very similar patterns, with significant expression of immune response genes in the active cluster (Appendix Table 8.3 B). Interestingly, the main difference between latent and control clusters was in DGE associated with cellular metabolic processes, primarily involved in protein and RNA processes (Appendix Table 8.3 C). A modular analysis was performed to schematically represent these patterns (Figure 6.10).

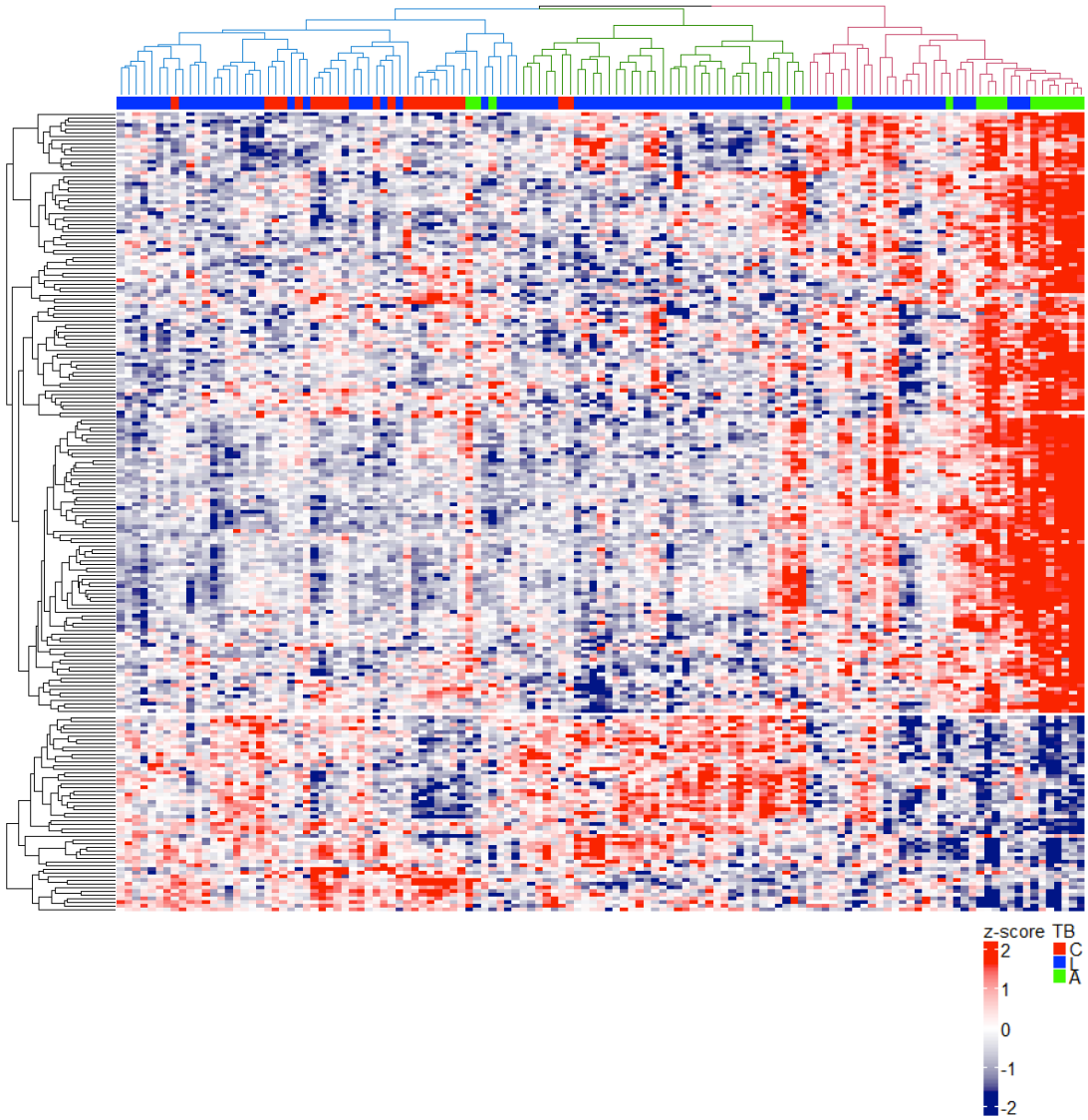


Figure 6.8 Pre-treatment differential gene expression in whole blood of the study cohort. A heatmap of differential gene expression derived from whole blood collected for individuals with active TB (n=18), LTBI (n=85) and healthy controls (n=22), before starting anti-TB treatment (where appropriate). Diagnostic groups are shown on the top bar as active disease (green blocks, A), LTBI (blue blocks, L) and controls (red blocks, C). Hierarchical cluster analysis revealed three distinct clusters based on DGE. Cluster 1 (blue dendrogram) contained almost all of the healthy controls. Cluster 2 (green dendrogram) consisted almost entirely of individuals with LTBI. Cluster 3 (red dendrogram) consisted of the majority of active patients. There was considerable overlap of LTBI patients into the other clusters. The y-axis was subject to unsupervised hierarchical clustering of similarity in gene expression and rows were scaled to z scores of gene expression (e.g. red indicates 2 SD from mean expression).

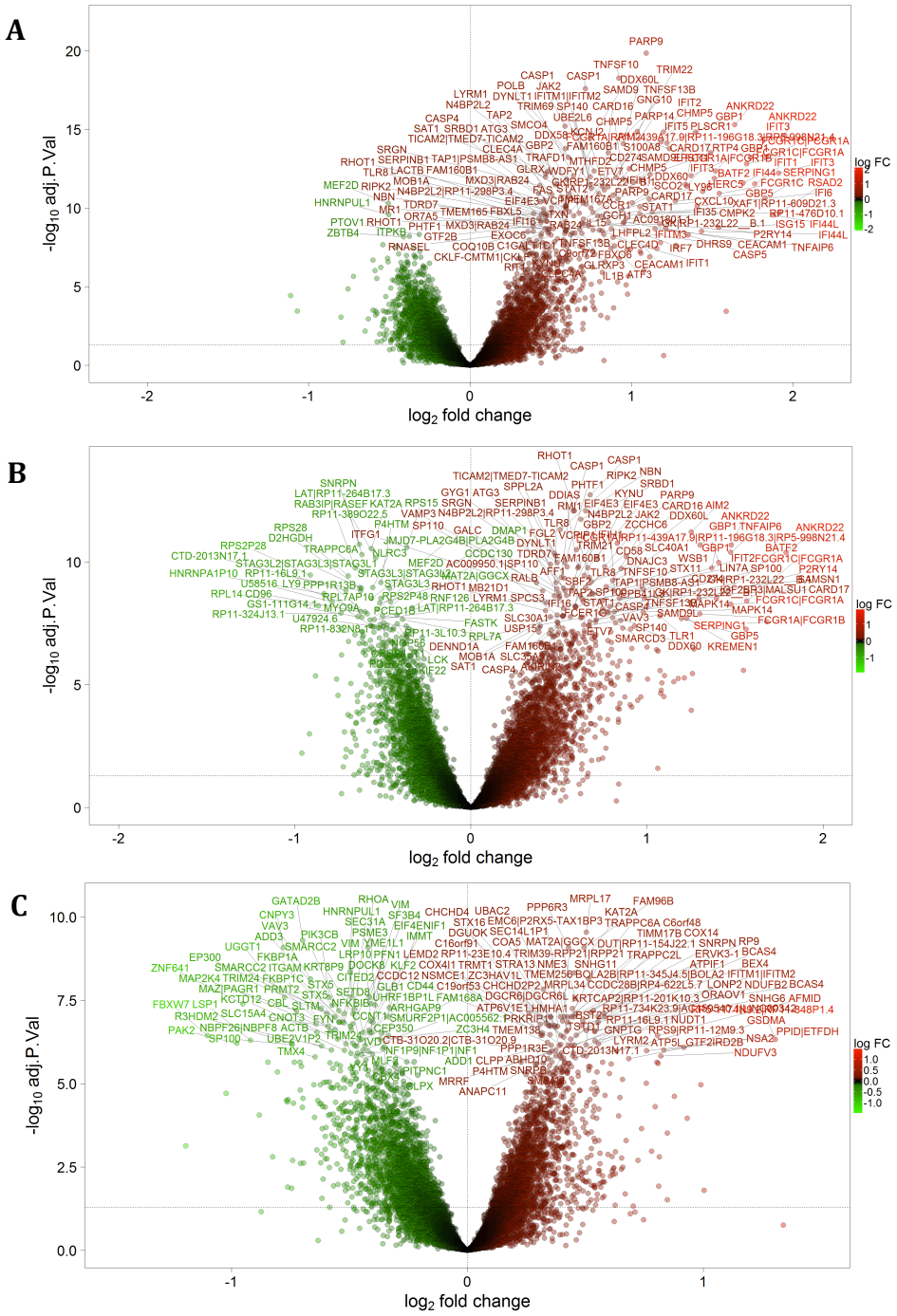


Figure 6.9 DGE between hierarchical clusters. Volcano plots showing the most significant DGE between groups. Comparisons are 'active' vs 'control' (A), 'active' vs 'latent' (B), and 'latent' vs 'control' clusters (C). The x-axis indicates the fold change in expression (red=increase in expression units; green=decrease) and the y-axis the significance.

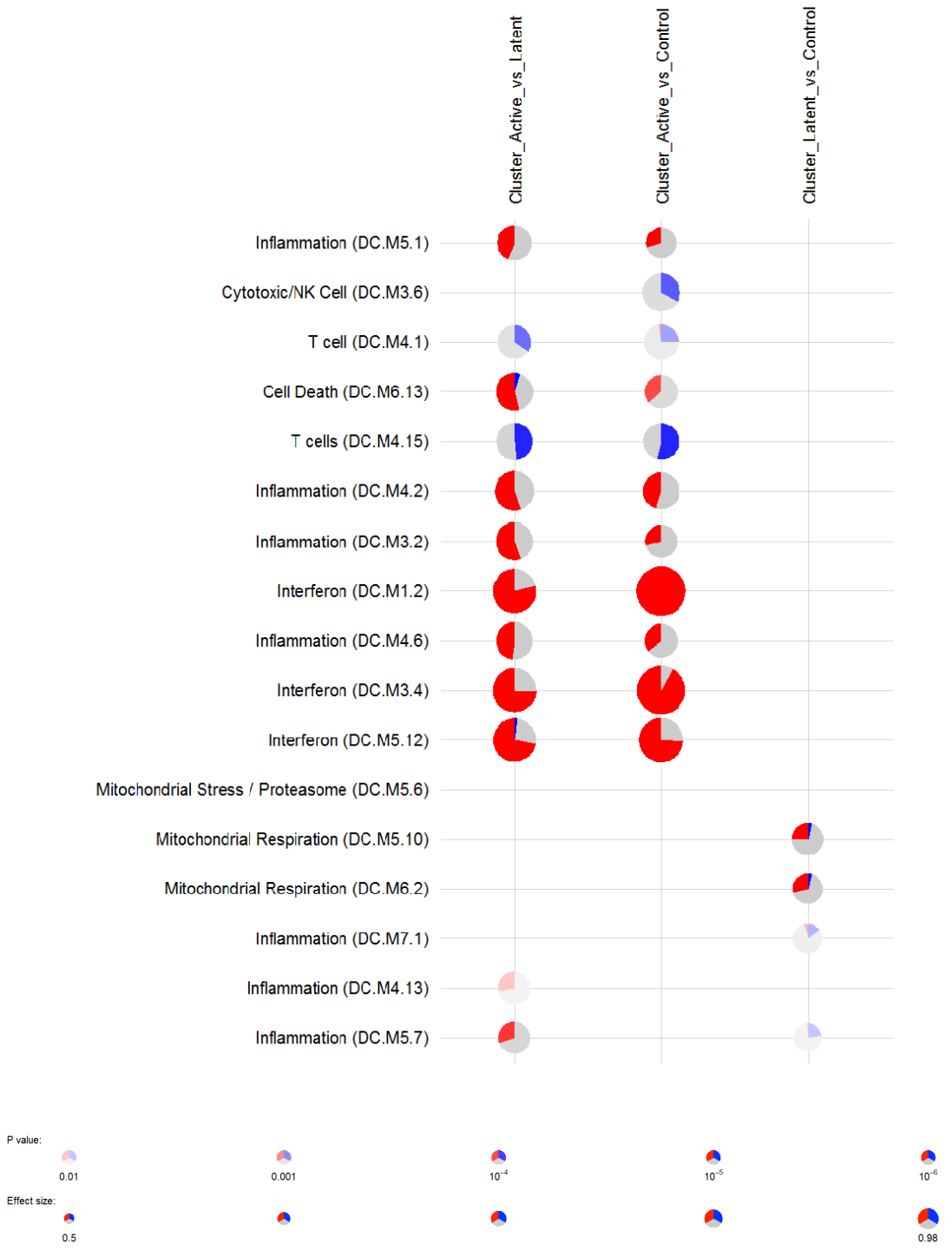


Figure 6.10 Modular analysis of DGE between clusters. Gene lists of significant DGE between pre-treatment clusters identified by hierarchical analysis were investigated by functional annotation. Modular analysis revealed prominence of inflammatory and interferon pathways in the active cluster. Red indicates upregulated in the cluster and blue downregulated, size the magnitude of the effect and transparency the p-value.

A comparative analysis of DGE seen in the current dataset with that reported by the prototypic whole blood transcriptomic study in TB was performed to assess the generalisability of the current study findings [235]. Using the analysis employed by Berry *et al*. and applying it to the current study dataset, there was significant agreement in clustering profiles (Figure 6.11). Using the Berry *et al.* dataset for training, machine learning could distinguish between active and latent patients in the current study with up to 80% accuracy. This earlier study identified a whole blood 393-transcript signature for active TB in intermediate and high-burden settings [235]. In addition, the authors went on to show a specific 86-transcript signature that discriminated active TB from other inflammatory and infectious diseases (both pulmonary and systemic) and which was dominated by a neutrophil-driven interferon inducible gene profile, consisting of both IFN-γ and type I IFN-αβ signalling [235]. When accounting for differences between the earlier and later versions of the microarrays used in the two studies and including only probes common to both, from the 209-transcript signature identified in the active cluster, 131 overlapped with either of the Berry *et al.* signatures (62.7%) (Figure 6.12). Within the 393-transcript signature, 121 genes overlapped and in the TB-specific signature of 86 transcripts, 12 genes were common to both. Overlapping 121/393 signatures included the genes *GBPs, CARD17, C1QB, TRIM22, FCGR1A, IFIH1, STAT1* and *SOCS1,* shown to be involved in immune responses, including innate immunity and defence responses, by functional classification. In contrast, the 12/86 overlapping transcripts were related to responses to wounding and regulation of apoptosis and programmed cell death following GO analysis. Subgroup analysis of the active TB patients did not reveal any differences in expression profile based on pulmonary or extra-pulmonary disease classification (data not shown).

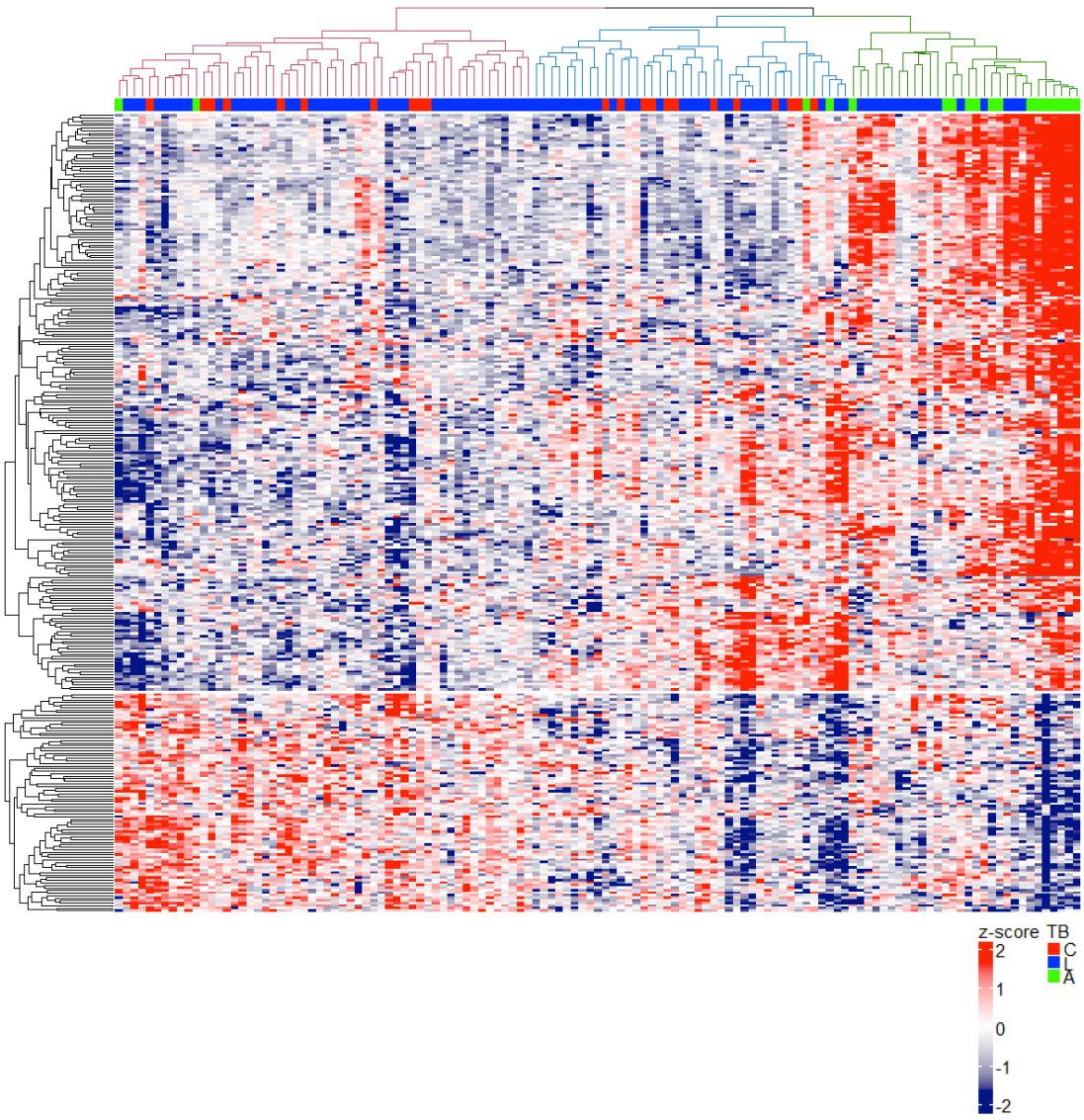


Figure 6.11 Pre-treatment differential gene expression using Berry *et al.* analysis. A heatmap of differential gene expression derived from whole blood collected for individuals with active TB (n=18), latent infection (n=85) and healthy controls (n=22), before starting anti-TB treatment (where appropriate). Diagnostic groups are shown on the top bar as active disease (green blocks, A), LTBI (blue blocks, L) and controls (red blocks, C). Hierarchical cluster analysis was performed using the parameters of Berry *et al.*

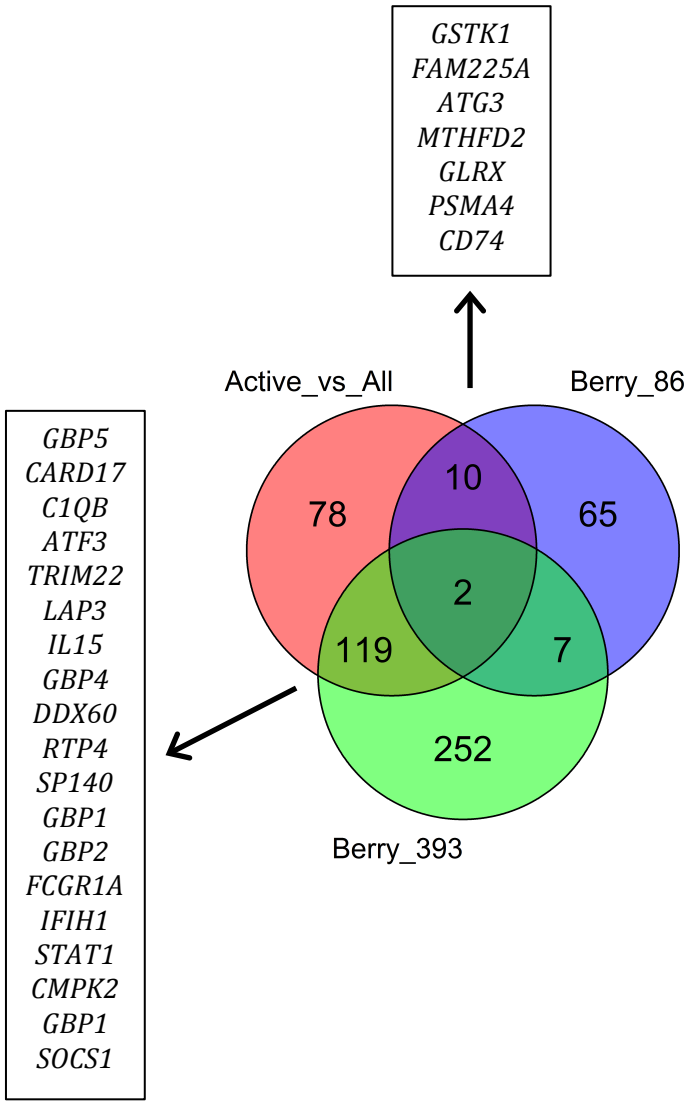


Figure 6.12 Overlap of active TB disease gene signatures identified by two independent studies. Comparison of genes differentially expressed between the active group (pre-treatment) and the combined group LTBI (pre-treatment) plus controls and the two key signatures described by Berry *et al.* Only probes present in Berry *et al.* and the current study as well as the highest expressed probe per gene was used for the comparison. The boxes contain some of the prominent genes overlapping between the studies (FDR 0.05).

On analysis of the whole blood MGIT net growth values as a continuous variable for both BCG and H37Rv, differences between the three clusters were observed (Figure 6.13). For BCG, there was a trend towards lower net growth in active cluster but this

did not reach significance (mean net growth for active, latent and control clusters: 0.32, 0.34 and 0.33 log_{10} cfu, respectively). However, H37Rv net growth was significantly lower in the active cluster compared with the control cluster (mean net growth: 0.53, 0.58 and 0.63 log_{10} cfu, respectively).

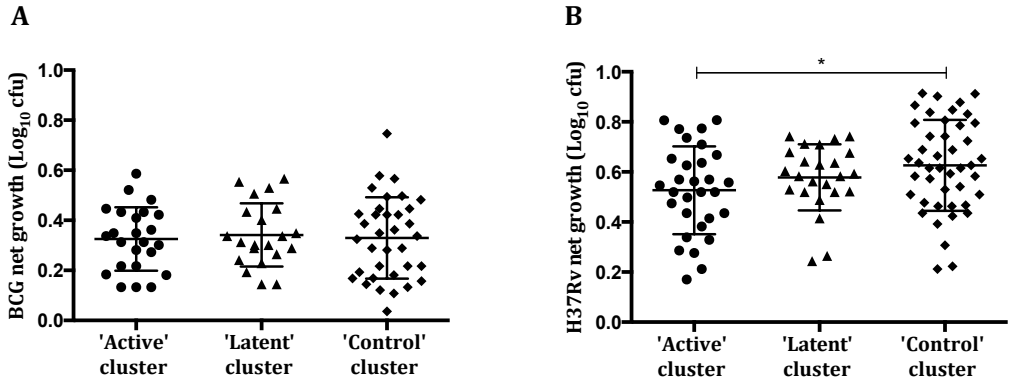


Figure 6.13 Relationship between pre-treatment MGIT net growth and DGE clusters. The relationship between pre-treatment whole blood MGIT net growth values for BCG Pasteur (A) and *M. tb* H37Rv (B) (where available) and the three clusters, as identified by hierarchical cluster analysis, was assessed. Points represent the mean of duplicates; bars represent mean values with the SD. The clusters can be notionally categorised on the basis of proportional contribution of each diagnostic group to each cluster. After testing for normality, a one-way multiple comparison ANOVA with Tukey's post-test correction was performed between the clusters. * represents a p-value of <0.05.

In order to assess the effect of treatment on DGE, the most significant genes for the differences between active TB subjects before and after anti-TB treatment and LTBI subjects before and after treatment were selected for hierarchical clustering. Hierarchical clustering was then performed on batch, age, gender and ethnicity subtracted residuals. A 1 – Pearson correlation was used as a dissimilarity matrix and distances were agglomerated using the complete linkage method of the hclust command in R. Two distinct clusters were identified, one of 19 and another of 48 subjects (Figure 6.14). All of the subjects previously grouped together in the active cluster occupied the larger (n=48) cluster, while the previous LTBI patients were within the smaller cluster. Examination of DGE in the clusters showed that there were significantly more changes among the active cluster within the latent cluster (Figure 6.15). Modular analysis confirmed this and also highlighted that there was little difference in the pattern of DGE following treatment among all individuals from controls.

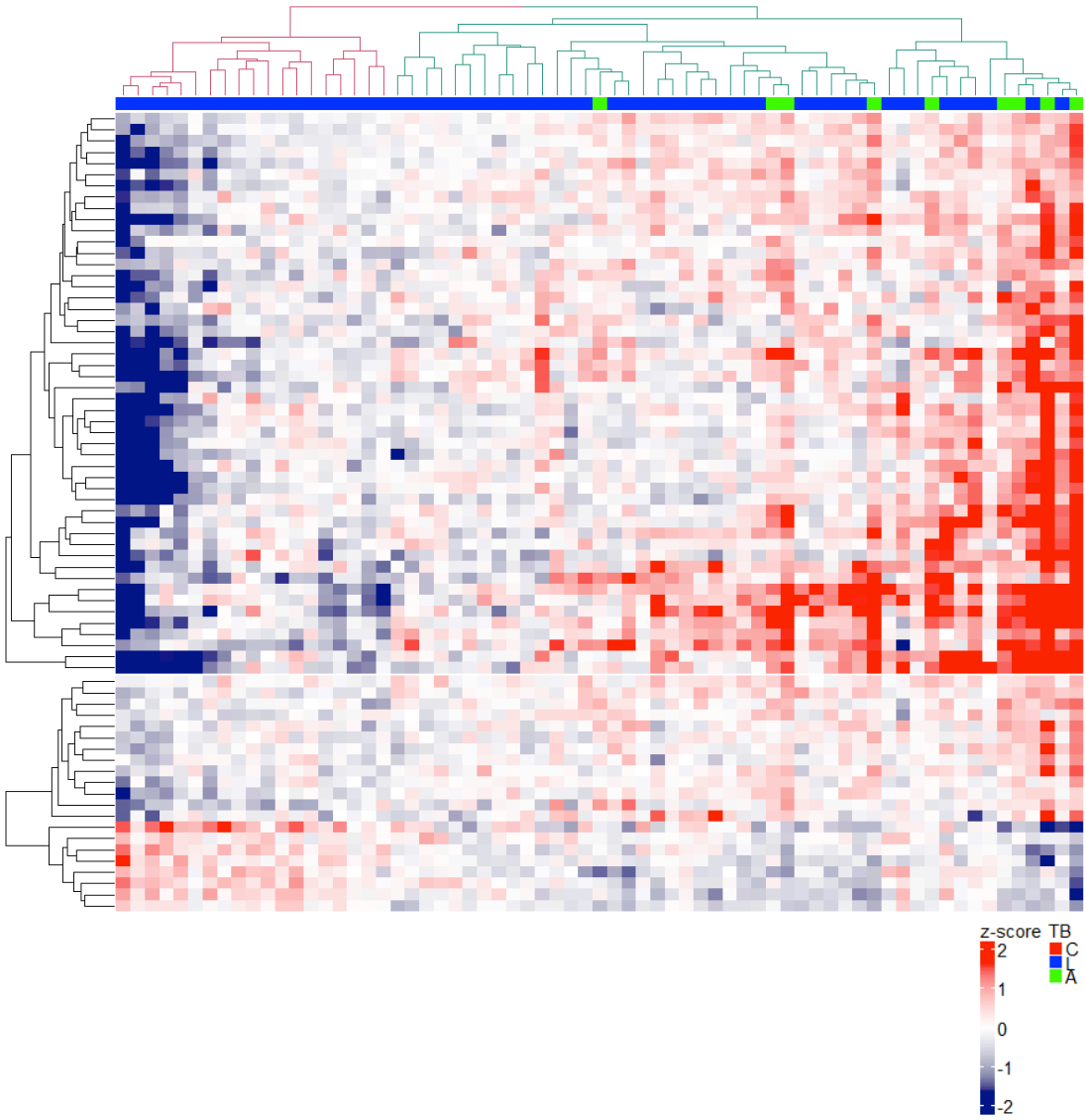


Figure 6.14 Changes in differential gene expression following anti-TB treatment. The most significant genes for the differences between active TB subjects before and after anti-TB treatment (n=9) and LTBI subjects before and after treatment (n=58) were selected for hierarchical clustering. A heatmap of differential gene expression based on this analysis is shown. Diagnostic groups are shown on the top bar as active disease (green blocks, A) and LTBI (blue blocks, L). The y-axis was subject to unsupervised hierarchical clustering of similarity in gene expression and rows were scaled to z scores of gene expression (e.g. red indicates 2 SD from mean expression).

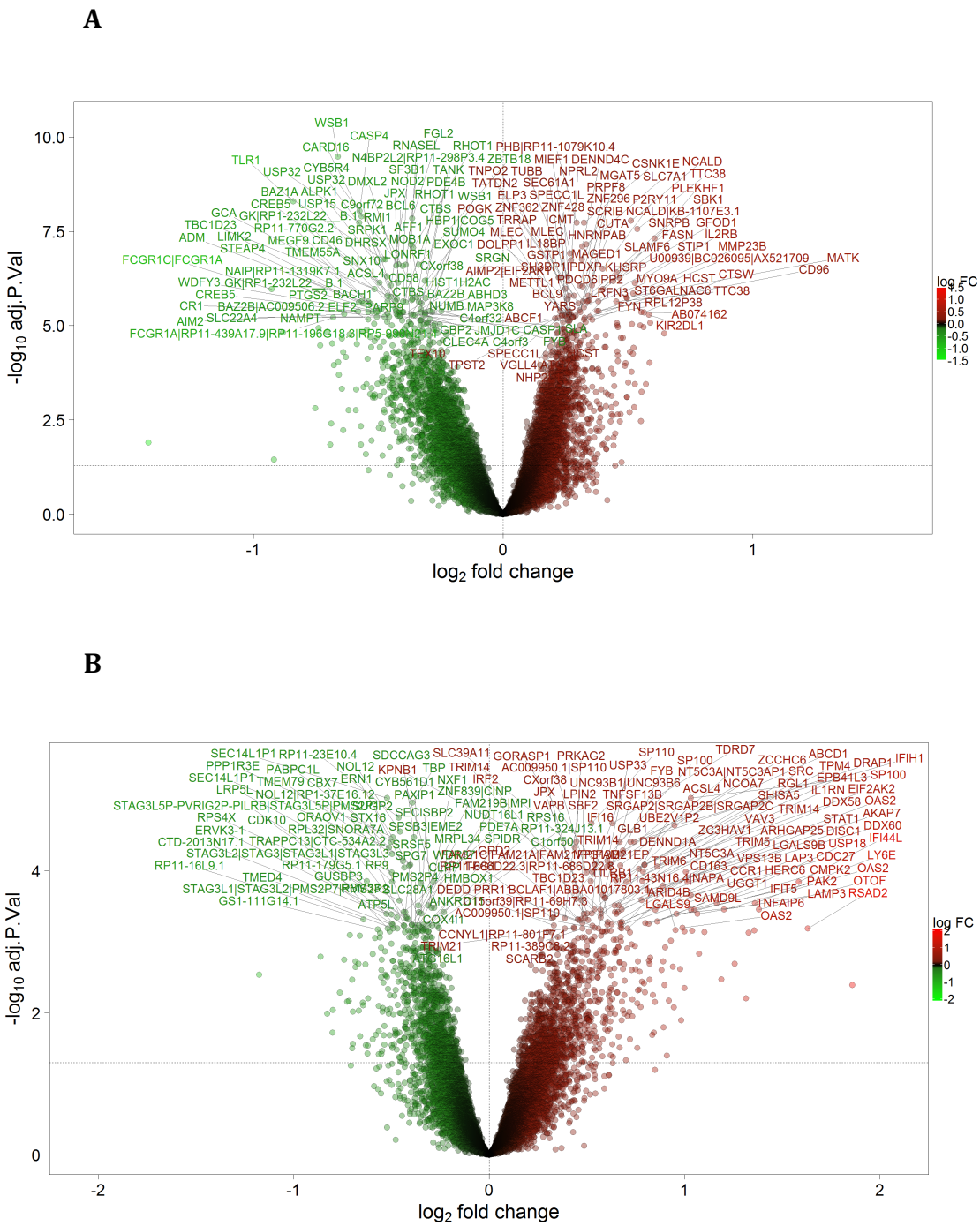


Figure 6.15 DGE in hierarchical clusters in response to TB treatment. Volcano plots showing the most significant DGE between groups identified by hierarchical clustering. Comparisons between the 'active' cluster before and after anti-TB treatment (A) and between the 'latent' cluster before and after treatment (B) are shown. The x-axis indicates the fold change in expression (red=increase in expression units; green=decrease) and the y-axis the significance (Benjamini-Hochberg adjusted p-value (the FDR).

6.4.4 Characterising monocyte subset phenotypes

As described, monocytes have a crucial role in the immune response to *M. tb* infection and therefore I sought to characterise the different subsets of these cells in PBMC isolated from the study cohort by five-colour flow cytometry. This included patients with active disease (n=17), those with LTBI (n=17) and healthy controls (n=10). The group of latently infected individuals consisted of samples from patients considered LTBI(a) (n=7) and LTBI(l) (n=10), based on MGIT data. Together with pre-treatment samples, matched samples collected after completion of anti-TB treatment were available for most of the participants (active n=11, LTBI n=14). Cells were visualized by size then a large gate was drawn around the monocyte cloud (Figure 6.16). An exclusion (negative) and inclusion (positive) gating strategy was then employed based on established approaches [530, 531]. After selecting live cells, CD3+, CD19+ and CD56+ cells were excluded. HLA-DR+ cells were then selected and were discriminated on a bivariate scatter plot of CD14+ versus CD16+. Double negative cells on this plot were removed as non-monocytes. Monocyte subsets were defined as CD14++CD16- (classical), CD14++CD16+ (intermediate), or CD14+CD16+ (non-classical) on the basis of FMO gating. The proportion of each subset of the total monocyte population was calculated. While there was no significant difference in the proportions of classical monocytes between active, LTBI and control groups, there was a trend for fewer classical monocytes among latently infected individuals (mean=90.4%, 85.3%, 88.2%, respectively) (Figure 6.17 A). Significant increases in the proportion of intermediate monocytes in *M. tb*-infected groups were seen, with more seen in LTBI (mean=5.9%, 8.7%, 1.9%, respectively) (Figure 6.17 B). Patients with active disease and LTBI also showed significantly fewer non-classical monocytes compared with healthy controls, with the lowest levels seen in the active TB patients (mean=3.6%, 5.9%, 9.4%, respectively) (Figure 6.17 C). There was a significant negative correlation between the

proportion of intermediate monocytes and MGIT BCG net growth (r=-0.43, p=0.02) and positive correlations between non-classical monocytes and net growth of both BCG and *M. tb* (r=0.41, p=0.03; r=0.33, p=0.03, respectively) (Figure 6.18). When the LTBI cohort was separated by ability to control bacillary grow into LTBI(a) and LTBI(l) and evaluated, a higher proportion of intermediate and lower proportion of non-classical monocytes were seen in the LTBI(a) subgroup, although these differences were not statistically significant (Figure 6.19).

Further work to characterise the monocyte subset profiles following anti-TB treatment showed that among active TB patients there were significant reductions in the proportion of intermediate and increases in non-classical monocytes in response to therapy, resulting in profiles similar to healthy controls (Figure 6.20). No changes in classical monocytes in the active group or changes in any subsets in the LTBI group taken as a whole were observed. However, on stratifying the LTBI individuals into LTBI(a) and LTBI(l), there was a trend for greater changes in proportions of intermediate and non-classical monocytes in the LTBI(a) subgroup, although these were not statistically significant (intermediate monocytes: pre- to post-, LTBI(a), mean=10.1% to 8.1%; LTBI(l), mean=7.7% to 7.2%; non-classical monocytes: pre- to post-, LTBI(a), mean=5.1% to 6.8%, ; LTBI(l), mean=6.6% to 6.0%) (Figure 6.21).

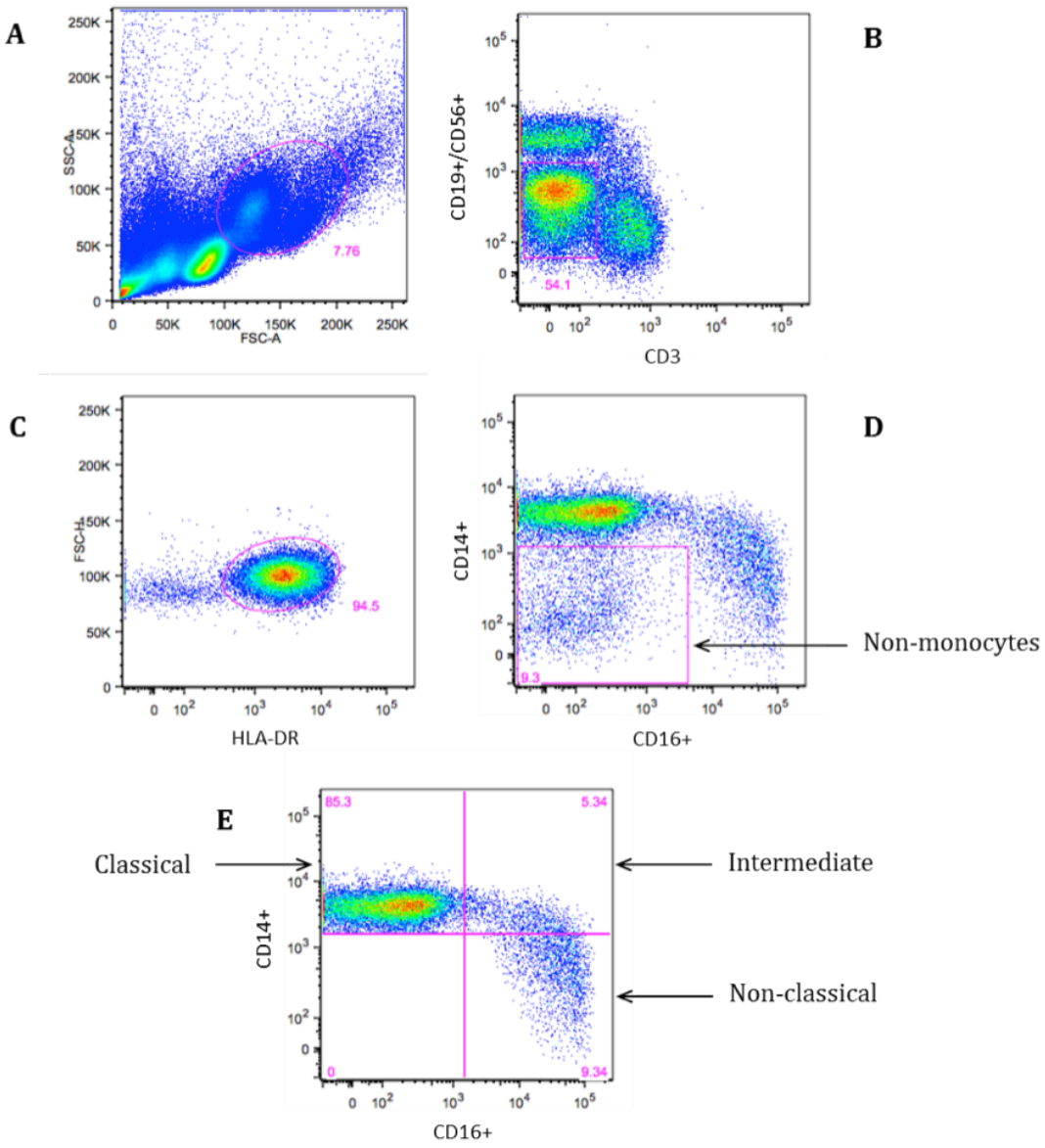


Figure 6.16 Monocyte subset gating strategy. Cells were visualized by size (FSC-A vs SSC-A) and a large gate was drawn around the monocyte cloud, excluding most cell debris (A). After selecting live cells, CD3+, CD19+ and CD56+ cells were all excluded (B). From the double negative cells, HLA-DR+ cells were then selected (C) and were discriminated on a bivariate scatter plot of CD14+ vs CD16+ (D). Double negative cells on this plot were removed as non-monocytes. Monocyte subsets were defined as CD14++CD16- (classical), CD14++CD16+ (intermediate), or CD14+CD16+ (non-classical) on the basis of FMO gating (E). The proportion of each subset of the total monocyte population was calculated.

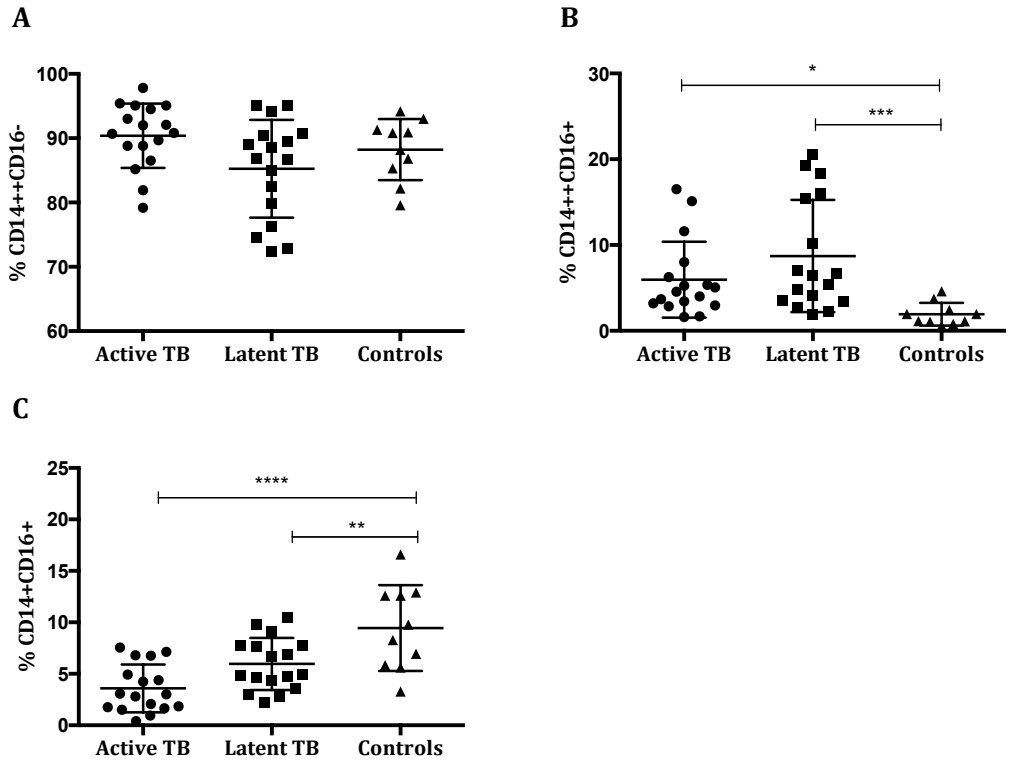


Figure 6.17 Pre-treatment monocyte subset characterisation. Monocyte subsets were characterised among patients with active TB disease (n=17), latent infection (n=17) and healthy controls (n=10) before starting anti-TB treatment (where appropriate). The proportions of classical (A), intermediate (B), and non-classical (C) monocytes were calculated from the total monocyte population. Points are single values and bars represent the mean with SD. After testing for normality, an ordinary one-way ANOVA with Tukey's correction (A and C) or a Kruskal-Wallis test with Dunn's correction for multiple comparisons (B) was performed. * represents a p-value of <0.05, ** a p-value of <0.005, *** a p-value of <0.0005 and **** a p-value of <0.0001.

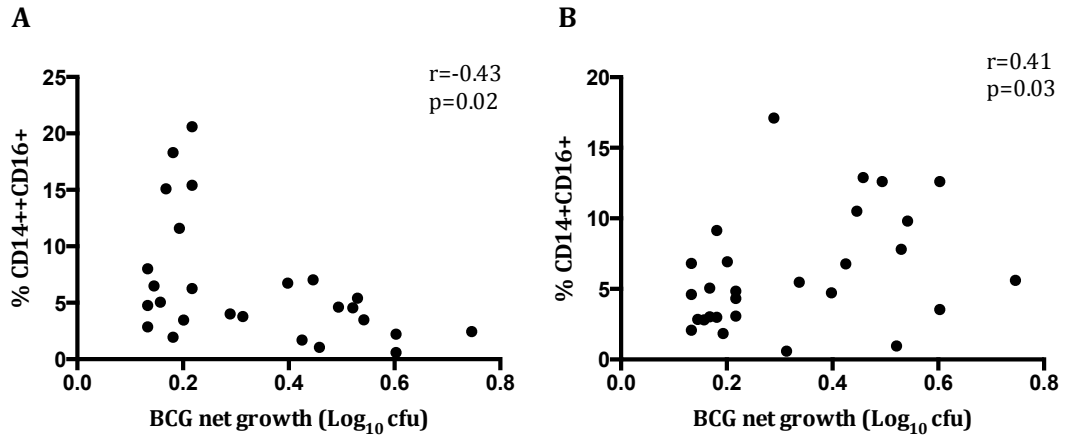


Figure 6.18 Correlations between baseline monocyte subsets and whole blood MGIT. The significance of correlations between the proportions of monocyte subsets and bacillary net growth seen in the MGIT assay were determined. A negative correlation between intermediate monocytes and net growth (A), and a positive correlation between non-classical monocytes and net growth (B) of BCG were seen. The latter was also seen with *M. tb* (data not shown). Spearman's r and associated p-values are shown.

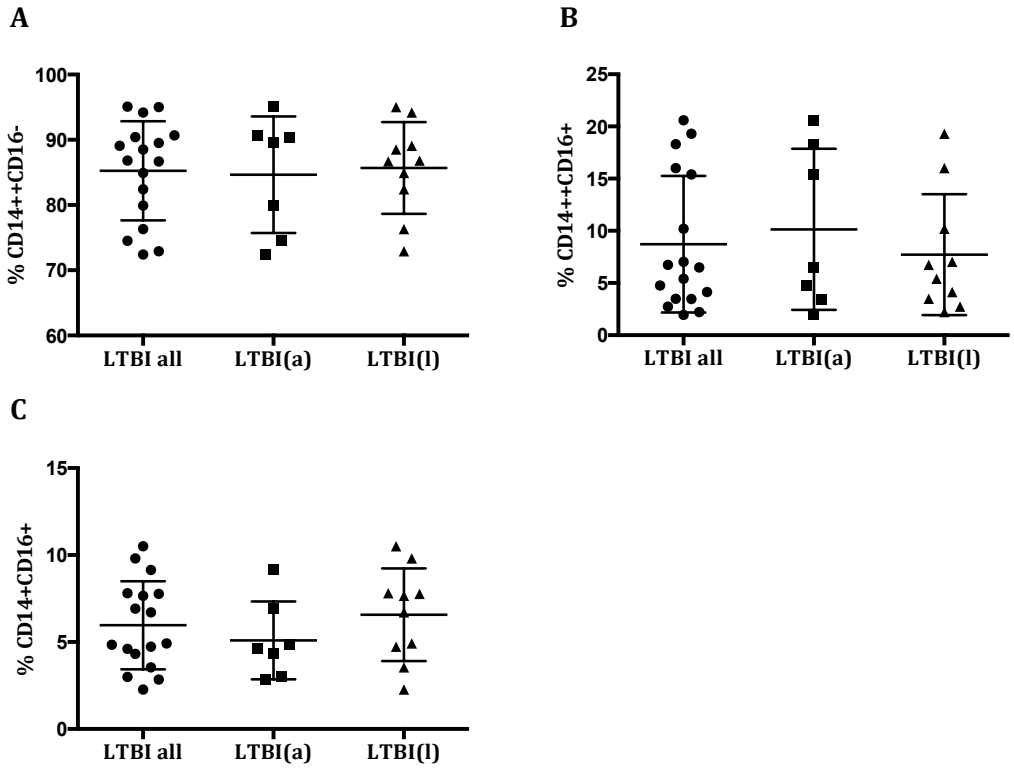


Figure 6.19 Baseline monocyte profiles in LTBI subgroups. The LTBI cohort was separated into LTBI(a) and LTBI(l) subgroups on the basis of mycobacterial control (n=7 and n=10, respectively). The proportions of classical (A), intermediate (B) and non-classical (C) monocytes were calculated from the total monocyte population. Points are single values and bars represent the mean with SD. After testing for normality, an unpaired t-test between LTBI(a) and LTBI(l) subgroups was performed. No statistically significant differences were observed.

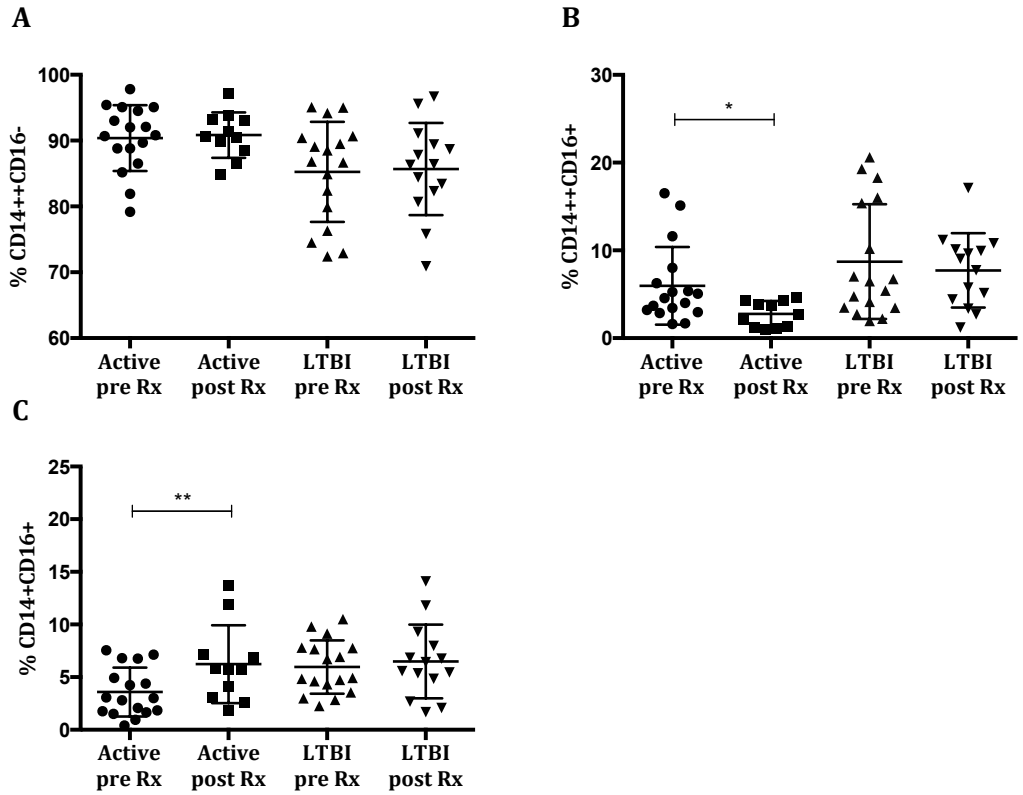


Figure 6.20 Changes in monocyte subsets following anti-TB treatment. Monocyte subsets were characterised among patients with active TB disease (n=11) and LTBI (n=14) after completing anti-TB treatment. The proportions of classical (A), intermediate (B) and non-classical (C) monocytes were calculated from the total monocyte population. Points are single values and bars represent the mean with SD. After testing for normality, an ordinary one-way ANOVA with Tukey's correction (A and C) or a Kruskal-Wallis test with Dunn's correction for multiple comparisons (B) was performed. * represents a p-value of <0.05 and ** a p-value of <0.005.

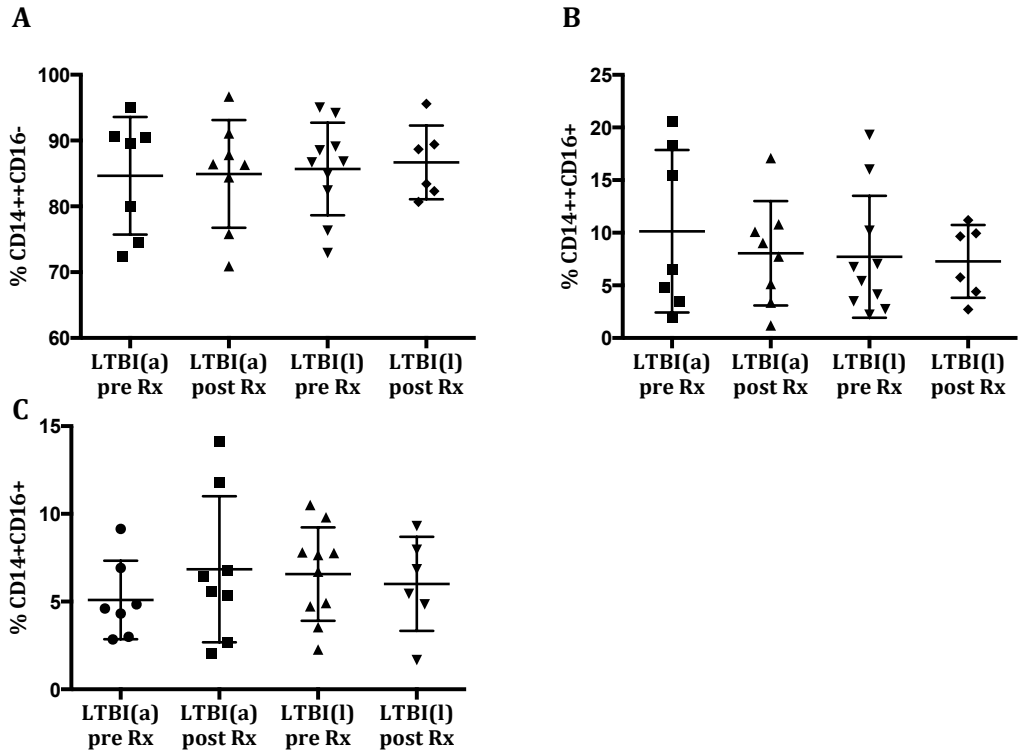


Figure 6.21 Post-treatment monocyte profiles in LTBI subgroups. The proportions of classical (A), intermediate (B) and non-classical (C) monocytes among LTBI(a) and LTBI(l) subgroups pre- and post-treatment for TB were determined. Points are single values and bars represent the mean with SD. After testing for normality, a Wilcoxon matched-pairs signed ranks test between LTBI(a) and LTBI(l) subgroups was performed. No statistically significant differences were observed.

6.4.5 Characterisation of functional T cell responses

The identification of *M. tb*-specific T cells producing one, two or three cytokines has been described in recent years and it has been suggested that this may reflect the immune response to varying mycobacterial load. Therefore I sought to evaluate such responses in this study, assessing IFN-γ, IL-2, TNF-α and IL-17 production, and to determine whether associations with stratified subgroups of LTBI patients occurred. PBMC isolated from patients with active disease (n=18), those with LTBI (n=20) and

healthy controls (n=10) were stimulated overnight with PPD, a pool of overlapping *M. tb*-specific peptides (ESAT-6/CFP-10), or SEB. An unstimulated negative control was also included. The frequency of CD4+ and CD8+ T cells was identified by surface staining and cytokine induction by intracellular staining (ICS) using multi-parameter flow cytometry (Figure 6.22-24). The background cytokine production in the unstimulated samples was subtracted from the stimulated conditions.

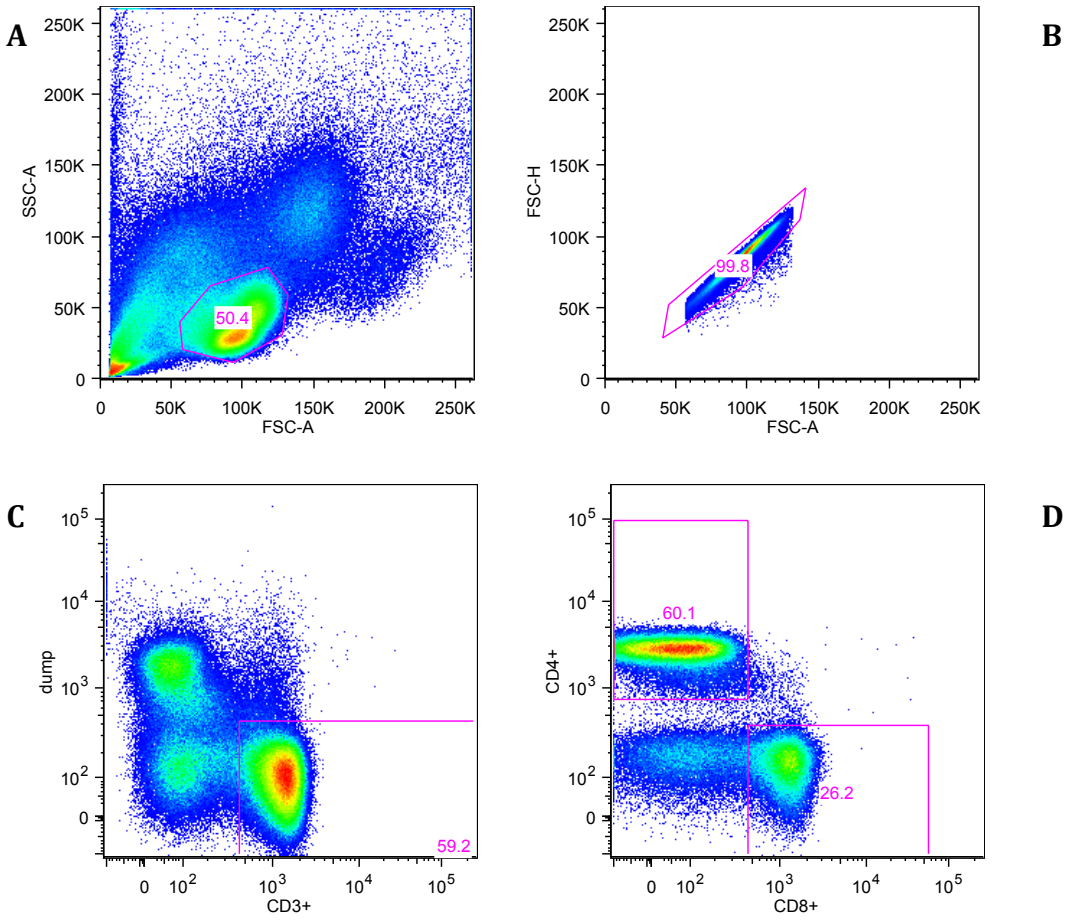


Figure 6.22 CD4+ and CD8+ T cell gating strategy. Cells were visualized by size (FSC-A vs SSC-A) and a large gate was drawn around the lymphocyte cloud, excluding most cell debris (A). Singlets and live cells were then selected (B). CD14+ and CD19+ cells (dump) were excluded and CD3+ T cells selected (C), after which CD4+ and CD8+ T cells were identified (D). The proportion of each population of the total CD3+ lymphocytes was calculated.

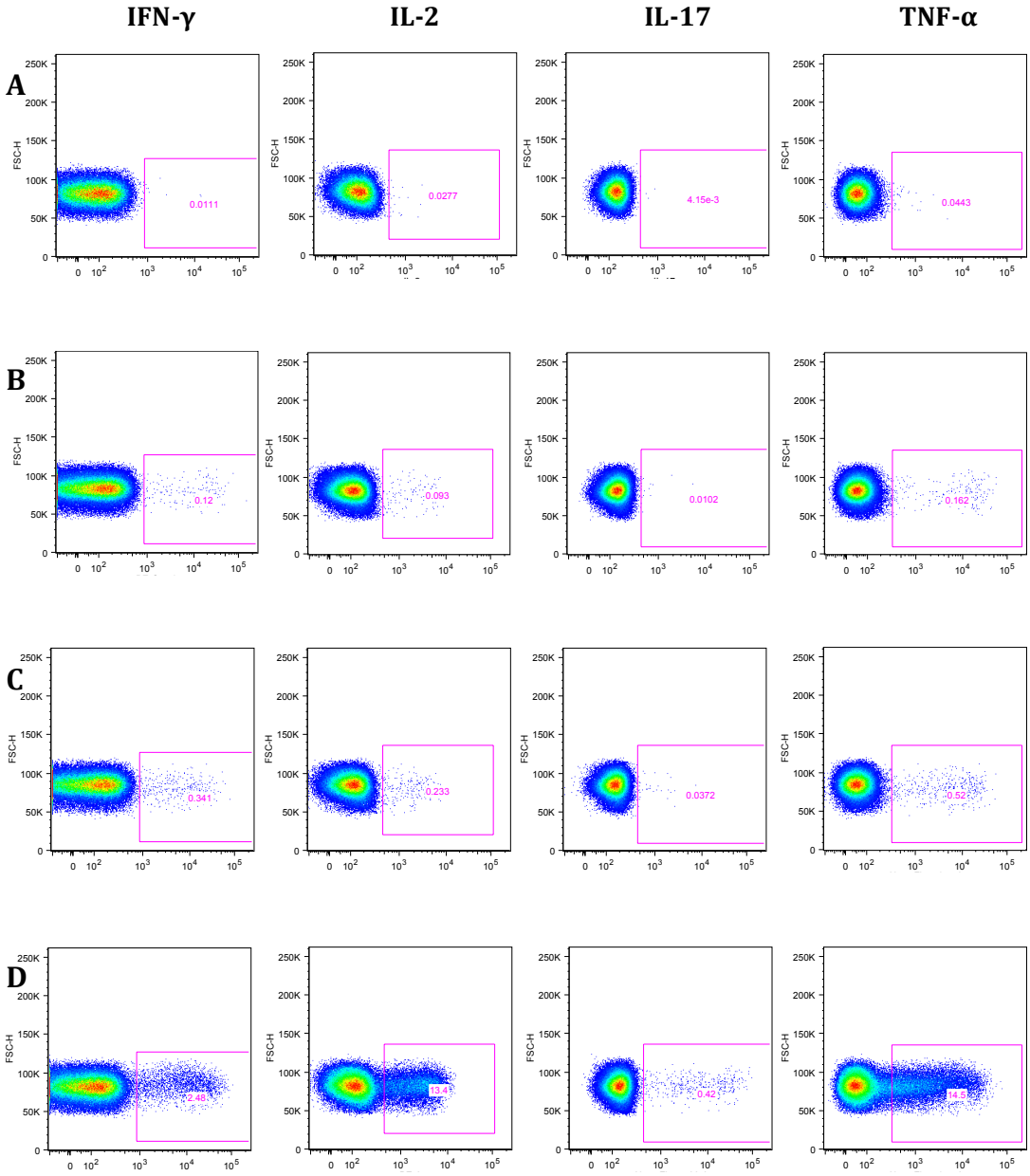


Figure 6.23 Functional CD4+ T cell characterisation. An example of flow cytometry plots showing the functional characterisation of CD4+ T cells. PBMC were unstimulated (A) or stimulated with an ESAT-6/CFP-10 peptide pool (B), PPD (C) or SEB (D). The proportion of CD4+ T cells producing IFN-γ, IL-2, IL-17 and TNF-α was calculated and background responses were subtracted.

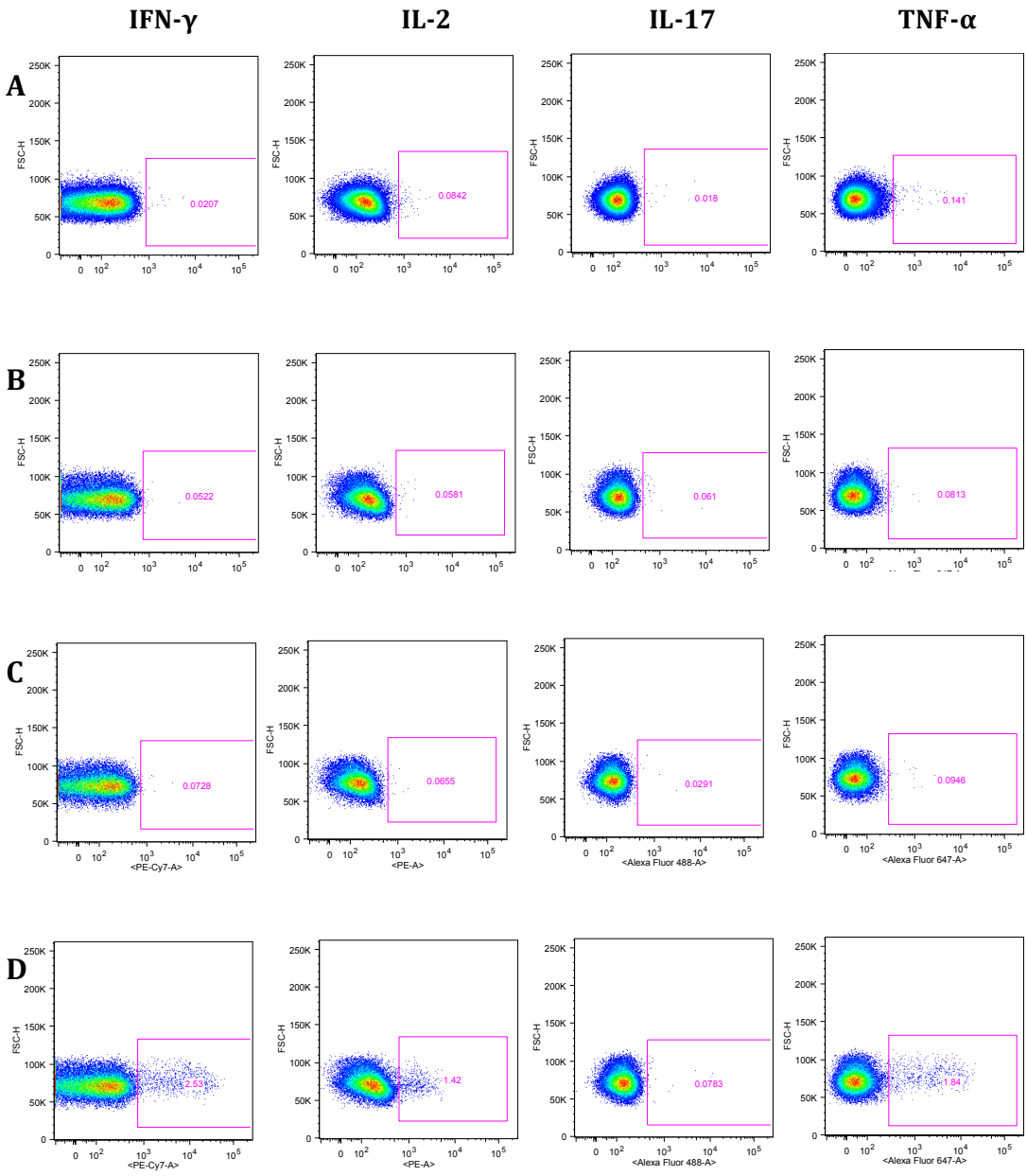


Figure 6.24 Functional CD8+ T cell characterisation. An example of flow cytometry plots showing the functional characterisation of CD8+ T cells. PBMC were unstimulated (A) or stimulated with an ESAT-6/CFP-10 peptide pool (B), PPD (C) or SEB (D). The proportion of CD8+ cells producing IFN-γ, IL-2, IL-17 and TNF-α was calculated and background responses were subtracted.

PPD stimulation induced the production of all four cytokines by both CD4+ and CD8+ T cells in each study group (Figure 6.25 A and B). The frequency of IFN-γ, IL-2, and TNF-α producing CD4+ T cells (total cytokine production) was considerably higher than CD8+ T cells and typically 10-20 fold differences were noted. In contrast, IL-17 production was very low in CD4+ T cells. While there was a trend for higher frequencies of IFN-γ, IL-2, and TNF-α producing CD4+ T cells in active and latent patients compared with healthy controls, no statistically significant differences in cytokine induction within each T cell subset was identified.

In contrast, stimulation with ESAT-6/CFP-10 peptides resulted in the induction of significantly greater numbers of IFN-γ, IL-2, and IL-17 producing CD4+ T cells among active TB and LTBI patients compared with healthy controls (Figure 6.25 C and D). There was no differences between the TB-infected subjects except in the case of IL-17 which was significantly higher in active patients compared to both LTBI and control groups. Interestingly, elevated responses in TNF-α production by CD4+ and CD8+ cells were seen among healthy controls, which was significant in CD8+ T cells. Considerably higher CD8+ responses were seen following ESAT-6/CFP-10 induction compared with PPD.

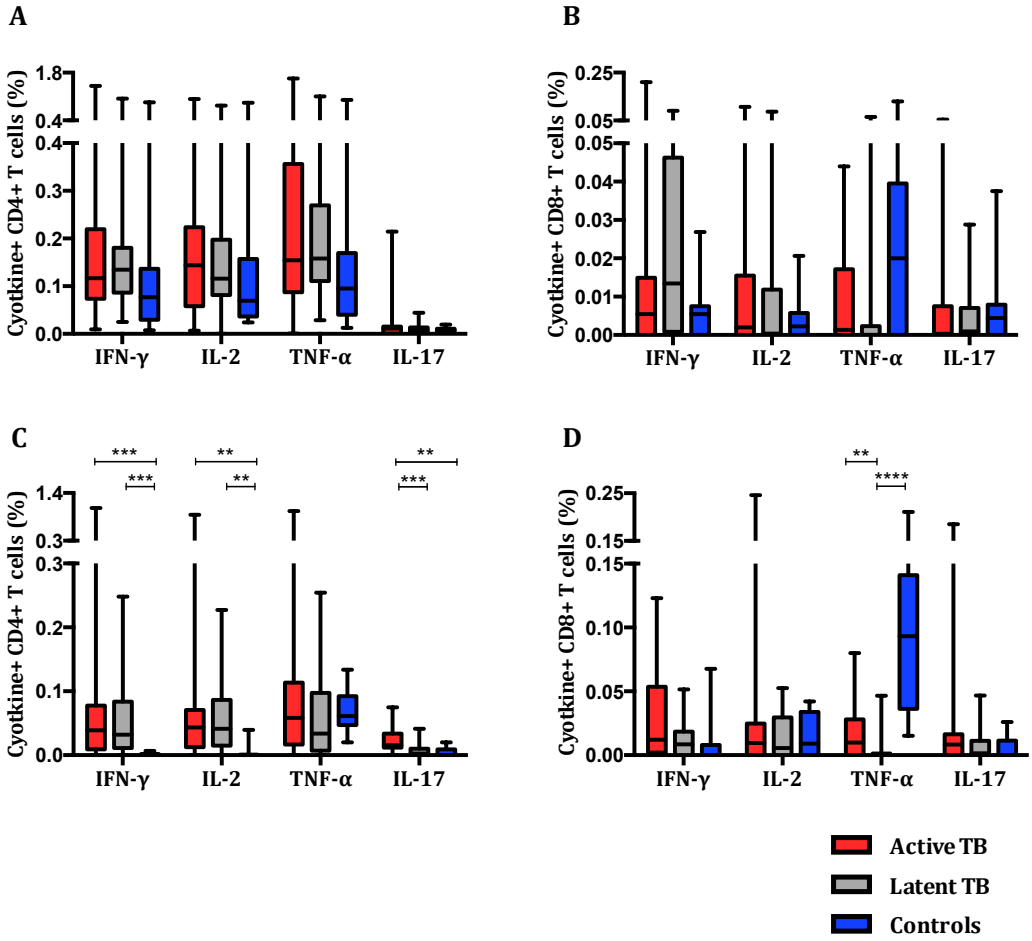


Figure 6.25 Pre-treatment T cell cytokine secretion. Pre-treatment PBMC from patients with active disease (n=18), LTBI (n=20) and healthy controls (n=10) were stimulated with either PPD or a peptide pool of ESAT-6/CFP-10 and the frequency of CD4+ and CD8+ T cells producing IFN-γ, IL-2, TNF-α and IL-17 was determined by flow cytometry. The frequencies of cytokine producing CD4+ and CD8+ T cells following stimulation with PPD (A & B, respectively) or ESAT-6/CFP-10 (C & D, respectively) are shown. Proportions of total CD4+ or CD8+ T cells are given. After testing for normality, a Kruskal-Wallis test with Dunn's correction for multiple comparisons was performed. ** represents a p-value of <0.005, *** a p-value of <0.0005 and **** a p-value of <0.0001.

On stratifying the LTBI individuals into LTBI(a) and LTBI(l), there was little difference in frequencies of IFN-γ, IL-2, TNF-α or IL-17 producing CD4+ or CD8+ T cells after PPD stimulation between the groups, although a trend for higher frequencies of IFN-γ and IL- 17 and fewer TNF-α-producing CD8+ T cells in the LTBI(a) subgroup was noted (Figure 6.26 A and B). With ESAT-6/CFP-10 stimulation, these relationships were similar. However, there were significantly more IL-2, and fewer TNF-α-producing CD8+ T cells, in the LTBI(a) subgroup, and a trend towards more CD8+ T cells producing IFN-γ in this group also (Figure 6.26 C and D). No significant changes in the frequencies of PPD- and *M. tb*-specific single cytokine-producing CD4+ or CD8+ T cells in response to anti-TB treatment were noted in either active disease or LTBI groups (Figure 6.27). This was also the case for LTBI subgroups (data not shown).

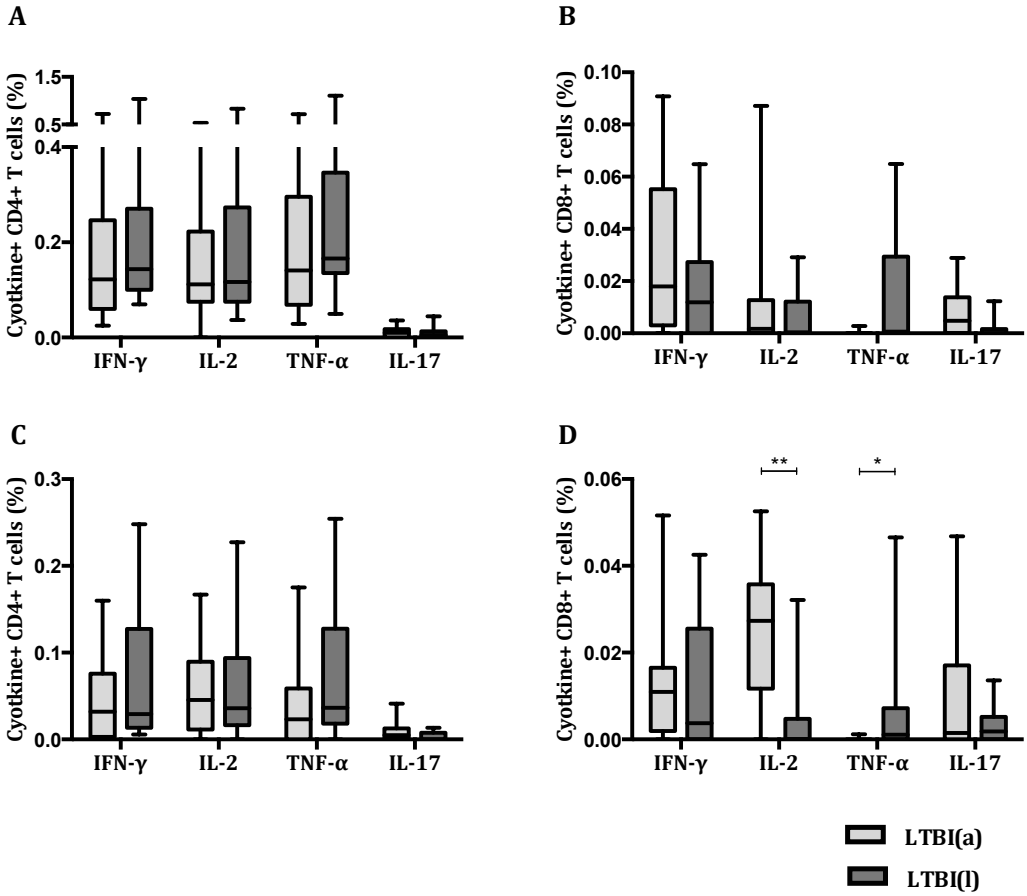


Figure 6.26 Baseline T cell cytokine secretion in LTBI subgroups. The LTBI cohort was separated into LTBI(a) and LTBI(l) subgroups on the basis of mycobacterial control (n=10 each). The frequencies of cytokine producing CD4+ and CD8+ T cells following stimulation with PPD (A & B, respectively) or ESAT-6/CFP-10 (C & D, respectively) are shown. Proportions of total CD4+ or CD8+ T cells are given. After testing for normality, an unpaired Mann-Whitney test between LTBI(a) and LTBI(l) subgroups was performed. * represents a p-value of <0.05 and ** a p-value of <0.01.

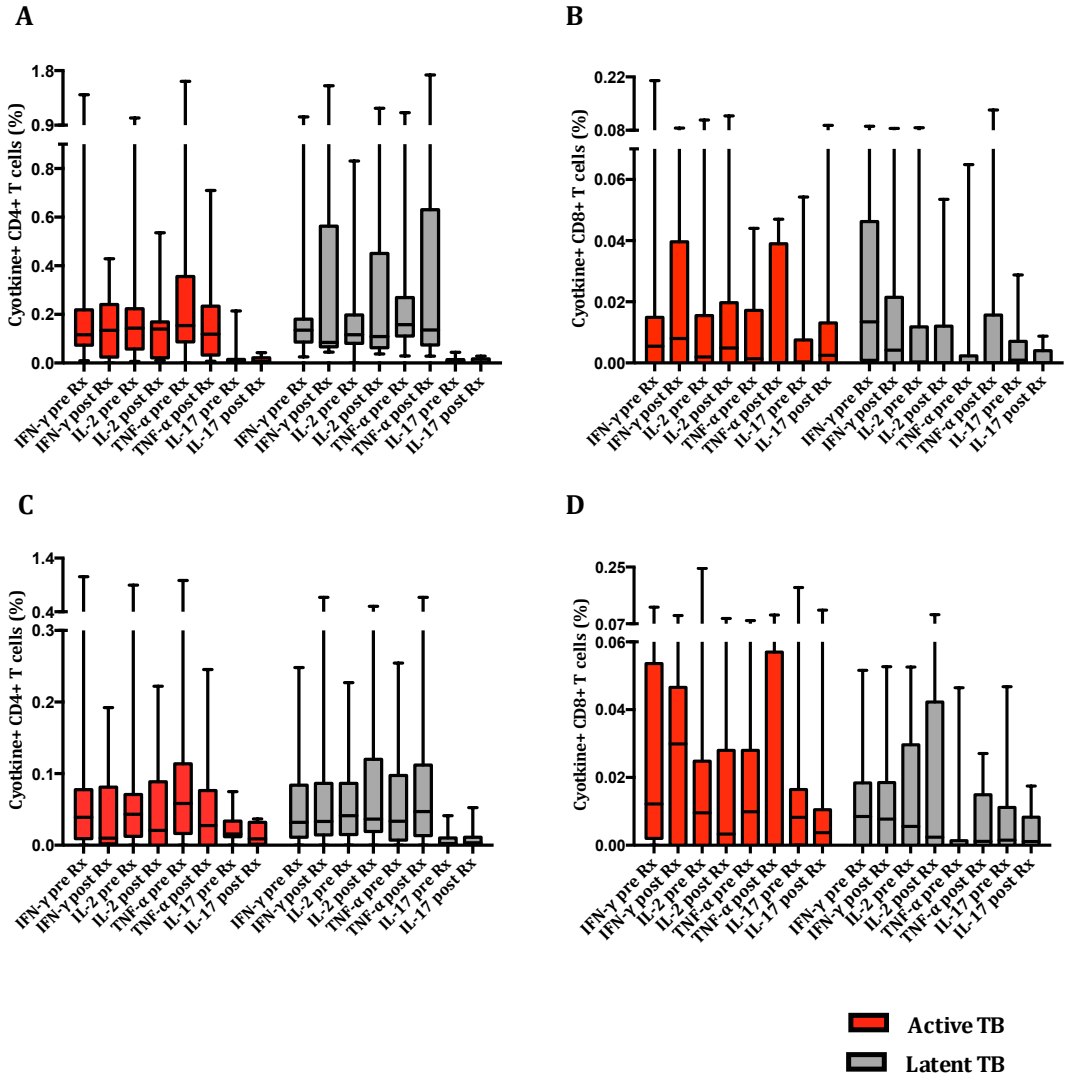


Figure 6.27 Changes in T cell cytokine secretion after treatment. PBMC isolated from patients after completion of treatment for active disease (n=11) and LTBI (n=14) were stimulated with either PPD or a peptide pool of ESAT-6/CFP-10 and the frequency of CD4+ and CD8+ T cells producing IFN-γ, IL-2, TNF-α and IL-17 was determined by flow cytometry. The frequencies of cytokine producing CD4+ and CD8+ T cells following stimulation with PPD (A & B, respectively) or ESAT-6/CFP-10 (C & D, respectively) are shown. Proportions of total CD4+ or CD8+ T cells are given. After testing for normality, a Wilcoxon matched-pairs signed rank test between pre- and post-treatment cytokine production was performed. No significant differences were observed.

In view of increasing evidence that CD4+ and CD8+ T cells producing more than one cytokine simultaneously may have important roles in TB immunity, the proportion of *M. tb*-specific polyfunctional T cells was also evaluated. Due to the very low frequency of IL-17 producing T cells, this cytokine was excluded from these analyses. Therefore polyfunctional cells are defined here as those T cells secreting IFN-γ, IL-2 and TNF-α and bifunctional cells as those secreting any combination of two of these cytokines.

Before treatment, and in response to ESAT-6/CFP-10 stimulation, patients with active TB disease showed a predominance of polyfunctional CD4+ T cells, followed by bifunctional then monofunctional cells (Figure 6.28). Following treatment, these proportions changed considerably, with a contraction of the polyfunctional CD4+ population and a substantial increase in monofunctional cells. The proportion of bifunctional CD4+ T cells was also reduced after anti-TB treatment. CD8+ T cells in this population were characterised by mostly bifunctional cells, followed by monofunctional cells and interestingly the proportion of bifunctional cells increased after treatment (Figure 6.29).

In the latently infected group as a whole, very few *M. tb*-specific monofunctional CD4+ T cells were observed (Figure 6.28). The proportion of polyfunctional CD4+ T cells dominated (even more so that in active patients) and bifunctional cells followed in magnitude. Again, after TB treatment, the frequency of polyfunctional cells declined with a concomitant increase in monofunctional CD4+ T cells, resulting in a profile very similar to the active TB patients after treatment. The CD8+ T cell profile in latent patients showed entirely monofunctional cells pre-treatment, with a contraction of this population and increase in bifunctional cells after treatment (Figure 6.29).

After stratifying the LTBI individuals into LTBI(a) and LTBI(l), some interesting patterns were noted. The proportion of *M. tb*-specific polyfunctional CD4+ T cells was

similar in both LTBI(a) and LTBI(l) groups (Figure 6.30 A and B). However, the LTBI(a) group demonstrated substantially more monofunctional CD4+ T cells than in LTBI(l), similar to the pattern seen in active patients (although bifunctional cells were more significant in the latter) (Figure 6.30 A). In contrast, after polyfunctional cells, it was bifunctional CD4+ T cells that occurred most frequently in the LTBI(l) group (Figure 6.30 B). Both LTBI subgroups showed declines in polyfunctional CD4+ T cells after treatment, although less so in the LTBI(l) group which showed a substantial increase in monofunctional cells in both subgroups (Figure 6.30 A and B). The CD8+ T cells in the LTBI(a) subgroup were predominantly single cytokine producers with some bifunctional cells, which changed little after treatment (Figure 6.30 C). In contrast, all CD8+ T cells in the LTBI(l) group were monofunctional and switched to bifunctional cells following anti-TB therapy (Figure 6.30 D). The frequencies of mono-, bi- and polyfunctional cytokine producing T cells are shown (Figure 6.31). Strikingly, healthy controls had evidence of only monofunctional CD4+ T cells, but CD8+ T cells were divided between a majority of monofunctional and minority of bifunctional cells (data not shown).

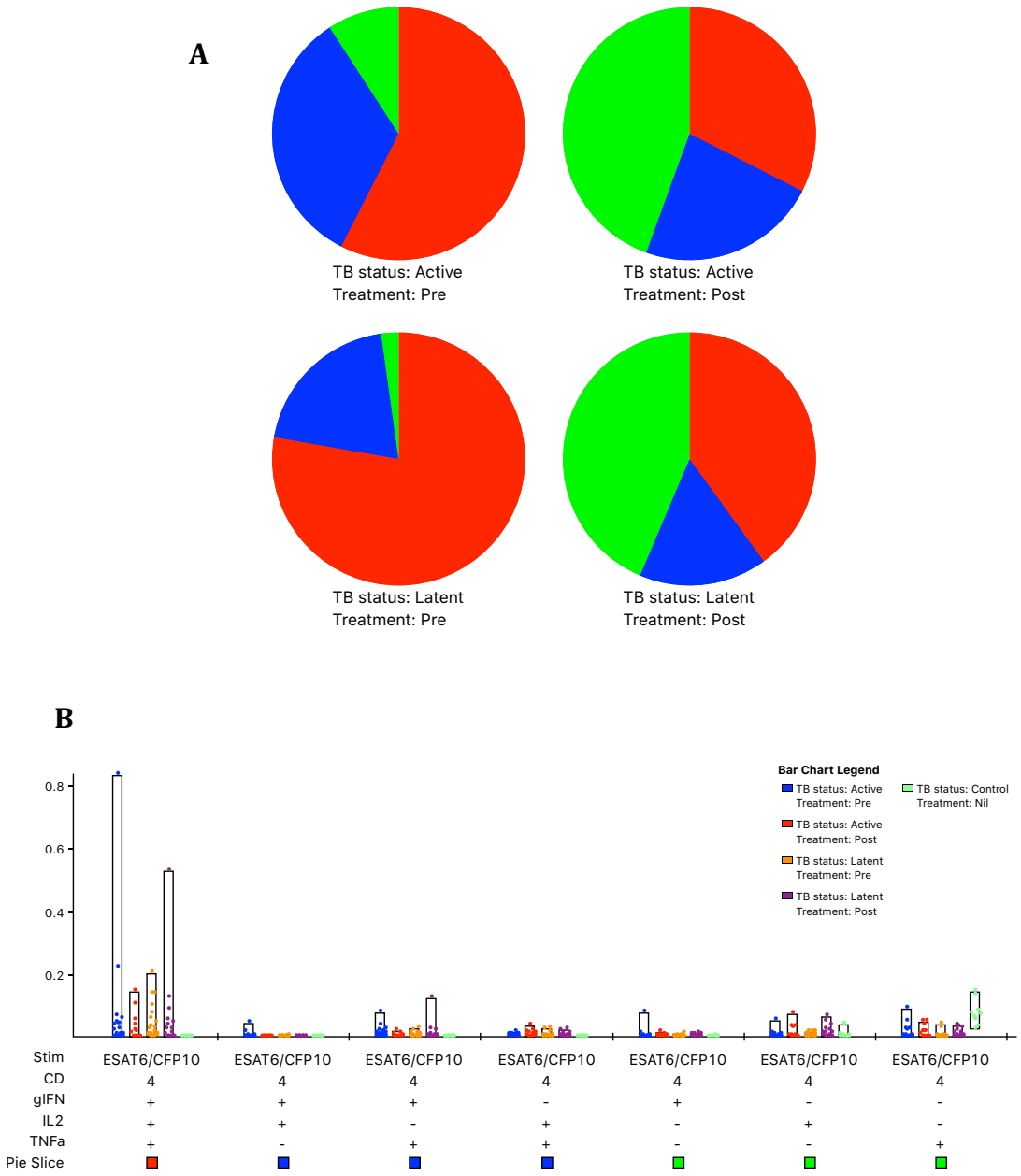


Figure 6.28 Polyfunctional CD4+ *M. tb*-specific cytokine responses. Pre-treatment and post-treatment CD4+ T cells producing one, two or three cytokines (IFN-γ, IL-2, and TNF-α) following stimulation with a peptide pool of ESAT-6/CFP-10 are shown. Median proportions of mono- (green), bi- (blue) and polyfunctional (red) CD4+ T cells are given (A), together with the frequency of responses (B) (corrected for background). IL-17 was excluded from the analysis due to the negligible responses seen in most subjects. Groups include active disease and LTBI. Healthy controls were monofunctional only (data not shown).

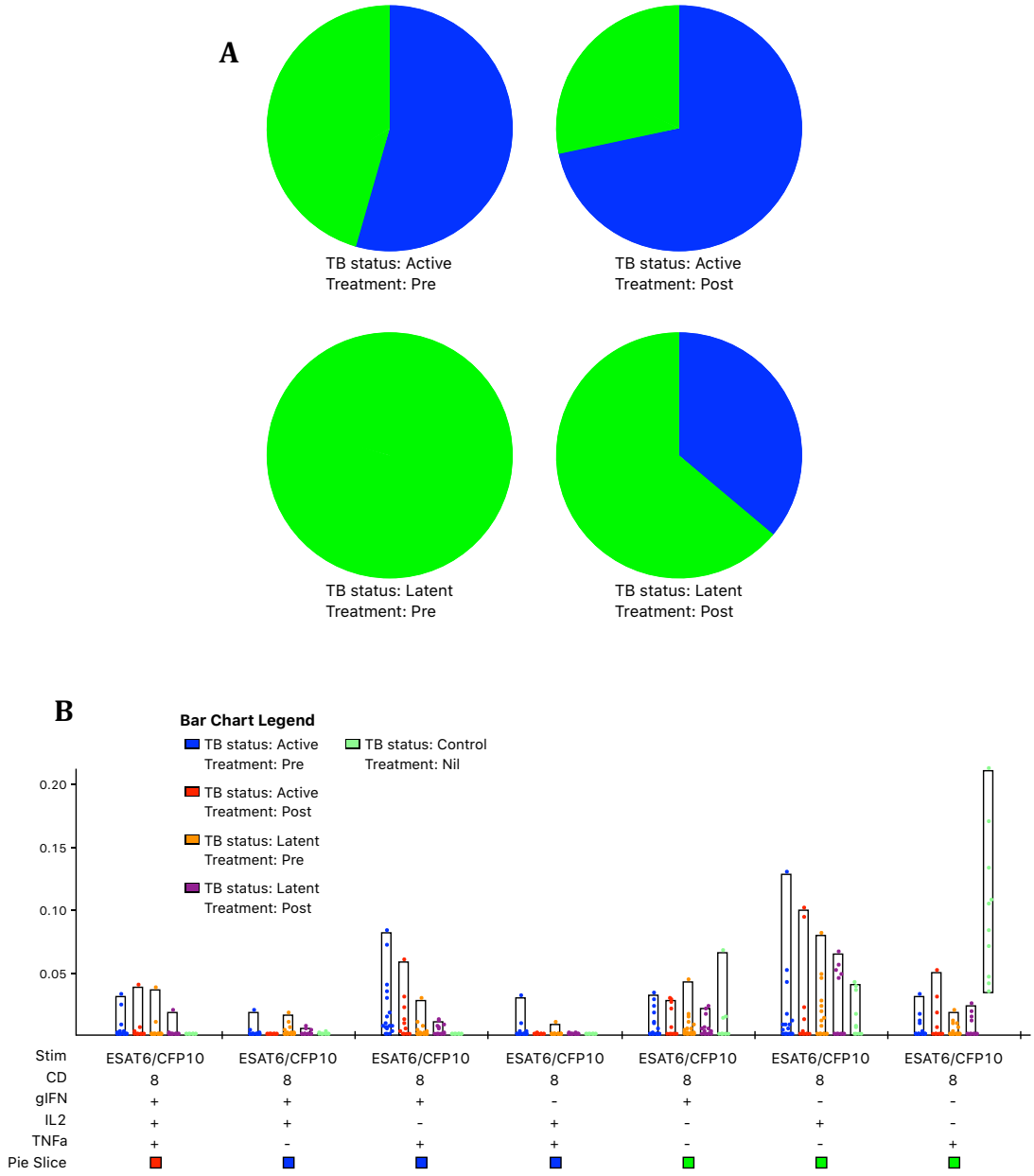


Figure 6.29 Polyfunctional CD8+ *M. tb*-specific cytokine responses. Pre-treatment and post-treatment CD8+ T cells producing one, two or three cytokines (IFN-γ, IL-2, and TNF-α) following stimulation with a peptide pool of ESAT-6/CFP-10 are shown. Median proportions of mono- (green), bi- (blue) and polyfunctional (red) CD8+ T cells are given (A), together with the frequency of responses (B) (corrected for background). IL-17 was excluded from the analysis due to the negligible responses seen in most subjects. Groups include active disease and LTBI. Healthy controls were monofunctional only (data not shown).

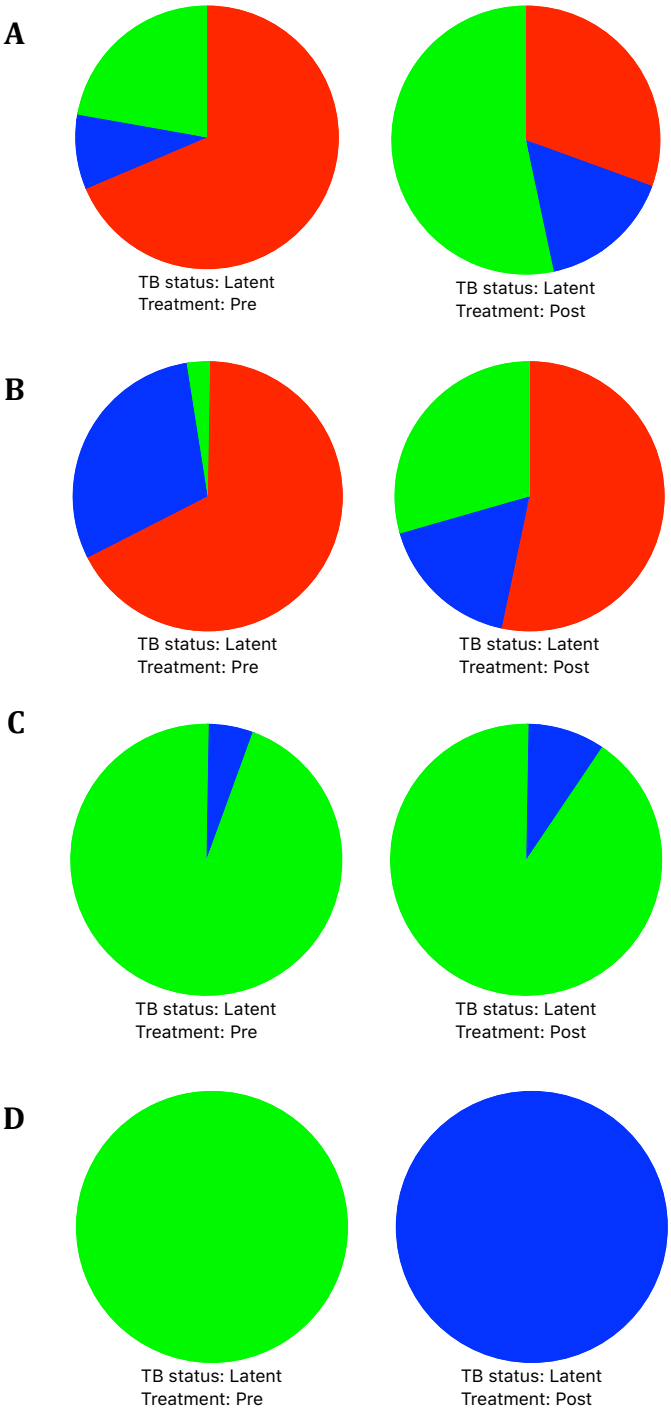


Figure 6.30 Proportions of polyfunctional T cells responses in stratified LTBI subgroups. Pre-treatment and post-treatment CD4+ and CD8+ T cells producing one, two or three cytokines (IFN-γ, IL-2, and TNF-α) following stimulation with a peptide pool of ESAT-6/CFP-10 are shown. Median proportions of mono- (green), bi- (blue) and polyfunctional (red) T cells are given as follows: CD4+ LTBI(a) (A) and LTBI(l) (B); CD8+ LTBI(a) (C) and LTBI(l) (D). IL-17 was excluded from the analysis due to the negligible responses seen in most subjects.

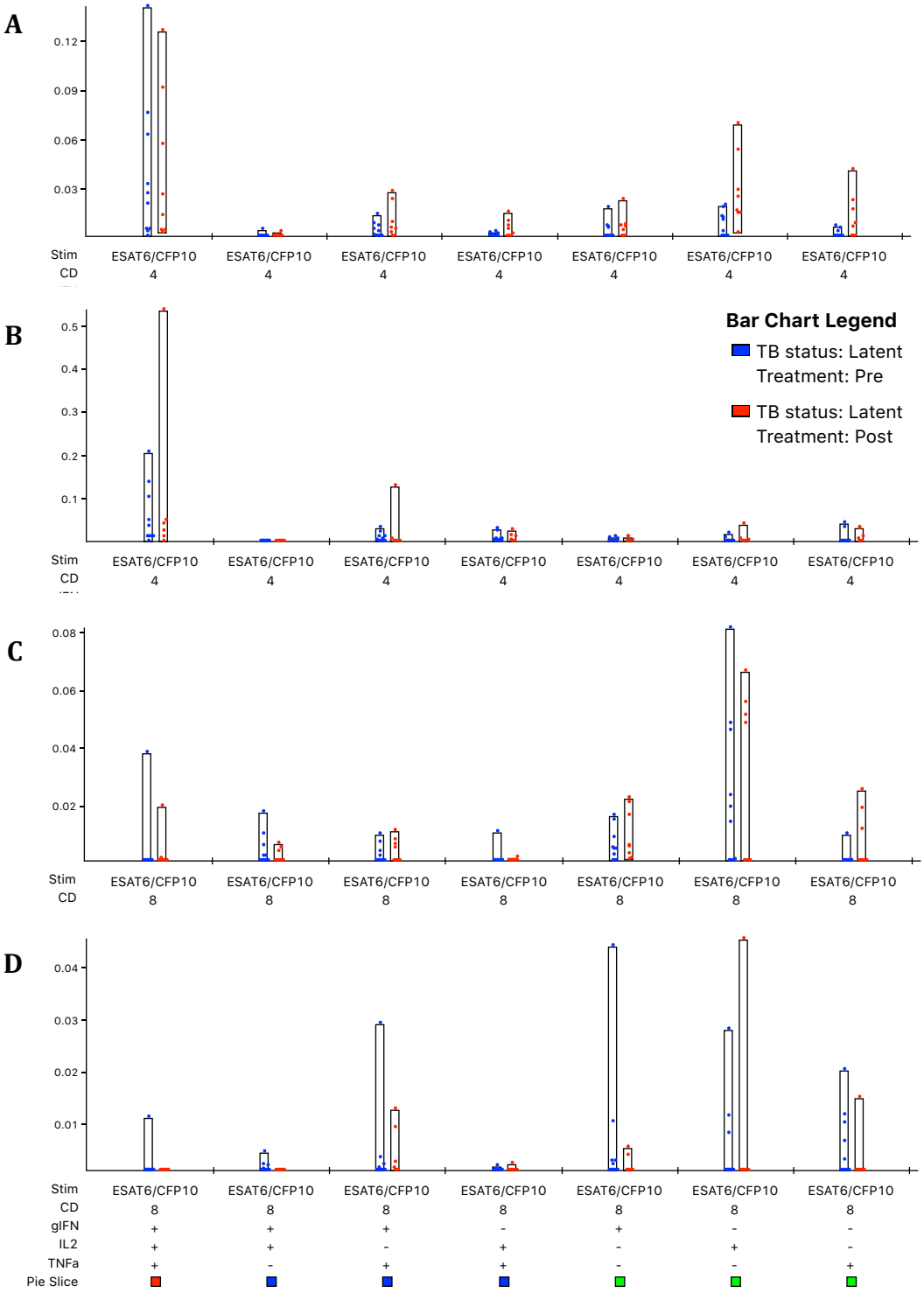


Figure 6.31 Frequencies of polyfunctional T cells responses in stratified LTBI subgroups. Pre-treatment and post-treatment CD4+ and CD8+ T cells responses following stimulation with ESAT-6/CFP-10 are shown. The frequency of T cell responses (corresponding to the preceding pie charts) are: CD4+ LTBI(a) (A) and LTBI(l) (B); CD8+ LTBI(a) (C) and LTBI(l) (D).

6.4.6 Characterising IgG subclass distribution

I evaluated the distribution of IgG subclass antibody responses to a variety of *M. tb*-specific antigens to determine whether these could delineate the spectrum of LTBI, particularly within the stratified LTBI subgroups. To date, most studies have focused on measuring total IgG or a single IgG subclass against limited types of antigens. In order to gain a broader understanding in this study population, the responses of IgG1, 2, 3 and 4 subclasses were investigated against both protein and non-protein antigens derived from *M. tb* H37Rv. Complex, composite antigens included culture filtrate and cell membrane fractions prepared from H37Rv, while single antigens included LAM and ESAT-6/CFP-10. Only pre-treatment (and control) serum samples were analysed because antibody persistence following successful treatment is highly variable, with reports ranging from a few months to 2 years. This seems dependent on individual factors, immunoglobulin class and subclass, and the antigens used in the ELISA [532, 533]. Therefore post-treatment samples were not tested. An initial screen of all IgG subclasses in pre-treatment serum samples from a subgroup of active TB patients (n=10) over several dilutions against all of the test antigens described above was performed. Negligible responses of IgG3 and IgG4 were detected above background, even at low dilutions, therefore only IgG1 and IgG2 were taken forward for further testing (data not shown). Initial intentions were to develop a semi-quantitative ELISA to allow for more intuitive comparisons of antibody levels. Within the host laboratory it has been suggested that, if the gradient of IgG ELISA OD values derived from a range of serum dilutions against a target antigen is similar to the gradient of an IgG standard concentration curve, then it may be possible to determine a semi-quantitative measure of immunoglobulin content in clinical samples. This has proven a valid approach in studies of humoral responses to candidate malaria vaccines (Draper, unpublished data). Standard curves were generated over a wide range of concentrations for each

IgG subclass. IgG1 and IgG2 responses to all of the test antigens in serum samples from active TB patients (n=10) were evaluated over several dilutions. Unfortunately, the serum OD gradients were found to differ too significantly from that of the concentration curves (>3SD of the standard curve mean *m* value for each IgG subclass), therefore this approach was not pursued. Potential reasons for this include different binding kinetics of antibody-antigen complex formation and the use of monoclonal IgG antibodies for generating the standard curve, which is in contrast to the polyclonal nature of human serum. While comparisons between subclasses are possible, without quantitative or semi-quantitative measures, only descriptions of patterns of IgG responses are appropriate.

Serum samples from patients with active TB (n=21), LTBI (n=30; LTBI(a) n=14; LTBI(l) n=16) and healthy controls (n=20) were analysed. IgG2 responses predominated, among which anti-LAM IgG2 in active TB patients generated the highest responses overall, followed by anti-culture filtrate IgG2 (median OD=0.50 and 0.28, respectively) (Figure 6.32). Significant differences in both IgG1 and IgG2 responses between active TB and controls were seen against all antigens. In addition, significant differences between TB and LTBI groups were also noted for IgG2 with every antigen, however for IgG1 this only occurred against LAM and culture filtrate. The only significant difference between LTBI and healthy controls was seen with anti-ESAT-6/CFP-10 IgG1 (Figure 6.32). There were correlations between IgG1 and IgG2 responses for each antigen and most significantly for LAM and culture filtrate (Table 6.2). Very interestingly, analysis of the whole population tested by ELISA (n=71) showed significant negative correlations between anti-ESAT-6/CFP-10 IgG1 ODs and the net growth of both BCG (r=-0.37, p=0.013) and H37Rv (r=-0.36, p=0.003). A weaker negative correlation between anti-culture filtrate IgG1 and H37Rv net growth was noted (r=-0.057, p=0.05). Furthermore, when the LTBI group was stratified by MGIT responses, a discriminatory

difference between LTBI(a) and LTBI(l) subgroups was seen with anti-ESAT-6/CFP-10 IgG1 (median OD=0.22 vs 0.084, p=0.05) (Figure 6.33). While there was a trend for higher anti-LAM IgG2 responses in the LTBI(a) subgroup, this was not significant (median OD=0.13 vs 0.071, p=0.3).

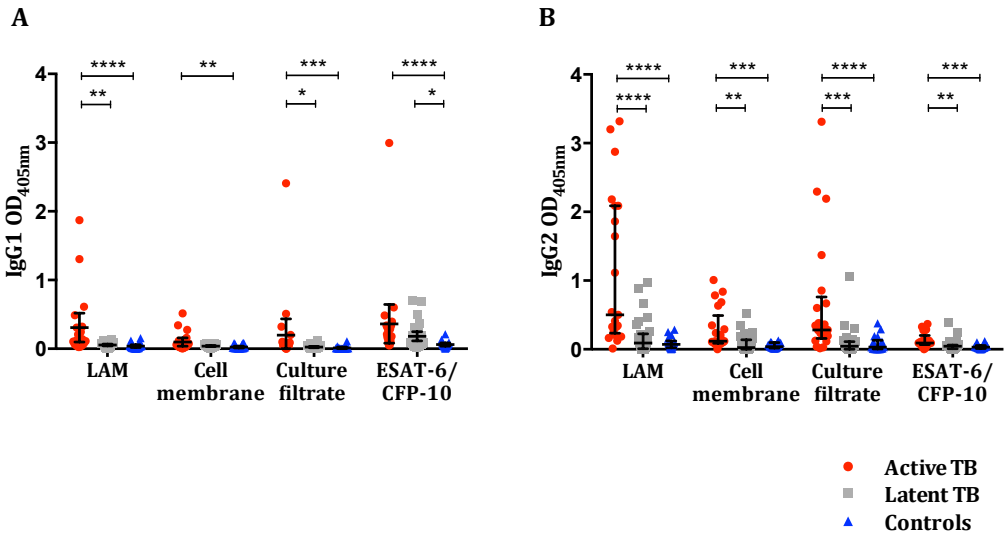


Figure 6.32 IgG antibody responses in TB. Antigen-specific IgG1 (A) and IgG2 (B) responses in pre-treatment samples from active TB (n=21), LTBI (n=30) and healthy control individuals (n=20) were determined by ELISA. Antigens used were *M. tb* H37Rv-derived LAM, cell membrane fraction, culture filtrate and ESAT-6/CFP-10. Optical densities (ODs) are reported following subtraction of the background. Points represent the mean of duplicates and bars are the median values with the interquartile range. After normality testing a Kruskal-Wallis test with Dunn's correction for multiple comparisons was performed for each antigen. * represents a p-value of <0.05, ** a p-value of <0.005, *** a p-value of <0.0005 and **** a p-value of <0.0001.

IgG subclasses	Antigen	r	p-value
IgG1 vs IgG2	LAM	0.59	<0.0001
	Cell membrane	0.31	0.01
	Culture filtrate	0.35	0.003
	ESAT-6/CFP-10	0.27	0.02

Table 6.2 Correlation of antigen-specific IgG1 and IgG2 antibody responses. The correlation between IgG1 and IgG2 responses, as measured by OD, against each antigen was evaluated by performing a Spearman correlation matrix. Spearman r correlation coefficients and associated p-values are shown.

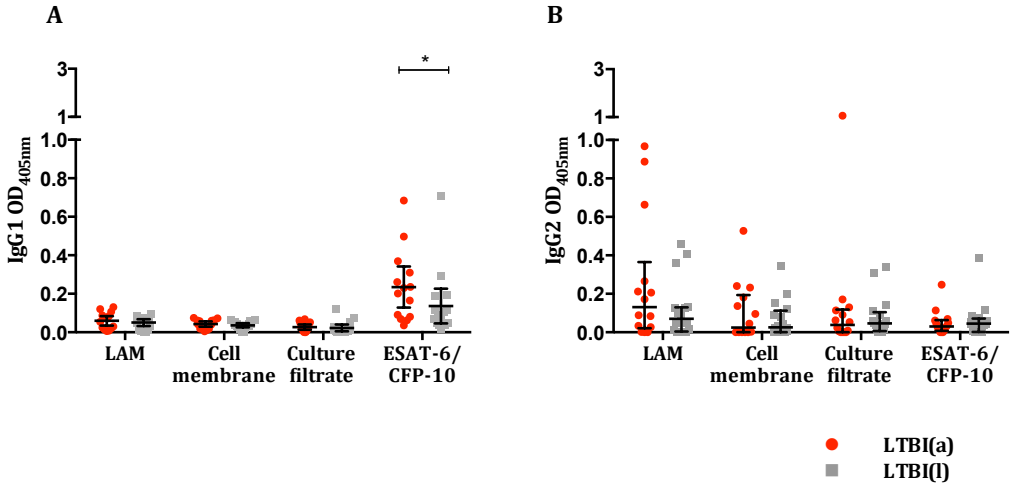


Figure 6.33 IgG antibody responses in LTBI subgroups. Antigen-specific IgG1 (A) and IgG2 (B) responses in pre-treatment samples from individuals with LTBI stratified by MGIT net growth as either LTBI(a) or LTBI(l) (n=14, n=16, respectively) were determined by ELISA. Antigens used were *M. tb* H37Rv-derived LAM, cell membrane fraction, culture filtrate and ESAT-6/CFP-10. Optical densities are reported following subtraction of the background. Points represent the mean of duplicates and bars are the median values with the interquartile range. After testing for normality, an unpaired Mann-Whitney test between LTBI(a) and LTBI(l) subgroups was performed. * represents a p-value of <0.05.

6.4.7 Evaluating B cell responses to TB

As discussed in Chapter 4, there is increasing interest in the possible role played by mycobacterial-specific B cells in the host immune response to *M. tb*. Evaluating these cells may provide a more dynamic, discriminative measure of the humoral response, as short-lived *M. tb*-specific plasmablasts (PBs) may reflect active infection whilst memory B cells (mBCs) may indicate resolved or subclinical infection [431, 439, 466-469]. Therefore I sought to characterise the profiles of *M. tb*-specific PBs and mBC in the study cohort and to investigate whether the PB:mBC ratio correlated with diagnostic classification and MGIT data. Having optimised an *ex vivo* ELISpot assay for determining BCG-specific PB and mBC responses following BCG vaccination, I applied the same approach but using a range of mycobacterial antigens which included cell membrane fraction, ESAT-6 and CFP-10 derived from *M. tb* H37Rv, and PPD. Unfortunately, several attempts of assay optimization were unsuccessful. Despite assessing multiple conditions such as varying antigen concentrations, number of PBMC and coating buffers etc., visualisation of well-defined spot forming cells was not achieved. Negative controls showed low to minimal background and positive controls (total IgG) were successful, however patient samples produced poorly-defined, small, granular spots, which was is in contrast to those identified during the earlier BCG vaccination study (data not shown). Patients with active disease showed patterns of responses to *M. tb* antigens that could be identified macroscopically (i.e. higher responses to cell membrane fraction than to ESAT-6 or CFP-10), but an automated ELISpot reader could not accurately enumerate spot forming cells. Given the very high cell requirement for B cell ELISpot assays and their labour intensive nature, further use of this methodology was not pursued.

6.4.8 The immunophenotypic characterisation of B cell subsets

Although it was not possible to study antigen-specific B cell profiles I sought to characterise the different subsets of these cells in PBMC isolated from patients using the flow cytometry panel previously described. This included patients with active disease (n=19), those with LTBI (n=18) and healthy controls (n=9). The group of latently infected individuals consisted of samples from patients considered LTBI(a) and LTBI(l) (n=9 each), based on MGIT data. B cell subsets were defined as CD19+CD10- (mature B cells), CD27+CD21- (activated mBC), CD27+CD21+ (classical mBC), CD27-CD21+ (naïve mBC) and CD27-CD21- (atypical mBC) on the basis of FMO gating. Mature B cells were calculated from the total lymphocyte population and other subsets as a proportion of mature B cells. Patients with active TB disease and LTBI had fewer mature B cells than healthy controls, but this was only significantly different between LTBI and control groups (median=16.6%, 12.7%, 19.7%, respectively) (Figure 6.34). While there was no significant difference in the proportions of naïve mBC between active, LTBI and control groups, there was a trend for increased frequency in active TB (median=75.1%, 68.4%, 64.4%, respectively). Interestingly, activated and atypical mBC were significantly elevated among individuals with active TB and LTBI while classical mBC were reduced in the active group (Figure 6.34). When the LTBI cohort was separated by ability to control bacillary grow into LTBI(a) and LTBI(l) and evaluated, no significant differences between any of the B cell subsets and LTBI subgroup were seen (Figure 6.35). However, evaluation of MGIT data as a continuous variable (where available) showed significant negative correlations between the proportion of activated and atypical mBCs and MGIT BCG net growth values ($r=-0.48$, $p=0.02$; $r=-0.56$, $p=0.007$ by Spearman's test, respectively) (Figure 6.36).

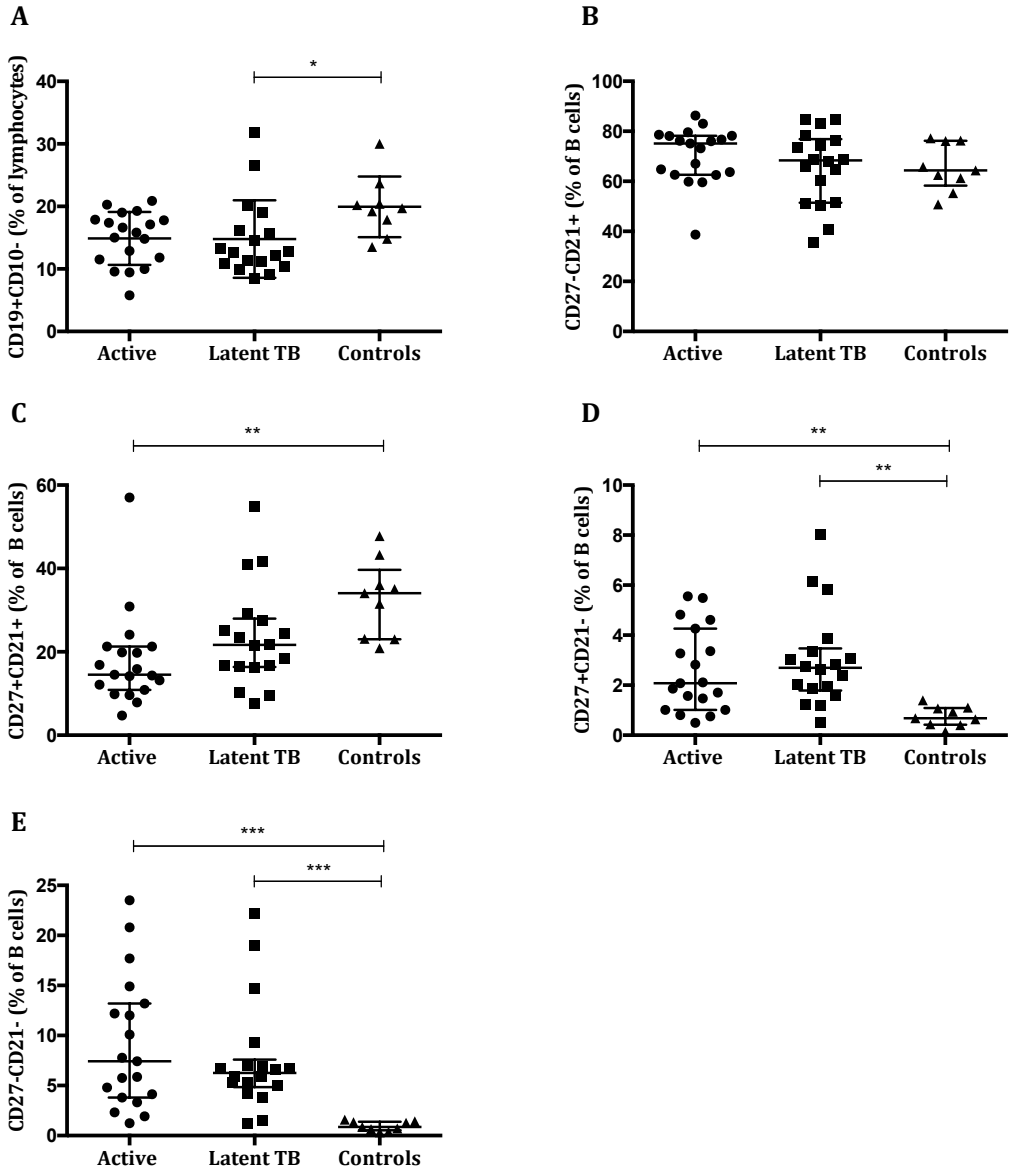


Figure 6.34 Pre-treatment B cell subset characterisation. B cell subsets were characterised among patients with active TB disease (n=19), latent infection (n=18) and healthy controls (n=9) before starting anti-TB treatment (where appropriate). The proportions of mature (A), naïve (B), classical (C), activated (D) and atypical (E) B cells were determined. Points are single values and bars represent the median with IQR. After testing for normality a Kruskal-Wallis test with Dunn's correction for multiple comparisons was performed. * represents a p-value of <0.05, ** a p-value of <0.005, *** a p-value of <0.0005 and **** a p-value of <0.0001.

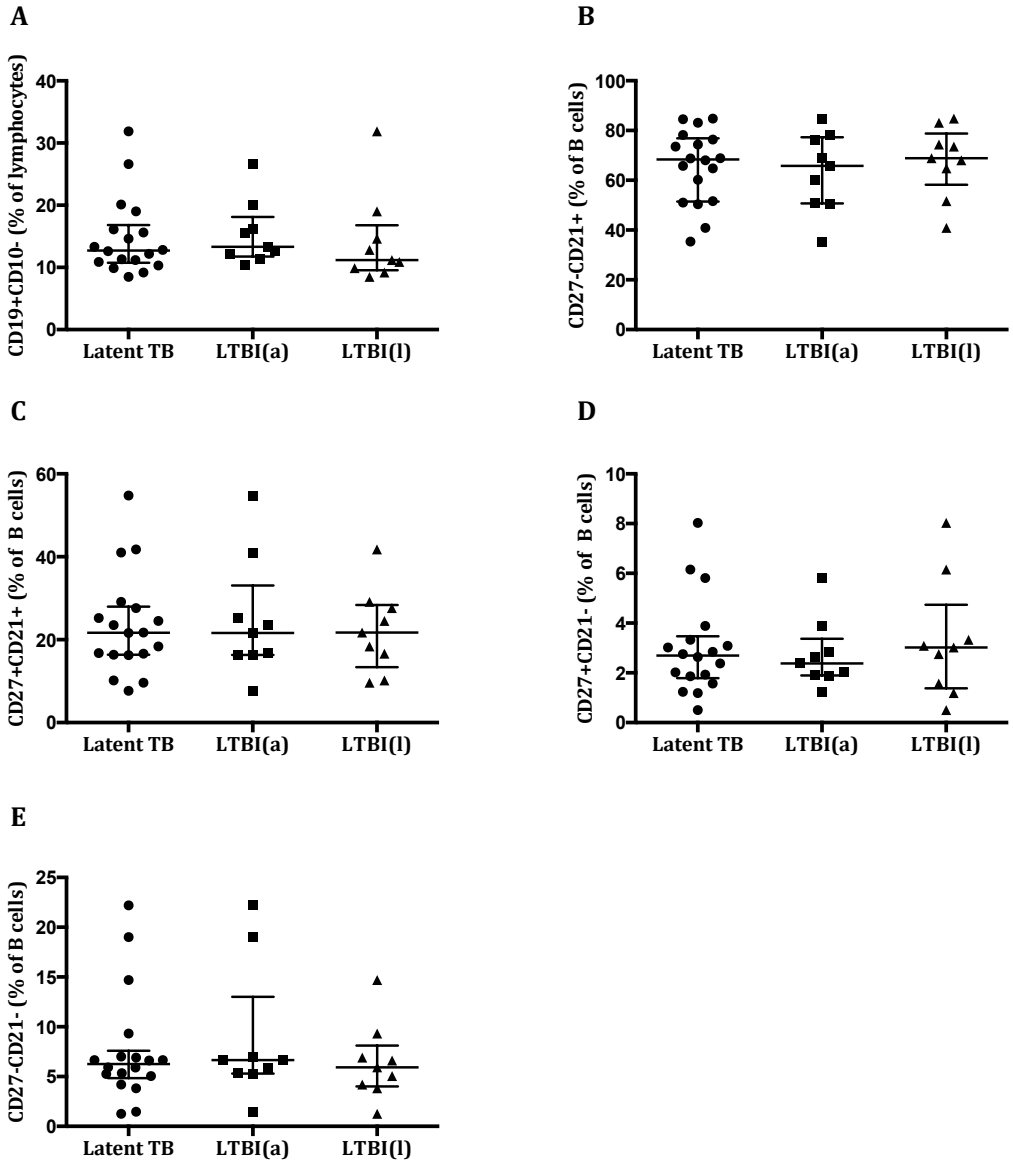


Figure 6.35 Baseline B cell profiles in LTBI subgroups. The LTBI cohort was separated into LTBI(a) and LTBI(l) (n=9 each) subgroups on the basis of mycobacterial control. The proportions of mature (A), naïve (B), classical (C), activated (D) and atypical (E) B cells were determined. Points are single values and bars represent the median with IQR. After testing for normality, an unpaired Mann-Whitney test between LTBI(a) and LTBI(l) subgroups was performed. No statistically significant differences were observed.

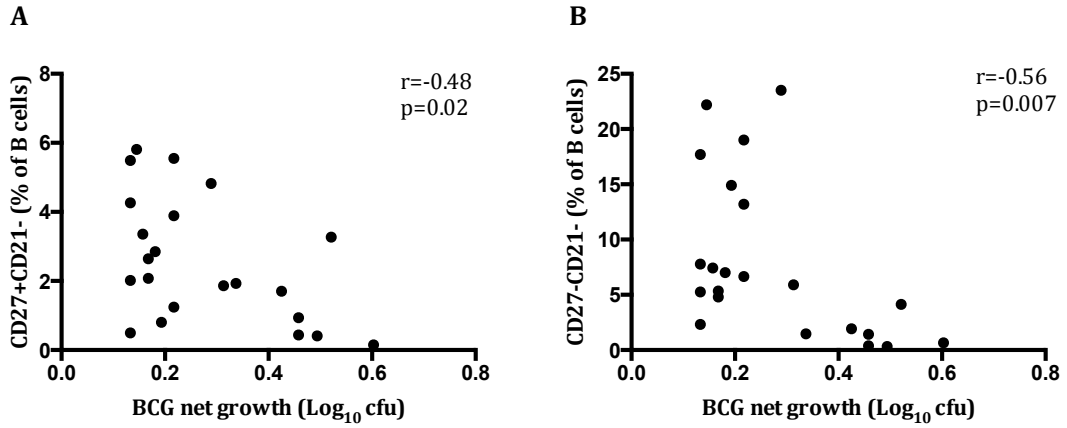


Figure 6.36 Correlations between baseline B cell subsets and whole blood MGIT. The significance of correlations between the proportions of B cell subsets and mycobacterial net growth in the MGIT assay were determined. Negatives correlations between the proportion of activated (A) and atypical (B) B cells and BCG net growth were seen. Spearman's r and associated p-values are shown.

6.5 Discussion

The aim of the experimental work undertaken in this chapter was to characterise the mycobacterial control profiles identified with the whole blood MGIT assay using several techniques. Serum cytokines, whole blood transcriptomics, cellular immunology and humoral responses were all investigated in the context of MGIT data in an attempt to better understand the spectrum of TB.

There has been increasing interest in evaluating cytokines and chemokines as potential immunodiagnostic markers for TB [534]. Several reports have recently identified putative biomarkers to differentiate between active disease and LTBI and also to monitor the efficacy of treatment. Biomarkers associated with the activity of Th1 cells and IFN-γ mediated signaling have been consistently shown to be elevated in patients with active TB. Inflammatory and Th2-related cytokines/chemokines are also increased in TB disease, but have generally been detected at lower concentrations and show poorer correlations [534]. To date, candidate biomarkers have included IP-10, IL-1RA, IL-2, IL-4, IL-8, TNF-α, MIP-1α and -1β, MCP-1, -2 and -3, VEGF and PDGF, many of which are in agreement with the findings reported in this study. However, there are some notable omissions and one of the reasons that almost half of the multiplex panel was undetected may be related to testing unstimulated serum samples, which is also a limitation in specificity. Most studies have typically stimulated whole blood with mycobacterial antigens in order to detect *M. tb*-specific responses. One of the difficulties of detecting biomarkers in unstimulated samples is that they will lack specificity for TB, and findings therefore likely reflect a generalised pro-inflammatory state. This has been highlighted recently with IP-10 in which unstimulated serum concentrations in patients with active TB correlated with a higher erythrocyte sedimentation rate (ESR) and were not significantly different from levels detected in

individuals with non-TB respiratory tract infections [535]. However, the main objective of evaluating serum cytokines and chemokines here was not to discriminate between different states of LTBI or assess the effect of treatment (although interesting profiles were seen), but rather to investigate the hypothesis that the magnitude of inhibition of bacillary growth measured by the *ex vivo* whole blood MGIT is related to the degree of *in vivo* immune activation, and therefore perhaps the issue about specificity is less problematic. Several correlations to support this hypothesis were observed. High serum levels of Gro and PDGF-BB at baseline correlated with enhanced mycobacterial control, while the converse was seen with TNF-α and MIP-1β. In addition, the dynamic response of many of the cytokines and chemokines measured following anti-TB treatment would infer some degree of mycobacterial specificity. Another advantage of this study was the size of the patient populations as most other studies have evaluated far fewer samples.

Together with IFN-γ, the Th1 cytokine TNF-α has a crucial role in the host immune response to *M. tb* infection. TNF-α is produced by macrophages, T cells, dendritic cells (DCs) and neutrophils and has multiple functions including activating macrophages and inducing chemokine production [536, 537]. In TB, TNF-α acts synergistically with IFN-γ resulting in intracellular bacillary killing through the production of reactive nitrogen intermediates [538]. TNF-α also increases the phagocytic capacity of macrophages and is pro-apoptotic, resulting in the presentation of mycobacterial antigens by DCs [373, 539]. It may also have a role in the formation and maintenance of the integrity of TB granulomas and is capable of controlling disease progression [181, 540, 541]. It has been proposed that one of the survival mechanisms employed by *M. tb* is to reduce the production of TNF [542]. Several animal models, including NHPs, mice and a zebrafish model, have provided evidence supporting a protective role for TNF in TB. Neutralisation of TNF with anti-TNF antibodies, disruption of the TNF receptor

gene or *TNF*$^{-/-}$ deficiency results in reactivation of infection, increased bacillary load and necrosis within granulomas, increased susceptibility to *M. tb* infection and higher mortality [543-546]. In humans, individuals receiving anti-TNF therapy for chronic inflammatory diseases such as rheumatoid arthritis with LTBI are at significant risk of reactivation to active disease. The rate of TB among such patients is five times higher than expected and typically results in disseminated or extrapulmonary disease, suggesting reactivation of previously controlled *M. tb* infection (17, 160).

While some studies have shown that the induction of TNF-α is greater in whole blood and PBMC from patients with active TB following stimulation with mycobacterial antigens, concentrations of TNF-α in unstimulated serum samples are very low, as seen in other chronic infections [547-549]. This may be due to sequestration of TNF-α to the site of infection and thus may reflect disease severity. Therefore, while healthy controls have low levels of TNF-α in the peripheral circulation, in the context of LTBI, higher levels could reflect control of infection, while low levels may infer failure of that control and resultant active disease. The data reported here are consistent with other reports. Moreover, the positive association with the degree of inhibition of bacillary growth seen in the MGIT assay could be interpreted as providing further evidence that less mycobacterial growth in this *ex vivo* system is an indication of disease status. Rather than using serum concentrations of TNF-α to distinguish *between* different states of *M. tb* infection, it could indicate disease status *within* the spectrum of LTBI, with lower concentrations suggesting more active or subclinical disease and higher levels adequate control. Supporting this hypothesis are findings that TNF-α is expressed in *M. tb*-infected tissues during latent infection and has a role in the containment of persistent TB, hence reactivation following attenuation of TNF-α responses [540, 541].

A similar paradigm was observed with levels of MIP-1β, which were also positively correlated with mycobacterial net growth. MIP-1β (CCL4) is a chemokine β peptide and chemoattractant to T helper cells and macrophages. It is secreted by activated macrophages, T cells, NK cells and DCs, and its production is induced by TNF-α, IFN-γ and IL-1 and suppressed by IL-4 and IL-10 [550, 551]. There is little literature concerning the role of MIP-1β in *M. tb* infection. One *in vitro* study found that *M. tb* induced significant MIP-1β secretion by alveolar macrophages and suppressed intracellular bacillary growth [552]. Interestingly, MIP-1β production was partly dependent on TNF-α as neutralizing antibodies against the latter attenuated its secretion. The authors suggested that MIP-1β may contribute to innate immune responses to *M. tb* infection and that its reduction may promote the intracellular survival of bacilli [552]. Lower levels have been observed in peripheral samples from pulmonary TB patients when compared with household contacts, and this may again represent sequestration as high expression has been noted in *M. tb*-infected tissue from humans and mice [553, 554]. Therefore, in the context of TB, higher serum concentrations of MIP-1β may characterise contained infection while lower levels occur in disease. While other significant correlations between pre-treatment serum cytokine concentrations and MGIA output were not seen, several analytes such as IL-4, IL-5 and IL-6 demonstrated a 'binomial distribution' across the three study groups (i.e. active=low, LTBI=high, control=low), similar to that seen with TNF-α and MIP-1β and warrant further investigation.

This is one of few observations of elevated concentrations of PDGF in *M. tb* infection. PDGF is an angiogenic growth factor and a potent mitogen for fibroblasts, smooth muscle cells and glial cells [555]. It is a dimeric glycoprotein composed of A and B polypeptide chains, which combine to generate three isoforms: AA, AB, BB [555]. It has been proposed that macrophage production of PDGF-BB is important in the

pathogenesis of chronic lung inflammation resulting in tissue fibrosis, such as that seen in TB [556]. An early report showed that PPD-stimulated lymphocytes from contacts of, and patients with, TB release IFN-γ, which can induce PDGF-BB expression in alveolar macrophages [556]. More recently, studies have shown increased serum levels of PDGF-BB in both stimulated and unstimulated samples from patients with pulmonary TB, which is associated with pulmonary fibrosis on HRCT and reduces significantly following treatment [199, 557, 558]. As previously discussed, there is significant heterogeneity of granulomas in TB and fibroblasts are an important cellular constituent of these structures. It is possible that serum PDGF-BB reflects the number, size and/or composition of pulmonary TB granulomas. The findings here agree with these other reports and the negative correlation between PDGF-BB levels and bacillary net growth may suggest the underlying state of infection. In summary, the strong correlations between unstimulated pre-treatment serum concentrations of several cytokines and chemokines with enhanced mycobacterial control seen in the MGIT assay may reflect immune activation along the spectrum of LTBI and may have utility in the risk stratification of individuals for reactivation.

Whole blood transcriptomics provides a powerful, unbiased measure of DGE at a moment in time. It is perhaps the archetypal 'omic' technology and has been the methodological approach taken by an increasing number of studies to identify novel biomarkers for TB. Most of these studies have focused on the diagnostic potential of transcriptomics and in particular to discriminate active TB disease from latent infection. Several common signatures have been associated with active TB, although the need to identify TB-specific profiles persists. The objective here was not to use DGE to discriminate between different states of TB disease and infection, but to investigate the proposed spectrum of TB in the context of functional MGIT data. As such, the design here contrasted with that of other studies and included many more patients with LTBI

and a heterogeneous group of active TB cases.

Analysis revealed distinct clusters which, on the whole, divided the study cohort by diagnostic group, although considerable overlap was seen especially with LTBI patients. In addition, the key transcriptomic signatures discriminating the cluster with most active TB patients from the other clusters containing mostly LTBI and healthy controls, was dominated by immune response pathways and included type I interferon signaling which have been previously shown to be important [235]. However, subsequent analysis also revealed the heterogeneity of the current study cohort. This is highlighted by the comparisons between the dataset here and that of Berry *et al.* While overlap between the active TB signature occurred and involved key genes that have been reported by several studies in the past, there were many non-overlapping genes between the two studies. There are several possible reasons for this, including different population characteristics, but most important is probably the heterogeneity of active disease types in the current study. While Berry *et al.* recruited only microbiologically confirmed pulmonary TB cases, this study had a diverse range of active presentations, both pulmonary and non-pulmonary, both culture confirmed and unconfirmed. This may account for some of the differences seen. To date, there are no other studies comparing DGE profiles in patients with pulmonary and extra-pulmonary TB and the lack of a clear difference in signature between these groups may suggest they exist on a continuum of pathology.

It is noteworthy that four of the 21 active TB patients in the earlier study were 'misclassified' by class prediction, while here four of 18 patients with active TB clustered with LTBI or control subjects. It has been proposed that such molecular heterogeneity could reflect clinical variance and indeed transcriptional signatures have been shown to correlate with disease severity and revert to that of healthy controls

after treatment [235, 277, 278]. Among the four 'misclassified' patients reported here, none were culture confirmed and two were extra-pulmonary cases. The only other study to recruit culture-negative TB cases found that the sensitivity of a signature for TB was 82.9% for the diagnosis of culture-confirmed TB, but ranged from 35.3-82.3% among patients with culture-negative TB and that this was dependent on estimates of the probability of true TB disease [286].

A particularly interesting aspect of DGE in TB studies is the clustering of LTBI individuals with active disease cases, and goes to the very heart of the question about a spectrum of infection. Here, almost two-thirds of the 'active' cluster contained patients with LTBI. This is higher than the 10-12% reported previously and is likely due to the heterogeneity of the active cohort here [235]. Indeed, when the Berry *et al.* analysis was applied to the current dataset, the cluster of 29 individuals that contained most of the active patients also consisted of 14 with LTBI, highlighting still further the diversity in the active group. One may also speculate that while such overlap is higher than would be expected in relation to the 10% lifetime risk of reactivating latent infection, it may signify the dynamic interaction between host and pathogen, which may be changing constantly for some individuals resulting in immune control and containment for some, or progression to active disease due to failure for others.

The rationale for performing these experiments was to use an unbiased methodology to provide an assessment of the whole blood MGIT assay data. Different magnitudes of mycobacterial growth control were associated with each hierarchical cluster, with less growth being observed in the clusters containing individuals with the most active disease. The overlap in DGE between clusters is similar to that seen with the MGIT data and again highlights the spectrum of responses proposed to exist in LTBI and disease. The lack of significant difference between clusters nominally defined as latent and

control could be because of improved classification of individuals by DGE. The contrasting view is that the MGIT assay may provide a more accurate measure of infection status, possibly because it is a stimulated, functional assay, with better discriminatory power. Similar trends of net growth between the clusters were seen with both BCG and *M. tb*, however the lack of significance with the former may also be due to the use of unstimulated samples in whole blood transcriptomics. There will undoubtedly be a fine balance between too much stimulation with a virulent strain of mycobacteria in the MGIT assay that overwhelms the ability to control growth and too little stimulation with an attenuated strain, which may fail to discriminate individuals above a baseline response. Differences between clusters and bacillary strain may also be due to the availability of fewer data points for BCG resulting in less power. While differences were seen with mycobacterial control as a continuous variable, the stratification of individuals into categories of ability to control growth failed to correlate with DGE profiles. Such classification may reduce resolution and discriminating power in the context of DGE. The use of centiles for stratification, while statistically robust, may not be appropriate and it would be interesting to examine other models.

However, overall these data suggest that the MGIT assay does provide an appropriate evaluation of the *M. tb* infection status of an infected host and correlates with clustering based on DGE profiles.

Finally, one of the novel aspects of this part of the study was the inclusion of patients with LTBI who had received three months of chemoprophylaxis. This has not been available to most other TB transcriptomic studies because they have occurred in TB endemic settings where treating LTBI is not routinely undertaken. The rationale for studying treatment responses among the LTBI cohort was to ascertain whether the

initial pre-treatment clustering of individuals was indeed based on presumed similarities in disease/infection status. One may hypothesise that individuals occupying similar positions within the TB spectrum may respond to treatment in a similar way, which could be identified by changes in DGE before and after therapy. It is especially interesting that the initial pre-treatment active cluster was so very different from the LTBI and control clusters, which showed very few differences between one another. As this active cluster contained so many individuals with LTBI it was important to study treatment-induced changes in DGE as a potential surrogate measure of bacillary burden. Following treatment there were very significant changes in the active cluster and when a new hierarchical analysis was performed on the basis of these changes, there was good concordance with earlier results. On the basis of DGE after treatment, all active patients that clustered together and 73% of the LTBI patients initially clustering with the actives repeated this pattern. One interpretation of this is that the initial clustering was accurate, and given the relationship between the transcriptomic data and the MGIT data, that the latter does indeed provide a valuable *ex vivo* functional readout that may be a surrogate marker of the *in vivo* host-*M. tb* relationship.

In terms of characterising monocyte subsets I found significant increases in intermediate and decreases in non-classical monocytes among individuals with active disease and LTBI, which changed significantly in the active group following anti-TB treatment. The consequences of such *in vivo* immune activation may be reflected in the enhanced mycobacterial control *ex vivo* observed in the MGIT assay. Significant correlations between pre-treatment intermediate and non-classical monocyte proportions and bacillary control were seen. Furthermore, when stratifying the LTBI group based in MGIT data, while no differences were seen between subgroups at baseline, those with an LTBI(a) profile showed the greatest changes in response to treatment and in a pattern similar to the active group.

Human peripheral monocytes are currently divided into three subsets based on the expression of the surface markers CD14 and CD16. Classical monocytes are defined as CD14++CD16- and account for 80-95% of the total monocyte population [559]. The functions of classical monocytes include phagocytic and anti-microbial peroxidase activity and they produce low levels of pro-inflammatory cytokines but high levels of IL-10 [560]. Non-classical monocytes express CD16 but lower levels of CD14 (CD14+CD16+, or CD14lowCD16+) and represent 5-10% of circulating monocytes. They have been termed 'patrolling' monocytes and appear to function by surveying the endothelium for signs of inflammation or damage which induces transmigration and the production of TNF-α and IL-1β [559]. Intermediate monocytes are typically the minor population of monocytes and are also positive for both markers but express more CD14 (CD14++CD16+, or CD14hiCD16+) and account for up to 5% of total monocytes. They are pro-inflammatory and produce high levels TNF-α, IL-1β and IL-6 (in response to LPS) [559, 560]. Changes in the proportions of monocyte subsets have been described for a number of diseases including sepsis, HIV infection, hepatitis B, rheumatoid arthritis, coronary artery disease, end stage renal failure and stroke [560].

In TB, increased frequencies of intermediate monocytes in active disease, compared with healthy controls, have been previously reported by several investigators, consistent with the findings here [561, 562]. In addition, these differences were lost following treatment [563]. Furthermore, a recent report also suggested that non-classical monocytes were also increased in patients with active TB, while others have failed to show a difference and I observed reduced numbers of non-classical monocytes in patients with active TB or LTBI [562, 564]. Interestingly, one study showed higher frequencies of intermediate monocytes in TST-positive versus -negative individuals and healthy controls. While the LTBI status was not known, there was a similar trend observed here among latently infected patients [565]. Important reasons for the

discrepancies between studies include different methodologies and gating strategies and highlight the lack of consensus in characterising monocyte subsets. Many studies analyse two subsets, CD14+CD16- and CD14+CD16+, which fails to discriminate between intermediate and non-classical monocytes. In addition, few studies employ FMOs to aid gating, which could over-estimate the contribution of non-classical monocytes. Finally, there are concerns that sample preparation may affect results, although it has been shown that while the total number of monocytes is reduced in cryopreserved versus fresh PBMC samples, the proportion of subsets does not differ [566]. Monocyte functional assays were not performed in this study however, it should be noted that stimulating purified monocytes rather than using whole blood may lead to experimental artifacts than may confound results [567].

While significant correlations between the proportions of certain monocyte subsets and the degree of mycobacterial growth inhibition in the MGIT were seen, stratifying patients on the basis of their whole blood MGIT responses did not provide any discriminatory value in the LTBI group. This may be an issue related to reduced power, and the magnitude of the change seen in response to anti-TB treatment in the LTBI(a) group may better reflect similarity with active patients. Studying additional elements, such as maturation markers or the functional capacity of monocytes to produce cytokines following *M. tb*-specific antigenic stimulation may improve the ability to show differences between LTBI(a) and LTBI(l) groups at baseline.

In terms of the T cell studies, over the past several years there has been increasing interest in profiling the functional capacity of CD4+ and CD8+ T cell subsets to investigate their potential as novel biomarkers of LTBI and disease. Functionality has been defined on the basis of single, double, or triple cytokine production, typically following stimulation with *M. tb*-specific antigens, and different profiles have been

associated with disease stage, mycobacterial load and response to treatment. However, many controversies exist and while some studies have suggested correlations with protection, others report links to TB disease severity [568, 569].

CD4+ T cells are crucial in protective immunity and host responses to TB and activate effector functions in macrophages that control intracellular *M. tb* growth and survival via the secretion of IFN-γ and TNF-α [568]. IL-2 is another cytokine key to Th1 response against TB and is required for T cell differentiation, effector functions and maintenance of memory [570]. Finally, the pro-inflammatory cytokine IL-17 is produced by Th17 cells following IL-23 induction and stimulates chemokine production and the recruitment of neutrophils to the site of infection. While its role in TB needs to be defined, there is some evidence that IL-17 may compromise the integrity of granulomas and therefore may contribute to the immunopathology of TB [571].

Interest in the role of polyfunctional T cells in TB stemmed from observations that the simultaneous production of multiple cytokines was associated with enhanced functional capacity to control chronic viral infections such as HIV [572]. It has been reported that polyfunctional T cells characterise protective antiviral immunity in chronic infections when antigenic load is low, whereas in acute infections with elevated antigenic burden, single IFN-γ-secreting T cells dominate the response and immune failure ensues [568]. In TB, early studies showed that polyfunctional CD4+ T cells producing IFN-γ, TNF-α, and IL-2 occurred at higher frequencies among patients with active disease compared to latently infected individuals and declined following treatment [573-579]. IFN-γ single and IFN-γ/IL-2 bifunctional CD4+ T cells seemed to characterise LTBI patients and therefore it was considered that the presence of multifunctional CD4+ T cells in TB patients was associated with the higher bacterial

loads and suggested failed immunity rather than a protective role [568]. However, more recently this view has been challenged, with the contrary findings of reduced frequencies of polyfunctional CD4+ T cells in patients with active TB disease, which increased with anti-TB therapy [63, 580, 581]. In the present study, the frequency of *M. tb*-specific polyfunctional CD4+ T cells in active patients was less than in latently infected individuals, consistent with recent studies [63, 580, 582]. In addition, active patients had more mono- and bifunctional CD4+ T cells, the former predominantly TNF-α secreting and the latter IFN-γ/TNF-α secreting, similar to the findings of other investigators [582, 583]. This is in agreement with the current paradigm of antiviral immunity as described above. Very interestingly, when patients with LTBI were stratified into subgroups based on MGIT responses, those with a profile of mycobacterial control similar to active patients had the greater frequency of monofunctional CD4+ T cells, among which IL-2 producing cells dominated. However, the frequency of IL-2 producing CD4+ T cells was considerably lower among the LTBI(a) versus LTBI(l) subgroups and it has previously been shown that in active TB disease *M. tb*-specific IL-2+ CD4+ T cells decline (both as polyfunctional and monofunctional entities) [584].

While the proportions of *M. tb*-specific polyfunctional CD4+ T cells were similar between the two LTBI groups, the magnitude of those responses were substantially greater in the LTBI(l) subgroup and may represent true quiescent infection and immune control. The striking dichotomous profile of CD4+ T cells within the LTBI group may assist in delineating the spectrum of TB and perhaps provides further evidence that MGIT responses may reflect immune activation in response to mycobacterial load.

CD8+ T cells also have a protective role in LTBI and work synergistically with CD4+ T cells [585]. CD8+ T cells appear to target *M. tb*-infected cells with high mycobacterial burdens and their effector functions include the secretion of cytotoxic molecules such as perforin, granzymes and granulysin which have direct cytolytic and anti-mycobacterial effects, and also the induction of apoptosis of infected cells [586-590]. Following activation, CD8+ T cells can also secret IFN-γ, TNF-α and IL-2. IFN-γ released by *M. tb*-specific $CD8^+$ T cells has been shown to provide protection against LTBI in both animal models and humans [586, 587, 589, 591].

Studies have shown that *M. tb*-specific CD8+ T cell responses are higher in patients with TB when compared with LTBI individuals, correlate with bacterial load and decline with successful anti-TB treatment [63, 580, 582, 592]. The phenotype of CD8+ T cells in active patients seems to one of effector memory, while in latently infected individuals terminally differentiated effector memory CD8+ T cells predominate [582]. Increased polyfunctional (IFN-γ/TNF-α/IL-2) CD8+ cells have been reported in LTBI patients and in active TB mono- and bifunctional TNF-α and IFN-γ occur [582].

In this study, no polyfunctional CD8+ cells were induced by stimulation with ESAT-6/CFP-10 in any study cohort, which has been previously reported [63]. In active TB patients dual secreting IFN-γ/TNF-α CD8+ T cells were predominant. Only monofunctional CD8+ cells were seen in the LTBI group, which were predominantly IFN-γ and IL-2 producing (consistent with prior studies), while stratifying the latently infected individuals showed clear differences in *M. tb*-specific CD8+ T cell between the LTBI(a) and LTBI(l) subgroups. In the LTBI(a) subgroup, bifunctional IFN-γ/TNF-α CD8+ were seen which was more consistent with the active TB group. Strikingly, the LTBI(l) subgroup remained wholly monofunctional cells. As with the CD4+ T cells responses, the LTBI(a) *M. tb*-specific CD8+ T cell profile shared most similarity with the

active TB disease group and given the basis of stratification was the whole blood MIGT assay, it further strengthens the hypothesis that functional MGIA can assist in delineating the spectrum of latent *M. tb* infection. The finding that there was a trend for more IL-17 producing CD8+ T cells in the LTBI(a) subgroup is very interesting. It has been reported that IL-17 is expressed predominantly in peripheral CD8+ rather than CD4+ T cells of active TB patients and this may therefore be a further indication of antigenic burden in the LTBI(a) group [593].

Finally, the effect of anti-TB therapy on T cells responses was very similar to other studies, with a relative reduction in the frequencies TNF-α and increase in IL-2 CD4+ T cell seen in active TB patients [594]. Furthermore, the contraction the polyfunctional CD4+ T cell population and rise in monofunctional cell is also consistent with other studies and suggests that with antigenic clearance, CD4+ T cells return to a resting state, although interestingly not to levels observed in healthy controls [579]. Post-treatment samples were collected relatively soon after completion of treatment and therefore longitudinal studies may be more informative in assessing the persistence of these T cells profiles. In terms of CD8+ T cells, the frequency of IFN-γ/TNF-α producing cells declined with treatment, although so did IL-2 CD8+ cells, which have previously been shown to increase [594]. An increasing proportion of monofunctional CD8+ T cells, replacing bi- and polyfunctional cells has been seen before, whereas here only increases on bifunctional occurred [579]. While most of the findings here are consistent with other studies, there are several reasons for the differences in the cytokine production profiles seen. These include the use of whole blood vs PBMC, different antigens and differences in subject characteristics and study setting and highlight the need for standardisation of methodologies and approaches.

The relative simplicity, robustness and cost-effectiveness of ELISAs make serodiagnostics attractive point-of-care tests for TB in resource-poor settings. Despite dozens of studies over many years, the detection of antibodies in sera against *M. tb* antigens has been limited by low sensitivity and specificity [475, 595]. Considerable inter-individual and geographic variations in antibody responses have been seen. Possible reasons for this include genetic and environmental factors at both the individual and population level, the effect of different infecting strains of *M. tb*, poor discriminating ability between active disease and latent infection and differences in the type and purity of antigens used [434, 475, 595-601].

Furthermore, many studies have focused on measuring either total IgG or a single IgG subclass against a single class of antigens. However, the humoral response to infection is characterised by great antibody diversity, with different subclasses inducing different effector functions. These include varying capacities to trigger FcγR-expressing cells, for phagocytosis or antibody-dependent cell-mediated cytotoxicity and complement activation [602]. The IgG class of antibodies is the most abundant of the five classes of human immunoglobulins, accounting for 10-20% of proteins in human serum. It provides the major component of most humoral responses to pathogens and is composed four subclasses, IgG1, 2, 3 and 4 [602]. The relative abundance of these subclasses is 60%, 32%, 4% and 4%, respectively [602]. These subclasses display preferences for antigens based on their biochemical structure, with IgG2 generally directed against carbohydrate and non-protein antigens, while IgG1, IgG3 and IgG4 bind to protein antigens [602].

Of the very few previous studies assessing IgG subclass distribution in the context of active TB, IgG1 and IgG2 responses predominated, which is perhaps unsurprising given their relative abundances, and is consistent with the findings of this study [603-605].

Indeed, given the negligible responses of IgG3 and IgG4 in the active TB disease patients on initial screening, further analysis of these subclasses in the remainder of the population was not pursued. Interestingly, one study has described loss of IgG2 responses and increases in IgG3 and IgG4 in individuals with HIV and *M. tb* co-infections and the authors suggested reduced Th1 cytokines and possibly HIV-induced isotype switching was the reason [605].

It is perhaps unsurprising to note the dominant IgG2 responses in patients with active disease and LTBI given that IgG2 is directed mainly against non-protein antigens and LAM is a glycolipid and the cell membrane fraction prepared from H37Rv contains a significant polysaccharide and lipid content. The composition of culture filtrate is mainly protein and the high responses to IgG2 were unexpected but may reflect polysaccharide contamination of the preparation, although a similar observation has been reported previously [604]. The finding that in active TB disease anti-LAM IgG2 responses dominate corresponds with the preference displayed by this subclass for non-protein antigens and has been reported by others [605]. The ability to discriminate between active TB and LTBI infection or controls with either IgG1 or IgG2 responses to most if not all antigens is also consistent with evidence that antibody titres are related to mycobacterial load and the severity of disease [606-608]. One of the difficulties with TB serodiagnostics is the large overlap in responses, particularly between uninfected healthy controls and individuals with latent infection [609]. Apart from ESAT-6/CFP-10 and LAM, the other antigen fractions were relatively crude preparations and together with LAM, are major structural constituents of mycobacteria with significant homology across species [459]. Prior NTM exposure could therefore account for high background levels of IgG, reducing the ability to separate LTBI from healthy controls. This may also be a similar scenario with BCG vaccination, which can generate significant increases in

IgG responses to cell membrane fraction, culture filtrate and LAM prepared from *M. tb* H37Rv (as was demonstrated in Chapter 4).

It is very interesting that IgG1 responses to the RD1-restricted protein antigens ESAT-6/CFP-10 could discriminate between latent infection and healthy controls. In addition, the strong negative association with these responses and MGIT assay mycobacterial net growth suggests that not only is this antigen specific for *M. tb*, but that it may reflect the bacillary burden and therefore the disease status. This is reinforced by differences in anti-ESAT-6/CFP-10 IgG1 responses seen between LTBI(a) and LTBI(l), with the former showing higher OD values then the latter, more consistent with an active disease phenotype. The significant heterogeneity among bacilli and associated pathology in both active disease and latent infection has already been discussed. ESAT-6 and CFP-10 are specific for *M. tb* and are mainly secreted during active bacterial replication [92]. There is evidence for ongoing bacillary replication in LTBI seen from the effect of chemoprophylaxis and the use of IGRAs from diagnosing LTBI, which rely on responses to ESAT-6 and CFP-10 antigens. Therefore, anti-ESAT-6/CFP-10 IgG1 responses may correlate with mycobacterial activity and have the potential to delineate the spectrum of TB infection. In contrast, the other antigens tested here are likely to be present irrespective of the replicative state of mycobacteria, which may account for the inability to dissect the LTBI subgroup.

As described in Chapter 4, one of the reasons for assessing different IgG subclass responses in TB arose from considering the spectrum of LTBI and parallels that can be drawn with leprosy. The causative mycobacteria, *M. tb* and *M. leprae,* share significant genomic homology and the pathology of both infections is characterised by chronic granulomatous disease. As proposed for *M. tb, M. leprae* causes a spectrum of presentations dependent on the host immune response, with milder pauci-bacillary

disease defined by Th1 and cell-mediated responses and more severe multi-bacillary infection dominated by Th2 and humoral responses [464]. Synergistic co-operation between B cells and Th cells is needed for an effective humoral response and it is possible to categorise Th cells on the basis of distinct patterns of cytokine production and their effects on humoral immunity [603]. IFN-γ, typically secreted by Th1 cells, can induce the secretion of IgG2 while the Th2 cytokine IL-10 causes class switching towards IgG1 and IgG3 subclass [610, 611]. However, it should be noted that while these associations are relatively clear and well defined in animal models, there is considerable overlap in humans, which may account for the contradictory observations reported to date [612]. Unfortunately, the non-quantitative nature of the assay used here precludes making conclusions about the Th1-Th2 paradigm and its relationship with humoral responses. While the accurate quantification of antibody concentrations is notoriously difficult to achieve, further work is warranted here to investigate the paradigm further as it may yield some interesting insights.

In view of the successful use of an *ex vivo* ELISpot assay in examining B cell responses to BCG vaccination, and the rationale for using this technique in the setting of TB disease, being unable to pursue its use was very disappointing. The characteristics of the spots, representing ASCs, were very different between vaccination and natural infection. Following BCG vaccination, ASCs were large, rounded and well-defined, whereas among individuals with TB disease much smaller, irregular spots occurred which were difficult to measure accurately. The patterns noted suggested that B cell responses were present and were consistent with IgG subclass ELISA data. This showed a profile of strong IgG2 response to cell membrane fraction, which was also seen with the B cell ELISpot assay, but quantitation of these responses was not possible. This may be due to differences in the antigens used or the patient samples. The former is perhaps less likely as the H37Rv cell membrane fraction is similar in its complex, composite

nature, to whole BCG and yet ASCs specific for the latter were clearly visible. The findings here are in contrast to the only published study of mycobacteria-specific B cell responses in TB, which showed an increased frequency of PBs in individuals with active disease and more mBCs in healthy controls [363]. Settings and patient populations were different between the studies but the experimental methodologies were similar [363]. This report does not comment on the characteristics of the ASCs enumerated or the settings used for automated counting.

Whilst it was not possible to characterise the phenotype of *M. tb*-specific B cells by flow cytometry, it was important to examine B cell subsets as little is known about their profile in the peripheral circulation of individuals with TB. The important role of cell-mediated immunity (CMI) in the control of TB is undisputed, but that of B cells has been little studied until recently. Reasons attributed to this relative neglect include the controversies associated with anti-TB serum therapy used in the late nineteenth century, together with the dichotomous view that CMI is directed towards intracellular pathogens while the target of the humoral response is extracellular organisms [433, 613, 614]. However, there is increasing evidence for a role of B cells and humoral immunity in defence against intracellular pathogens as shown for *Chlamydia trachomatis, Salmonella enterica, Leishmania major* and *Plasmodium* species, among others [433]. It has also been highlighted that intracellular pathogens, including *M .tb*, probably reside in the extracellular compartment for some time during the infective process and would therefore be susceptible to humoral responses [615]. Animal models have shown that B cell deficiency results in increased pulmonary pathology and mortality following *M. tb* challenge [616]. B cell functions include the modulation of T cell responses through antigen presentation and the action of cytokines and antibodies, resulting in T cell activation, polarization, modification of effector functions and the development of T cell memory [433]. B cells also regulate macrophage function, which

is likely to be important in the context of TB [433]. Recent evidence suggests that B cells exist in discrete clusters in the lymphocytic cuff of TB granulomas, forming germinal centre-like structures, that may function to perpetuate the local host response to *M. tb* through T cell modulation [433, 460].

Several previous studies using flow cytometry have shown reduced numbers of total B cells in the peripheral blood of patients with pulmonary TB and LTBI compared with healthy individuals, although there are also reports of no differences or increased CD19+ cells in active TB [235, 439, 564, 617-620]. Interestingly, whole blood transcriptomics have also shown a modular TB signature with a decreased abundance of B cell transcripts [235]. Very few studies have gone on to assess B cell subsets. One study which examined the frequencies of circulating CD4+ T follicular helper cells in TB also characterised the distribution of B cells and reported no differences any of the major subsets between patients with active TB or LTBI [621]. Crucially, this study did not include healthy controls to compare against, and on close review of the data the frequencies of B cell subsets are very similar to those found here [621]. In the current study, individuals with active TB and LTBI showed reduced frequencies of mature B cells, consistent with previous reports. In addition, significant increases in activated and atypical mBCs were observed and fewer classical mBC in active TB patients. An earlier report showing increased activated circulating B cells in MDR-TB patients suggested that this may derive from cytokines inducing B cell activation and proliferation, such as IL-6, although no differences in serum levels were detected [620]. In contrast, the concentration of IL-6 was significantly elevated in the serum of both active TB and LTBI patients here.

One of the most interesting findings was of the increased atypical mBCs. Atypical mBCs, also termed tissue-like mBCs, were first described in the lymphoid tissue of healthy

individuals and it was proposed that these cells might protect against pathogens through modulatory cytokine secretion [622]. However, subsequent studies in HIV infection suggested that atypical mBCs are hyporesponsive or exhausted cells and have a poor capacity for differentiation, cytokine and antibody production, and demonstrate upregulated inhibitory pathways when compared to classical mBCs [623-625]. One hypothesis is that atypical mBCs are generated from dysfunctional germinal centre reactions or arise from pre-existing classical mBCs, in either case resulting in diminished classical mBC responses [623]. The reduction in classical mBCs seen here may support the proposal that atypical mBCs are derived from this population. Atypical mBCs have recently been shown to be greatly expanded in individuals living in malaria-endemic areas and it is thought that repeated infection with *Plasmodium falciparum* may induce the generation of atypical mBCs that interfere with the acquisition of malaria immunity [626-629]. It has very recently been shown that increased proportions of atypical mBCs occur in active TB patients and individuals with LTBI [630]. These mBCs showed impaired proliferation, immunoglobulin- and cytokine-production, which resolved following successful treatment. If the presence of atypical mBCs is a hallmark of chronic infection, it is tantalizing to speculate that they may have a role in TB and represent failure of B cell responses that may contribute to reactivation of latent infection and progression to active disease. They may also explain the difficulties encountered with profiling *M. tb*-specific mBCs by *ex vivo* ELISpot.

Strong negative correlations between the proportion of atypical and activated mBCs with MGIT BCG growth were seen. However, as in the case with certain monocyte subsets, different subgroups of LTBI patients could not be discriminated using stratified parameters. Identification of other surface markers or examining the functional capacity of these cells in response to *M. tb*-specific antigenic stimulation may provide better resolution.

There were several limitations to this aspect of the study. Current methods do not allow for the identification of *M. tb*-specific B cell subsets but his would be an important development for future work. Furthermore, the frequencies in peripheral blood may not represent those in important compartments such as secondary lymphoid organs or granulomas. Finally, increased or decreased subset frequencies may be a result of shifts in other B cell subsets and while measuring the relative proportions of subsets is typically performed, determining absolute B cell counts will also be important.

Conclusions and future work

7 Conclusions and future work

7.1 Main findings & conclusions

The aim of this study was to use an *ex vivo* whole blood functional assay to measure the capacity of individuals to control mycobacterial growth based on the hypothesis that this could be a surrogate biomarker for *in vivo* TB status. I then sought to characterise different control profiles using a multi-platform approach, and found several interesting correlations and associations that warrant further investigation.

Despite the significant progress that has been made with global control programmes, TB remains a huge challenge to health and still causes significant morbidity and mortality worldwide. Together with enhanced diagnostics, shorter and more effective treatment regimens and improved vaccines, there is increasing awareness of the need to tackle the huge burden of LTBI if control and elimination of TB is to be achieved. However, the magnitude of the reservoir of latent infection is such that targeted preventative therapy will be required as a pragmatic solution to the problem. Unfortunately, current diagnostics do not have the resolution to accurately identify individuals at risk of progressing to active TB disease. Therefore, there is an urgent need to find novel biomarkers and while much work has been undertake in this area, an incomplete understanding of the immunopathogenesis of TB has hampered progress. This is highlighted by the recent suggestion that rather than a simple binary classification of active disease or latent infection, a dynamic interaction between host and pathogen probably exists. As such, states of active disease and latent infection possibly correspond to partially overlapping regions on a spectrum that reflect the changing balance of interactions over time. It is proposed that this continuous spectrum includes elements ranging from innate and acquired immunity, quiescent and

subclinical infection, and fulminant disease. Evidence supporting this hypothesis has come from epidemiological observations, an increasing appreciation of the heterogeneity of the granuloma and mycobacterial diversity, and recent studies of the nature of the host immune response to TB through the characterisation of T cell polyfunctionality and patterns of differential gene expression in response to *M .tb*. Delineating this spectrum would not only improve our understanding of TB, but also has the potential to identify individuals occupying a part of the spectrum that corresponds to the highest risk of progression to active disease, therefore facilitating targeted treatment of LTBI. Considering the complexity of TB, it is probable that a biosignature, rather than a single biomarker, will provide a correlate of TB risk or protection. Recently, experimental approaches based on 'omic' technologies have been used in TB biosignature discovery and while these offer the advantages of being unbiased, hypothesis generating, and generate large datasets, they are typically used in isolation. A combinatorial approach, which uses several different experimental platforms to measure independent variables, has been shown to increase the power of biosignatures and predictive models.

MGIAs provide an unbiased, summative assessment of a range of immune mechanisms and their complex interactions and may have an important role in dissecting the host immune response to *M. tb*. This is particularly relevant for TB, given the conflicting data on the role of T cells, macrophages, neutrophils, humoral responses and other immune effector mechanisms in mycobacterial control. No studies had previously used a MGIA to assess anti-mycobacterial immunogenicity in patients with TB. A whole blood assay includes both cellular and non-cellular components of the compartment, but also has the advantage of minimal sample manipulation.

The initial part of this study was designed to assess the appropriateness of a whole blood MGIA for the above application and to gain some insight into underlying mechanisms of action. I have shown, using mycobacteria of different virulence, that the BACTEC MGIT system is very reproducible and demonstrates levels of intra- and inter-assay variability well within the recommended limits of acceptability for a functional assay. Differential gene expression studies indicated that while many similarities between human transcriptomic responses to BCG and *M. tb* occur in the MGIT assay, there are some important differences probably related to varying virulence and therefore studying responses to a range of mycobacteria was an appropriate approach. Finally, cellular depletion studies highlighted not only the technical difficulties of removing certain cell factions from whole blood with as little sample manipulation as possible, but also that there is considerable heterogeneity in the responses of individuals following such depletions. This is an apt demonstration of inter-individual variation and underscores the value of the whole blood MGIT assay in capturing such heterogeneity as a single functional measure, reflecting all cellular and non-cellular constituents of the sample.

Subsequent work benefited from working with individuals recently vaccinated with BCG to assess its effect on MGIT mycobacterial control and also for assay development. Whilst the strains and routes of introduction are clearly different from natural infection with *M. tb*, BCG vaccination offers a unique opportunity as a 'mycobacterial challenge' model to measure anti-mycobacterial responses. It is a valuable model of contemporaneous mycobacterial exposure. The MGIT assay identified enhanced bacillary growth control in response to BCG vaccination, supporting earlier evidence that this assay can indeed detect differential inhibitory capacities following recent challenge. The rationale for developing B cell-based assays has been extensively discussed in the context of the wider study. Humoral responses may reflect antigenic

burden and therefore could have a role in dissecting the spectrum of TB in which the position an individual occupies on the spectrum will probably be significantly influenced by the bacillary load and its interaction with host immune responses. BCG vaccinees did generate specific B cell responses following 'challenge' and demonstrated the proof-of-concept of this approach for onward application to the main study.

The next phase of the study was crucial to meet the overall objectives, as the requirement to enroll a broad range of patients with active TB disease, a large cohort with LTBI and appropriately matched healthy controls, was fundamental to study the spectrum of mycobacterial responses. Despite the logistical challenges of clinical necessity (in terms of avoiding delays to starting treatment) and the distances between centers and the host laboratory, over 200 participants were recruited to the study in a multi-centre approach, with post-treatment samples collected from the majority. The demographic profile of volunteers was generally consistent with the profile of patients currently seen in the UK. The clinical heterogeneity of patients with active TB was an important aspect to replicate the diversity in this part of the spectrum of TB. Baseline haematology parameters showed some very interesting results, including increased ML ratio and platelet counts among individuals with TB, which also overlapped substantially with the LTBI group. The ML ratio is interesting as it may have a prognostic value not only in active disease but also in predicting risk of reactivation. The potential function of platelets as immunomodulators rather than merely a non-specific marker of inflammation is fascinating. Of course, the main objective here was to assess differential functional responses and the whole blood MGIT was able to discriminate between individuals assigned to conventional diagnostic groups, although considerable overlap occurred. Mycobacterial growth followed a hierarchical pattern of active TB<latent infection<healthy controls, and the increased bacillary control seen in patients with the highest burden of infection may reflect a general state of immune

activation. These findings were consistent with earlier work in the study showing enhanced growth control after mycobacterial exposure in the form of BCG vaccination and the differences in the discriminatory power of the MGIT assay seen with mycobacterial strains of varying virulence supported the experimental approach. The wide range of MGIT assay responses seen among latently infected participants is consistent with the concept of a spectrum of TB, and while wholly speculative, it is attractive to propose that some individuals, perhaps with subclinical disease, demonstrated immune activation and thus bacillary control similar to the active group, whilst others with quiescent infection clustered with the healthy controls. The effect of anti-TB treatment, which resulted in increases in bacillary net growth and therefore a reduction in mycobacterial control were very interesting, particularly considering the magnitude of the changes seen in different diagnostic groups. Individuals with the highest bacillary burden, and therefore the greatest immune activation, showed the greatest changes in growth control after successful treatment. Changes in haematological measures and some of the previous correlations between certain cell types and growth control agree with this hypothesis.

Finally, characterisation of these differential MGIT assay responses was undertaken using a range of experimental techniques in an attempt to generate a biosignature for the spectrum observed. Unbiased methods using unselected samples provided a powerful approach. Whole blood transcriptomics and multiplex cytokine and chemokine assays applied to the majority of the study cohort revealed some fascinating patterns and overlap. Differential gene expression dominated by type I interferon and inflammatory signatures were noted not only in active TB patients but also many individuals with LTBI. Clustering analysis based on transcriptomic data showed clear associations with MGIT assay responses and the modulation of patterns of gene expression following treatment would suggest that these are not mere artifacts.

Assessing responses to anti-TB therapy in the LTBI group was novel and provided further evidence that there exists a subset of individuals defined clinically as latently infected, but who are more similar in characteristics to patients with active TB disease. This was also the case with certain cytokines and chemokines, and especially IL-6 and PDGF, which showed strong correlations with mycobacterial growth control. In addition, these assays showed certain 'bimodal' patterns, such as with TNF-α and MIP-1β, which may have future potential in developing predictive models of risk. Immunology assays used selected samples, based on stratification using MGIT data, and also showed interesting correlations with mycobacterial control. Increases in inflammatory monocytes, polyfunctional T cells, activated and atypical memory B cells and IgG1 responses to RD1-restricted *M. tb*-specific antigens all demonstrated correlations or associations with MGIT data, either as a continuous and categorical variable. These findings may not only give some insight into host immune responses to *M. tb* and the spectrum of those responses, but also tentatively suggest a biosignature for reactivation and progression. There are many potential confounders with this part of the study, including the lack of a standard for validating MGIT responses, and also the issue of co-dependent variables and the relationship between dependence and correlation. As discussed, current diagnostics are limited, their interpretation can be complex, and the lack of a 'gold standard' makes assessment of new techniques difficult. Furthermore, while many different platforms were used to study multiple biomarkers to mitigate against problems with assessing co-dependent variables, it is almost impossible to avoid this because of the integrated nature of the human immune system. However, one may conclude that the findings of this study could be extended in further work to assess the utility of a putative biosignature of risk (or protection) in TB.

7.2 Future work

The results of the work presented here have raised several interesting findings that warrant further investigation, some of which I discuss below.

7.2.1 Biomarker refinement and pre-clinical evaluation

The findings reported here could be refined further and potentially evaluated in pre-clinical animal models before consideration of field studies. While a possible limitation of using peripheral blood samples is that they may not simulate the immunological milieu of the pulmonary granuloma, TB biosignatures will invariably rely on such samples and therefore their use is appropriate. However, how these samples are processed for subsequent exploratory studies is important. The MGIT assay used whole blood whereas the immunology assays relied on cryopreserved PBMC. This was a logistical necessity in early phases of the study but future work could involve immunophenotyping and functional characterisation of immune cells in stimulated whole blood. This would avoid the significant processing required in PBMC isolation and any concerns about the effects of cryopreservation and thawing on cell attributes. Apart from the T cell studies, other cellular immunology only examined phenotypic characteristics based on identifying surface markers. It is possible that functional studies would not only yield interesting immunological data but also refine the contribution of these cells to any predictive model. Increased frequencies of inflammatory monocytes and activated and atypical memory B cells were seen, but there are no data pertaining to their function, particularly in response to *M. tb*-specific antigens. This would be important to study, as both quantitative and qualitative factors are likely to be relevant to control. With such refinement of the biosignature, it may then be possible to test its predictive value in relevant animal models of TB. As discussed earlier, most small animals are poor models for human LTBI but there have

been several recent and exciting advances with NHP models. Low dose *M. tb* infection in Cynomolgus macaques can result in active disease and latent infection, and combining imaging and tissue studies which use microbiological, histological, immunological and molecular techniques, are powerful tools in studying the various manifestations of *M. tb* infection [206, 213, 215]. Such a model could be used to assess the predictive ability of biosignatures for TB reactivation and progression.

7.2.2 Evaluation of a putative biosignature of TB reactivation

Does the pattern of biomarkers identified in this study among individuals with a diagnosis of LTBI, which suggests a profile of subclinical disease, have any clinical application? Can a putative biosignature of reactivation risk be developed and validated? These are fundamental questions about the translational potential of the study findings. Given that several biomarkers increase the power of predictive models, several elements could be used in a longitudinal assessment of disease risk, including differential gene expression, cytokine markers, profiles of polyfunctional T cells, and changes in monocyte and B cell subsets. However, there would be several obstacles to validating such a biosignature in the field. Firstly, any such study would be both long and costly and require a sufficient sample size for robust statistical power. A recent prospective cohort study assessing an RNA signature for TB disease risk enrolled almost 11,000 participants with a two-year follow-up [289]. The costs and infrastructure required to undertake such a study are huge. In addition, in order to see an effect, patients could only be recruited in countries where preventative treatment is not routinely administered as part of public health policy. An immediate problem with this is that such countries are typically in TB endemic settings (hence the policy) with high burdens of ongoing exposure and transmission. The uncertainty of whether TB disease resulted from reactivation or re-infection would be a significant confounder.

Comprehensive follow-up and history of exposure risk would be essential and may, to some degree, mitigate against this. Alternatively, a moderate disease burden setting may be more appropriate for such a study.

7.2.3 Further MGIT assay characterisation

While a significant amount of work was performed to characterise the whole blood MGIT assay and understand underlying mechanisms, there is scope for further work in this area. Over time, the reagents available for depleting cells from whole blood have increased, as have the reported efficiencies. It would be interesting to re-visit this aspect of the work with the aim of recruiting more volunteers, improving depletion efficiency and perhaps exploring different combinations of cell depletions. In addition, using samples from patients with active TB disease and LTBI may provide further insight into the functional contributions of these cells to mycobacterial growth control. The transcriptomic time-course studies were particularly interesting in showing the effect of virulent *M. tb* on mitochondria-related signatures, which is the first such demonstration in human whole blood and consistent with very recent data using cell culture [375]. Extending these studies to other strains of mycobacteria of different virulence, including clinical isolates, could further this knowledge, and would be technically easier because one could use focused qRT-PCR specific for key mitochondrial genes rather than a complex and costly transcriptomic approach. Finally, it would be interesting to examine whether the number and subsets of key immune cells change over the duration of the MGIT assay. Multiparametric flow cytometry with whole blood could be used for this, and combining surface staining with ICS would provide both phenotypic and functional information.

7.2.4 Exploring B cell responses to mycobacteria

There is increasing evidence for a role of B cells in TB and the finding here that there are clear shifts in B cell subsets associated with TB infection and disease is fascinating and warrants further examination. It was not technically possible to study plasmablast frequencies or IgG+ cells to gain insight into isotype class switching, but this would be an important future consideration, as would the assessment of changes in subsets in patients following anti-TB treatment. The development of *M. tb*-specific labels for flow cytometric studies in order to identify antigen-specific B cells would be significant advance in understanding their relative contributions to the profiles observed. As previously discussed, perhaps the use of two or more complex markers may be of value to achieve this. Furthermore, little is currently known about the origin, development or functional capacity of atypical memory B cells and it would be beneficial to examine these elements to further delineate their association with TB. Finally, the finding that specific plasmablast and memory B cell responses are induced following BCG vaccination is novel. While the critical role of T cells in generating vaccine induced immunity against TB is accepted, B cells have not been studied in any detail. Greater appreciation of their function, if any in this context, may benefit the development of effective TB vaccines, which is notoriously difficult to achieve. Extending the studies performed here to assess the longitudinal kinetics of B cell development and persistence to mycobacterial antigens would be a suitable first step.

Appendix

8 Appendix

8.1 MGIT standard curve

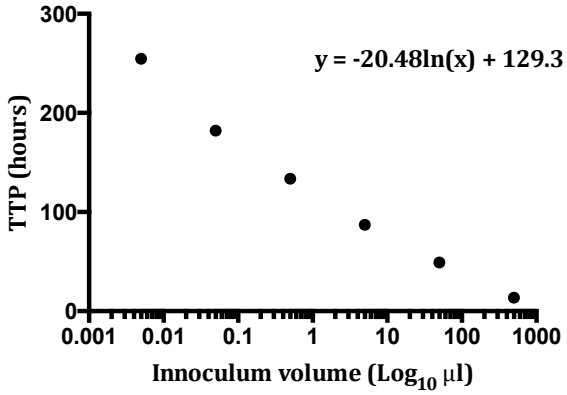


Figure 8.1 Example MGIT standard curve. Inoculum volume is plotted against time-to-positivity (TTP) to generate a standard curve, defined by the equation: *y = m (ln x) + c* where y is TTP, m is the slope and c is the y intercept.

8.2 Reagents and solutions

Reagent	Supplier	Catalogue No.
4-Nitrophenyl phosphate (20mg)	Sigma Aldrich	N2765
AlexaFluor 488 microscale protein labeling kit	Invitrogen	A30006
Anti-human CD3 AlexaFluor 700 (clone UCHT1)	eBioscience	56-0038-42
Anti-human CD4 APC (clone RPA-T4)	BioLegend	300514
Anti-human CD4 Pacific Blue (clone RPA-T4)	BioLegend	300521
Anti-human CD8 APC-H7 (clone SK1)	Becton Dickinson	641400
Anti-human CD8 Qdot605 (clone RPA-T8)	eBioscience	93-0088-42
Anti-human CD10 APC (clone HI10a)	Becton Dickinson	332777
Anti-human CD14 Pacific Blue (clone 61D3)	eBioscience	48-0149
Anti-human CD14 ECD (clone RMO52)	Beckman Coulter	IM2707U
Anti-human CD14 PE (clone HCD14)	BioLegend	325606
Anti-human CD16 PE-Cy7 (clone 3G8)	BioLegend	302016
Anti-human CD19 PECy5 (clone HIB19)	BioLegend	302210
Anti-human CD19 ECD (clone J3-119)	Beckman Coulter	A07770
Anti-human CD19 PB (clone SJ25-C1)	Life Technologies	MHCD1928
Anti-human CD19 PECy7 (clone SJ25-C1)	Becton Dickinson	560911
Anti-human CD20 eFl780 (APC-Cy7) (clone 2H7)	eBioscience	47-0209
Anti-human CD21 eFl450 (Pacific Blue) (clone HB5)	eBioscience	9048-0219-025
Anti-human CD27 Qdot605 (clone CLB-27/1)	Invitrogen	Q10065
Anti-human CD28	Becton Dickinson	340975
Anti-human CD38-PECy5 (clone HIT2)	eBioscience	15-0389
Anti-human CD49d	Becton Dickinson	340976
Anti-human CD56 PE Cy7 (clone MEM-188)	BioLegend	304628
Anti-human CD56 PB (clone MEM-188)	BioLegend	304629
Anti-human CD66b FITC (clone G10F5)	BioLegend	305104
Anti-human HLA-DR APC-Cy7 (clone L243)	BioLegend	307618
Anti-human IgG1 Fc biotin conjugated (clone HP6070)	Life Technologies	MH1515
Anti-human IgG2 biotin conjugated (clone HP6002)	Life Technologies	05-3540
Anti-human IgG3 biotin conjugated (clone HP6050)	Life Technologies	MH1512
Anti-human IgG4 biotin conjugated (clone HP6025)	Life Technologies	MH1542
Anti-human IgG-PE (clone G18-145)	Becton Dickinson	560951
Anti-human IFNγ Pe-Cy7 (clone 45.B3)	eBioscience	25-7319-82
Anti-human IL-2 PE (clone MQ1-17H12)	eBioscience	12-7029-42

Anti-human IL-17 AF488 (clone BL168)	BioLegend	512308
Anti-human TNFα AF-647 (clone MAb11)	BioLegend	502916
Anti-mouse Ig/κ compensation beads	Becton Dickinson	552843
Aqua LIVE/DEAD stain	Life technologies	L34957
BACTEC Mycobacterial Growth Indicator Tubes	Becton Dickinson	245122
BCG Pasteur	In-house	n/a
BCG SSI	Statens Serum Inst.	n/a
BCIP/NBT (plus) solution (ELISpot developing)	Europa	M0711A
Benzonase nuclease	Novagen	70664-3
Bovine Serum Albumin (BSA)	Sigma Aldrich	A8531
Brefeldin A	Sigma Aldrich	B7651
Carbonate buffer capsules	Sigma Aldrich	C-3041
Casein blocking buffer	ThermoFisher	37528
CASYTON solution	Roche Diagnostics	43001
Cell membrane fraction *M. tb* H37Rv	BEI Resources	NR-14831
CFP-10 *M. tb* H37Rv peptide array	BEI Resources	NR-34825
CFP-10 *M. tb* H37Rv recombinant protein	BEI Resources	NR-14869
Culture filtrate proteins *M. tb* H37Rv	BEI Resources	NR-14825
Deionised water	In-house	n/a
Diethanolamine buffer (5x)	ThermoFisher	34064
Dimethyl sulfoxide (DMSO)	Sigma Aldrich	D2650
Dulbeco's PBS	Sigma Aldrich	D8537
EasySep® Human Whole Blood CD3 Positive Selection Kit	StemCell Tech.	18081
EasySep® Human Buffy Coat CD14 Selection Kit	StemCell Tech.	18088
EasySep® Human Whole Blood CD19 Selection Kit	StemCell Tech.	18084
EasySep® Human Whole Blood CD66b Selection Kit	StemCell Tech.	18682
ESAT-6 *M. tb* H37Rv recombinant protein	BEI Resources	NR-14868
ESAT-6 *M. tb* H37Rv peptide array	BEI Resources	NR-34824
Ethanol	Sigma Aldrich	32221
Extravidin-AP	Sigma	E2636
FACS stain buffer (BSA/NaN3)	Becton Dickinson	554657
Foetal calf serum (FCS)	Sigma Aldrich	F2442
GLOBINclear kit	ThermoFisher	AM1980
Goat anti-human γ-chain whole IgG alkaline phosphatase conjugate	Sigma Aldrich	A3187
Goat anti-human- polyclonal IgG	Invitrogen	H17000

HEPES	Sigma Aldrich	H3375
HumanHT-12 v4.0 Expression BeadChip Kit	Illumina	BD-103-0604
Human IFN-γ ELISpot^{BASIC} (ALP)	Mabtech	3420-2A
Illumina TotalPrep-96 RNA Amplification Kit	Thermo Fisher	4393543
L-glutamine (4mM)	Sigma Aldrich	G7513
Lightning-Link® Fluorescein Conjugation Kit	Innova Biosciences	707-0010
Lipoarabinomannan *M. tb* H37Rv	BEI Resources	NR-14848
Lymphoprep	StemCell Tech.	7801
Mycobacterium tuberculosis H37Rv	BEI Resources	NR-15404
Middlebrook 7H10 agar	Becton Dickinson	295964
Middlebrook 7H9 broth	Becton Dickinson	271310
Milliplex Map Kit Human Cytokine/Chemokine Magnetic Bead Panel Multiplex	Millipore	HCYTMAG-60K-PX41
Native human IgG1	AbD Serotec	5219-3004
Native human IgG2	AbD Serotec	5225-3004
Native human IgG3	AbD Serotec	5248-3004
Native human IgG4	AbD Serotec	5254-3004
OADC enrichment	Becton Dickinson	245116
PANTA antibiotics	Becton Dickinson	245114
PAXgene blood RNA kit	Qiagen	762174
Penicillin-streptomycin solution (100U/100µg)	Sigma Aldrich	P0781
Perm/Wash buffer	Becton Dickinson	554723
Phosphate buffered Saline (PBS)	Sigma Aldrich	D8662
Phytohaemagglutinin (PHA)	Sigma Aldrich	L8902
Pooled Human AB Serum (PHS)	Sigma Aldrich	H4522
Purified Protein Derivative (PPD)	Statens Serum Inst.	2390
RNA 6000 Nano Kit	Agilent	5067-1511
RPMI 1640 media	Sigma Aldrich	R0883
Staphylococcal endotoxin B (SEB)	Sigma Aldrich	S4881
Tween 20	Sigma Aldrich	P7949
Tween 80	Becton Dickinson	231181
Whole cell lysate *M. tb* H37Rv	BEI Resources	NR-14822

Table 8.1 Reagents. A list of reagents used in this study.

Solution	Composition
Agar 7H10	900ml dH_20 + 19.7g Middlebrook agar base + 5ml glycerol (+ 100ml OADC after autoclaving and cooling below 55°C)
Cryopreservation medium	80% foetal calf serum (FCS) with 20% DMSO
ELISpot coating buffer	1 packet of ELISpot coating buffer powder reconstituted in 1 litre of dH_20 and filtered using a 0.22μM filter
FACS buffer	1% FCS in PBS
Middlebrook 7H9	4.7g/l 7H9 powder made up with water and 0.05% Tween 80 and supplemented with 10% OADC after autoclaving and cooling below 55°C
PBS	0.01M: NaCl 0.138M, KCl 0.0027M, pH 7.4; made by dissolving tablets in dH_2O
R0	RPMI 1640 supplemented with 2mM L-glutamine and 100U/ml penicillin and streptomycin sulphate (pen-strep)
R10	RPMI 1640 supplemented with 10% serum, 2mM L-glutamine and 100U/ml penicillin and streptomycin sulphate
RPMI-MGIT	RPMI 1640 media with HEPES supplemented with 2mM L-glutamine and 10% PHS

Table 8.2 Solutions. A list of solutions used in this study.

8.3 Supplementary transcriptomic data

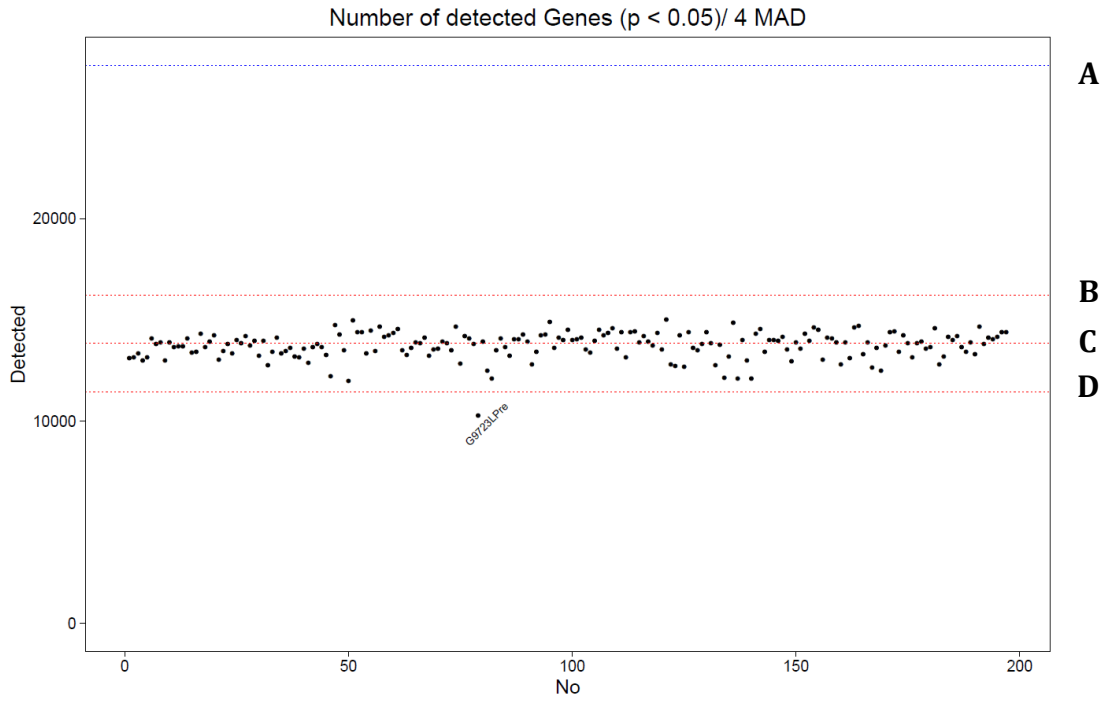


Figure 8.2 Quality control evaluation by probe detection. A plot of the number of samples (x-axis) against the number of genes on the array (y-axis) with at least one probe passing the detection p-value of 0.05 in at least 10% of all samples. Samples with more than 4 times the median absolute deviation (MAD) from the median were excluded (n=1). Dashed lines correspond to: the total number of genes represented on the array, ~27,000 (A), the median number of detected genes (C) and three robust SDs above and below the average (B and D).

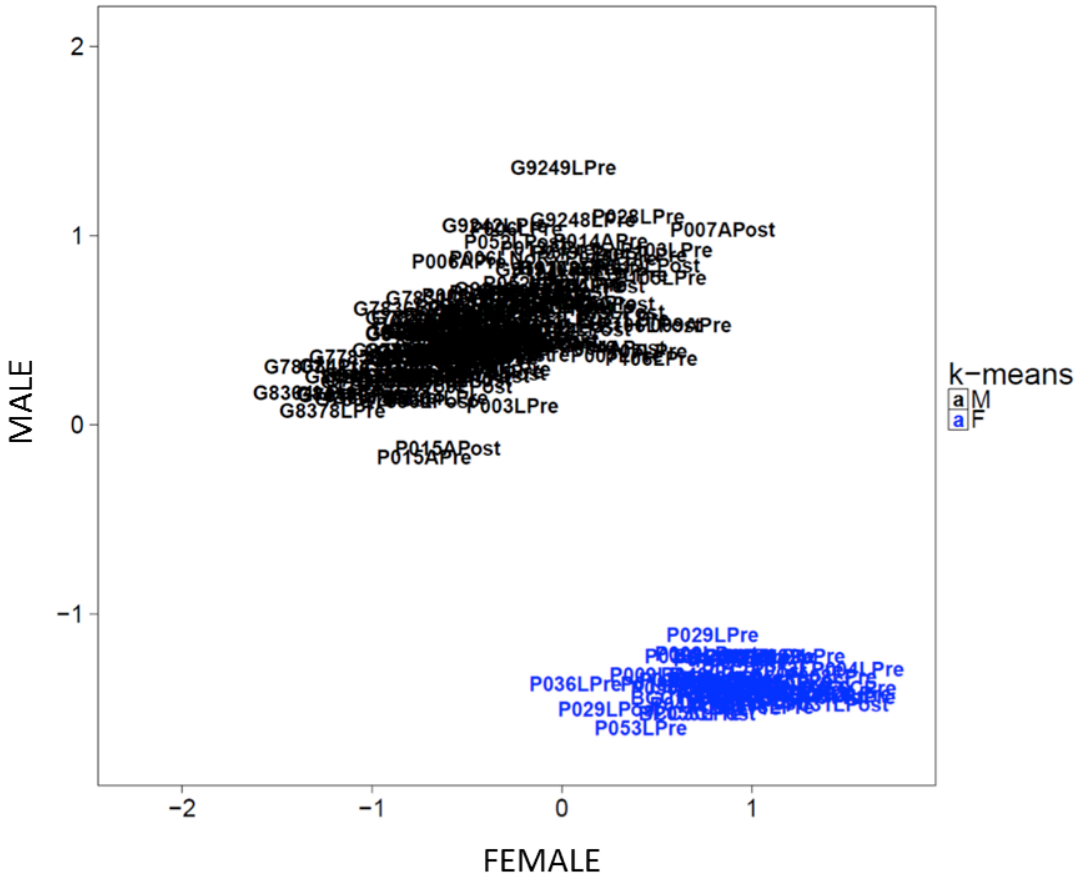


Figure 8.3 Quality control evaluation with gender classification. Z-score (scaled expression) of the most upregulated genes for male and female subjects are shown. k-means clustering was used to separate the two groups and no outliers were detected based on the gender labels provided (i.e. no mislabeled samples were identified).

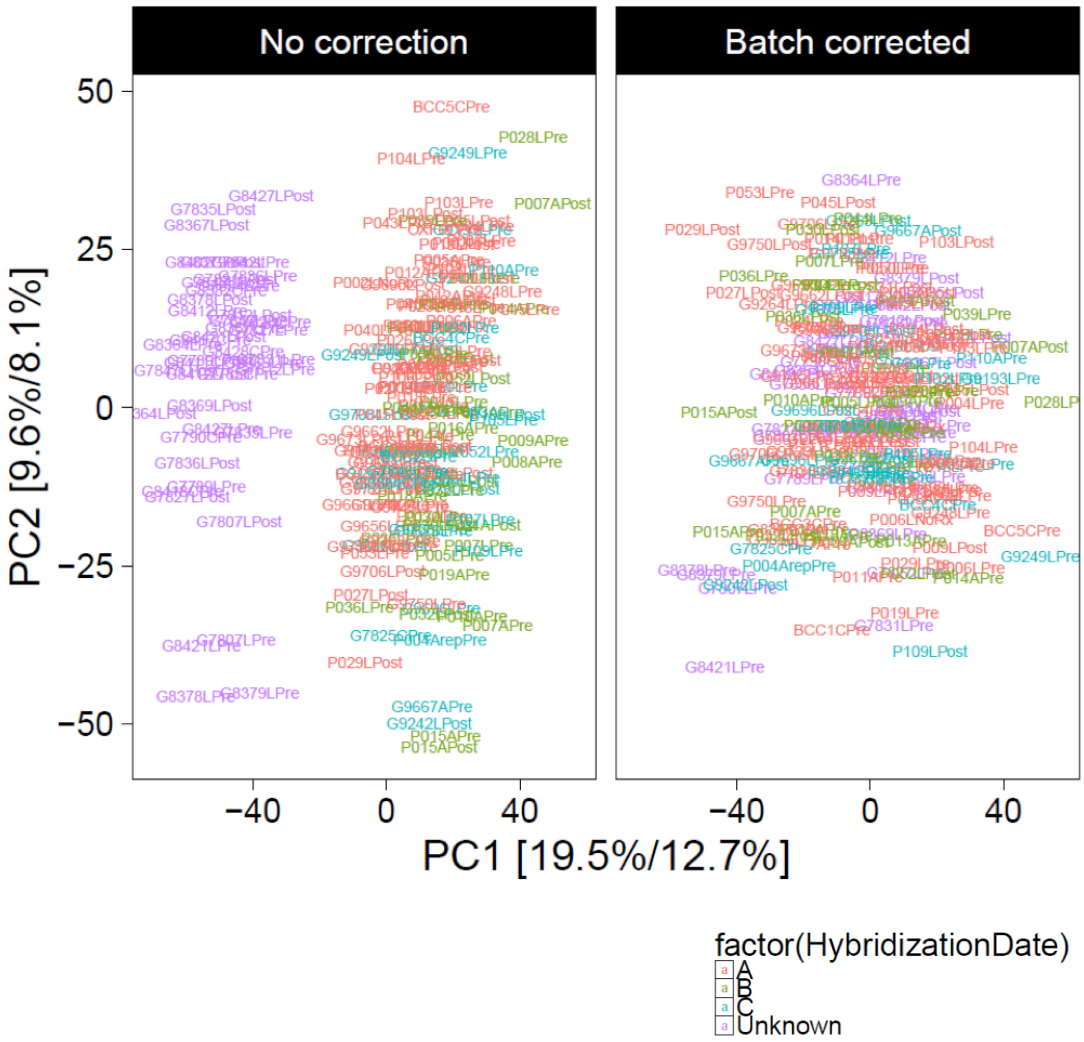


Figure 8.4 Assessing microarray processing batch effect. Principal components analysis (PCA) was performed on all samples and detected probes and the first two principal components are shown in the left hand panel (no correction). Each sample is colour coded according to one of the four hybridization dates. Hybridization batch effects were then removed and the first two principal components after PCA are shown in the right panel.

A

GO Term	n	Up	Down	Up p-value	Down p-value
innate immune response	853	158	68	2.01×10^{-29}	0.50
immune response	1323	205	115	1.96×10^{-27}	0.15
type I interferon signalling pathway	68	39	4	4.17×10^{-27}	0.79
cellular response to type I interferon	68	39	4	4.17×10^{-27}	0.79
response to type I interferon	72	40	5	4.92×10^{-27}	0.68
defence response to other organism	391	92	22	1.06×10^{-24}	0.96
defence response	1360	202	104	1.41×10^{-24}	0.67
regulation of innate immune response	346	80	26	4.61×10^{-21}	0.64
immune system process	2037	254	183	5.53×10^{-20}	0.03
response to external biotic stimulus	671	117	41	1.69×10^{-19}	0.97

B

GO Term	n	Up	Down	Up p-value	Down p-value
defence response	1360	285	104	7.66×10^{-32}	0.99
innate immune response	853	207	61	1.17×10^{-31}	0.99
immune response	1323	279	110	1.31×10^{-31}	0.98
immune system process	2037	368	181	8.46×10^{-28}	0.96
regulation of innate immune response	346	105	23	4.35×10^{-24}	0.98
response to stress	3061	481	281	9.52×10^{-23}	0.96
regulation of defence response	614	147	54	8.38×10^{-22}	0.86
positive regulation of immune response	553	136	51	2.47×10^{-21}	0.75
activation of immune response	448	118	40	3.49×10^{-21}	0.79
immune effector process	615	145	56	7.72×10^{-21}	0.79

C

GO Term	n	Up	Down	Up p-value	Down p-value
structural constituent of ribosome	193	75	3	5.68×10^{-37}	1.00
ribosomal subunit	155	64	0	1.59×10^{-33}	1.00
ribosome	212	72	2	4.43×10^{-31}	1.00
translational termination	177	65	1	1.97×10^{-30}	1.00
translational elongation	204	69	5	1.08×10^{-29}	1.00
cytosolic ribosome	100	47	0	5.98×10^{-28}	1.00
intracellular ribonucleoprotein complex	648	126	51	9.13×10^{-27}	0.84
ribonucleoprotein complex	648	126	51	9.13×10^{-27}	0.84
selenocysteine metabolic process	89	42	0	3.44×10^{-25}	1.00
serine family amino acid metabolic process	116	45	0	1.51×10^{-22}	1.00

Table 8.3 GO DGE annotation top tables. The top 10 functional pathways identified by GO analysis of the most significant DGE comparisons between 'active' vs 'control' clusters (A), 'active' vs 'latent' clusters (B) and 'latent' vs 'control' clusters (C). Clusters were generated from hierarchical analysis as previously described.

References

1. Wirth T, Hildebrand F, Allix-Beguec C, Wolbeling F, Kubica T, Kremer K*, et al.* Origin, spread and demography of the Mycobacterium tuberculosis complex. *PLoS Pathog* 2008,**4**:e1000160.
2. Hershberg R, Lipatov M, Small PM, Sheffer H, Niemann S, Homolka S*, et al.* High functional diversity in Mycobacterium tuberculosis driven by genetic drift and human demography. *PLoS Biol* 2008,**6**:e311.
3. Gagneux S. Host-pathogen coevolution in human tuberculosis. *Philos Trans R Soc Lond B Biol Sci* 2012,**367**:850-859.
4. Esmail H, Barry CE, 3rd, Young DB, Wilkinson RJ. The ongoing challenge of latent tuberculosis. *Philos Trans R Soc Lond B Biol Sci* 2014,**369**:20130437.
5. WHO. 2015 Global tuberculosis report. In. Geneva, Switzerland: World Health Organisation; 2015.
6. Richter E, Weizenegger M, Rusch-Gerdes S, Niemann S. Evaluation of genotype MTBC assay for differentiation of clinical Mycobacterium tuberculosis complex isolates. *J Clin Microbiol* 2003,**41**:2672-2675.
7. Wayne LG. Microbiology of tubercle bacilli. *Am Rev Respir Dis* 1982,**125**:31-41.
8. Grange JM. Mycobacterium bovis infection in human beings. *Tuberculosis (Edinb)* 2001,**81**:71-77.
9. Park D, Qin H, Jain S, Preziosi M, Minuto JJ, Mathews WC*, et al.* Tuberculosis due to Mycobacterium bovis in patients coinfected with human immunodeficiency virus. *Clin Infect Dis* 2010,**51**:1343-1346.
10. McNeil MR, Brennan PJ. Structure, function and biogenesis of the cell envelope of mycobacteria in relation to bacterial physiology, pathogenesis and drug resistance; some thoughts and possibilities arising from recent structural information. *Res Microbiol* 1991,**142**:451-463.
11. Loudon RG, Roberts RM. Droplet expulsion from the respiratory tract. *Am Rev Respir Dis* 1967,**95**:435-442.
12. Loudon RG, Roberts RM. Singing and the dissemination of tuberculosis. *Am Rev Respir Dis* 1968,**98**:297-300.
13. Escombe AR, Moore DA, Gilman RH, Navincopa M, Ticona E, Mitchell B*, et al.* Upper-room ultraviolet light and negative air ionization to prevent tuberculosis transmission. *PLoS Med* 2009,**6**:e43.
14. O'Shea MK, Wilson D. Tuberculosis and the military. *J R Army Med Corps* 2013,**159**:190-199.
15. Chaisson RE, Nachega JB. *Tuberculosis*. 5th ed. Oxford: Oxford University Press; 2010.
16. Barnes PF, Bloch AB, Davidson PT, Snider DE, Jr. Tuberculosis in patients with human immunodeficiency virus infection. *N Engl J Med* 1991,**324**:1644-1650.
17. Comstock GW. Epidemiology of tuberculosis. *Am Rev Respir Dis* 1982,**125**:8-15.
18. Lawn SD, Zumla AI. Tuberculosis. *Lancet* 2011,**378**:57-72.
19. Palaci M, Dietze R, Hadad DJ, Ribeiro FK, Peres RL, Vinhas SA*, et al.* Cavitary disease and quantitative sputum bacillary load in cases of pulmonary tuberculosis. *J Clin Microbiol* 2007,**45**:4064-4066.
20. Ernst JD. The immunological life cycle of tuberculosis. *Nat Rev Immunol* 2012,**12**:581-591.
21. O'Garra A, Redford PS, McNab FW, Bloom CI, Wilkinson RJ, Berry MP. The immune response in tuberculosis. *Annu Rev Immunol* 2013,**31**:475-527.
22. Arango L, Brewin AW, Murray JF. The spectrum of tuberculosis as currently seen in a metropolitan hospital. *Am Rev Respir Dis* 1973,**108**:805-812.
23. MacGregor RR. A year's experience with tuberculosis in a private urban teaching hospital in the postsanatorium era. *Am J Med* 1975,**58**:221-228.

24. Poulsen A. Some clinical features of tuberculosis. *Acta Tuberc Scand* 1957,**33**:37-92; concl.
25. Choyke PL, Sostman HD, Curtis AM, Ravin CE, Chen JT, Godwin JD*, et al.* Adult-onset pulmonary tuberculosis. *Radiology* 1983,**148**:357-362.
26. Krysl J, Korzeniewska-Kosela M, Muller NL, FitzGerald JM. Radiologic features of pulmonary tuberculosis: an assessment of 188 cases. *Can Assoc Radiol J* 1994,**45**:101-107.
27. Khan MA, Kovnat DM, Bachus B, Whitcomb ME, Brody JS, Snider GL. Clinical and roentgenographic spectrum of pulmonary tuberculosis in the adult. *Am J Med* 1977,**62**:31-38.
28. Farman DP, Speir WA, Jr. Initial roentgenographic manifestations of bacteriologically proven Mycobacterium tuberculosis. Typical or atypical? *Chest* 1986,**89**:75-77.
29. Poppius H, Thomander K. Segmentary distribution of cavities; a radiologic study of 500 consecutive cases of cavernous pulmonary tuberculosis. *Ann Med Intern Fenn* 1957,**46**:113-119.
30. Tuberculosis. In: *NG33 Guidence (TB) 2016*. London: National Institute for Health and Care Excellence; 2016.
31. Greenberg SD, Frager D, Suster B, Walker S, Stavropoulos C, Rothpearl A. Active pulmonary tuberculosis in patients with AIDS: spectrum of radiographic findings (including a normal appearance). *Radiology* 1994,**193**:115-119.
32. Bakari M, Arbeit RD, Mtei L, Lyimo J, Waddell R, Matee M*, et al.* Basis for treatment of tuberculosis among HIV-infected patients in Tanzania: the role of chest x-ray and sputum culture. *BMC Infect Dis* 2008,**8**:32.
33. Reid MJ, Shah NS. Approaches to tuberculosis screening and diagnosis in people with HIV in resource-limited settings. *Lancet Infect Dis* 2009,**9**:173-184.
34. Huebner RE, Schein MF, Bass JB, Jr. The tuberculin skin test. *Clin Infect Dis* 1993,**17**:968-975.
35. Dye C, Bassili A, Bierrenbach AL, Broekmans JF, Chadha VK, Glaziou P*, et al.* Measuring tuberculosis burden, trends, and the impact of control programmes. *Lancet Infect Dis* 2008,**8**:233-243.
36. Rieder HL. Methodological issues in the estimation of the tuberculosis problem from tuberculin surveys. *Tuber Lung Dis* 1995,**76**:114-121.
37. Aggerbeck H, Giemza R, Joshi P, Tingskov PN, Hoff ST, Boyle J*, et al.* Randomised clinical trial investigating the specificity of a novel skin test (C-Tb) for diagnosis of M. tuberculosis infection. *PLoS One* 2013,**8**:e64215.
38. Hoff ST, Peter JG, Theron G, Pascoe M, Tingskov PN, Aggerbeck H*, et al.* Sensitivity of C-Tb: a novel RD-1-specific skin test for the diagnosis of tuberculosis infection. *Eur Respir J* 2016,**47**:919-928.
39. Dye C, Scheele S, Dolin P, Pathania V, Raviglione MC. Consensus statement. Global burden of tuberculosis: estimated incidence, prevalence, and mortality by country. WHO Global Surveillance and Monitoring Project. *JAMA* 1999,**282**:677-686.
40. Styblo K. The relationship between the risk of tuberculous infection and the risk of developing infectious tuberculosis. *Bull Int Union Tuberc Lung Dis* 1985,**60**:117-119.
41. Dye C. Breaking a law: tuberculosis disobeys Styblo's rule. *Bull World Health Organ* 2008,**86**:4.
42. van Leth F, van der Werf MJ, Borgdorff MW. Prevalence of tuberculous infection and incidence of tuberculosis: a re-assessment of the Styblo rule. *Bull World Health Organ* 2008,**86**:20-26.

43. Gagneux S. Genetic diversity in Mycobacterium tuberculosis. *Curr Top Microbiol Immunol* 2013,**374**:1-25.
44. Koch R. A Further Communication on a Remedy for Tuberculosis. *Br Med J* 1891,**1**:125-127.
45. Dharmadhikari AS, Basaraba RJ, Van Der Walt ML, Weyer K, Mphahlele M, Venter K*, et al.* Natural infection of guinea pigs exposed to patients with highly drug-resistant tuberculosis. *Tuberculosis (Edinb)* 2011,**91**:329-338.
46. Escombe AR, Oeser C, Gilman RH, Navincopa M, Ticona E, Martinez C*, et al.* The detection of airborne transmission of tuberculosis from HIV-infected patients, using an in vivo air sampling model. *Clin Infect Dis* 2007,**44**:1349-1357.
47. Mills CC, O'Grady F, Riley RL. Tuberculin conversion in the "naturally infected" guinea pig. *Bull Johns Hopkins Hosp* 1960,**106**:36-45.
48. Ferebee SH. Controlled chemoprophylaxis trials in tuberculosis. A general review. *Bibl Tuberc* 1970,**26**:28-106.
49. Menzies D. Interpretation of repeated tuberculin tests. Boosting, conversion, and reversion. *Am J Respir Crit Care Med* 1999,**159**:15-21.
50. Targeted tuberculin testing and treatment of latent tuberculosis infection. This official statement of the American Thoracic Society was adopted by the ATS Board of Directors, July 1999. This is a Joint Statement of the American Thoracic Society (ATS) and the Centers for Disease Control and Prevention (CDC). This statement was endorsed by the Council of the Infectious Diseases Society of America. (IDSA), September 1999, and the sections of this statement. *Am J Respir Crit Care Med* 2000,**161**:S221-247.
51. Lalvani A, Nagvenkar P, Udwadia Z, Pathan AA, Wilkinson KA, Shastri JS*, et al.* Enumeration of T cells specific for RD1-encoded antigens suggests a high prevalence of latent Mycobacterium tuberculosis infection in healthy urban Indians. *J Infect Dis* 2001,**183**:469-477.
52. Lalvani A, Pathan AA, McShane H, Wilkinson RJ, Latif M, Conlon CP*, et al.* Rapid detection of Mycobacterium tuberculosis infection by enumeration of antigen-specific T cells. *Am J Respir Crit Care Med* 2001,**163**:824-828.
53. Menzies D, Pai M, Comstock G. Meta-analysis: new tests for the diagnosis of latent tuberculosis infection: areas of uncertainty and recommendations for research. *Ann Intern Med* 2007,**146**:340-354.
54. Pai M, Zwerling A, Menzies D. Systematic review: T-cell-based assays for the diagnosis of latent tuberculosis infection: an update. *Ann Intern Med* 2008,**149**:177-184.
55. Pathan AA, Wilkinson KA, Wilkinson RJ, Latif M, McShane H, Pasvol G*, et al.* High frequencies of circulating IFN-gamma-secreting CD8 cytotoxic T cells specific for a novel MHC class I-restricted Mycobacterium tuberculosis epitope in M. tuberculosis-infected subjects without disease. *Eur J Immunol* 2000,**30**:2713-2721.
56. Kang YA, Lee HW, Yoon HI, Cho B, Han SK, Shim YS*, et al.* Discrepancy between the tuberculin skin test and the whole-blood interferon gamma assay for the diagnosis of latent tuberculosis infection in an intermediate tuberculosis-burden country. *JAMA* 2005,**293**:2756-2761.
57. Mahomed H, Hughes EJ, Hawkridge T, Minnies D, Simon E, Little F*, et al.* Comparison of mantoux skin test with three generations of a whole blood IFN-gamma assay for tuberculosis infection. *Int J Tuberc Lung Dis* 2006,**10**:310-316.
58. Mancuso JD, Mazurek GH, Tribble D, Olsen C, Aronson NE, Geiter L*, et al.* Discordance among commercially available diagnostics for latent tuberculosis infection. *Am J Respir Crit Care Med* 2012,**185**:427-434.

59. Pai M, Joshi R, Dogra S, Zwerling AA, Gajalakshmi D, Goswami K*, et al.* T-cell assay conversions and reversions among household contacts of tuberculosis patients in rural India. *Int J Tuberc Lung Dis* 2009,**13**:84-92.
60. Perry S, Sanchez L, Yang S, Agarwal Z, Hurst P, Parsonnet J. Reproducibility of QuantiFERON-TB gold in-tube assay. *Clin Vaccine Immunol* 2008,**15**:425-432.
61. van Zyl-Smit RN, Pai M, Peprah K, Meldau R, Kieck J, Juritz J*, et al.* Within-subject variability and boosting of T-cell interferon-gamma responses after tuberculin skin testing. *Am J Respir Crit Care Med* 2009,**180**:49-58.
62. Banaei N, Gaur RL, Pai M. Interferon Gamma Release Assays for Latent Tuberculosis: What Are the Sources of Variability? *J Clin Microbiol* 2016,**54**:845-850.
63. Day CL, Abrahams DA, Lerumo L, Janse van Rensburg E, Stone L, O'Rie T*, et al.* Functional capacity of Mycobacterium tuberculosis-specific T cell responses in humans is associated with mycobacterial load. *J Immunol* 2011,**187**:2222-2232.
64. Kaushal D, Mehra S, Didier PJ, Lackner AA. The non-human primate model of tuberculosis. *J Med Primatol* 2012,**41**:191-201.
65. Mehra S, Golden NA, Dutta NK, Midkiff CC, Alvarez X, Doyle LA*, et al.* Reactivation of latent tuberculosis in rhesus macaques by coinfection with simian immunodeficiency virus. *J Med Primatol* 2011,**40**:233-243.
66. Adetifa IM, Ota MO, Walther B, Hammond AS, Lugos MD, Jeffries DJ*, et al.* Decay kinetics of an interferon gamma release assay with anti-tuberculosis therapy in newly diagnosed tuberculosis cases. *PLoS One* 2010,**5**.
67. Chee CB, KhinMar KW, Gan SH, Barkham TM, Pushparani M, Wang YT. Latent tuberculosis infection treatment and T-cell responses to Mycobacterium tuberculosis-specific antigens. *Am J Respir Crit Care Med* 2007,**175**:282-287.
68. Lee SH, Lew WJ, Kim HJ, Lee HK, Lee YM, Cho CH*, et al.* Serial interferon-gamma release assays after rifampicin prophylaxis in a tuberculosis outbreak. *Respir Med* 2010,**104**:448-453.
69. Comstock GW, Livesay VT, Woolpert SF. The prognosis of a positive tuberculin reaction in childhood and adolescence. *Am J Epidemiol* 1974,**99**:131-138.
70. Diel R, Loddenkemper R, Nienhaus A. Predictive value of interferon-gamma release assays and tuberculin skin testing for progression from latent TB infection to disease state: a meta-analysis. *Chest* 2012,**142**:63-75.
71. Higuchi K, Harada N, Fukazawa K, Mori T. Relationship between whole-blood interferon-gamma responses and the risk of active tuberculosis. *Tuberculosis (Edinb)* 2008,**88**:244-248.
72. Metcalfe JZ, Cattamanchi A, Vittinghoff E, Ho C, Grinsdale J, Hopewell PC*, et al.* Evaluation of quantitative IFN-gamma response for risk stratification of active tuberculosis suspects. *Am J Respir Crit Care Med* 2010,**181**:87-93.
73. Rangaka MX, Wilkinson KA, Glynn JR, Ling D, Menzies D, Mwansa-Kambafwile J*, et al.* Predictive value of interferon-gamma release assays for incident active tuberculosis: a systematic review and meta-analysis. *Lancet Infect Dis* 2012,**12**:45-55.
74. Watkins RE, Brennan R, Plant AJ. Tuberculin reactivity and the risk of tuberculosis: a review. *Int J Tuberc Lung Dis* 2000,**4**:895-903.
75. Diel R, Loddenkemper R, Niemann S, Meywald-Walter K, Nienhaus A. Negative and positive predictive value of a whole-blood interferon-gamma release assay for developing active tuberculosis: an update. *Am J Respir Crit Care Med* 2011,**183**:88-95.
76. Mahomed H, Hawkridge T, Verver S, Abrahams D, Geiter L, Hatherill M*, et al.* The tuberculin skin test versus QuantiFERON TB Gold(R) in predicting

tuberculosis disease in an adolescent cohort study in South Africa. *PLoS One* 2011,**6**:e17984.
77. Smieja MJ, Marchetti CA, Cook DJ, Smaill FM. Isoniazid for preventing tuberculosis in non-HIV infected persons. *Cochrane Database Syst Rev* 2000:Cd001363.
78. Salgame P, Geadas C, Collins L, Jones-Lopez E, Ellner JJ. Latent tuberculosis infection--Revisiting and revising concepts. *Tuberculosis (Edinb)* 2015,**95**:373-384.
79. Pai M. Spectrum of latent tuberculosis - existing tests cannot resolve the underlying phenotypes. *Nat Rev Microbiol* 2010,**8**:242; author reply 242.
80. Dye C, Hosseini M, Watt C. Did we reach the 2005 targets for tuberculosis control? *Bull World Health Organ* 2007,**85**:364-369.
81. WHO. The Global Plan to Stop TB 2011-2015 In. Geneva: World Health Organization; 2010.
82. Dye C, Glaziou P, Floyd K, Raviglione M. Prospects for tuberculosis elimination. *Annu Rev Public Health* 2013,**34**:271-286.
83. Dye C, Williams BG. Eliminating human tuberculosis in the twenty-first century. *J R Soc Interface* 2008,**5**:653-662.
84. Bloom BR, Atun R. Back to the future: Rethinking global control of tuberculosis. *Sci Transl Med* 2016,**8**:329ps327.
85. Mao TE, Okada K, Yamada N, Peou S, Ota M, Saint S*, et al.* Cross-sectional studies of tuberculosis prevalence in Cambodia between 2002 and 2011. *Bull World Health Organ* 2014,**92**:573-581.
86. Shapiro AE, Variava E, Rakgokong MH, Moodley N, Luke B, Salimi S*, et al.* Community-based targeted case finding for tuberculosis and HIV in household contacts of patients with tuberculosis in South Africa. *Am J Respir Crit Care Med* 2012,**185**:1110-1116.
87. Wood R, Middelkoop K, Myer L, Grant AD, Whitelaw A, Lawn SD*, et al.* Undiagnosed tuberculosis in a community with high HIV prevalence: implications for tuberculosis control. *Am J Respir Crit Care Med* 2007,**175**:87-93.
88. Kritzinger FE, den Boon S, Verver S, Enarson DA, Lombard CJ, Borgdorff MW*, et al.* No decrease in annual risk of tuberculosis infection in endemic area in Cape Town, South Africa. *Trop Med Int Health* 2009,**14**:136-142.
89. Yuen CM, Amanullah F, Dharmadhikari A, Nardell EA, Seddon JA, Vasilyeva I*, et al.* Turning off the tap: stopping tuberculosis transmission through active case-finding and prompt effective treatment. *Lancet* 2015,**386**:2334-2343.
90. Abu-Raddad LJ, Sabatelli L, Achterberg JT, Sugimoto JD, Longini IM, Jr., Dye C*, et al.* Epidemiological benefits of more-effective tuberculosis vaccines, drugs, and diagnostics. *Proc Natl Acad Sci U S A* 2009,**106**:13980-13985.
91. Barry CE, 3rd, Boshoff HI, Dartois V, Dick T, Ehrt S, Flynn J*, et al.* The spectrum of latent tuberculosis: rethinking the biology and intervention strategies. *Nat Rev Microbiol* 2009,**7**:845-855.
92. Mack U, Migliori GB, Sester M, Rieder HL, Ehlers S, Goletti D*, et al.* LTBI: latent tuberculosis infection or lasting immune responses to M. tuberculosis? A TBNET consensus statement. *Eur Respir J* 2009,**33**:956-973.
93. Young DB, Gideon HP, Wilkinson RJ. Eliminating latent tuberculosis. *Trends Microbiol* 2009,**17**:183-188.
94. Kasprowicz VO, Churchyard G, Lawn SD, Squire SB, Lalvani A. Diagnosing latent tuberculosis in high-risk individuals: rising to the challenge in high-burden areas. *J Infect Dis* 2011,**204 Suppl 4**:S1168-1178.

95. Sutherland JS, Hill PC, Adetifa IM, de Jong BC, Donkor S, Joosten SA*, et al.* Identification of probable early-onset biomarkers for tuberculosis disease progression. *PLoS One* 2011,**6**:e25230.
96. Cardona PJ. A dynamic reinfection hypothesis of latent tuberculosis infection. *Infection* 2009,**37**:80-86.
97. Gengenbacher M, Kaufmann SH. Mycobacterium tuberculosis: success through dormancy. *FEMS Microbiol Rev* 2012,**36**:514-532.
98. Young D, Stark J, Kirschner D. Systems biology of persistent infection: tuberculosis as a case study. *Nat Rev Microbiol* 2008,**6**:520-528.
99. Daniel TM. The history of tuberculosis. *Respir Med* 2006,**100**:1862-1870.
100. Gideon HP, Flynn JL. Latent tuberculosis: what the host "sees"? *Immunol Res* 2011,**50**:202-212.
101. Robertson BD, Altmann D, Barry C, Bishai B, Cole S, Dick T*, et al.* Detection and treatment of subclinical tuberculosis. *Tuberculosis (Edinb)* 2012,**92**:447-452.
102. Vynnycky E, Fine PE. The natural history of tuberculosis: the implications of age-dependent risks of disease and the role of reinfection. *Epidemiol Infect* 1997,**119**:183-201.
103. Borgdorff MW, Sebek M, Geskus RB, Kremer K, Kalisvaart N, van Soolingen D. The incubation period distribution of tuberculosis estimated with a molecular epidemiological approach. *Int J Epidemiol* 2011,**40**:964-970.
104. McCarthy OR. Asian immigrant tuberculosis--the effect of visiting Asia. *Br J Dis Chest* 1984,**78**:248-253.
105. Cohen T, Murray M. Incident tuberculosis among recent US immigrants and exogenous reinfection. *Emerg Infect Dis* 2005,**11**:725-728.
106. Andrews JR, Noubary F, Walensky RP, Cerda R, Losina E, Horsburgh CR. Risk of progression to active tuberculosis following reinfection with Mycobacterium tuberculosis. *Clin Infect Dis* 2012,**54**:784-791.
107. Brooks-Pollock E, Becerra MC, Goldstein E, Cohen T, Murray MB. Epidemiologic inference from the distribution of tuberculosis cases in households in Lima, Peru. *J Infect Dis* 2011,**203**:1582-1589.
108. Sutherland I, Svandova E, Radhakrishna S. The development of clinical tuberculosis following infection with tubercle bacilli. 1. A theoretical model for the development of clinical tuberculosis following infection, linking from data on the risk of tuberculous infection and the incidence of clinical tuberculosis in the Netherlands. *Tubercle* 1982,**63**:255-268.
109. Lurie MB. A correlation between the histological changes and the fate of living tubercle bacilli in the organs of reinfected rabbits. *J Exp Med* 1933,**57**:181-201.
110. Whalen CC, Zalwango S, Chiunda A, Malone L, Eisenach K, Joloba M*, et al.* Secondary attack rate of tuberculosis in urban households in Kampala, Uganda. *PLoS One* 2011,**6**:e16137.
111. Ellner JJ. Immunoregulation in TB: observations and implications. *Clin Transl Sci* 2010,**3**:23-28.
112. Marx FM, Dunbar R, Enarson DA, Williams BG, Warren RM, van der Spuy GD*, et al.* The temporal dynamics of relapse and reinfection tuberculosis after successful treatment: a retrospective cohort study. *Clin Infect Dis* 2014,**58**:1676-1683.
113. Lillebaek T, Dirksen A, Baess I, Strunge B, Thomsen VO, Andersen AB. Molecular evidence of endogenous reactivation of Mycobacterium tuberculosis after 33 years of latent infection. *J Infect Dis* 2002,**185**:401-404.
114. Stead WW. Pathogenesis of the sporadic case of tuberculosis. *N Engl J Med* 1967,**277**:1008-1012.

115. Steinbruck P, Dankova D, Edwards LB, Doster B, Livesay VT. Tuberculosis risk in persons with "fibrotic" x-ray lesions. *Bull Int Union Tuberc* 1972,**47**:135-159.
116. Vaara J, Kokkola K. Inactive pulmonary lesions: a potent risk factor of tuberculosis. *Ann Clin Res* 1975,**7**:331-333.
117. Antonucci G, Girardi E, Raviglione MC, Ippolito G. Risk factors for tuberculosis in HIV-infected persons. A prospective cohort study. The Gruppo Italiano di Studio Tubercolosi e AIDS (GISTA). *JAMA* 1995,**274**:143-148.
118. Corbett EL, Watt CJ, Walker N, Maher D, Williams BG, Raviglione MC*, et al.* The growing burden of tuberculosis: global trends and interactions with the HIV epidemic. *Arch Intern Med* 2003,**163**:1009-1021.
119. Golub JE, Saraceni V, Cavalcante SC, Pacheco AG, Moulton LH, King BS*, et al.* The impact of antiretroviral therapy and isoniazid preventive therapy on tuberculosis incidence in HIV-infected patients in Rio de Janeiro, Brazil. *AIDS* 2007,**21**:1441-1448.
120. Guelar A, Gatell JM, Verdejo J, Podzamczer D, Lozano L, Aznar E*, et al.* A prospective study of the risk of tuberculosis among HIV-infected patients. *AIDS* 1993,**7**:1345-1349.
121. Havlir DV, Getahun H, Sanne I, Nunn P. Opportunities and challenges for HIV care in overlapping HIV and TB epidemics. *JAMA* 2008,**300**:423-430.
122. Martinez-Pino I, Sambeat MA, Lacalle-Remigio JR, Domingo P. Incidence of tuberculosis in HIV-infected patients in Spain: the impact of treatment for LTBI. *Int J Tuberc Lung Dis* 2013,**17**:1545-1551.
123. Elzi L, Schlegel M, Weber R, Hirschel B, Cavassini M, Schmid P*, et al.* Reducing tuberculosis incidence by tuberculin skin testing, preventive treatment, and antiretroviral therapy in an area of low tuberculosis transmission. *Clin Infect Dis* 2007,**44**:94-102.
124. Corbett EL, Bandason T, Cheung YB, Munyati S, Godfrey-Faussett P, Hayes R*, et al.* Epidemiology of tuberculosis in a high HIV prevalence population provided with enhanced diagnosis of symptomatic disease. *PLoS Med* 2007,**4**:e22.
125. Fan WC, Liu CJ, Hong YC, Feng JY, Su WJ, Chien SH*, et al.* Long-term risk of tuberculosis in haematopoietic stem cell transplant recipients: a 10-year nationwide study. *Int J Tuberc Lung Dis* 2015,**19**:58-64.
126. Gomez-Reino JJ, Carmona L, Angel Descalzo M. Risk of tuberculosis in patients treated with tumor necrosis factor antagonists due to incomplete prevention of reactivation of latent infection. *Arthritis Rheum* 2007,**57**:756-761.
127. Jick SS, Lieberman ES, Rahman MU, Choi HK. Glucocorticoid use, other associated factors, and the risk of tuberculosis. *Arthritis Rheum* 2006,**55**:19-26.
128. Lichtenstein IH, MacGregor RR. Mycobacterial infections in renal transplant recipients: report of five cases and review of the literature. *Rev Infect Dis* 1983,**5**:216-226.
129. Lopez de Castilla D, Schluger NW. Tuberculosis following solid organ transplantation. *Transpl Infect Dis* 2010,**12**:106-112.
130. Wallis RS, Broder M, Wong J, Lee A, Hoq L. Reactivation of latent granulomatous infections by infliximab. *Clin Infect Dis* 2005,**41 Suppl 3**:S194-198.
131. Corbett EL, Churchyard GJ, Clayton TC, Williams BG, Mulder D, Hayes RJ*, et al.* HIV infection and silicosis: the impact of two potent risk factors on the incidence of mycobacterial disease in South African miners. *AIDS* 2000,**14**:2759-2768.
132. Kamboj M, Sepkowitz KA. The risk of tuberculosis in patients with cancer. *Clin Infect Dis* 2006,**42**:1592-1595.

133. Ludvigsson JF, Wahlstrom J, Grunewald J, Ekbom A, Montgomery SM. Coeliac disease and risk of tuberculosis: a population based cohort study. *Thorax* 2007,**62**:23-28.
134. Pablos-Mendez A, Blustein J, Knirsch CA. The role of diabetes mellitus in the higher prevalence of tuberculosis among Hispanics. *Am J Public Health* 1997,**87**:574-579.
135. Pien FD, Younoszai BG, Pien BC. Mycobacterial infections in patients with chronic renal disease. *Infect Dis Clin North Am* 2001,**15**:851-876.
136. Steiger Z, Nickel WO, Shannon GJ, Nedwicki EG, Higgins RF. Pulmonary tuberculosis after gastric resection. *Am J Surg* 1976,**131**:668-671.
137. Edwards LB, Livesay VT, Acquaviva FA, Palmer CE. Height, weight, tuberculous infection, and tuberculous disease. *Arch Environ Health* 1971,**22**:106-112.
138. Palmer CE, Jablon S, Edwards PQ. Tuberculosis morbidity of young men in relation to tuberculin sensitivity and body build. *Am Rev Tuberc* 1957,**76**:517-539.
139. Getahun H, Matteelli A, Chaisson RE, Raviglione M. Latent Mycobacterium tuberculosis infection. *N Engl J Med* 2015,**372**:2127-2135.
140. Menzies D, Al Jahdali H, Al Otaibi B. Recent developments in treatment of latent tuberculosis infection. *Indian J Med Res* 2011,**133**:257-266.
141. Comstock GW. How much isoniazid is needed for prevention of tuberculosis among immunocompetent adults? *Int J Tuberc Lung Dis* 1999,**3**:847-850.
142. Silva AP, Hill P, Belo MT, Rabelo SG, Menzies D, Trajman A. Non-completion of latent tuberculous infection treatment among children in Rio de Janeiro State, Brazil. *Int J Tuberc Lung Dis* 2016,**20**:479-486.
143. Moro RN, Borisov AS, Saukkonen J, Khan A, Sterling TR, Villarino ME*, et al.* Factors Associated With Noncompletion of Latent Tuberculosis Infection Treatment: Experience From the PREVENT TB Trial in the United States and Canada. *Clin Infect Dis* 2016.
144. LoBue PA, Moser KS. Use of isoniazid for latent tuberculosis infection in a public health clinic. *Am J Respir Crit Care Med* 2003,**168**:443-447.
145. Jasmer RM, Snyder DC, Chin DP, Hopewell PC, Cuthbert SS, Antonio Paz E*, et al.* Twelve months of isoniazid compared with four months of isoniazid and rifampin for persons with radiographic evidence of previous tuberculosis: an outcome and cost-effectiveness analysis. *Am J Respir Crit Care Med* 2000,**162**:1648-1652.
146. Hermans SM, Grant AD, Chihota V, Lewis JJ, Vynnycky E, Churchyard GJ*, et al.* The timing of tuberculosis after isoniazid preventive therapy among gold miners in South Africa: a prospective cohort study. *BMC Med* 2016,**14**:45.
147. Den Boon S, Matteelli A, Ford N, Getahun H. Continuous isoniazid for the treatment of latent tuberculosis infection in people living with HIV. *Aids* 2016,**30**:797-801.
148. Samandari T, Agizew TB, Nyirenda S, Tedla Z, Sibanda T, Mosimaneotsile B*, et al.* Tuberculosis incidence after 36 months' isoniazid prophylaxis in HIV-infected adults in Botswana: a posttrial observational analysis. *Aids* 2015,**29**:351-359.
149. Martinson NA, Barnes GL, Moulton LH, Msandiwa R, Hausler H, Ram M*, et al.* New regimens to prevent tuberculosis in adults with HIV infection. *N Engl J Med* 2011,**365**:11-20.
150. Golub JE, Cohn S, Saraceni V, Cavalcante SC, Pacheco AG, Moulton LH*, et al.* Long-term protection from isoniazid preventive therapy for tuberculosis in HIV-infected patients in a medium-burden tuberculosis setting: the TB/HIV in Rio (THRio) study. *Clin Infect Dis* 2015,**60**:639-645.

151. Sumner T, Houben RM, Rangaka MX, Maartens G, Boulle A, Wilkinson RJ*, et al.* Post-treatment effect of isoniazid preventive therapy on tuberculosis incidence in HIV-infected individuals on antiretroviral therapy. *Aids* 2016,**30**:1279-1286.
152. Leung CC, Rieder HL, Lange C, Yew WW. Treatment of latent infection with Mycobacterium tuberculosis: update 2010. *Eur Respir J* 2011,**37**:690-711.
153. Fox W, Ellard GA, Mitchison DA. Studies on the treatment of tuberculosis undertaken by the British Medical Research Council tuberculosis units, 1946-1986, with relevant subsequent publications. *Int J Tuberc Lung Dis* 1999,**3**:S231-279.
154. Ford CB, Lin PL, Chase MR, Shah RR, Iartchouk O, Galagan J*, et al.* Use of whole genome sequencing to estimate the mutation rate of Mycobacterium tuberculosis during latent infection. *Nat Genet* 2011,**43**:482-486.
155. Stagg HR, Zenner D, Harris RJ, Munoz L, Lipman MC, Abubakar I. Treatment of latent tuberculosis infection: a network meta-analysis. *Ann Intern Med* 2014,**161**:419-428.
156. Johnson JL, Okwera A, Hom DL, Mayanja H, Mutuluuza Kityo C, Nsubuga P*, et al.* Duration of efficacy of treatment of latent tuberculosis infection in HIV-infected adults. *Aids* 2001,**15**:2137-2147.
157. Houben RM, Sumner T, Grant AD, White RG. Ability of preventive therapy to cure latent Mycobacterium tuberculosis infection in HIV-infected individuals in high-burden settings. *Proc Natl Acad Sci U S A* 2014,**111**:5325-5330.
158. Sterling TR, Villarino ME, Borisov AS, Shang N, Gordin F, Bliven-Sizemore E*, et al.* Three months of rifapentine and isoniazid for latent tuberculosis infection. *N Engl J Med* 2011,**365**:2155-2166.
159. Shepardson D, Marks SM, Chesson H, Kerrigan A, Holland DP, Scott N*, et al.* Cost-effectiveness of a 12-dose regimen for treating latent tuberculous infection in the United States. *Int J Tuberc Lung Dis* 2013,**17**:1531-1537.
160. Seddon JA, Hesseling AC, Finlayson H, Fielding K, Cox H, Hughes J*, et al.* Preventive therapy for child contacts of multidrug-resistant tuberculosis: a prospective cohort study. *Clin Infect Dis* 2013,**57**:1676-1684.
161. Bamrah S, Brostrom R, Dorina F, Setik L, Song R, Kawamura LM*, et al.* Treatment for LTBI in contacts of MDR-TB patients, Federated States of Micronesia, 2009-2012. *Int J Tuberc Lung Dis* 2014,**18**:912-918.
162. Esmail H, Barry CE, 3rd, Wilkinson RJ. Understanding latent tuberculosis: the key to improved diagnostic and novel treatment strategies. *Drug Discov Today* 2012,**17**:514-521.
163. Zumla AI, Gillespie SH, Hoelscher M, Philips PP, Cole ST, Abubakar I*, et al.* New antituberculosis drugs, regimens, and adjunct therapies: needs, advances, and future prospects. *Lancet Infect Dis* 2014,**14**:327-340.
164. Williams K, Minkowski A, Amoabeng O, Peloquin CA, Taylor D, Andries K*, et al.* Sterilizing activities of novel combinations lacking first- and second-line drugs in a murine model of tuberculosis. *Antimicrob Agents Chemother* 2012,**56**:3114-3120.
165. Grosset JH, Singer TG, Bishai WR. New drugs for the treatment of tuberculosis: hope and reality. *Int J Tuberc Lung Dis* 2012,**16**:1005-1014.
166. Andersen P. Vaccine strategies against latent tuberculosis infection. *Trends Microbiol* 2007,**15**:7-13.
167. Aagaard C, Hoang T, Dietrich J, Cardona PJ, Izzo A, Dolganov G*, et al.* A multistage tuberculosis vaccine that confers efficient protection before and after exposure. *Nat Med* 2011,**17**:189-194.

168. Vilaplana C, Montane E, Pinto S, Barriocanal AM, Domenech G, Torres F*, et al.* Double-blind, randomized, placebo-controlled Phase I Clinical Trial of the therapeutical antituberculous vaccine RUTI. *Vaccine* 2010,**28**:1106-1116.
169. O'Shea MK, McShane H. A review of clinical models for the evaluation of human TB vaccines. *Hum Vaccin Immunother* 2016:1-11.
170. Lin PL, Flynn JL. Understanding latent tuberculosis: a moving target. *J Immunol* 2010,**185**:15-22.
171. Coussens AK, Wilkinson RJ, Hanifa Y, Nikolayevskyy V, Elkington PT, Islam K*, et al.* Vitamin D accelerates resolution of inflammatory responses during tuberculosis treatment. *Proc Natl Acad Sci U S A* 2012,**109**:15449-15454.
172. Martineau AR. Old wine in new bottles: vitamin D in the treatment and prevention of tuberculosis. *Proc Nutr Soc* 2012,**71**:84-89.
173. Martineau AR, Nhamoyebonde S, Oni T, Rangaka MX, Marais S, Bangani N*, et al.* Reciprocal seasonal variation in vitamin D status and tuberculosis notifications in Cape Town, South Africa. *Proc Natl Acad Sci U S A* 2011,**108**:19013-19017.
174. Oei W, Nishiura H. The relationship between tuberculosis and influenza death during the influenza (H1N1) pandemic from 1918-19. *Comput Math Methods Med* 2012,**2012**:124861.
175. Redford PS, Mayer-Barber KD, McNab FW, Stavropoulos E, Wack A, Sher A*, et al.* Influenza A virus impairs control of Mycobacterium tuberculosis coinfection through a type I interferon receptor-dependent pathway. *J Infect Dis* 2014,**209**:270-274.
176. Wilkinson RJ, Llewelyn M, Toossi Z, Patel P, Pasvol G, Lalvani A*, et al.* Influence of vitamin D deficiency and vitamin D receptor polymorphisms on tuberculosis among Gujarati Asians in west London: a case-control study. *Lancet* 2000,**355**:618-621.
177. Joshi R, Reingold AL, Menzies D, Pai M. Tuberculosis among health-care workers in low- and middle-income countries: a systematic review. *PLoS Med* 2006,**3**:e494.
178. Marks SM, Taylor Z, Qualls NL, Shrestha-Kuwahara RJ, Wilce MA, Nguyen CH. Outcomes of contact investigations of infectious tuberculosis patients. *Am J Respir Crit Care Med* 2000,**162**:2033-2038.
179. Morrison J, Pai M, Hopewell PC. Tuberculosis and latent tuberculosis infection in close contacts of people with pulmonary tuberculosis in low-income and middle-income countries: a systematic review and meta-analysis. *Lancet Infect Dis* 2008,**8**:359-368.
180. Stead WW. Management of health care workers after inadvertent exposure to tuberculosis: a guide for the use of preventive therapy. *Ann Intern Med* 1995,**122**:906-912.
181. Clay H, Volkman HE, Ramakrishnan L. Tumor necrosis factor signaling mediates resistance to mycobacteria by inhibiting bacterial growth and macrophage death. *Immunity* 2008,**29**:283-294.
182. Martineau AR, Newton SM, Wilkinson KA, Kampmann B, Hall BM, Nawroly N*, et al.* Neutrophil-mediated innate immune resistance to mycobacteria. *J Clin Invest* 2007,**117**:1988-1994.
183. Sia JK, Georgieva M, Rengarajan J. Innate Immune Defenses in Human Tuberculosis: An Overview of the Interactions between Mycobacterium tuberculosis and Innate Immune Cells. *J Immunol Res* 2015,**2015**:747543.
184. Cobat A, Barrera LF, Henao H, Arbelaez P, Abel L, Garcia LF*, et al.* Tuberculin skin test reactivity is dependent on host genetic background in Colombian tuberculosis household contacts. *Clin Infect Dis* 2012,**54**:968-971.

185. Cobat A, Gallant CJ, Simkin L, Black GF, Stanley K, Hughes J*, et al.* High heritability of antimycobacterial immunity in an area of hyperendemicity for tuberculosis disease. *J Infect Dis* 2010,**201**:15-19.
186. Cobat A, Gallant CJ, Simkin L, Black GF, Stanley K, Hughes J*, et al.* Two loci control tuberculin skin test reactivity in an area hyperendemic for tuberculosis. *J Exp Med* 2009,**206**:2583-2591.
187. Cobat A, Poirier C, Hoal E, Boland-Auge A, de La Rocque F, Corrard F*, et al.* Tuberculin skin test negativity is under tight genetic control of chromosomal region 11p14-15 in settings with different tuberculosis endemicities. *J Infect Dis* 2015,**211**:317-321.
188. Fennelly KP, Jones-Lopez EC, Ayakaka I, Kim S, Menyha H, Kirenga B*, et al.* Variability of infectious aerosols produced during coughing by patients with pulmonary tuberculosis. *Am J Respir Crit Care Med* 2012,**186**:450-457.
189. Anibarro L, Trigo M, Villaverde C, Pena A, Gonzalez-Fernandez A. Tuberculin skin test and interferon-gamma release assay show better correlation after the tuberculin 'window period' in tuberculosis contacts. *Scand J Infect Dis* 2011,**43**:424-429.
190. Lee SW, Oh DK, Lee SH, Kang HY, Lee CT, Yim JJ. Time interval to conversion of interferon-gamma release assay after exposure to tuberculosis. *Eur Respir J* 2011,**37**:1447-1452.
191. Ribeiro-Rodrigues R, Kim S, Coelho da Silva FD, Uzelac A, Collins L, Palaci M*, et al.* Discordance of tuberculin skin test and interferon gamma release assay in recently exposed household contacts of pulmonary TB cases in Brazil. *PLoS One* 2014,**9**:e96564.
192. Shah M, Kasambira TS, Adrian PV, Madhi SA, Martinson NA, Dorman SE. Longitudinal analysis of QuantiFERON-TB Gold In-Tube in children with adult household tuberculosis contact in South Africa: a prospective cohort study. *PLoS One* 2011,**6**:e26787.
193. Anderson ST, Williams AJ, Brown JR, Newton SM, Simsova M, Nicol MP*, et al.* Transmission of Mycobacterium tuberculosis undetected by tuberculin skin testing. *Am J Respir Crit Care Med* 2006,**173**:1038-1042.
194. Ewer K, Millington KA, Deeks JJ, Alvarez L, Bryant G, Lalvani A. Dynamic antigen-specific T-cell responses after point-source exposure to Mycobacterium tuberculosis. *Am J Respir Crit Care Med* 2006,**174**:831-839.
195. Rangaka MX, Wilkinson KA, Seldon R, Van Cutsem G, Meintjes GA, Morroni C*, et al.* Effect of HIV-1 infection on T-Cell-based and skin test detection of tuberculosis infection. *Am J Respir Crit Care Med* 2007,**175**:514-520.
196. Dorman SE, Belknap R, Graviss EA, Reves R, Schluger N, Weinfurter P*, et al.* Interferon-gamma release assays and tuberculin skin testing for diagnosis of latent tuberculosis infection in healthcare workers in the United States. *Am J Respir Crit Care Med* 2014,**189**:77-87.
197. Hill PC, Brookes RH, Fox A, Jackson-Sillah D, Jeffries DJ, Lugos MD*, et al.* Longitudinal assessment of an ELISPOT test for Mycobacterium tuberculosis infection. *PLoS Med* 2007,**4**:e192.
198. Slater ML, Welland G, Pai M, Parsonnet J, Banaei N. Challenges with QuantiFERON-TB Gold assay for large-scale, routine screening of U.S. healthcare workers. *Am J Respir Crit Care Med* 2013,**188**:1005-1010.
199. Zwerling A, Benedetti A, Cojocariu M, McIntosh F, Pietrangelo F, Behr MA*, et al.* Repeat IGRA testing in Canadian health workers: conversions or unexplained variability? *PLoS One* 2013,**8**:e54748.

200. Pai M, Joshi R, Dogra S, Mendiratta DK, Narang P, Kalantri S*, et al.* Serial testing of health care workers for tuberculosis using interferon-gamma assay. *Am J Respir Crit Care Med* 2006,**174**:349-355.
201. Yoshiyama T, Harada N, Higuchi K, Nakajima Y, Ogata H. Estimation of incidence of tuberculosis infection in health-care workers using repeated interferon-gamma assays. *Epidemiol Infect* 2009,**137**:1691-1698.
202. Flynn JL, Chan J, Lin PL. Macrophages and control of granulomatous inflammation in tuberculosis. *Mucosal Immunol* 2011,**4**:271-278.
203. Ramakrishnan L. Revisiting the role of the granuloma in tuberculosis. *Nat Rev Immunol* 2012,**12**:352-366.
204. Egen JG, Rothfuchs AG, Feng CG, Winter N, Sher A, Germain RN. Macrophage and T cell dynamics during the development and disintegration of mycobacterial granulomas. *Immunity* 2008,**28**:271-284.
205. Shaler CR, Horvath CN, Jeyanathan M, Xing Z. Within the Enemy's Camp: contribution of the granuloma to the dissemination, persistence and transmission of Mycobacterium tuberculosis. *Front Immunol* 2013,**4**:30.
206. Capuano SV, 3rd, Croix DA, Pawar S, Zinovik A, Myers A, Lin PL*, et al.* Experimental Mycobacterium tuberculosis infection of cynomolgus macaques closely resembles the various manifestations of human M. tuberculosis infection. *Infect Immun* 2003,**71**:5831-5844.
207. Skoura E, Zumla A, Bomanji J. Imaging in tuberculosis. *Int J Infect Dis* 2015,**32**:87-93.
208. Yang CM, Hsu CH, Lee CM, Wang FC. Intense uptake of [F-18]-fluoro-2 deoxy-D-glucose in active pulmonary tuberculosis. *Ann Nucl Med* 2003,**17**:407-410.
209. Hara T, Kosaka N, Suzuki T, Kudo K, Niino H. Uptake rates of 18F-fluorodeoxyglucose and 11C-choline in lung cancer and pulmonary tuberculosis: a positron emission tomography study. *Chest* 2003,**124**:893-901.
210. Goo JM, Im JG, Do KH, Yeo JS, Seo JB, Kim HY*, et al.* Pulmonary tuberculoma evaluated by means of FDG PET: findings in 10 cases. *Radiology* 2000,**216**:117-121.
211. Park IN, Ryu JS, Shim TS. Evaluation of therapeutic response of tuberculoma using F-18 FDG positron emission tomography. *Clin Nucl Med* 2008,**33**:1-3.
212. Jeong YJ, Paeng JC, Nam HY, Lee JS, Lee SM, Yoo CG*, et al.* (18)F-FDG positron-emission tomography/computed tomography findings of radiographic lesions suggesting old healed tuberculosis. *J Korean Med Sci* 2014,**29**:386-391.
213. Lin PL, Pawar S, Myers A, Pegu A, Fuhrman C, Reinhart TA*, et al.* Early events in Mycobacterium tuberculosis infection in cynomolgus macaques. *Infect Immun* 2006,**74**:3790-3803.
214. Via LE, Lin PL, Ray SM, Carrillo J, Allen SS, Eum SY*, et al.* Tuberculous granulomas are hypoxic in guinea pigs, rabbits, and nonhuman primates. *Infect Immun* 2008,**76**:2333-2340.
215. Lin PL, Rodgers M, Smith L, Bigbee M, Myers A, Bigbee C*, et al.* Quantitative comparison of active and latent tuberculosis in the cynomolgus macaque model. *Infect Immun* 2009,**77**:4631-4642.
216. Lin PL, Ford CB, Coleman MT, Myers AJ, Gawande R, Ioerger T*, et al.* Sterilization of granulomas is common in active and latent tuberculosis despite within-host variability in bacterial killing. *Nat Med* 2014,**20**:75-79.
217. Loring WW, Melvin I, Vandiviere HM, Willis HS. The death and resurrection of the tubercle bacillus. *Trans Am Clin Climatol Assoc* 1955,**67**:132-138.
218. Feldman WH, Baggenstoss AH. The residual infectivity of the primary complex of tuberculosis. *Am J Pathol* 1938,**14**:473-490.473.

219. Feldman WH, Baggenstoss AH. The occurrence of virulent tubercle bacilli in presumably non-tuberculous lung tissue. *Am J Pathol* 1939,**15**:501-515.
220. Rachman H, Strong M, Ulrichs T, Grode L, Schuchhardt J, Mollenkopf H*, et al.* Unique transcriptome signature of Mycobacterium tuberculosis in pulmonary tuberculosis. *Infect Immun* 2006,**74**:1233-1242.
221. Timm J, Post FA, Bekker LG, Walther GB, Wainwright HC, Manganelli R*, et al.* Differential expression of iron-, carbon-, and oxygen-responsive mycobacterial genes in the lungs of chronically infected mice and tuberculosis patients. *Proc Natl Acad Sci U S A* 2003,**100**:14321-14326.
222. Fenhalls G, Stevens L, Moses L, Bezuidenhout J, Betts JC, Helden Pv P*, et al.* In situ detection of Mycobacterium tuberculosis transcripts in human lung granulomas reveals differential gene expression in necrotic lesions. *Infect Immun* 2002,**70**:6330-6338.
223. Zhang Y. Persistent and dormant tubercle bacilli and latent tuberculosis. *Front Biosci* 2004,**9**:1136-1156.
224. Sherman DR, Voskuil M, Schnappinger D, Liao R, Harrell MI, Schoolnik GK. Regulation of the Mycobacterium tuberculosis hypoxic response gene encoding alpha -crystallin. *Proc Natl Acad Sci U S A* 2001,**98**:7534-7539.
225. Park HD, Guinn KM, Harrell MI, Liao R, Voskuil MI, Tompa M*, et al.* Rv3133c/dosR is a transcription factor that mediates the hypoxic response of Mycobacterium tuberculosis. *Mol Microbiol* 2003,**48**:833-843.
226. Rustad TR, Harrell MI, Liao R, Sherman DR. The enduring hypoxic response of Mycobacterium tuberculosis. *PLoS One* 2008,**3**:e1502.
227. Lin MY, Ottenhoff TH. Not to wake a sleeping giant: new insights into host-pathogen interactions identify new targets for vaccination against latent Mycobacterium tuberculosis infection. *Biol Chem* 2008,**389**:497-511.
228. Black GF, Thiel BA, Ota MO, Parida SK, Adegbola R, Boom WH*, et al.* Immunogenicity of novel DosR regulon-encoded candidate antigens of Mycobacterium tuberculosis in three high-burden populations in Africa. *Clin Vaccine Immunol* 2009,**16**:1203-1212.
229. Demissie A, Leyten EM, Abebe M, Wassie L, Aseffa A, Abate G*, et al.* Recognition of stage-specific mycobacterial antigens differentiates between acute and latent infections with Mycobacterium tuberculosis. *Clin Vaccine Immunol* 2006,**13**:179-186.
230. Geluk A, Lin MY, van Meijgaarden KE, Leyten EM, Franken KL, Ottenhoff TH*, et al.* T-cell recognition of the HspX protein of Mycobacterium tuberculosis correlates with latent M. tuberculosis infection but not with M. bovis BCG vaccination. *Infect Immun* 2007,**75**:2914-2921.
231. Leyten EM, Lin MY, Franken KL, Friggen AH, Prins C, van Meijgaarden KE*, et al.* Human T-cell responses to 25 novel antigens encoded by genes of the dormancy regulon of Mycobacterium tuberculosis. *Microbes Infect* 2006,**8**:2052-2060.
232. Roupie V, Romano M, Zhang L, Korf H, Lin MY, Franken KL*, et al.* Immunogenicity of eight dormancy regulon-encoded proteins of Mycobacterium tuberculosis in DNA-vaccinated and tuberculosis-infected mice. *Infect Immun* 2007,**75**:941-949.
233. Gideon HP, Wilkinson KA, Rustad TR, Oni T, Guio H, Kozak RA*, et al.* Hypoxia induces an immunodominant target of tuberculosis specific T cells absent from common BCG vaccines. *PLoS Pathog* 2010,**6**:e1001237.
234. Wilkinson KA, Stewart GR, Newton SM, Vordermeier HM, Wain JR, Murphy HN*, et al.* Infection biology of a novel alpha-crystallin of Mycobacterium tuberculosis: Acr2. *J Immunol* 2005,**174**:4237-4243.

235. Berry MP, Graham CM, McNab FW, Xu Z, Bloch SA, Oni T*, et al.* An interferon-inducible neutrophil-driven blood transcriptional signature in human tuberculosis. *Nature* 2010,**466**:973-977.
236. Biomarkers and surrogate endpoints: preferred definitions and conceptual framework. *Clin Pharmacol Ther* 2001,**69**:89-95.
237. Weiner J, Maertzdorf J, Kaufmann SH. The dual role of biomarkers for understanding basic principles and devising novel intervention strategies in tuberculosis. *Ann N Y Acad Sci* 2013,**1283**:22-29.
238. Walzl G, Ronacher K, Hanekom W, Scriba TJ, Zumla A. Immunological biomarkers of tuberculosis. *Nat Rev Immunol* 2011,**11**:343-354.
239. Davies PD, Pai M. The diagnosis and misdiagnosis of tuberculosis. *Int J Tuberc Lung Dis* 2008,**12**:1226-1234.
240. Parrish NM, Carroll KC. Role of the clinical mycobacteriology laboratory in diagnosis and management of tuberculosis in low-prevalence settings. *J Clin Microbiol* 2011,**49**:772-776.
241. Swai HF, Mugusi FM, Mbwambo JK. Sputum smear negative pulmonary tuberculosis: sensitivity and specificity of diagnostic algorithm. *BMC Res Notes* 2011,**4**:475.
242. Haas CT, Roe JK, Pollara G, Mehta M, Noursadeghi M. Diagnostic 'omics' for active tuberculosis. *BMC Med* 2016,**14**:37.
243. Lagier JC, Edouard S, Pagnier I, Mediannikov O, Drancourt M, Raoult D. Current and past strategies for bacterial culture in clinical microbiology. *Clin Microbiol Rev* 2015,**28**:208-236.
244. Boehme CC, Saacks S, O'Brien RJ. The changing landscape of diagnostic services for tuberculosis. *Semin Respir Crit Care Med* 2013,**34**:17-31.
245. Dinnes J, Deeks J, Kunst H, Gibson A, Cummins E, Waugh N*, et al.* A systematic review of rapid diagnostic tests for the detection of tuberculosis infection. *Health Technol Assess* 2007,**11**:1-196.
246. O'Shea MK, Koh GC, Munang M, Smith G, Banerjee A, Dedicoat M. Time-to-detection in culture predicts risk of Mycobacterium tuberculosis transmission: a cohort study. *Clin Infect Dis* 2014,**59**:177-185.
247. Barnard M, Gey van Pittius NC, van Helden PD, Bosman M, Coetzee G, Warren RM. The diagnostic performance of the GenoType MTBDRplus version 2 line probe assay is equivalent to that of the Xpert MTB/RIF assay. *J Clin Microbiol* 2012,**50**:3712-3716.
248. Crudu V, Stratan E, Romancenco E, Allerheiligen V, Hillemann A, Moraru N. First evaluation of an improved assay for molecular genetic detection of tuberculosis as well as rifampin and isoniazid resistances. *J Clin Microbiol* 2012,**50**:1264-1269.
249. Blakemore R, Nabeta P, Davidow AL, Vadwai V, Tahirli R, Munsamy V*, et al.* A multisite assessment of the quantitative capabilities of the Xpert MTB/RIF assay. *Am J Respir Crit Care Med* 2011,**184**:1076-1084.
250. Boehme CC, Nabeta P, Hillemann D, Nicol MP, Shenai S, Krapp F*, et al.* Rapid molecular detection of tuberculosis and rifampin resistance. *N Engl J Med* 2010,**363**:1005-1015.
251. Steingart KR, Sohn H, Schiller I, Kloda LA, Boehme CC, Pai M*, et al.* Xpert(R) MTB/RIF assay for pulmonary tuberculosis and rifampicin resistance in adults. *Cochrane Database Syst Rev* 2013,**1**:CD009593.
252. Hesseling AC, Walzl G, Enarson DA, Carroll NM, Duncan K, Lukey PT*, et al.* Baseline sputum time to detection predicts month two culture conversion and relapse in non-HIV-infected patients. *Int J Tuberc Lung Dis* 2010,**14**:560-570.

253. Johnson JL, Hadad DJ, Dietze R, Maciel EL, Sewali B, Gitta P*, et al.* Shortening treatment in adults with noncavitary tuberculosis and 2-month culture conversion. *Am J Respir Crit Care Med* 2009,**180**:558-563.
254. Al-Muhsen S, Casanova JL. The genetic heterogeneity of mendelian susceptibility to mycobacterial diseases. *J Allergy Clin Immunol* 2008,**122**:1043-1051; quiz 1052-1043.
255. Diedrich CR, Flynn JL. HIV-1/mycobacterium tuberculosis coinfection immunology: how does HIV-1 exacerbate tuberculosis? *Infect Immun* 2011,**79**:1407-1417.
256. Flynn JL, Chan J, Triebold KJ, Dalton DK, Stewart TA, Bloom BR. An essential role for interferon gamma in resistance to Mycobacterium tuberculosis infection. *J Exp Med* 1993,**178**:2249-2254.
257. Bhatt K, Verma S, Ellner JJ, Salgame P. Quest for correlates of protection against tuberculosis. *Clin Vaccine Immunol* 2015,**22**:258-266.
258. Nakaya HI, Pulendran B. Vaccinology in the era of high-throughput biology. *Philos Trans R Soc Lond B Biol Sci* 2015,**370**.
259. Elias D, Akuffo H, Britton S. PPD induced in vitro interferon gamma production is not a reliable correlate of protection against Mycobacterium tuberculosis. *Trans R Soc Trop Med Hyg* 2005,**99**:363-368.
260. Kagina BM, Abel B, Scriba TJ, Hughes EJ, Keyser A, Soares A*, et al.* Specific T cell frequency and cytokine expression profile do not correlate with protection against tuberculosis after bacillus Calmette-Guerin vaccination of newborns. *Am J Respir Crit Care Med* 2010,**182**:1073-1079.
261. Mittrucker HW, Steinhoff U, Kohler A, Krause M, Lazar D, Mex P*, et al.* Poor correlation between BCG vaccination-induced T cell responses and protection against tuberculosis. *Proc Natl Acad Sci U S A* 2007,**104**:12434-12439.
262. Fletcher HA, Snowden MA, Landry B, Rida W, Satti I, Harris SA*, et al.* T-cell activation is an immune correlate of risk in BCG vaccinated infants. *Nat Commun* 2016,**7**:11290.
263. Ottenhoff TH, Ellner JJ, Kaufmann SH. Ten challenges for TB biomarkers. *Tuberculosis (Edinb)* 2012,**92 Suppl 1**:S17-20.
264. Wallis RS, Kim P, Cole S, Hanna D, Andrade BB, Maeurer M*, et al.* Tuberculosis biomarkers discovery: developments, needs, and challenges. *Lancet Infect Dis* 2013,**13**:362-372.
265. Weiner J, 3rd, Kaufmann SH. Recent advances towards tuberculosis control: vaccines and biomarkers. *J Intern Med* 2014,**275**:467-480.
266. Zhu J, He F, Wang J, Yu J. Modeling transcriptome based on transcript-sampling data. *PLoS One* 2008,**3**:e1659.
267. Jacobsen M, Mattow J, Repsilber D, Kaufmann SH. Novel strategies to identify biomarkers in tuberculosis. *Biol Chem* 2008,**389**:487-495.
268. Jacobsen M, Repsilber D, Gutschmidt A, Neher A, Feldmann K, Mollenkopf HJ*, et al.* Candidate biomarkers for discrimination between infection and disease caused by Mycobacterium tuberculosis. *J Mol Med (Berl)* 2007,**85**:613-621.
269. Lesho E, Forestiero FJ, Hirata MH, Hirata RD, Cecon L, Melo FF*, et al.* Transcriptional responses of host peripheral blood cells to tuberculosis infection. *Tuberculosis (Edinb)* 2011,**91**:390-399.
270. Lu C, Wu J, Wang H, Wang S, Diao N, Wang F*, et al.* Novel biomarkers distinguishing active tuberculosis from latent infection identified by gene expression profile of peripheral blood mononuclear cells. *PLoS One* 2011,**6**:e24290.

271. Maertzdorf J, Ota M, Repsilber D, Mollenkopf HJ, Weiner J, Hill PC*, et al.* Functional correlations of pathogenesis-driven gene expression signatures in tuberculosis. *PLoS One* 2011,**6**:e26938.
272. Maertzdorf J, Repsilber D, Parida SK, Stanley K, Roberts T, Black G*, et al.* Human gene expression profiles of susceptibility and resistance in tuberculosis. *Genes Immun* 2011,**12**:15-22.
273. Maertzdorf J, Weiner J, 3rd, Mollenkopf HJ, Bauer T, Prasse A, Muller-Quernheim J*, et al.* Common patterns and disease-related signatures in tuberculosis and sarcoidosis. *Proc Natl Acad Sci U S A* 2012,**109**:7853-7858.
274. Mistry R, Cliff JM, Clayton CL, Beyers N, Mohamed YS, Wilson PA*, et al.* Gene-expression patterns in whole blood identify subjects at risk for recurrent tuberculosis. *J Infect Dis* 2007,**195**:357-365.
275. Sutherland JS, Loxton AG, Haks MC, Kassa D, Ambrose L, Lee JS*, et al.* Differential gene expression of activating Fcgamma receptor classifies active tuberculosis regardless of human immunodeficiency virus status or ethnicity. *Clin Microbiol Infect* 2014,**20**:O230-238.
276. Kaforou M, Wright VJ, Oni T, French N, Anderson ST, Bangani N*, et al.* Detection of tuberculosis in HIV-infected and -uninfected African adults using whole blood RNA expression signatures: a case-control study. *PLoS Med* 2013,**10**:e1001538.
277. Cliff JM, Lee JS, Constantinou N, Cho JE, Clark TG, Ronacher K*, et al.* Distinct phases of blood gene expression pattern through tuberculosis treatment reflect modulation of the humoral immune response. *J Infect Dis* 2013,**207**:18-29.
278. Bloom CI, Graham CM, Berry MP, Wilkinson KA, Oni T, Rozakeas F*, et al.* Detectable changes in the blood transcriptome are present after two weeks of antituberculosis therapy. *PLoS One* 2012,**7**:e46191.
279. Joosten SA, Fletcher HA, Ottenhoff TH. A helicopter perspective on TB biomarkers: pathway and process based analysis of gene expression data provides new insight into TB pathogenesis. *PLoS One* 2013,**8**:e73230.
280. Blankley S, Graham CM, Levin J, Turner J, Berry MP, Bloom CI*, et al.* A 380-gene meta-signature of active tuberculosis compared with healthy controls. *Eur Respir J* 2016,**47**:1873-1876.
281. Maertzdorf J, McEwen G, Weiner J, 3rd, Tian S, Lader E, Schriek U*, et al.* Concise gene signature for point-of-care classification of tuberculosis. *EMBO Mol Med* 2015,**8**:86-95.
282. Maji A, Misra R, Kumar Mondal A, Kumar D, Bajaj D, Singhal A*, et al.* Expression profiling of lymph nodes in tuberculosis patients reveal inflammatory milieu at site of infection. *Sci Rep* 2015,**5**:15214.
283. Subbian S, Tsenova L, Kim MJ, Wainwright HC, Visser A, Bandyopadhyay N*, et al.* Lesion-Specific Immune Response in Granulomas of Patients with Pulmonary Tuberculosis: A Pilot Study. *PLoS One* 2015,**10**:e0132249.
284. Gideon HP, Phuah J, Myers AJ, Bryson BD, Rodgers MA, Coleman MT*, et al.* Variability in tuberculosis granuloma T cell responses exists, but a balance of pro- and anti-inflammatory cytokines is associated with sterilization. *PLoS Pathog* 2015,**11**:e1004603.
285. Koth LL, Solberg OD, Peng JC, Bhakta NR, Nguyen CP, Woodruff PG. Sarcoidosis blood transcriptome reflects lung inflammation and overlaps with tuberculosis. *Am J Respir Crit Care Med* 2011,**184**:1153-1163.
286. Anderson ST, Kaforou M, Brent AJ, Wright VJ, Banwell CM, Chagaluka G*, et al.* Diagnosis of childhood tuberculosis and host RNA expression in Africa. *N Engl J Med* 2014,**370**:1712-1723.

287. Walter ND, Miller MA, Vasquez J, Weiner M, Chapman A, Engle M*, et al.* Blood Transcriptional Biomarkers for Active Tuberculosis among Patients in the United States: a Case-Control Study with Systematic Cross-Classifier Evaluation. *J Clin Microbiol* 2016,**54**:274-282.
288. Bloom CI, Graham CM, Berry MP, Rozakeas F, Redford PS, Wang Y*, et al.* Transcriptional blood signatures distinguish pulmonary tuberculosis, pulmonary sarcoidosis, pneumonias and lung cancers. *PLoS One* 2013,**8**:e70630.
289. Zak DE, Penn-Nicholson A, Scriba TJ, Thompson E, Suliman S, Amon LM*, et al.* A blood RNA signature for tuberculosis disease risk: a prospective cohort study. *Lancet* 2016.
290. Sloot R, Schim van der Loeff MF, van Zwet EW, Haks MC, Keizer ST, Scholing M*, et al.* Biomarkers Can Identify Pulmonary Tuberculosis in HIV-infected Drug Users Months Prior to Clinical Diagnosis. *EBioMedicine* 2015,**2**:172-179.
291. Fu Y, Yi Z, Wu X, Li J, Xu F. Circulating microRNAs in patients with active pulmonary tuberculosis. *J Clin Microbiol* 2011,**49**:4246-4251.
292. Iannaccone M, Dorhoi A, Kaufmann SH. Host-directed therapy of tuberculosis: what is in it for microRNA? *Expert Opin Ther Targets* 2014,**18**:491-494.
293. Liu Y, Wang X, Jiang J, Cao Z, Yang B, Cheng X. Modulation of T cell cytokine production by miR-144* with elevated expression in patients with pulmonary tuberculosis. *Mol Immunol* 2011,**48**:1084-1090.
294. Wang C, Yang S, Sun G, Tang X, Lu S, Neyrolles O*, et al.* Comparative miRNA expression profiles in individuals with latent and active tuberculosis. *PLoS One* 2011,**6**:e25832.
295. Wang Z, Gerstein M, Snyder M. RNA-Seq: a revolutionary tool for transcriptomics. *Nat Rev Genet* 2009,**10**:57-63.
296. Wu J, Lu C, Diao N, Zhang S, Wang S, Wang F*, et al.* Analysis of microRNA expression profiling identifies miR-155 and miR-155* as potential diagnostic markers for active tuberculosis: a preliminary study. *Hum Immunol* 2012,**73**:31-37.
297. Wu LS, Lee SW, Huang KY, Lee TY, Hsu PW, Weng JT. Systematic expression profiling analysis identifies specific microRNA-gene interactions that may differentiate between active and latent tuberculosis infection. *Biomed Res Int* 2014,**2014**:895179.
298. Agranoff D, Fernandez-Reyes D, Papadopoulos MC, Rojas SA, Herbster M, Loosemore A*, et al.* Identification of diagnostic markers for tuberculosis by proteomic fingerprinting of serum. *Lancet* 2006,**368**:1012-1021.
299. Deng C, Lin M, Hu C, Li Y, Gao Y, Cheng X*, et al.* Establishing a serologic decision tree model of extrapulmonary tuberculosis by MALDI-TOF MS analysis. *Diagn Microbiol Infect Dis* 2011,**71**:144-150.
300. Kunnath-Velayudhan S, Salamon H, Wang HY, Davidow AL, Molina DM, Huynh VT*, et al.* Dynamic antibody responses to the Mycobacterium tuberculosis proteome. *Proc Natl Acad Sci U S A* 2010,**107**:14703-14708.
301. Liu Q, Chen X, Hu C, Zhang R, Yue J, Wu G*, et al.* Serum protein profiling of smear-positive and smear-negative pulmonary tuberculosis using SELDI-TOF mass spectrometry. *Lung* 2010,**188**:15-23.
302. Sartain MJ, Slayden RA, Singh KK, Laal S, Belisle JT. Disease state differentiation and identification of tuberculosis biomarkers via native antigen array profiling. *Mol Cell Proteomics* 2006,**5**:2102-2113.
303. De Groote MA, Nahid P, Jarlsberg L, Johnson JL, Weiner M, Muzanyi G*, et al.* Elucidating novel serum biomarkers associated with pulmonary tuberculosis treatment. *PLoS One* 2013,**8**:e61002.

304. Achkar JM, Cortes L, Croteau P, Yanofsky C, Mentinova M, Rajotte I*, et al.* Host Protein Biomarkers Identify Active Tuberculosis in HIV Uninfected and Co-infected Individuals. *EBioMedicine* 2015,**2**:1160-1168.
305. Nahid P, Bliven-Sizemore E, Jarlsberg LG, De Groote MA, Johnson JL, Muzanyi G*, et al.* Aptamer-based proteomic signature of intensive phase treatment response in pulmonary tuberculosis. *Tuberculosis (Edinb)* 2014,**94**:187-196.
306. Ou Q, Liu X, Cheng X. An iTRAQ approach to quantitative proteome analysis of cerebrospinal fluid from patients with tuberculous meningitis. *Biosci Trends* 2013,**7**:186-192.
307. Song SH, Han M, Choi YS, Dan KS, Yang MG, Song J*, et al.* Proteomic profiling of serum from patients with tuberculosis. *Ann Lab Med* 2014,**34**:345-353.
308. Tanaka T, Sakurada S, Kano K, Takahashi E, Yasuda K, Hirano H*, et al.* Identification of tuberculosis-associated proteins in whole blood supernatant. *BMC Infect Dis* 2011,**11**:71.
309. Wang C, Wei LL, Shi LY, Pan ZF, Yu XM, Li TY*, et al.* Screening and identification of five serum proteins as novel potential biomarkers for cured pulmonary tuberculosis. *Sci Rep* 2015,**5**:15615.
310. Xu DD, Deng DF, Li X, Wei LL, Li YY, Yang XY*, et al.* Discovery and identification of serum potential biomarkers for pulmonary tuberculosis using iTRAQ-coupled two-dimensional LC-MS/MS. *Proteomics* 2014,**14**:322-331.
311. Zhang X, Liu F, Li Q, Jia H, Pan L, Xing A*, et al.* A proteomics approach to the identification of plasma biomarkers for latent tuberculosis infection. *Diagn Microbiol Infect Dis* 2014,**79**:432-437.
312. Liu J, Jiang T, Jiang F, Xu D, Wei L, Wang C*, et al.* Comparative proteomic analysis of serum diagnosis patterns of sputum smear-positive pulmonary tuberculosis based on magnetic bead separation and mass spectrometry analysis. *Int J Clin Exp Med* 2015,**8**:2077-2085.
313. Liu J, Jiang T, Wei L, Yang X, Wang C, Zhang X*, et al.* The discovery and identification of a candidate proteomic biomarker of active tuberculosis. *BMC Infect Dis* 2013,**13**:506.
314. Liu JY, Jin L, Zhao MY, Zhang X, Liu CB, Zhang YX*, et al.* New serum biomarkers for detection of tuberculosis using surface-enhanced laser desorption/ionization time-of-flight mass spectrometry. *Clin Chem Lab Med* 2011,**49**:1727-1733.
315. Sandhu G, Battaglia F, Ely BK, Athanasakis D, Montoya R, Valencia T*, et al.* Discriminating active from latent tuberculosis in patients presenting to community clinics. *PLoS One* 2012,**7**:e38080.
316. Xu D, Li Y, Li X, Wei LL, Pan Z, Jiang TT*, et al.* Serum protein S100A9, SOD3, and MMP9 as new diagnostic biomarkers for pulmonary tuberculosis by iTRAQ-coupled two-dimensional LC-MS/MS. *Proteomics* 2015,**15**:58-67.
317. Zhang J, Wu X, Shi L, Liang Y, Xie Z, Yang Y*, et al.* Diagnostic serum proteomic analysis in patients with active tuberculosis. *Clin Chim Acta* 2012,**413**:883-887.
318. Al-Tarawneh SK, Border MB, Dibble CF, Bencharit S. Defining salivary biomarkers using mass spectrometry-based proteomics: a systematic review. *OMICS* 2011,**15**:353-361.
319. Kaddurah-Daouk R, Kristal BS, Weinshilboum RM. Metabolomics: a global biochemical approach to drug response and disease. *Annu Rev Pharmacol Toxicol* 2008,**48**:653-683.
320. Nanda T, Das M, Tripathy K, Ravi Teja Y. Metabolomics: The Future of Systems Biology. *J Comput Sci Syst Biol* 2011,**S13**.
321. Griffin JL, Shockcor JP. Metabolic profiles of cancer cells. *Nat Rev Cancer* 2004,**4**:551-561.

322. Sabatine MS, Liu E, Morrow DA, Heller E, McCarroll R, Wiegand R, *et al.* Metabolomic identification of novel biomarkers of myocardial ischemia. *Circulation* 2005,**112**:3868-3875.
323. Wang TJ, Larson MG, Vasan RS, Cheng S, Rhee EP, McCabe E, *et al.* Metabolite profiles and the risk of developing diabetes. *Nat Med* 2011,**17**:448-453.
324. Banday KM, Pasikanti KK, Chan EC, Singla R, Rao KV, Chauhan VS, *et al.* Use of urine volatile organic compounds to discriminate tuberculosis patients from healthy subjects. *Anal Chem* 2011,**83**:5526-5534.
325. Mahapatra S, Hess AM, Johnson JL, Eisenach KD, DeGroote MA, Gitta P, *et al.* A metabolic biosignature of early response to anti-tuberculosis treatment. *BMC Infect Dis* 2014,**14**:53.
326. Phillips M, Basa-Dalay V, Bothamley G, Cataneo RN, Lam PK, Natividad MP, *et al.* Breath biomarkers of active pulmonary tuberculosis. *Tuberculosis (Edinb)* 2010,**90**:145-151.
327. Weiner J, 3rd, Parida SK, Maertzdorf J, Black GF, Repsilber D, Telaar A, *et al.* Biomarkers of inflammation, immunosuppression and stress with active disease are revealed by metabolomic profiling of tuberculosis patients. *PLoS One* 2012,**7**:e40221.
328. Mason S, van Furth AM, Mienie LJ, Engelke UF, Wevers RA, Solomons R, *et al.* A hypothetical astrocyte-microglia lactate shuttle derived from a H NMR metabolomics analysis of cerebrospinal fluid from a cohort of South African children with tuberculous meningitis. *Metabolomics* 2015,**11**:822-837.
329. Tientcheu LD, Maertzdorf J, Weiner J, Adetifa IM, Mollenkopf HJ, Sutherland JS, *et al.* Differential transcriptomic and metabolic profiles of M. africanum- and M. tuberculosis-infected patients after, but not before, drug treatment. *Genes Immun* 2015,**16**:347-355.
330. Frediani JK, Jones DP, Tukvadze N, Uppal K, Sanikidze E, Kipiani M, *et al.* Plasma metabolomics in human pulmonary tuberculosis disease: a pilot study. *PLoS One* 2014,**9**:e108854.
331. McShane LM, Polley MY. Development of omics-based clinical tests for prognosis and therapy selection: the challenge of achieving statistical robustness and clinical utility. *Clin Trials* 2013,**10**:653-665.
332. Rodgers JL, Nicewander WA, Toothaker L. Linearly independent, orthogonal, and uncorrelated variables. *Am Stat* 1984,**38**:133-134.
333. Musselwhite LW, Andrade BB, Ellenberg SS, Tierney A, Belaunzaran-Zamudio PF, Rupert A, *et al.* Vitamin D, d-dimer, Interferon gamma, and sCD14 Levels are Independently Associated with Immune Reconstitution Inflammatory Syndrome: A Prospective, International Study. *EBioMedicine* 2016,**4**:115-123.
334. Furman D, Jojic V, Kidd B, Shen-Orr S, Price J, Jarrell J, *et al.* Apoptosis and other immune biomarkers predict influenza vaccine responsiveness. *Mol Syst Biol* 2013,**9**:659.
335. Gibot S, Bene MC, Noel R, Massin F, Guy J, Cravoisy A, *et al.* Combination biomarkers to diagnose sepsis in the critically ill patient. *Am J Respir Crit Care Med* 2012,**186**:65-71.
336. Weiner J, 3rd, Kaufmann SH, Maertzdorf J. High-throughput data analysis and data integration for vaccine trials. *Vaccine* 2015.
337. Maertzdorf J, Weiner J, 3rd, Kaufmann SH. Enabling biomarkers for tuberculosis control. *Int J Tuberc Lung Dis* 2012,**16**:1140-1148.
338. Chaussabel D, Quinn C, Shen J, Patel P, Glaser C, Baldwin N, *et al.* A modular analysis framework for blood genomics studies: application to systemic lupus erythematosus. *Immunity* 2008,**29**:150-164.

339. Banchereau R, Jordan-Villegas A, Ardura M, Mejias A, Baldwin N, Xu H*, et al.* Host immune transcriptional profiles reflect the variability in clinical disease manifestations in patients with Staphylococcus aureus infections. *PLoS One* 2012,**7**:e34390.
340. Chiche L, Jourde-Chiche N, Whalen E, Presnell S, Gersuk V, Dang K*, et al.* Modular transcriptional repertoire analyses of adults with systemic lupus erythematosus reveal distinct type I and type II interferon signatures. *Arthritis Rheumatol* 2014,**66**:1583-1595.
341. Youmans GP. Mechanisms of immunity in tuberculosis. *Pathobiol Annu* 1979,**9**:137-162.
342. Crowle AJ, May M. Preliminary demonstration of human tuberculoimmunity in vitro. *Infect Immun* 1981,**31**:453-464.
343. Crowle AJ, Ross EJ, May MH. Inhibition by 1,25(OH)2-vitamin D3 of the multiplication of virulent tubercle bacilli in cultured human macrophages. *Infect Immun* 1987,**55**:2945-2950.
344. Rook GA, Steele J, Fraher L, Barker S, Karmali R, O'Riordan J*, et al.* Vitamin D3, gamma interferon, and control of proliferation of Mycobacterium tuberculosis by human monocytes. *Immunology* 1986,**57**:159-163.
345. Steele J, Flint KC, Pozniak AL, Hudspith B, Johnson MM, Rook GA. Inhibition of virulent Mycobacterium tuberculosis by murine peritoneal macrophages and human alveolar lavage cells: the effects of lymphokines and recombinant gamma interferon. *Tubercle* 1986,**67**:289-294.
346. Cheng SH, Walker L, Poole J, Aber VR, Walker KB, Mitchison DA*, et al.* Demonstration of increased anti-mycobacterial activity in peripheral blood monocytes after BCG vaccination in British school children. *Clin Exp Immunol* 1988,**74**:20-25.
347. Cheng SH, Walker KB, Lowrie DB, Mitchison DA, Swamy R, Datta M*, et al.* Monocyte antimycobacterial activity before and after Mycobacterium bovis BCG vaccination in Chingleput, India, and London, United Kingdom. *Infect Immun* 1993,**61**:4501-4503.
348. Silver RF, Li Q, Boom WH, Ellner JJ. Lymphocyte-dependent inhibition of growth of virulent Mycobacterium tuberculosis H37Rv within human monocytes: requirement for CD4+ T cells in purified protein derivative-positive, but not in purified protein derivative-negative subjects. *J Immunol* 1998,**160**:2408-2417.
349. Hoft DF, Worku S, Kampmann B, Whalen CC, Ellner JJ, Hirsch CS*, et al.* Investigation of the relationships between immune-mediated inhibition of mycobacterial growth and other potential surrogate markers of protective Mycobacterium tuberculosis immunity. *J Infect Dis* 2002,**186**:1448-1457.
350. Worku S, Hoft DF. In vitro measurement of protective mycobacterial immunity: antigen-specific expansion of T cells capable of inhibiting intracellular growth of bacille Calmette-Guerin. *Clin Infect Dis* 2000,**30 Suppl 3**:S257-261.
351. Kampmann B, Gaora PO, Snewin VA, Gares MP, Young DB, Levin M. Evaluation of human antimycobacterial immunity using recombinant reporter mycobacteria. *J Infect Dis* 2000,**182**:895-901.
352. Kampmann B, Tena GN, Mzazi S, Eley B, Young DB, Levin M. Novel human in vitro system for evaluating antimycobacterial vaccines. *Infect Immun* 2004,**72**:6401-6407.
353. Tena GN, Young DB, Eley B, Henderson H, Nicol MP, Levin M*, et al.* Failure to control growth of mycobacteria in blood from children infected with human immunodeficiency virus and its relationship to T cell function. *J Infect Dis* 2003,**187**:1544-1551.

354. Burl S, Holder BS, Lo BK, Kampmann B. Optimisation of a functional mycobacterial growth-inhibition assay to improve its suitability for infant TB vaccine studies. *J Immunol Methods* 2013,**394**:121-124.
355. Newton S, Martineau A, Kampmann B. A functional whole blood assay to measure viability of mycobacteria, using reporter-gene tagged BCG or M.Tb (BCGlux/M.Tb lux). *J Vis Exp* 2011.
356. Wallis RS, Palaci M, Vinhas S, Hise AG, Ribeiro FC, Landen K*, et al.* A whole blood bactericidal assay for tuberculosis. *J Infect Dis* 2001,**183**:1300-1303.
357. Cheon SH, Kampmann B, Hise AG, Phillips M, Song HY, Landen K*, et al.* Bactericidal activity in whole blood as a potential surrogate marker of immunity after vaccination against tuberculosis. *Clin Diagn Lab Immunol* 2002,**9**:901-907.
358. Wallis RS, Vinhas SA, Johnson JL, Ribeiro FC, Palaci M, Peres RL*, et al.* Whole blood bactericidal activity during treatment of pulmonary tuberculosis. *J Infect Dis* 2003,**187**:270-278.
359. Janulionis E, Sofer C, Schwander SK, Nevels D, Kreiswirth B, Shashkina E*, et al.* Survival and replication of clinical Mycobacterium tuberculosis isolates in the context of human innate immunity. *Infect Immun* 2005,**73**:2595-2601.
360. Wallis RS, Vinhas S, Janulionis E. Strain specificity of antimycobacterial immunity in whole blood culture after cure of tuberculosis. *Tuberculosis (Edinb)* 2009,**89**:221-224.
361. Fletcher HA, Tanner R, Wallis RS, Meyer J, Manjaly ZR, Harris S*, et al.* Inhibition of mycobacterial growth in vitro following primary but not secondary vaccination with Mycobacterium bovis BCG. *Clin Vaccine Immunol* 2013,**20**:1683-1689.
362. Harris SA, Meyer J, Satti I, Marsay L, Poulton ID, Tanner R*, et al.* Evaluation of a human BCG challenge model to assess antimycobacterial immunity induced by BCG and a candidate tuberculosis vaccine, MVA85A, alone and in combination. *J Infect Dis* 2014,**209**:1259-1268.
363. Sebina I, Biraro IA, Dockrell HM, Elliott AM, Cose S. Circulating B-lymphocytes as potential biomarkers of tuberculosis infection activity. *PLoS One* 2014,**9**:e106796.
364. Kang JS, Cherian A, Gan SH, Lee TH, Lee KC, Chee CB*, et al.* Strong purified protein derivative responses are associated with poor mycobacterium inhibition in latent TB. *Eur Respir J* 2010,**36**:348-354.
365. Tanner R. Development of mycobacterial growth inhibition assays for the early evaluation and gating of novel TB vaccine candidates. University of Oxford: Oxford; 2015:282.
366. Bouza E, Diaz-Lopez MD, Moreno S, Bernaldo de Quiros JC, Vicente T, Berenguer J. Mycobacterium tuberculosis bacteremia in patients with and without human immunodeficiency virus infection. *Arch Intern Med* 1993,**153**:496-500.
367. McDonald LC, Archibald LK, Rheanpumikankit S, Tansuphaswadikul S, Eampokalap B, Nwanyanawu O*, et al.* Unrecognised Mycobacterium tuberculosis bacteraemia among hospital inpatients in less developed countries. *Lancet* 1999,**354**:1159-1163.
368. Tuomela M, Stanescu I, Krohn K. Validation overview of bio-analytical methods. *Gene Ther* 2005,**12 Suppl 1**:S131-138.
369. Marrero J, Trujillo C, Rhee KY, Ehrt S. Glucose phosphorylation is required for Mycobacterium tuberculosis persistence in mice. *PLoS Pathog* 2013,**9**:e1003116.
370. Lowe DM, Redford PS, Wilkinson RJ, O'Garra A, Martineau AR. Neutrophils in tuberculosis: friend or foe? *Trends Immunol* 2012,**33**:14-25.

371. Banerjee S, Farhana A, Ehtesham NZ, Hasnain SE. Iron acquisition, assimilation and regulation in mycobacteria. *Infect Genet Evol* 2011,**11**:825-838.
372. Smith I. Mycobacterium tuberculosis pathogenesis and molecular determinants of virulence. *Clin Microbiol Rev* 2003,**16**:463-496.
373. Keane J, Balcewicz-Sablinska MK, Remold HG, Chupp GL, Meek BB, Fenton MJ*, et al.* Infection by Mycobacterium tuberculosis promotes human alveolar macrophage apoptosis. *Infect Immun* 1997,**65**:298-304.
374. Gan H, Lee J, Ren F, Chen M, Kornfeld H, Remold HG. Mycobacterium tuberculosis blocks crosslinking of annexin-1 and apoptotic envelope formation on infected macrophages to maintain virulence. *Nat Immunol* 2008,**9**:1189-1197.
375. Jamwal S, Midha MK, Verma HN, Basu A, Rao KV, Manivel V. Characterizing virulence-specific perturbations in the mitochondrial function of macrophages infected with Mycobacterium tuberculosis. *Sci Rep* 2013,**3**:1328.
376. Pym AS, Brodin P, Brosch R, Huerre M, Cole ST. Loss of RD1 contributed to the attenuation of the live tuberculosis vaccines Mycobacterium bovis BCG and Mycobacterium microti. *Mol Microbiol* 2002,**46**:709-717.
377. Lewis KN, Liao R, Guinn KM, Hickey MJ, Smith S, Behr MA*, et al.* Deletion of RD1 from Mycobacterium tuberculosis mimics bacille Calmette-Guerin attenuation. *J Infect Dis* 2003,**187**:117-123.
378. Lee J, Repasy T, Papavinasasundaram K, Sassetti C, Kornfeld H. Mycobacterium tuberculosis induces an atypical cell death mode to escape from infected macrophages. *PLoS One* 2011,**6**:e18367.
379. Kaku T, Kawamura I, Uchiyama R, Kurenuma T, Mitsuyama M. RD1 region in mycobacterial genome is involved in the induction of necrosis in infected RAW264 cells via mitochondrial membrane damage and ATP depletion. *FEMS Microbiol Lett* 2007,**274**:189-195.
380. Bain BJ. Ethnic and sex differences in the total and differential white cell count and platelet count. *J Clin Pathol* 1996,**49**:664-666.
381. Kirkland TN, Viriyakosol S. Structure-function analysis of soluble and membrane-bound CD14. *Prog Clin Biol Res* 1998,**397**:79-87.
382. Ratledge C. Iron, mycobacteria and tuberculosis. *Tuberculosis (Edinb)* 2004,**84**:110-130.
383. Subbian S, Bandyopadhyay N, Tsenova L, O'Brien P, Khetani V, Kushner NL*, et al.* Early innate immunity determines outcome of Mycobacterium tuberculosis pulmonary infection in rabbits. *Cell Commun Signal* 2013,**11**:60.
384. Ratcliffe HL, Palladino VS. Tuberculosis induced by droplet nuclei infection; initial homogeneous response of small mammals (rats, mice, guinea pigs, and hamsters) to human and to bovine bacilli, and the rate and pattern of tubercle development. *J Exp Med* 1953,**97**:61-68.
385. Eum SY, Kong JH, Hong MS, Lee YJ, Kim JH, Hwang SH*, et al.* Neutrophils are the predominant infected phagocytic cells in the airways of patients with active pulmonary TB. *Chest* 2010,**137**:122-128.
386. Cassidy JP, Bryson DG, Pollock JM, Evans RT, Forster F, Neill SD. Early lesion formation in cattle experimentally infected with Mycobacterium bovis. *J Comp Pathol* 1998,**119**:27-44.
387. Turner OC, Basaraba RJ, Orme IM. Immunopathogenesis of pulmonary granulomas in the guinea pig after infection with Mycobacterium tuberculosis. *Infect Immun* 2003,**71**:864-871.
388. Cassidy JP, Martineau AR. Innate resistance to tuberculosis in man, cattle and laboratory animal models: nipping disease in the bud? *J Comp Pathol* 2014,**151**:291-308.

389. Kisich KO, Higgins M, Diamond G, Heifets L. Tumor necrosis factor alpha stimulates killing of Mycobacterium tuberculosis by human neutrophils. *Infect Immun* 2002,**70**:4591-4599.
390. Stead WW, Senner JW, Reddick WT, Lofgren JP. Racial differences in susceptibility to infection by Mycobacterium tuberculosis. *N Engl J Med* 1990,**322**:422-427.
391. Suter E. Multiplication of tubercle bacilli within mononuclear phagocytes in tissue cultures derived from normal animals and animals vaccinated with BCG. *J Exp Med* 1953,**97**:235-245.
392. Takeda K, Akira S. Toll-like receptors in innate immunity. *Int Immunol* 2005,**17**:1-14.
393. Scott HM, Flynn JL. Mycobacterium tuberculosis in chemokine receptor 2-deficient mice: influence of dose on disease progression. *Infect Immun* 2002,**70**:5946-5954.
394. Rutledge BJ, Rayburn H, Rosenberg R, North RJ, Gladue RP, Corless CL*, et al.* High level monocyte chemoattractant protein-1 expression in transgenic mice increases their susceptibility to intracellular pathogens. *J Immunol* 1995,**155**:4838-4843.
395. Peters W, Scott HM, Chambers HF, Flynn JL, Charo IF, Ernst JD. Chemokine receptor 2 serves an early and essential role in resistance to Mycobacterium tuberculosis. *Proc Natl Acad Sci U S A* 2001,**98**:7958-7963.
396. Mamtani M, Mummidi S, Ramsuran V, Pham MH, Maldonado R, Begum K*, et al.* Influence of variations in CCL3L1 and CCR5 on tuberculosis in a northwestern Colombian population. *J Infect Dis* 2011,**203**:1590-1594.
397. Flores-Villanueva PO, Ruiz-Morales JA, Song CH, Flores LM, Jo EK, Montano M*, et al.* A functional promoter polymorphism in monocyte chemoattractant protein-1 is associated with increased susceptibility to pulmonary tuberculosis. *J Exp Med* 2005,**202**:1649-1658.
398. Shen C, Assche GV, Colpaert S, Maerten P, Geboes K, Rutgeerts P*, et al.* Adalimumab induces apoptosis of human monocytes: a comparative study with infliximab and etanercept. *Aliment Pharmacol Ther* 2005,**21**:251-258.
399. Keane J, Gershon S, Wise RP, Mirabile-Levens E, Kasznica J, Schwieterman WD*, et al.* Tuberculosis associated with infliximab, a tumor necrosis factor alpha-neutralizing agent. *N Engl J Med* 2001,**345**:1098-1104.
400. Strauss-Ayali D, Conrad SM, Mosser DM. Monocyte subpopulations and their differentiation patterns during infection. *J Leukoc Biol* 2007,**82**:244-252.
401. Naranbhai V, Fletcher HA, Tanner R, O'Shea MK, McShane H, Fairfax BP*, et al.* Distinct Transcriptional and Anti-Mycobacterial Profiles of Peripheral Blood Monocytes Dependent on the Ratio of Monocytes: Lymphocytes. *EBioMedicine* 2015,**2**:1619-1626.
402. Naranbhai V, Hill AV, Abdool Karim SS, Naidoo K, Abdool Karim Q, Warimwe GM*, et al.* Ratio of monocytes to lymphocytes in peripheral blood identifies adults at risk of incident tuberculosis among HIV-infected adults initiating antiretroviral therapy. *J Infect Dis* 2014,**209**:500-509.
403. Merekoulias G, Alexopoulos EC, Belezos T, Panagiotopoulou E, Jelastopulu DM. Lymphocyte to monocyte ratio as a screening tool for influenza. *PLoS Curr* 2010,**2**:RRN1154.
404. Warimwe GM, Murungi LM, Kamuyu G, Nyangweso GM, Wambua J, Naranbhai V, *et al.* The ratio of monocytes to lymphocytes in peripheral blood correlates with increased susceptibility to clinical malaria in Kenyan children. *PLoS One* 2013,**8**:e57320.

405. Muller-Sieburg CE, Cho RH, Thoman M, Adkins B, Sieburg HB. Deterministic regulation of hematopoietic stem cell self-renewal and differentiation. *Blood* 2002,**100**:1302-1309.
406. Muller-Sieburg CE, Sieburg HB, Bernitz JM, Cattarossi G. Stem cell heterogeneity: implications for aging and regenerative medicine. *Blood* 2012,**119**:3900-3907.
407. Pang WW, Price EA, Sahoo D, Beerman I, Maloney WJ, Rossi DJ*, et al.* Human bone marrow hematopoietic stem cells are increased in frequency and myeloid-biased with age. *Proc Natl Acad Sci U S A* 2011,**108**:20012-20017.
408. Schroeder T. Hematopoietic stem cell heterogeneity: subtypes, not unpredictable behavior. *Cell Stem Cell* 2010,**6**:203-207.
409. Baldridge MT, King KY, Boles NC, Weksberg DC, Goodell MA. Quiescent haematopoietic stem cells are activated by IFN-gamma in response to chronic infection. *Nature* 2010,**465**:793-797.
410. Das B, Kashino SS, Pulu I, Kalita D, Swami V, Yeger H*, et al.* CD271(+) bone marrow mesenchymal stem cells may provide a niche for dormant Mycobacterium tuberculosis. *Sci Transl Med* 2013,**5**:170ra113.
411. Kato K. Effect of tuberculin test on monocyte-lymphocyte ratio in children. *J Pediatr* 1935,**7**:238-244.
412. Orme IM. The Achilles heel of BCG. *Tuberculosis (Edinb)* 2010,**90**:329-332.
413. Rosenthal SR, Loewinsohne, Graham ML, Liveright D, Thorne G, Johnson V. BCG vaccination against tuberculosis in Chicago. A twenty-year study statistically analyzed. *Pediatrics* 1961,**28**:622-641.
414. Comstock GW, Woolpert SF, Livesay VT. Tuberculosis studies in Muscogee County, Georgia. Twenty-year evaluation of a community trial of BCG vaccination. *Public Health Rep* 1976,**91**:276-280.
415. Fifteen year follow up of trial of BCG vaccines in south India for tuberculosis prevention. Tuberculosis Research Centre (ICMR), Chennai. *Indian J Med Res* 1999,**110**:56-69.
416. Aronson NE, Santosham M, Comstock GW, Howard RS, Moulton LH, Rhoades ER*, et al.* Long-term efficacy of BCG vaccine in American Indians and Alaska Natives: A 60-year follow-up study. *Jama* 2004,**291**:2086-2091.
417. Balu S, Reljic R, Lewis MJ, Pleass RJ, McIntosh R, van Kooten C*, et al.* A novel human IgA monoclonal antibody protects against tuberculosis. *J Immunol* 2011,**186**:3113-3119.
418. Buccheri S, Reljic R, Caccamo N, Meraviglia S, Ivanyi J, Salerno A*, et al.* Prevention of the post-chemotherapy relapse of tuberculous infection by combined immunotherapy. *Tuberculosis (Edinb)* 2009,**89**:91-94.
419. Chambers MA, Gavier-Widen D, Hewinson RG. Antibody bound to the surface antigen MPB83 of Mycobacterium bovis enhances survival against high dose and low dose challenge. *FEMS Immunol Med Microbiol* 2004,**41**:93-100.
420. Guirado E, Amat I, Gil O, Diaz J, Arcos V, Caceres N*, et al.* Passive serum therapy with polyclonal antibodies against Mycobacterium tuberculosis protects against post-chemotherapy relapse of tuberculosis infection in SCID mice. *Microbes Infect* 2006,**8**:1252-1259.
421. Hamasur B, Haile M, Pawlowski A, Schroder U, Kallenius G, Svenson SB. A mycobacterial lipoarabinomannan specific monoclonal antibody and its F(ab') fragment prolong survival of mice infected with Mycobacterium tuberculosis. *Clin Exp Immunol* 2004,**138**:30-38.
422. Olivares N, Leon A, Lopez Y, Puig A, Cadiz A, Falero G*, et al.* The effect of the administration of human gamma globulins in a model of BCG infection in mice. *Tuberculosis (Edinb)* 2006,**86**:268-272.

423. Roy E, Stavropoulos E, Brennan J, Coade S, Grigorieva E, Walker B*, et al.* Therapeutic efficacy of high-dose intravenous immunoglobulin in Mycobacterium tuberculosis infection in mice. *Infect Immun* 2005,**73**:6101-6109.
424. Teitelbaum R, Glatman-Freedman A, Chen B, Robbins JB, Unanue E, Casadevall A*, et al.* A mAb recognizing a surface antigen of Mycobacterium tuberculosis enhances host survival. *Proc Natl Acad Sci U S A* 1998,**95**:15688-15693.
425. Williams A, Reljic R, Naylor I, Clark SO, Falero-Diaz G, Singh M*, et al.* Passive protection with immunoglobulin A antibodies against tuberculous early infection of the lungs. *Immunology* 2004,**111**:328-333.
426. de Valliere S, Abate G, Blazevic A, Heuertz RM, Hoft DF. Enhancement of innate and cell-mediated immunity by antimycobacterial antibodies. *Infect Immun* 2005,**73**:6711-6720.
427. Hamasur B, Haile M, Pawlowski A, Schroder U, Williams A, Hatch G*, et al.* Mycobacterium tuberculosis arabinomannan-protein conjugates protect against tuberculosis. *Vaccine* 2003,**21**:4081-4093.
428. Kunnath-Velayudhan S, Davidow AL, Wang HY, Molina DM, Huynh VT, Salamon H*, et al.* Proteome-scale antibody responses and outcome of Mycobacterium tuberculosis infection in nonhuman primates and in tuberculosis patients. *J Infect Dis* 2012,**206**:697-705.
429. Costello AM, Kumar A, Narayan V, Akbar MS, Ahmed S, Abou-Zeid C*, et al.* Does antibody to mycobacterial antigens, including lipoarabinomannan, limit dissemination in childhood tuberculosis? *Trans R Soc Trop Med Hyg* 1992,**86**:686-692.
430. Achkar JM, Chan J, Casadevall A. B cells and antibodies in the defense against Mycobacterium tuberculosis infection. *Immunol Rev* 2015,**264**:167-181.
431. Ashenafi S, Aderaye G, Zewdie M, Raqib R, Bekele A, Magalhaes I*, et al.* BCG-specific IgG-secreting peripheral plasmablasts as a potential biomarker of active tuberculosis in HIV negative and HIV positive patients. *Thorax* 2013,**68**:269-276.
432. Chan J, Mehta S, Bharrhan S, Chen Y, Achkar JM, Casadevall A*, et al.* The role of B cells and humoral immunity in Mycobacterium tuberculosis infection. *Semin Immunol* 2014,**26**:588-600.
433. Kozakiewicz L, Phuah J, Flynn J, Chan J. The role of B cells and humoral immunity in Mycobacterium tuberculosis infection. *Adv Exp Med Biol* 2013,**783**:225-250.
434. Abebe F, Bjune G. The protective role of antibody responses during Mycobacterium tuberculosis infection. *Clin Exp Immunol* 2009,**157**:235-243.
435. Arias-Bouda LM, Kuijper S, Van der Werf A, Nguyen LN, Jansen HM, Kolk AH. Changes in avidity and level of immunoglobulin G antibodies to Mycobacterium tuberculosis in sera of patients undergoing treatment for pulmonary tuberculosis. *Clin Diagn Lab Immunol* 2003,**10**:702-709.
436. Demkow U, Filewska M, Michalowska-Mitczuk D, Kus J, Jagodzinski J, Zielonka T*, et al.* Heterogeneity of antibody response to myobacterial antigens in different clinical manifestations of pulmonary tuberculosis. *J Physiol Pharmacol* 2007,**5**:117-127.
437. Legesse M, Ameni G, Medhin G, Mamo G, Franken KL, Ottenhoff TH*, et al.* IgA response to ESAT-6/CFP-10 and Rv2031 antigens varies in culture-confirmed pulmonary tuberculosis patients, healthy Mycobacterium tuberculosis infected and non-infected individuals in a tuberculosis endemic setting, Ethiopia. *Scand J Immunol* 2013,**29**:12080.

438. Maglione PJ, Chan J. How B cells shape the immune response against Mycobacterium tuberculosis. *Eur J Immunol* 2009,**39**:676-686.
439. Hernandez J, Velazquez C, Valenzuela O, Robles-Zepeda R, Ruiz-Bustos E, Navarro M*, et al.* Low number of peripheral blood B lymphocytes in patients with pulmonary tuberculosis. *Immunol Invest* 2010,**39**:197-205.
440. Sebina I, Cliff JM, Smith SG, Nogaro S, Webb EL, Riley EM*, et al.* Long-lived memory B-cell responses following BCG vaccination. *PLoS One* 2012,**7**:11.
441. Rodrigues LC, Pereira SM, Cunha SS, Genser B, Ichihara MY, de Brito SC*, et al.* Effect of BCG revaccination on incidence of tuberculosis in school-aged children in Brazil: the BCG-REVAC cluster-randomised trial. *Lancet* 2005,**366**:1290-1295.
442. Abubakar I, Pimpin L, Ariti C, Beynon R, Mangtani P, Sterne JA*, et al.* Systematic review and meta-analysis of the current evidence on the duration of protection by bacillus Calmette-Guerin vaccination against tuberculosis. *Health Technol Assess* 2013,**17**:1-372, v-vi.
443. Andersen P, Doherty TM. The success and failure of BCG - implications for a novel tuberculosis vaccine. *Nat Rev Microbiol* 2005,**3**:656-662.
444. Colditz GA, Berkey CS, Mosteller F, Brewer TF, Wilson ME, Burdick E*, et al.* The efficacy of bacillus Calmette-Guerin vaccination of newborns and infants in the prevention of tuberculosis: meta-analyses of the published literature. *Pediatrics* 1995,**96**:29-35.
445. Colditz GA, Brewer TF, Berkey CS, Wilson ME, Burdick E, Fineberg HV*, et al.* Efficacy of BCG vaccine in the prevention of tuberculosis. Meta-analysis of the published literature. *JAMA* 1994,**271**:698-702.
446. Fine PE. Variation in protection by BCG: implications of and for heterologous immunity. *Lancet* 1995,**346**:1339-1345.
447. Bennett AR, Gorak-Stolinska P, Ben-Smith A, Floyd S, de Lara CM, Weir RE*, et al.* The PPD-specific T-cell clonal response in UK and Malawian subjects following BCG vaccination: a new repertoire evolves over 12 months. *Vaccine* 2006,**24**:2617-2626.
448. Black GF, Weir RE, Floyd S, Bliss L, Warndorff DK, Crampin AC*, et al.* BCG-induced increase in interferon-gamma response to mycobacterial antigens and efficacy of BCG vaccination in Malawi and the UK: two randomised controlled studies. *Lancet* 2002,**359**:1393-1401.
449. Weir RE, Black GF, Nazareth B, Floyd S, Stenson S, Stanley C*, et al.* The influence of previous exposure to environmental mycobacteria on the interferon-gamma response to bacille Calmette-Guerin vaccination in southern England and northern Malawi. *Clin Exp Immunol* 2006,**146**:390-399.
450. Black GF, Fine PEM, Warndorff DK, Floyd S, Weir RE, Blackwell JM*, et al.* Relationship between IFN-gamma and skin test responsiveness to Mycobacterium tuberculosis PPD in healthy, non-BCG-vaccinated young adults in Northern Malawi. *Int J Tuberc Lung Dis* 2001,**5**:664-672.
451. Mangtani P, Abubakar I, Ariti C, Beynon R, Pimpin L, Fine PE*, et al.* Protection by BCG vaccine against tuberculosis: a systematic review of randomized controlled trials. *Clin Infect Dis* 2014,**58**:470-480.
452. Brandt L, Feino Cunha J, Weinreich Olsen A, Chilima B, Hirsch P, Appelberg R*, et al.* Failure of the Mycobacterium bovis BCG vaccine: some species of environmental mycobacteria block multiplication of BCG and induction of protective immunity to tuberculosis. *Infect Immun* 2002,**70**:672-678.
453. Elias D, Akuffo H, Britton S. Helminthes could influence the outcome of vaccines against TB in the tropics. *Parasite Immunol* 2006,**28**:507-513.

454. Elias D, Akuffo H, Pawlowski A, Haile M, Schon T, Britton S. Schistosoma mansoni infection reduces the protective efficacy of BCG vaccination against virulent Mycobacterium tuberculosis. *Vaccine* 2005,**23**:1326-1334.
455. Elias D, Britton S, Aseffa A, Engers H, Akuffo H. Poor immunogenicity of BCG in helminth infected population is associated with increased in vitro TGF-beta production. *Vaccine* 2008,**26**:3897-3902.
456. Elias D, Wolday D, Akuffo H, Petros B, Bronner U, Britton S. Effect of deworming on human T cell responses to mycobacterial antigens in helminth-exposed individuals before and after bacille Calmette-Guerin (BCG) vaccination. *Clin Exp Immunol* 2001,**123**:219-225.
457. Hoft DF, Kemp EB, Marinaro M, Cruz O, Kiyono H, McGhee JR*, et al.* A double-blind, placebo-controlled study of Mycobacterium-specific human immune responses induced by intradermal bacille Calmette-Guerin vaccination. *J Lab Clin Med* 1999,**134**:244-252.
458. Chen T, Blanc C, Eder AZ, Prados-Rosales R, Souza AC, Kim RS*, et al.* Association of Human Antibodies to Arabinomannan with Enhanced Mycobacterial Opsonophagocytosis and Intracellular Growth Reduction. *J Infect Dis* 2016.
459. Mishra AK, Driessen NN, Appelmelk BJ, Besra GS. Lipoarabinomannan and related glycoconjugates: structure, biogenesis and role in Mycobacterium tuberculosis physiology and host-pathogen interaction. *FEMS Microbiol Rev* 2011,**35**:1126-1157.
460. Ulrichs T, Kosmiadi GA, Trusov V, Jorg S, Pradl L, Titukhina M*, et al.* Human tuberculous granulomas induce peripheral lymphoid follicle-like structures to orchestrate local host defence in the lung. *J Pathol* 2004,**204**:217-228.
461. Phuah JY, Mattila JT, Lin PL, Flynn JL. Activated B cells in the granulomas of nonhuman primates infected with Mycobacterium tuberculosis. *Am J Pathol* 2012,**181**:508-514.
462. Lazaro FP, Werneck RI, Mackert CC, Cobat A, Prevedello FC, Pimentel RP*, et al.* A major gene controls leprosy susceptibility in a hyperendemic isolated population from north of Brazil. *J Infect Dis* 2010,**201**:1598-1605.
463. Styblo K. Recent advances in epidemiological research in tuberculosis. *Adv Tuberc Res* 1980,**20**:1-63.
464. Salgame P, Abrams JS, Clayberger C, Goldstein H, Convit J, Modlin RL*, et al.* Differing lymphokine profiles of functional subsets of human CD4 and CD8 T cell clones. *Science* 1991,**254**:279-282.
465. Teles RM, Graeber TG, Krutzik SR, Montoya D, Schenk M, Lee DJ*, et al.* Type I interferon suppresses type II interferon-triggered human anti-mycobacterial responses. *Science* 2013,**339**:1448-1453.
466. Sebina I, Cliff JM, Smith SG, Nogaro S, Webb EL, Riley EM*, et al.* Long-lived memory B-cell responses following BCG vaccination. *PLoS One* 2012,**7**:e51381.
467. Rekha RS, Kamal SM, Andersen P, Rahim Z, Hoq MI, Ara G*, et al.* Validation of the ALS assay in adult patients with culture confirmed pulmonary tuberculosis. *PLoS One* 2011,**6**:e16425.
468. Raqib R, Rahman J, Kamaluddin AK, Kamal SM, Banu FA, Ahmed S*, et al.* Rapid diagnosis of active tuberculosis by detecting antibodies from lymphocyte secretions. *J Infect Dis* 2003,**188**:364-370.
469. Raqib R, Kamal SM, Rahman MJ, Rahim Z, Banu S, Bardhan PK*, et al.* Use of antibodies in lymphocyte secretions for detection of subclinical tuberculosis infection in asymptomatic contacts. *Clin Diagn Lab Immunol* 2004,**11**:1022-1027.

470. Sze DM, Toellner KM, Garcia de Vinuesa C, Taylor DR, MacLennan IC. Intrinsic constraint on plasmablast growth and extrinsic limits of plasma cell survival. *J Exp Med* 2000,**192**:813-821.
471. Tarte K, Zhan F, De Vos J, Klein B, Shaughnessy J, Jr. Gene expression profiling of plasma cells and plasmablasts: toward a better understanding of the late stages of B-cell differentiation. *Blood* 2003,**102**:592-600.
472. Tangye SG, Tarlinton DM. Memory B cells: effectors of long-lived immune responses. *Eur J Immunol* 2009,**39**:2065-2075.
473. Rosado MM, Scarsella M, Pandolfi E, Cascioli S, Giorda E, Chionne P*, et al.* Switched memory B cells maintain specific memory independently of serum antibodies: the hepatitis B example. *Eur J Immunol* 2011,**41**:1800-1808.
474. Kelly DF, Pollard AJ, Moxon ER. Immunological memory: the role of B cells in long-term protection against invasive bacterial pathogens. *Jama* 2005,**294**:3019-3023.
475. Steingart KR, Henry M, Laal S, Hopewell PC, Ramsay A, Menzies D*, et al.* Commercial serological antibody detection tests for the diagnosis of pulmonary tuberculosis: a systematic review. *PLoS Med* 2007,**4**:e202.
476. Chan ED, Heifets L, Iseman MD. Immunologic diagnosis of tuberculosis: a review. *Tuber Lung Dis* 2000,**80**:131-140.
477. Saletti G, Cuburu N, Yang JS, Dey A, Czerkinsky C. Enzyme-linked immunospot assays for direct ex vivo measurement of vaccine-induced human humoral immune responses in blood. *Nat Protoc* 2013,**8**:1073-1087.
478. Halliley JL, Kyu S, Kobie JJ, Walsh EE, Falsey AR, Randall TD*, et al.* Peak frequencies of circulating human influenza-specific antibody secreting cells correlate with serum antibody response after immunization. *Vaccine* 2010,**28**:3582-3587.
479. Elias SC, Choudhary P, de Cassan SC, Biswas S, Collins KA, Halstead FD*, et al.* Analysis of human B-cell responses following ChAd63-MVA MSP1 and AMA1 immunization and controlled malaria infection. *Immunology* 2014,**141**:628-644.
480. Blanchard-Rohner G, Pulickal AS, Jol-van der Zijde CM, Snape MD, Pollard AJ. Appearance of peripheral blood plasma cells and memory B cells in a primary and secondary immune response in humans. *Blood* 2009,**114**:4998-5002.
481. Tangye SG, Avery DT, Deenick EK, Hodgkin PD. Intrinsic differences in the proliferation of naive and memory human B cells as a mechanism for enhanced secondary immune responses. *J Immunol* 2003,**170**:686-694.
482. Blink EJ, Light A, Kallies A, Nutt SL, Hodgkin PD, Tarlinton DM. Early appearance of germinal center-derived memory B cells and plasma cells in blood after primary immunization. *J Exp Med* 2005,**201**:545-554.
483. Lanzavecchia A, Sallusto F. Human B cell memory. *Curr Opin Immunol* 2009,**21**:298-304.
484. Moody MA, Haynes BF. Antigen-specific B cell detection reagents: use and quality control. *Cytometry A* 2008,**73**:1086-1092.
485. Kardava L, Moir S, Shah N, Wang W, Wilson R, Buckner CM*, et al.* Abnormal B cell memory subsets dominate HIV-specific responses in infected individuals. *J Clin Invest* 2014,**124**:3252-3262.
486. Doucett VP, Gerhard W, Owler K, Curry D, Brown L, Baumgarth N. Enumeration and characterization of virus-specific B cells by multicolor flow cytometry. *J Immunol Methods* 2005,**303**:40-52.
487. Dall'Stella R, Krieger MA, Burger M, Agottani JB, Chahad-Ehlers S, Thomaz-Soccol V. Development of bioprocess for the production of purified protein

derivative with Brazilian strains of Mycobacterium tuberculosis for diagnosis use. *J Biotechnol* 2007,**127**:278-287.
488. Borsuk S, Newcombe J, Mendum TA, Dellagostin OA, McFadden J. Identification of proteins from tuberculin purified protein derivative (PPD) by LC-MS/MS. *Tuberculosis (Edinb)* 2009,**89**:423-430.
489. Townsend SE, Goodnow CC, Cornall RJ. Single epitope multiple staining to detect ultralow frequency B cells. *J Immunol Methods* 2001,**249**:137-146.
490. Amanna IJ, Slifka MK. Quantitation of rare memory B cell populations by two independent and complementary approaches. *J Immunol Methods* 2006,**317**:175-185.
491. Minassian AM, Satti I, Poulton ID, Meyer J, Hill AV, McShane H. A human challenge model for Mycobacterium tuberculosis using Mycobacterium bovis bacille Calmette-Guerin. *J Infect Dis* 2012,**205**:1035-1042.
492. Minassian AM, Ronan EO, Poyntz H, Hill AV, McShane H. Preclinical development of an in vivo BCG challenge model for testing candidate TB vaccine efficacy. *PLoS One* 2011,**6**:e19840.
493. 2011 Census. In: *Population and Household Estimates for England and Wales* London: Office of National Statistics 2011.
494. Tuberculosis in Birmingham. In: *TB in Birmingham - A Report of the Health & Adults Overview and Scrutiny Committee*. Birmingham: Birmingham City Council; 2012.
495. Reports of cases of tuberculosis to enhanced tuberculosis surveillance systems: United Kingdom, 2000 to 2014 In. London: Public Health England; 2015.
496. Koh GC, Hawthorne G, Turner AM, Kunst H, Dedicoat M. Tuberculosis incidence correlates with sunshine: an ecological 28-year time series study. *PLoS One* 2013,**8**:e57752.
497. O'Shea MK, Fletcher TE, Beeching NJ, Dedicoat M, Spence D, McShane H*, et al.* Tuberculin skin testing and treatment modulates interferon-gamma release assay results for latent tuberculosis in migrants. *PLoS One* 2014,**9**:e97366.
498. Donald PR, Maritz JS, Diacon AH. The pharmacokinetics and pharmacodynamics of rifampicin in adults and children in relation to the dosage recommended for children. *Tuberculosis (Edinb)* 2011,**91**:196-207.
499. Acocella G. Clinical pharmacokinetics of rifampicin. *Clin Pharmacokinet* 1978,**3**:108-127.
500. Tuberculosis in England. In: *2015 report (presenting data to end of 2014) version 1.1*. London: Public Health England; 2015.
501. Whitley E, Ball J. Statistics review 4: sample size calculations. *Crit Care* 2002,**6**:335-341.
502. Lowe DM, Bandara AK, Packe GE, Barker RD, Wilkinson RJ, Griffiths CJ*, et al.* Neutrophilia independently predicts death in tuberculosis. *Eur Respir J* 2013,**42**:1752-1757.
503. Sabin FR, Doan CA, Cunningham RS. Studies of the blood in experimental tuberculosis: the monocyte-lymphocyte ratio; the anemia-leucopenia phase. *Trans 22nd Annu Meeting Natl Tuberc Assoc* 1926,**22**:252-256.
504. Doan CA, Sabin FR. The relation of the tubercle and the monocyte:lymphocyte ratio to resistance and susceptibilty in tuberculosis. *J Exp Med* 1930,**IV**:113-152.
505. Rogers PM. A study of the blood monocytes in children with tuberculosis. *N Engl J Med* 1928,**198**:740-749.
506. Naranbhai V, Moodley D, Chipato T, Stranix-Chibanda L, Nakabaiito C, Kamateeka M*, et al.* The association between the ratio of monocytes: lymphocytes and risk of tuberculosis among HIV-infected postpartum women. *J Acquir Immune Defic Syndr* 2014,**67**:573-575.

507. Naranbhai V, Kim S, Fletcher H, Cotton MF, Violari A, Mitchell C*, et al.* The association between the ratio of monocytes:lymphocytes at age 3 months and risk of tuberculosis (TB) in the first two years of life. *BMC Med* 2014,**12**:120.
508. Wang J, Yin Y, Wang X, Pei H, Kuai S, Gu L*, et al.* Ratio of monocytes to lymphocytes in peripheral blood in patients diagnosed with active tuberculosis. *Braz J Infect Dis* 2015,**19**:125-131.
509. Denis M, Wedlock DN, Buddle BM. Ability of T cell subsets and their soluble mediators to modulate the replication of Mycobacterium bovis in bovine macrophages. *Cell Immunol* 2004,**232**:1-8.
510. Carpenter E, Fray L, Gormley E. Cellular responses and Mycobacterium bovis BCG growth inhibition by bovine lymphocytes. *Immunol Cell Biol* 1997,**75**:554-560.
511. Rakotosamimanana N, Richard V, Raharimanga V, Gicquel B, Doherty TM, Zumla A*, et al.* Biomarkers for risk of developing active tuberculosis in contacts of TB patients: a prospective cohort study. *Eur Respir J* 2015,**46**:1095-1103.
512. Lee SW, Kang YA, Yoon YS, Um SW, Lee SM, Yoo CG*, et al.* The prevalence and evolution of anemia associated with tuberculosis. *J Korean Med Sci* 2006,**21**:1028-1032.
513. Weiss G. Pathogenesis and treatment of anaemia of chronic disease. *Blood Rev* 2002,**16**:87-96.
514. Baynes RD, Flax H, Bothwell TH, Bezwoda WR, Atkinson P, Mendelow B. Red blood cell distribution width in the anemia secondary to tuberculosis. *Am J Clin Pathol* 1986,**85**:226-229.
515. Nemeth E, Rivera S, Gabayan V, Keller C, Taudorf S, Pedersen BK*, et al.* IL-6 mediates hypoferremia of inflammation by inducing the synthesis of the iron regulatory hormone hepcidin. *J Clin Invest* 2004,**113**:1271-1276.
516. Means RT, Jr. Recent developments in the anemia of chronic disease. *Curr Hematol Rep* 2003,**2**:116-121.
517. Kassa E, Enawgaw B, Gelaw A, Gelaw B. Effect of anti-tuberculosis drugs on hematological profiles of tuberculosis patients attending at University of Gondar Hospital, Northwest Ethiopia. *BMC Hematol* 2016,**16**:1.
518. Yeaman MR. Platelets in defense against bacterial pathogens. *Cell Mol Life Sci* 2010,**67**:525-544.
519. Semple JW, Italiano JE, Jr., Freedman J. Platelets and the immune continuum. *Nat Rev Immunol* 2011,**11**:264-274.
520. Li Z, Yang F, Dunn S, Gross AK, Smyth SS. Platelets as immune mediators: their role in host defense responses and sepsis. *Thromb Res* 2011,**127**:184-188.
521. Kornerup KN, Salmon GP, Pitchford SC, Liu WL, Page CP. Circulating platelet-neutrophil complexes are important for subsequent neutrophil activation and migration. *J Appl Physiol (1985)* 2010,**109**:758-767.
522. Feng Y, Dorhoi A, Mollenkopf HJ, Yin H, Dong Z, Mao L*, et al.* Platelets direct monocyte differentiation into epithelioid-like multinucleated giant foam cells with suppressive capacity upon mycobacterial stimulation. *J Infect Dis* 2014,**210**:1700-1710.
523. Clark SR, Ma AC, Tavener SA, McDonald B, Goodarzi Z, Kelly MM*, et al.* Platelet TLR4 activates neutrophil extracellular traps to ensnare bacteria in septic blood. *Nat Med* 2007,**13**:463-469.
524. Feng Y, Yin H, Mai G, Mao L, Yue J, Xiao H*, et al.* Elevated serum levels of CCL17 correlate with increased peripheral blood platelet count in patients with active tuberculosis in China. *Clin Vaccine Immunol* 2011,**18**:629-632.
525. Yakar F, Yildiz N, Yakar A, Kilicaslan Z. Isoniazid- and rifampicin-induced thrombocytopenia. *Multidiscip Respir Med* 2013,**8**:13.

526. Tozkoparan E, Deniz O, Ucar E, Bilgic H, Ekiz K. Changes in platelet count and indices in pulmonary tuberculosis. *Clin Chem Lab Med* 2007,**45**:1009-1013.
527. Sahin F, Yazar E, Yildiz P. Prominent features of platelet count, plateletcrit, mean platelet volume and platelet distribution width in pulmonary tuberculosis. *Multidiscip Respir Med* 2012,**7**:38.
528. Freyne B, Marchant A, Curtis N. BCG-associated heterologous immunity, a historical perspective: experimental models and immunological mechanisms. *Trans R Soc Trop Med Hyg* 2015,**109**:46-51.
529. Creating the gene ontology resource: design and implementation. *Genome Res* 2001,**11**:1425-1433.
530. Tallone T, Turconi G, Soldati G, Pedrazzini G, Moccetti T, Vassalli G. Heterogeneity of human monocytes: an optimized four-color flow cytometry protocol for analysis of monocyte subsets. *J Cardiovasc Transl Res* 2011,**4**:211-219.
531. Abeles RD, McPhail MJ, Sowter D, Antoniades CG, Vergis N, Vijay GK*, et al.* CD14, CD16 and HLA-DR reliably identifies human monocytes and their subsets in the context of pathologically reduced HLA-DR expression by CD14(hi) /CD16(neg) monocytes: Expansion of CD14(hi) /CD16(pos) and contraction of CD14(lo) /CD16(pos) monocytes in acute liver failure. *Cytometry A* 2012,**81**:823-834.
532. Mattos AM, Chaves AS, Franken KL, Figueiredo BB, Ferreira AP, Ottenhoff TH*, et al.* Detection of IgG1 antibodies against Mycobacterium tuberculosis DosR and Rpf antigens in tuberculosis patients before and after chemotherapy. *Tuberculosis (Edinb)* 2016,**96**:65-70.
533. Imaz MS, Zerbini E. Antibody response to culture filtrate antigens of Mycobacterium tuberculosis during and after treatment of tuberculosis patients. *Int J Tuberc Lung Dis* 2000,**4**:562-569.
534. Chegou NN, Heyckendorf J, Walzl G, Lange C, Ruhwald M. Beyond the IFN-gamma horizon: biomarkers for immunodiagnosis of infection with Mycobacterium tuberculosis. *Eur Respir J* 2014,**43**:1472-1486.
535. Clifford V, Tebruegge M, Zufferey C, Germano S, Denholm J, Street A*, et al.* Serum IP-10 in the diagnosis of latent and active tuberculosis. *J Infect* 2015,**71**:696-698.
536. Pasparakis M, Alexopoulou L, Douni E, Kollias G. Tumour necrosis factors in immune regulation: everything that's interesting is...new! *Cytokine Growth Factor Rev* 1996,**7**:223-229.
537. Vassalli P. The pathophysiology of tumor necrosis factors. *Annu Rev Immunol* 1992,**10**:411-452.
538. Yu K, Mitchell C, Xing Y, Magliozzo RS, Bloom BR, Chan J. Toxicity of nitrogen oxides and related oxidants on mycobacteria: M. tuberculosis is resistant to peroxynitrite anion. *Tuber Lung Dis* 1999,**79**:191-198.
539. Miller EA, Ernst JD. Illuminating the black box of TNF action in tuberculous granulomas. *Immunity* 2008,**29**:175-177.
540. Mohan VP, Scanga CA, Yu K, Scott HM, Tanaka KE, Tsang E*, et al.* Effects of tumor necrosis factor alpha on host immune response in chronic persistent tuberculosis: possible role for limiting pathology. *Infect Immun* 2001,**69**:1847-1855.
541. Chakravarty SD, Zhu G, Tsai MC, Mohan VP, Marino S, Kirschner DE*, et al.* Tumor necrosis factor blockade in chronic murine tuberculosis enhances granulomatous inflammation and disorganizes granulomas in the lungs. *Infect Immun* 2008,**76**:916-926.

542. Cavalcanti YV, Brelaz MC, Neves JK, Ferraz JC, Pereira VR. Role of TNF-Alpha, IFN-Gamma, and IL-10 in the Development of Pulmonary Tuberculosis. *Pulm Med* 2012,**2012**:745483.
543. Bean AG, Roach DR, Briscoe H, France MP, Korner H, Sedgwick JD*, et al.* Structural deficiencies in granuloma formation in TNF gene-targeted mice underlie the heightened susceptibility to aerosol Mycobacterium tuberculosis infection, which is not compensated for by lymphotoxin. *J Immunol* 1999,**162**:3504-3511.
544. Kaneko H, Yamada H, Mizuno S, Udagawa T, Kazumi Y, Sekikawa K*, et al.* Role of tumor necrosis factor-alpha in Mycobacterium-induced granuloma formation in tumor necrosis factor-alpha-deficient mice. *Lab Invest* 1999,**79**:379-386.
545. Iliopoulos A, Psathakis K, Aslanidis S, Skagias L, Sfikakis PP. Tuberculosis and granuloma formation in patients receiving anti-TNF therapy. *Int J Tuberc Lung Dis* 2006,**10**:588-590.
546. Harris J, Keane J. How tumour necrosis factor blockers interfere with tuberculosis immunity. *Clin Exp Immunol* 2010,**161**:1-9.
547. Zijlstra EE, van der Poll T, Mevissen M. Soluble receptors for tumor necrosis factor as markers of disease activity in visceral leishmaniasis. *J Infect Dis* 1995,**171**:498-501.
548. Juffermans NP, Verbon A, van Deventer SJ, van Deutekom H, Speelman P, van der Poll T. Tumor necrosis factor and interleukin-1 inhibitors as markers of disease activity of tuberculosis. *Am J Respir Crit Care Med* 1998,**157**:1328-1331.
549. Godfried MH, van der Poll T, Jansen J, Romijin JA, Schattenkerk JK, Endert E*, et al.* Soluble receptors for tumour necrosis factor: a putative marker of disease progression in HIV infection. *Aids* 1993,**7**:33-36.
550. Sherry B, Espinoza M, Manogue KR, Cerami A. Induction of the chemokine beta peptides, MIP-1 alpha and MIP-1 beta, by lipopolysaccharide is differentially regulated by immunomodulatory cytokines gamma-IFN, IL-10, IL-4, and TGF-beta. *Mol Med* 1998,**4**:648-657.
551. Maurer M, von Stebut E. Macrophage inflammatory protein-1. *Int J Biochem Cell Biol* 2004,**36**:1882-1886.
552. Saukkonen JJ, Bazydlo B, Thomas M, Strieter RM, Keane J, Kornfeld H. Beta-chemokines are induced by Mycobacterium tuberculosis and inhibit its growth. *Infect Immun* 2002,**70**:1684-1693.
553. Rangel-Santiago JF, Baay-Guzman GJ, Duran-Padilla MA, Lopez-Bochm KA, Garcia-Romero BL, Hernandez-Cueto DD*, et al.* A novel role of Yin-Yang-1 in pulmonary tuberculosis through the regulation of the chemokine CCL4. *Tuberculosis (Edinb)* 2016,**96**:87-95.
554. Chegou NN, Black GF, Kidd M, van Helden PD, Walzl G. Host markers in QuantiFERON supernatants differentiate active TB from latent TB infection: preliminary report. *BMC Pulm Med* 2009,**9**:21.
555. Westermark B, Heldin CH. Platelet-derived growth factor. Structure, function and implications in normal and malignant cell growth. *Acta Oncol* 1993,**32**:101-105.
556. Wangoo A, Taylor IK, Haynes AR, Shaw RJ. Up-regulation of alveolar macrophage platelet-derived growth factor-B (PDGF-B) mRNA by interferon-gamma from Mycobacterium tuberculosis antigen (PPD)-stimulated lymphocytes. *Clin Exp Immunol* 1993,**94**:43-50.
557. Ameglio F, Casarini M, Capoluongo E, Mattia P, Puglisi G, Giosue S. Post-treatment changes of six cytokines in active pulmonary tuberculosis: differences between patients with stable or increased fibrosis. *Int J Tuberc Lung Dis* 2005,**9**:98-104.

558. Anbarasu D, Raja CP, Raja A. Multiplex analysis of cytokines/chemokines as biomarkers that differentiate healthy contacts from tuberculosis patients in high endemic settings. *Cytokine* 2013,**61**:747-754.
559. Wong KL, Yeap WH, Tai JJ, Ong SM, Dang TM, Wong SC. The three human monocyte subsets: implications for health and disease. *Immunol Res* 2012,**53**:41-57.
560. Yang J, Zhang L, Yu C, Yang XF, Wang H. Monocyte and macrophage differentiation: circulation inflammatory monocyte as biomarker for inflammatory diseases. *Biomark Res* 2014,**2**:1.
561. Vanham G, Edmonds K, Qing L, Hom D, Toossi Z, Jones B*, et al.* Generalized immune activation in pulmonary tuberculosis: co-activation with HIV infection. *Clin Exp Immunol* 1996,**103**:30-34.
562. Castano D, Garcia LF, Rojas M. Increased frequency and cell death of CD16+ monocytes with Mycobacterium tuberculosis infection. *Tuberculosis (Edinb)* 2011,**91**:348-360.
563. Sanchez MD, Garcia Y, Montes C, Paris SC, Rojas M, Barrera LF*, et al.* Functional and phenotypic changes in monocytes from patients with tuberculosis are reversed with treatment. *Microbes Infect* 2006,**8**:2492-2500.
564. Barcelos W, Martins-Filho OA, Guimaraes TM, Oliveira MH, Spindola-de-Miranda S, Carvalho BN*, et al.* Peripheral blood mononuclear cells immunophenotyping in pulmonary tuberculosis patients before and after treatment. *Microbiol Immunol* 2006,**50**:597-605.
565. Barcelos W, Sathler-Avelar R, Martins-Filho OA, Carvalho BN, Guimaraes TM, Miranda SS*, et al.* Natural killer cell subpopulations in putative resistant individuals and patients with active Mycobacterium tuberculosis infection. *Scand J Immunol* 2008,**68**:92-102.
566. Appleby LJ, Nausch N, Midzi N, Mduluza T, Allen JE, Mutapi F. Sources of heterogeneity in human monocyte subsets. *Immunol Lett* 2013,**152**:32-41.
567. Mukherjee R, Kanti Barman P, Kumar Thatoi P, Tripathy R, Kumar Das B, Ravindran B. Non-Classical monocytes display inflammatory features: Validation in Sepsis and Systemic Lupus Erythematous. *Sci Rep* 2015,**5**:13886.
568. Prezzemolo T, Guggino G, La Manna MP, Di Liberto D, Dieli F, Caccamo N. Functional Signatures of Human CD4 and CD8 T Cell Responses to Mycobacterium tuberculosis. *Front Immunol* 2014,**5**:180.
569. da Silva MV, Tiburcio MG, Machado JR, Silva DA, Rodrigues DB, Rodrigues V*, et al.* Complexity and Controversies over the Cytokine Profiles of T Helper Cell Subpopulations in Tuberculosis. *J Immunol Res* 2015,**2015**:639107.
570. Hoyer KK, Dooms H, Barron L, Abbas AK. Interleukin-2 in the development and control of inflammatory disease. *Immunol Rev* 2008,**226**:19-28.
571. Torrado E, Cooper AM. IL-17 and Th17 cells in tuberculosis. *Cytokine Growth Factor Rev* 2010,**21**:455-462.
572. Almeida JR, Price DA, Papagno L, Arkoub ZA, Sauce D, Bornstein E*, et al.* Superior control of HIV-1 replication by CD8+ T cells is reflected by their avidity, polyfunctionality, and clonal turnover. *J Exp Med* 2007,**204**:2473-2485.
573. Caccamo N, Guggino G, Joosten SA, Gelsomino G, Di Carlo P, Titone L*, et al.* Multifunctional CD4(+) T cells correlate with active Mycobacterium tuberculosis infection. *Eur J Immunol* 2010,**40**:2211-2220.
574. Caccamo N, Guggino G, Meraviglia S, Gelsomino G, Di Carlo P, Titone L*, et al.* Analysis of Mycobacterium tuberculosis-specific CD8 T-cells in patients with active tuberculosis and in individuals with latent infection. *PLoS One* 2009,**4**:e5528.

575. Chiacchio T, Petruccioli E, Vanini V, Butera O, Cuzzi G, Petrone L*, et al.* Higher frequency of T-cell response to M. tuberculosis latency antigen Rv2628 at the site of active tuberculosis disease than in peripheral blood. *PLoS One* 2011,**6**:e27539.
576. Sargentini V, Mariotti S, Carrara S, Gagliardi MC, Teloni R, Goletti D*, et al.* Cytometric detection of antigen-specific IFN-gamma/IL-2 secreting cells in the diagnosis of tuberculosis. *BMC Infect Dis* 2009,**9**:99.
577. Sester U, Fousse M, Dirks J, Mack U, Prasse A, Singh M*, et al.* Whole-blood flow-cytometric analysis of antigen-specific CD4 T-cell cytokine profiles distinguishes active tuberculosis from non-active states. *PLoS One* 2011,**6**:e17813.
578. Sutherland JS, Adetifa IM, Hill PC, Adegbola RA, Ota MO. Pattern and diversity of cytokine production differentiates between Mycobacterium tuberculosis infection and disease. *Eur J Immunol* 2009,**39**:723-729.
579. Young JM, Adetifa IM, Ota MO, Sutherland JS. Expanded polyfunctional T cell response to mycobacterial antigens in TB disease and contraction post-treatment. *PLoS One* 2010,**5**:e11237.
580. Harari A, Rozot V, Bellutti Enders F, Perreau M, Stalder JM, Nicod LP*, et al.* Dominant TNF-alpha+ Mycobacterium tuberculosis-specific CD4+ T cell responses discriminate between latent infection and active disease. *Nat Med* 2011,**17**:372-376.
581. Marin ND, Paris SC, Rojas M, Garcia LF. Functional profile of CD4+ and CD8+ T cells in latently infected individuals and patients with active TB. *Tuberculosis (Edinb)* 2013,**93**:155-166.
582. Rozot V, Vigano S, Mazza-Stalder J, Idrizi E, Day CL, Perreau M*, et al.* Mycobacterium tuberculosis-specific CD8+ T cells are functionally and phenotypically different between latent infection and active disease. *Eur J Immunol* 2013,**43**:1568-1577.
583. Petruccioli E, Petrone L, Vanini V, Sampaolesi A, Gualano G, Girardi E*, et al.* IFNgamma/TNFalpha specific-cells and effector memory phenotype associate with active tuberculosis. *J Infect* 2013,**66**:475-486.
584. Jasenosky LD, Scriba TJ, Hanekom WA, Goldfeld AE. T cells and adaptive immunity to Mycobacterium tuberculosis in humans. *Immunol Rev* 2015,**264**:74-87.
585. Ladel CH, Daugelat S, Kaufmann SH. Immune response to Mycobacterium bovis bacille Calmette Guerin infection in major histocompatibility complex class I- and II-deficient knock-out mice: contribution of CD4 and CD8 T cells to acquired resistance. *Eur J Immunol* 1995,**25**:377-384.
586. Brighenti S, Andersson J. Induction and regulation of CD8+ cytolytic T cells in human tuberculosis and HIV infection. *Biochem Biophys Res Commun* 2010,**396**:50-57.
587. Chen CY, Huang D, Wang RC, Shen L, Zeng G, Yao S*, et al.* A critical role for CD8 T cells in a nonhuman primate model of tuberculosis. *PLoS Pathog* 2009,**5**:e1000392.
588. Levine B, Mizushima N, Virgin HW. Autophagy in immunity and inflammation. *Nature* 2011,**469**:323-335.
589. Mazzaccaro RJ, Stenger S, Rock KL, Porcelli SA, Brenner MB, Modlin RL*, et al.* Cytotoxic T lymphocytes in resistance to tuberculosis. *Adv Exp Med Biol* 1998,**452**:85-101.
590. Lewinsohn DA, Heinzel AS, Gardner JM, Zhu L, Alderson MR, Lewinsohn DM. Mycobacterium tuberculosis-specific CD8+ T cells preferentially recognize heavily infected cells. *Am J Respir Crit Care Med* 2003,**168**:1346-1352.

591. Bruns H, Meinken C, Schauenberg P, Harter G, Kern P, Modlin RL*, et al.* Anti-TNF immunotherapy reduces CD8+ T cell-mediated antimicrobial activity against Mycobacterium tuberculosis in humans. *J Clin Invest* 2009,**119**:1167-1177.
592. Nyendak MR, Park B, Null MD, Baseke J, Swarbrick G, Mayanja-Kizza H*, et al.* Mycobacterium tuberculosis specific CD8(+) T cells rapidly decline with antituberculosis treatment. *PLoS One* 2013,**8**:e81564.
593. Dheda K, Chang JS, Lala S, Huggett JF, Zumla A, Rook GA. Gene expression of IL17 and IL23 in the lungs of patients with active tuberculosis. *Thorax* 2008,**63**:566-568.
594. Feruglio SL, Tonby K, Kvale D, Dyrhol-Riise AM. Early dynamics of T helper cell cytokines and T regulatory cells in response to treatment of active Mycobacterium tuberculosis infection. *Clin Exp Immunol* 2015,**179**:454-465.
595. Steingart KR, Flores LL, Dendukuri N, Schiller I, Laal S, Ramsay A*, et al.* Commercial serological tests for the diagnosis of active pulmonary and extrapulmonary tuberculosis: an updated systematic review and meta-analysis. *PLoS Med* 2011,**8**:e1001062.
596. Reed MB, Gagneux S, Deriemer K, Small PM, Barry CE, 3rd. The W-Beijing lineage of Mycobacterium tuberculosis overproduces triglycerides and has the DosR dormancy regulon constitutively upregulated. *J Bacteriol* 2007,**189**:2583-2589.
597. Lyashchenko K, Colangeli R, Houde M, Al Jahdali H, Menzies D, Gennaro ML. Heterogeneous antibody responses in tuberculosis. *Infect Immun* 1998,**66**:3936-3940.
598. Hoff ST, Abebe M, Ravn P, Range N, Malenganisho W, Rodriques DS*, et al.* Evaluation of Mycobacterium tuberculosis--specific antibody responses in populations with different levels of exposure from Tanzania, Ethiopia, Brazil, and Denmark. *Clin Infect Dis* 2007,**45**:575-582.
599. Bothamley GH. Serological diagnosis of tuberculosis. *Eur Respir J Suppl* 1995,**20**:676s-688s.
600. Baumann R, Kaempfer S, Chegou NN, Oehlmann W, Loxton AG, Kaufmann SH*, et al.* Serologic diagnosis of tuberculosis by combining Ig classes against selected mycobacterial targets. *J Infect* 2014,**69**:581-589.
601. Abebe F, Holm-Hansen C, Wiker HG, Bjune G. Progress in serodiagnosis of Mycobacterium tuberculosis infection. *Scand J Immunol* 2007,**66**:176-191.
602. Vidarsson G, Dekkers G, Rispens T. IgG subclasses and allotypes: from structure to effector functions. *Front Immunol* 2014,**5**:520.
603. Sousa AO, Henry S, Maroja FM, Lee FK, Brum L, Singh M*, et al.* IgG subclass distribution of antibody responses to protein and polysaccharide mycobacterial antigens in leprosy and tuberculosis patients. *Clin Exp Immunol* 1998,**111**:48-55.
604. Hussain R, Dawood G, Abrar N, Toossi Z, Minai A, Dojki M*, et al.* Selective increases in antibody isotypes and immunoglobulin G subclass responses to secreted antigens in tuberculosis patients and healthy household contacts of the patients. *Clin Diagn Lab Immunol* 1995,**2**:726-732.
605. Da Costa CT, Khanolkar-Young S, Elliott AM, Wasunna KM, McAdam KP. Immunoglobulin G subclass responses to mycobacterial lipoarabinomannan in HIV-infected and non-infected patients with tuberculosis. *Clin Exp Immunol* 1993,**91**:25-29.
606. Turneer M, Van Vooren JP, De Bruyn J, Serruys E, Dierckx P, Yernault JC. Humoral immune response in human tuberculosis: immunoglobulins G, A, and M directed against the purified P32 protein antigen of Mycobacterium bovis bacillus Calmette-Guerin. *J Clin Microbiol* 1988,**26**:1714-1719.

607. Ivanyi J. Serodiagnosis of tuberculosis: due to shift track. *Tuberculosis (Edinb)* 2012,**92**:31-37.
608. Cole RA, Lu HM, Shi YZ, Wang J, De-Hua T, Zhou AT. Clinical evaluation of a rapid immunochromatographic assay based on the 38 kDa antigen of Mycobacterium tuberculosis on patients with pulmonary tuberculosis in China. *Tuber Lung Dis* 1996,**77**:363-368.
609. Perley CC, Frahm M, Click EM, Dobos KM, Ferrari G, Stout JE*, et al.* The human antibody response to the surface of Mycobacterium tuberculosis. *PLoS One* 2014,**9**:e98938.
610. Kawano Y, Noma T. Role of interleukin-2 and interferon-gamma in inducing production of IgG subclasses in lymphocytes of human newborns. *Immunology* 1996,**88**:40-48.
611. Briere F, Servet-Delprat C, Bridon JM, Saint-Remy JM, Banchereau J. Human interleukin 10 induces naive surface immunoglobulin D+ (sIgD+) B cells to secrete IgG1 and IgG3. *J Exp Med* 1994,**179**:757-762.
612. Kaplan C, Valdez JC, Chandrasekaran R, Eibel H, Mikecz K, Glant TT*, et al.* Th1 and Th2 cytokines regulate proteoglycan-specific autoantibody isotypes and arthritis. *Arthritis Res* 2002,**4**:54-58.
613. Glatman-Freedman A, Casadevall A. Serum therapy for tuberculosis revisited: reappraisal of the role of antibody-mediated immunity against Mycobacterium tuberculosis. *Clin Microbiol Rev* 1998,**11**:514-532.
614. Collins FM. Cellular antimicrobial immunity. *CRC Crit Rev Microbiol* 1978,**7**:27-91.
615. Grosset J. Mycobacterium tuberculosis in the extracellular compartment: an underestimated adversary. *Antimicrob Agents Chemother* 2003,**47**:833-836.
616. Maglione PJ, Xu J, Chan J. B cells moderate inflammatory progression and enhance bacterial containment upon pulmonary challenge with Mycobacterium tuberculosis. *J Immunol* 2007,**178**:7222-7234.
617. Wu YE, Zhang SW, Peng WG, Li KS, Li K, Jiang JK*, et al.* Changes in lymphocyte subsets in the peripheral blood of patients with active pulmonary tuberculosis. *J Int Med Res* 2009,**37**:1742-1749.
618. Montes Santiago J, Gambon Deza F, Pacheco Carracedo M, Cerda Mota T. [Cellular immune response in tuberculosis: analysis of T-lymphocytes and their subsets, B-lymphocytes and natural cytotoxic cells in different tuberculosis states and body fluids]. *Rev Clin Esp* 1996,**196**:223-227.
619. Corominas M, Cardona V, Gonzalez L, Cayla JA, Rufi G, Mestre M*, et al.* B-lymphocytes and co-stimulatory molecules in Mycobacterium tuberculosis infection. *Int J Tuberc Lung Dis* 2004,**8**:98-105.
620. Abreu MT, Carvalheiro H, Rodrigues-Sousa T, Domingos A, Segorbe-Luis A, Rodrigues-Santos P*, et al.* Alterations in the peripheral blood B cell subpopulations of multidrug-resistant tuberculosis patients. *Clin Exp Med* 2014,**14**:423-429.
621. Kumar NP, Sridhar R, Hanna LE, Banurekha VV, Nutman TB, Babu S. Decreased frequencies of circulating CD4(+) T follicular helper cells associated with diminished plasma IL-21 in active pulmonary tuberculosis. *PLoS One* 2014,**9**:e111098.
622. Ehrhardt GR, Hsu JT, Gartland L, Leu CM, Zhang S, Davis RS*, et al.* Expression of the immunoregulatory molecule FcRH4 defines a distinctive tissue-based population of memory B cells. *J Exp Med* 2005,**202**:783-791.
623. Portugal S, Tipton CM, Sohn H, Kone Y, Wang J, Li S*, et al.* Malaria-associated atypical memory B cells exhibit markedly reduced B cell receptor signaling and effector function. *Elife* 2015,**4**.

624. Ehrhardt GR, Hijikata A, Kitamura H, Ohara O, Wang JY, Cooper MD. Discriminating gene expression profiles of memory B cell subpopulations. *J Exp Med* 2008,**205**:1807-1817.
625. Moir S, Ho J, Malaspina A, Wang W, DiPoto AC, O'Shea MA*, et al.* Evidence for HIV-associated B cell exhaustion in a dysfunctional memory B cell compartment in HIV-infected viremic individuals. *J Exp Med* 2008,**205**:1797-1805.
626. Weiss GE, Crompton PD, Li S, Walsh LA, Moir S, Traore B*, et al.* Atypical memory B cells are greatly expanded in individuals living in a malaria-endemic area. *J Immunol* 2009,**183**:2176-2182.
627. Weiss GE, Clark EH, Li S, Traore B, Kayentao K, Ongoiba A*, et al.* A positive correlation between atypical memory B cells and Plasmodium falciparum transmission intensity in cross-sectional studies in Peru and Mali. *PLoS One* 2011,**6**:e15983.
628. Sullivan RT, Ssewanyana I, Wamala S, Nankya F, Jagannathan P, Tappero JW*, et al.* B cell sub-types following acute malaria and associations with clinical immunity. *Malar J* 2016,**15**:139.
629. Illingworth J, Butler NS, Roetynck S, Mwacharo J, Pierce SK, Bejon P*, et al.* Chronic exposure to Plasmodium falciparum is associated with phenotypic evidence of B and T cell exhaustion. *J Immunol* 2013,**190**:1038-1047.
630. Joosten SA, van Meijgaarden KE, Del Nonno F, Baiocchini A, Petrone L, Vanini V*, et al.* Patients with Tuberculosis Have a Dysfunctional Circulating B-Cell Compartment, Which Normalizes following Successful Treatment. *PLoS Pathog* 2016,**12**:e1005687.